Third Benchmark Workshop

on

NUMERICAL ANALYSIS OF DAMS

Paris, France
September 29–30, 1994

Organized by
the **ICOLD**
"ad-hoc" Committee on Computational Aspects
of Dam Analysis and Design

Under the auspices of the
French Committee on Large Dams
in cooperation with

COYNE ET BELLIER
Bureau d'Ingénieurs Conseils

and

CNEH
ELECTRICITE DE FRANCE

Volume II

Third Benchmark Workshop on
NUMERICAL ANALYSIS OF DAMS
Gennevilliers, France, September 29-30, 1994

THEME A2

Evaluation of critical uniform temperature decrease for a cracked buttress dam

PRESENTATION

&

REFERENCE INFORMATION AND DATA

Third Benchmark Workshop on Numerical Analysis of Dams
Gennevilliers (France) - September 29-30, 1994

Theme A2 :

EVALUATION OF CRITICAL UNIFORM TEMPERATURE DECREASE FOR A CRACKED BUTTRESS DAM

GENERAL ASPECTS

G.GIUSEPPETTI

Chairman of the "ad-hoc Committee on Computational Aspects of Dam Analysis and Design"

Theme A2 is concerned with the numerical evaluation of a uniform temperature decrease that gives rise to the propagation of a pre-existant crack in a buttress dam.
The reason why such topic has been included as a theme of the BW is obvious considering the large number of existing dams in which crackings are present. In fact many dams exhibit cracks whose main causes can be identified as follows:

a) during construction

- shrinkage
- heat idration process and subsequent cooling
- dead load effects
- prestressing due to joints injection

b) during operation

- extreme environmental temperatures
- chemical influences (alkali-aggregate reactions, action of sulphates, etc.)
- deformation of rock abutments and foundation
- earthquakes
- water loadings (hydrostatic and uplift pressures)

Such causes are well summarized in the table 1, presented by R.Widman at 15th ICOLD Congress held in Lausanne, 1985.

TIME		DUE TO: LOAD CASE	DUE TO: SPECIAL CONDITION	LOCATION: DIRECTION	LOCATION: INITIATION AT
DURING CONSTRUCTION	RESTRAINT	INTERIOR TEMPERATURE DIFFERENCIES	EARLY HARDENED CONCRETE	VERTICAL	CONCRETE SURFACE
			HARDENED CONCRETE	STEEP	ROCK SURFACE
		SHRINKAGE		NO PREDOMINANT LOCATION	
	LOAD	DEAD LOAD		HORIZONTAL	DOWNSTREAM FACE
		PRESTRESSING	INJECTION OF VERTICAL JOINTS		
DURING OPERATION	RESTRAINT	EXTREME EXTERNAL TEMPERATURES	VOLUME CHANGES OF CONCRETE	NO PREDOMINANT LOCATION	
		CHEMICAL INFLUENCES			
	LOAD	WATERLOAD	DEFORMATIONS OF DAM BODY	HORIZONTAL	NEAR UPSTREAM DAM TOE
			DEFORMATIONS OF VALLEY FLANKS	VERTICAL	DOWNSTREAM SURFACE
			LOCAL DEFORMATIONS OF ROCK IRREGULARITIES OF ROCK EXCAVATION	STEEP	ROCK SURFACE
		EARTHQUAKE		NO PREDOMINANT LOCATION	

Table 1

With regard to numerical modelling of cracking phenomena, different methods can be adopted according to the kind of problem to be solved. In the table 2 such methods are briefly summarized:

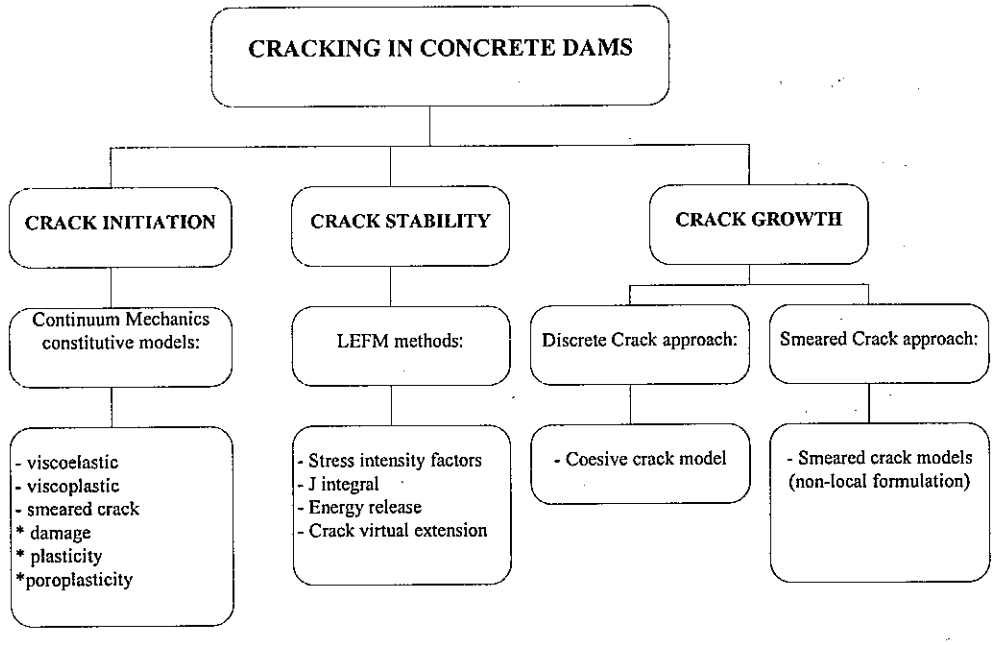

Table 2

In the Theme A2 a crack stability problem is proposed.
Five different lenghts of the crack have been assumed to carry out the analyses. In the exercise just the evaluation of the critical uniform temperature decrease is requested, i.e. a temperature variation which gives rise to a critical stress state at the tip of the crack that causes the initiation of the propagation of the crack itself.

THIRD BENCHMARK WORKSHOP ON NUMERICAL ANALYSIS OF DAMS

THEME A2: Buttress dam

Evaluation of critical uniform temperature decrease for a cracked buttress dam

INTRODUCTION

Several analyses are requested in order to evaluate the uniform temperature decrease which gives rises to a critical stress state at the upper tip of the crack, and consequently causes the initiation of the propagation of the crack itself. The value of the temperature decrease above defined, and some other results specified in the following, are requested with reference to five different crack lengths.

The analyses have to be carried out according to two different schemes:

- rigid foundation
- deformable foundation

For both cases, a plane (2-D) analysis (plane stress for the buttress and plane strain for the foundation) is required.
Information to perform the analyses will be provided in the following chapters.

1.0 GEOMETRICAL DATA

The main geometrical data are reported in figure 1. The analyses should be carried out with reference to the following five different crack lengths L:

0.5 m ; 2. m ; 10. m ; 20. m ; 40.m

With reference to the deformable foundation scheme, a semicircular foundation zone with a radius of 300 m shoud be taken into account.
The Finite Element meshes relevant to both rigid and deformable foundation are represented in figures 2-11. Meshes data are recorded on the diskette enclosed as Annex 1. Considering that for this kind of problems the suitable Finite Element meshes are tightly connected with the algorithm adopted for the analyses, the FE meshes enclosed for the present Theme A2 have to be considered just as a suggestion.
Alternative numerical methods as Boundary Element Method could be used as well.

2.0 PHYSICAL-MECHANICAL PARAMETERS

The following data have to be assumed in the numerical analyses:

2.1 -Concrete:

- Young's elastic modulus $E_c = 3.0\ exp^{10}\ Nm^{-2}$
- Poisson ratio coefficient $v = 0.16$
- Thermal dilatation coefficient $a = 1.0\ exp^{-5}\ {}^{\circ}C^{-1}$
- Toughness $K_c = 2.3\ exp^{6}\ Nm^{-3/2}$

2.2 -Rock (deformable foundation):

- Young's elastic modulus $E_r = 1.0\ exp^{10}\ Nm^{-2}$
- Poisson ratio coefficient $v = 0.2$

3.0 Loading condition

A uniform thermal distribution in the dam (both slab and webs) have to be considered. This is to be intended as a variation with reference to the average (unstressed) state, which is assumed conventionally to correspond to a uniform temperature of 0°C.
The foundation is assumed to remain at constant average (0°C) temperature.

4.0 PRESENTATION OF RESULTS

In order to simplify the comparison of results obtained by different participants, it would be worthwile collecting a selected set of results (temperatures and displacements) according to the forms suggested in tables 1-6.
In addition, contour maps of horizontal and vertical displacements are requested.
Participants are kindly asked to provide all data mentioned above recorded on a diskette.

TABLE 1.

RIGID FOUNDATION

L m	DT °C	d_{max} m	yd_{max} m
0.5			
2.0			
10.			
20.			
40.			

L = crack length (m)

DT = critical temperature variation that gives rises to crack propagation (°C)

d_{max} = maximum crack opening (m)

yd_{max} = maximum crack opening level (m)

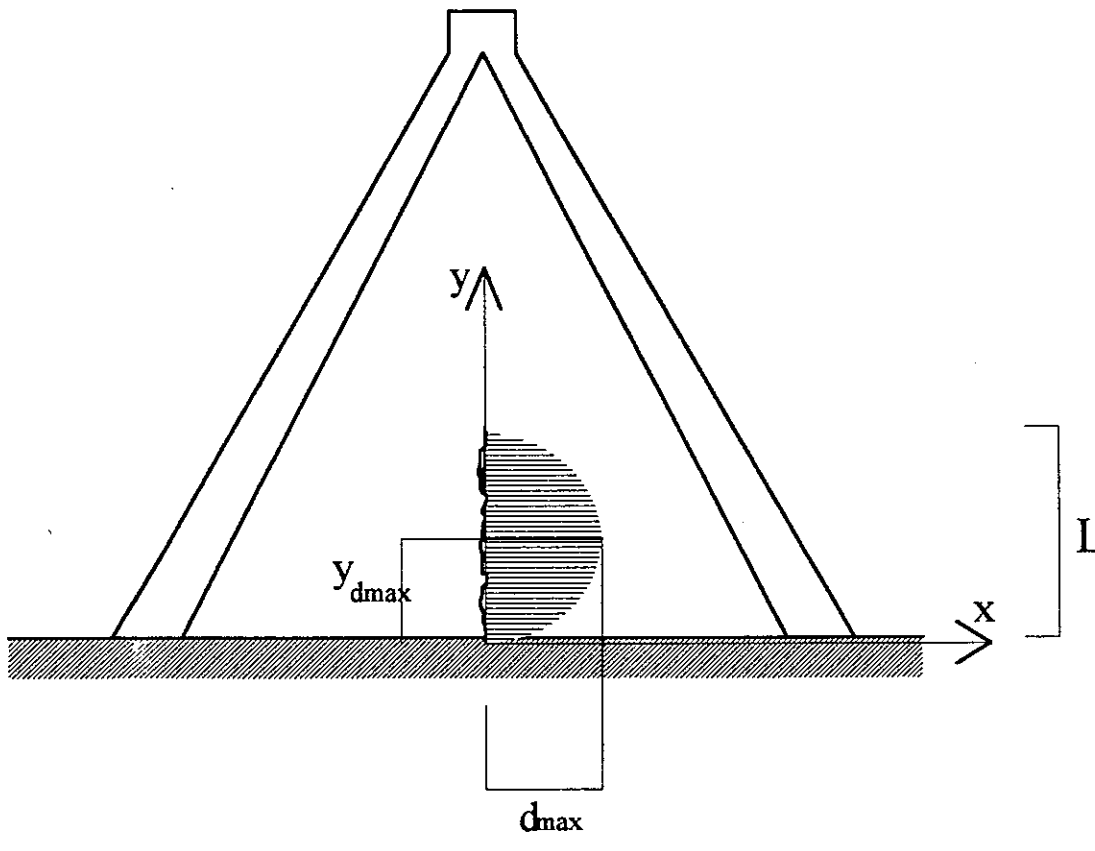

TABLE 2.

DEFORMABLE FOUNDATION

L m	DT °C	d_{max} m	yd_{max} m
0.5			
2.0			
10.			
20.			
40.			

L = crack length (m)

DT = critical temperature variation that gives rises to crack propagation (°C)

d_{max} = maximum crack opening (m)

yd_{max} = maximum crack opening level (m)

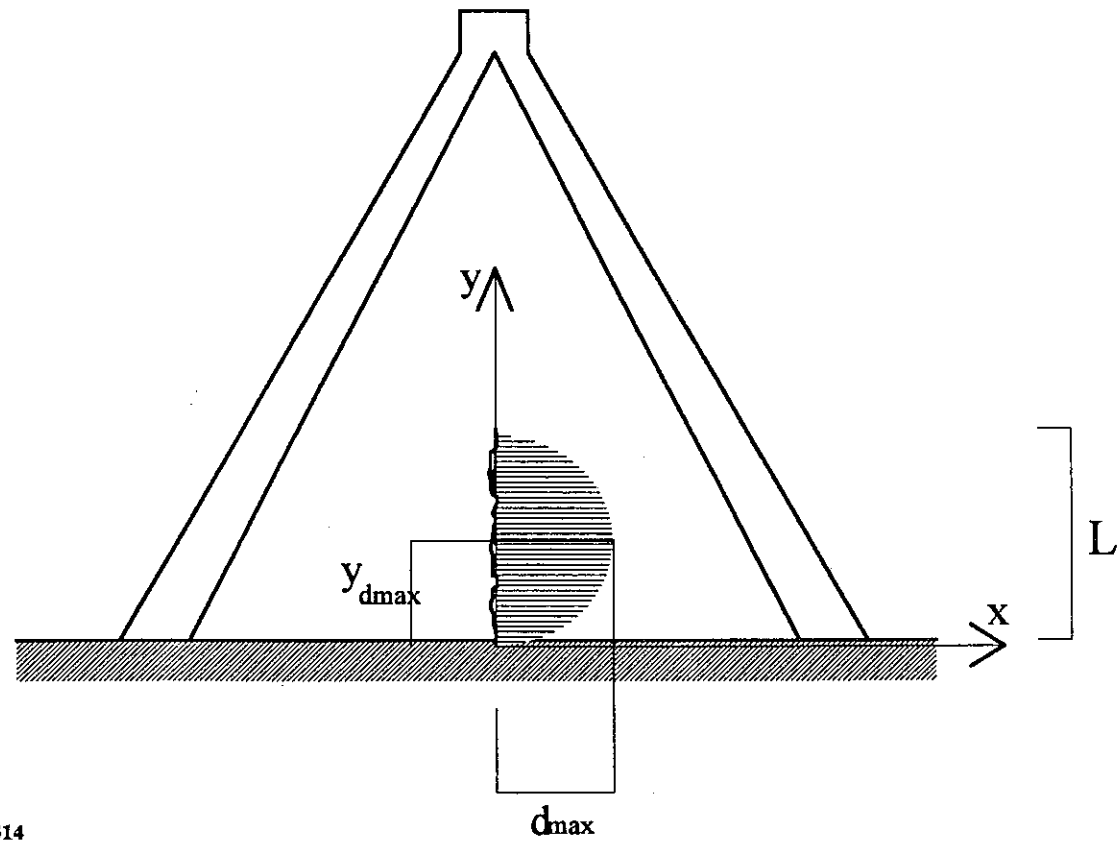

TABLE 3.

RIGID FOUNDATION

y m	ux(y) m

y = level of node along the crack (m)
ux(y) = horizontal displacement for the node at level y (m)

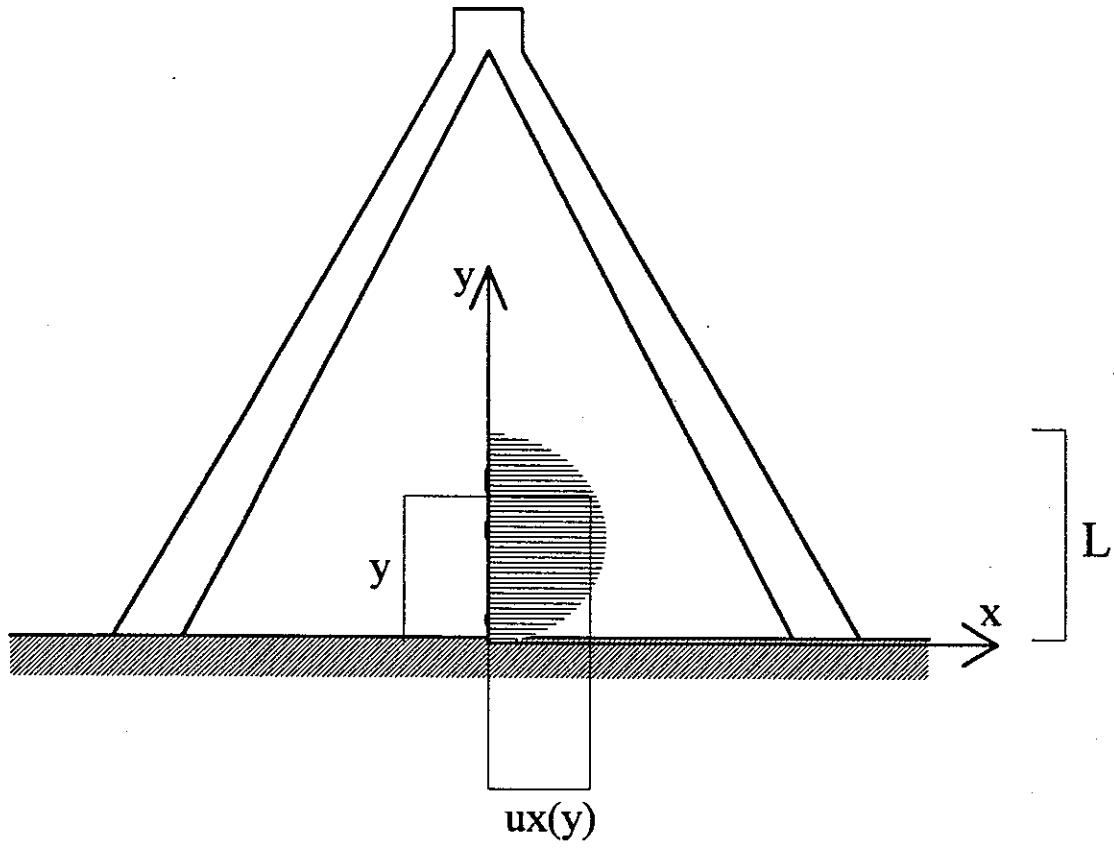

TABLE 4.

DEFORMABLE FOUNDATION

y m	ux(y) m

y = level of node along the crack (m)
ux(y) = horizontal displacement for the node at level y (m)

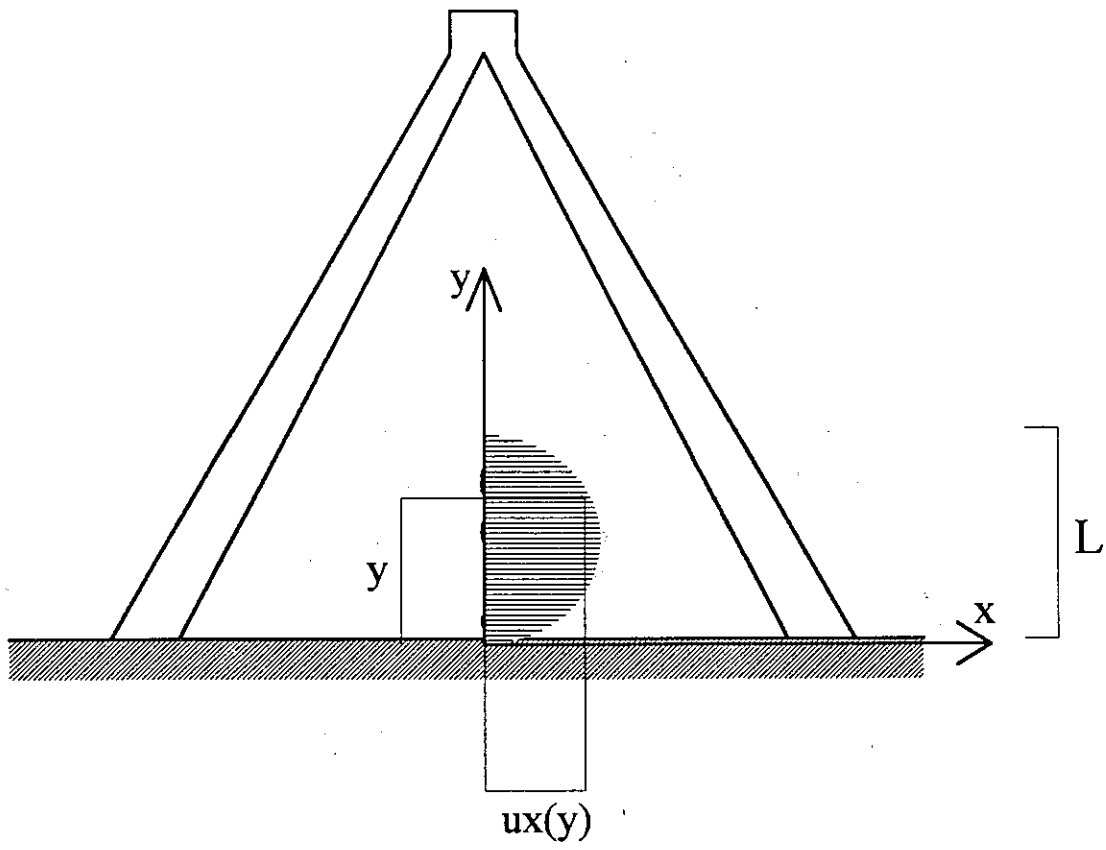

TABLE 5.

RIGID FOUNDATION

x(y=L/2) m	ux(x) m

x(y=L/2) = abscissa of node along the crack axis (horizontal straight line at level y=L/2) (m)

ux(x) = corresponding horizontal displacement (m)

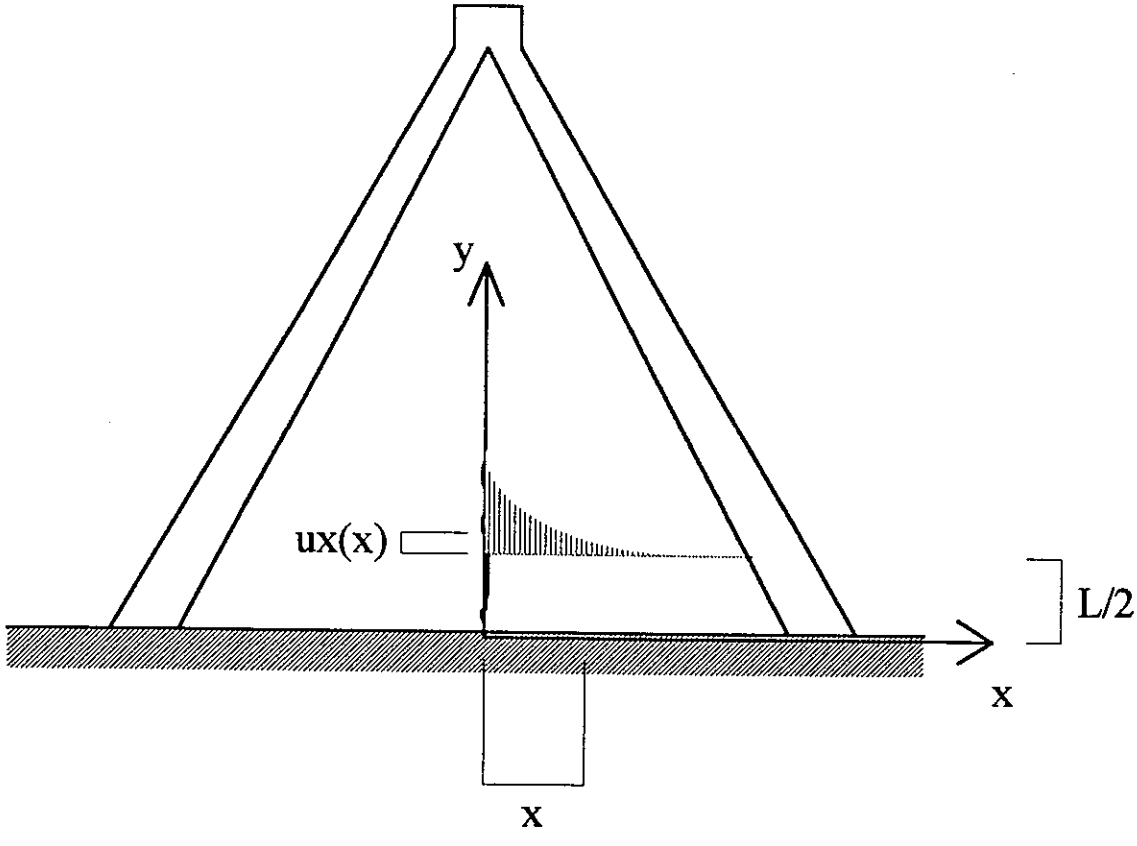

TABLE 6.

DEFORMABLE FOUNDATION

x(y=L/2) m	ux(x) m

x(y=L/2) = abscissa of node along the crack axis (horizontal straigh line at level y=L/2) (m)

ux(x) = corresponding horizontal displacement (m)

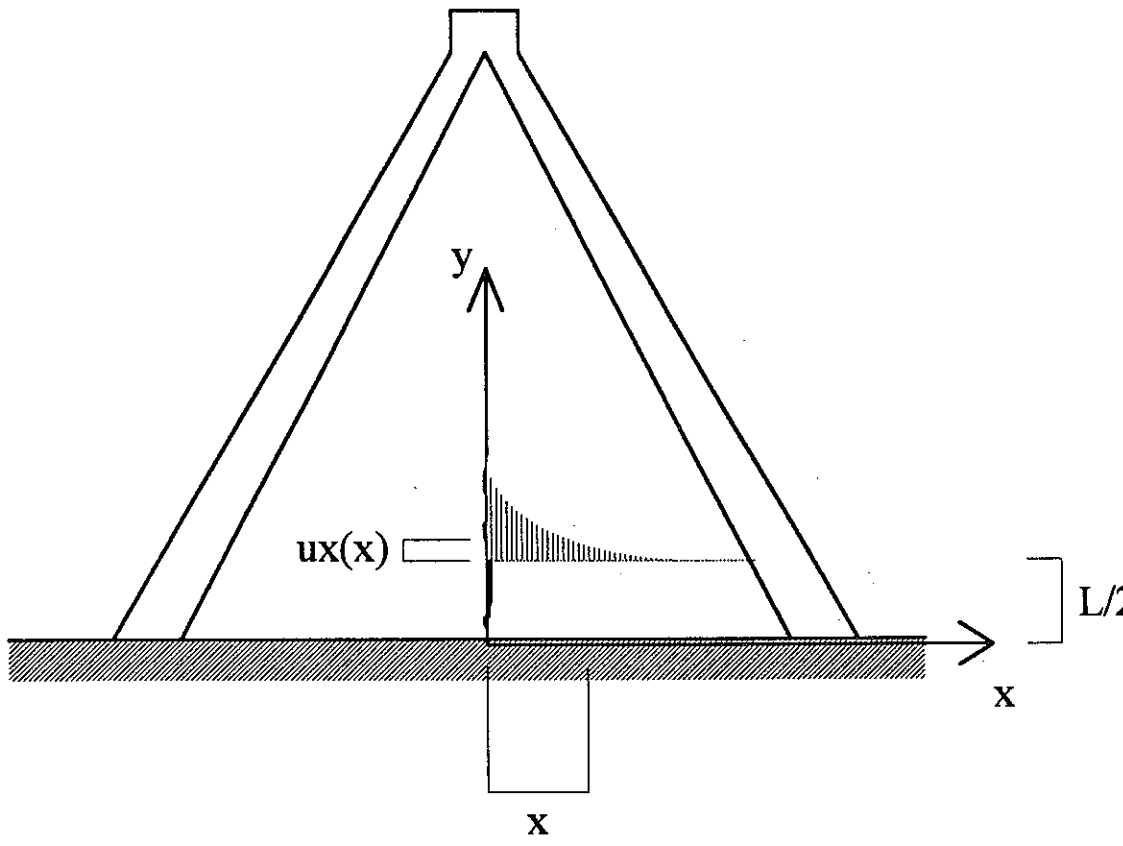

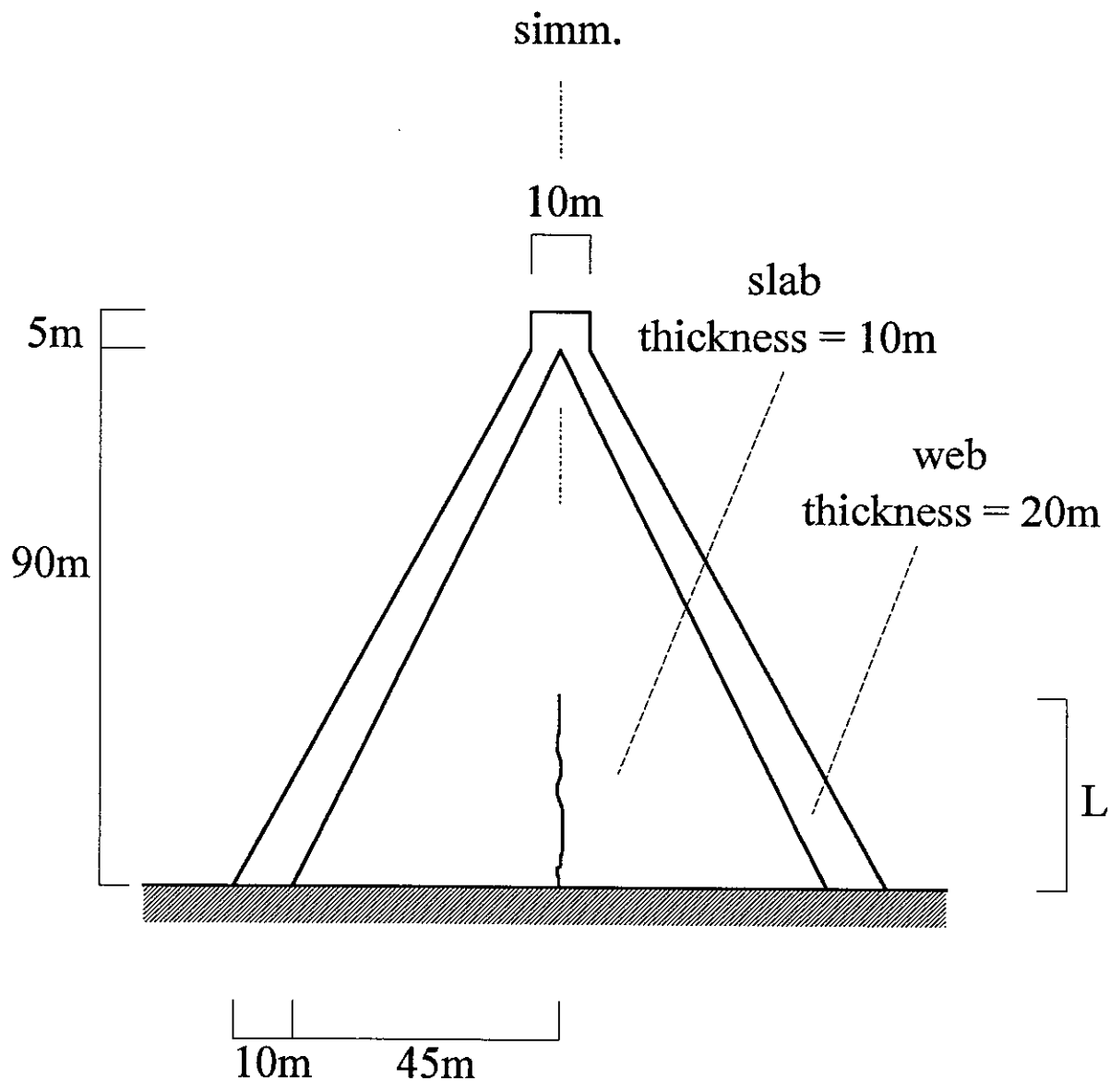

fig. 1 - Geometrical data

fig. 2 - Crack length 0.5 m : Dam and Foundation mesh

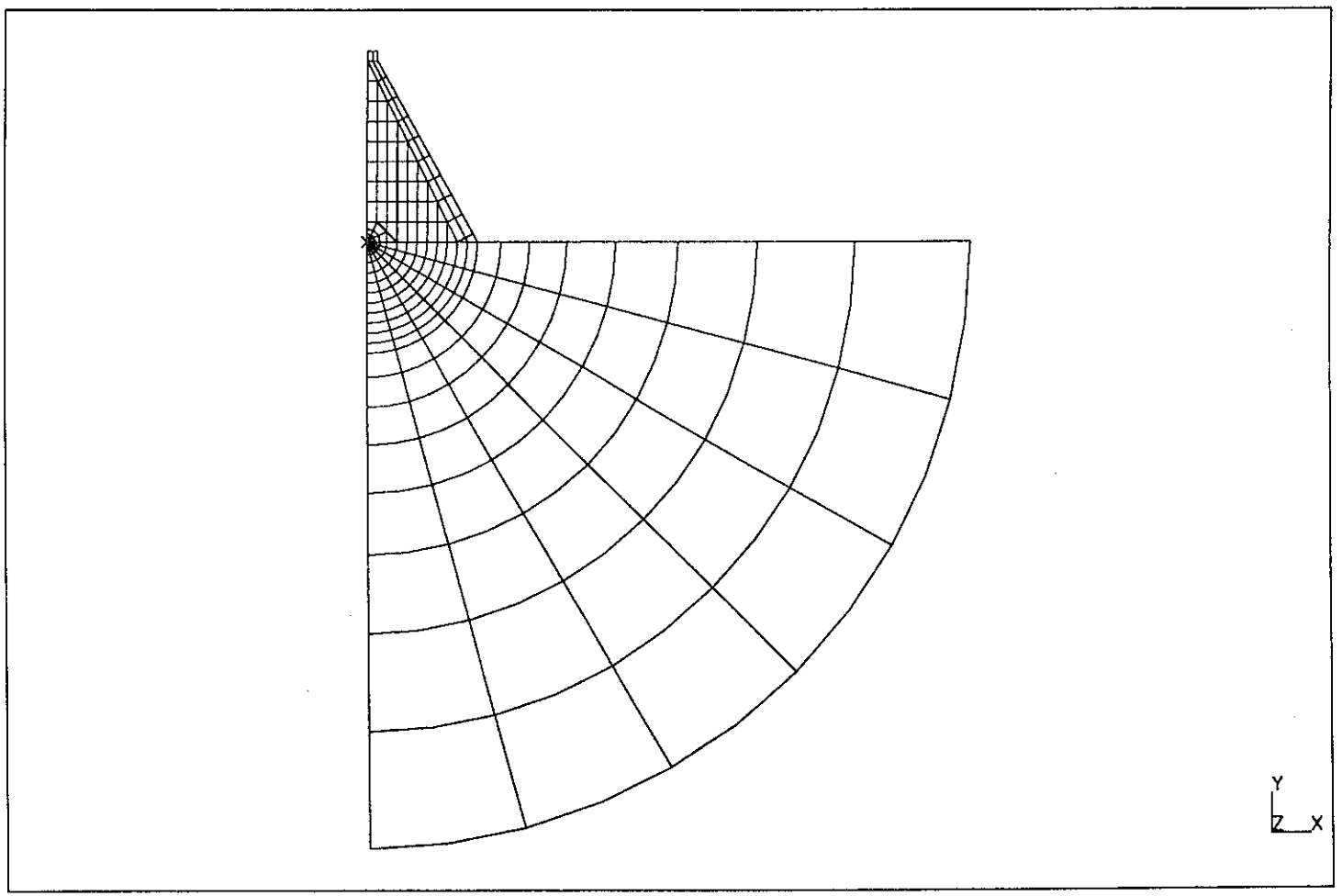

fig. 3a - Crack length 0.5 m : Dam mesh

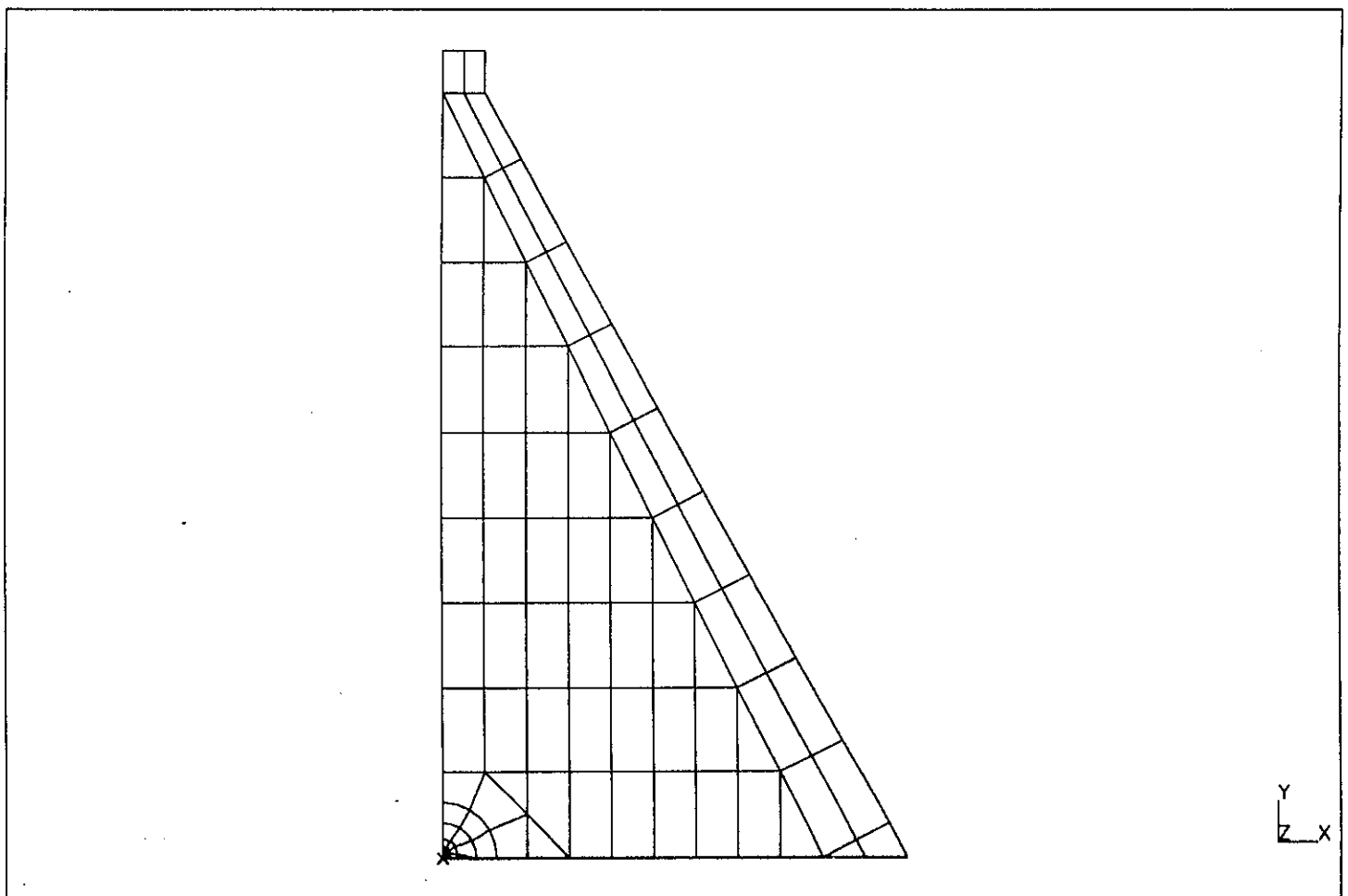

fig. 3b - Crack length 0.5 m : mesh zoom near the crack

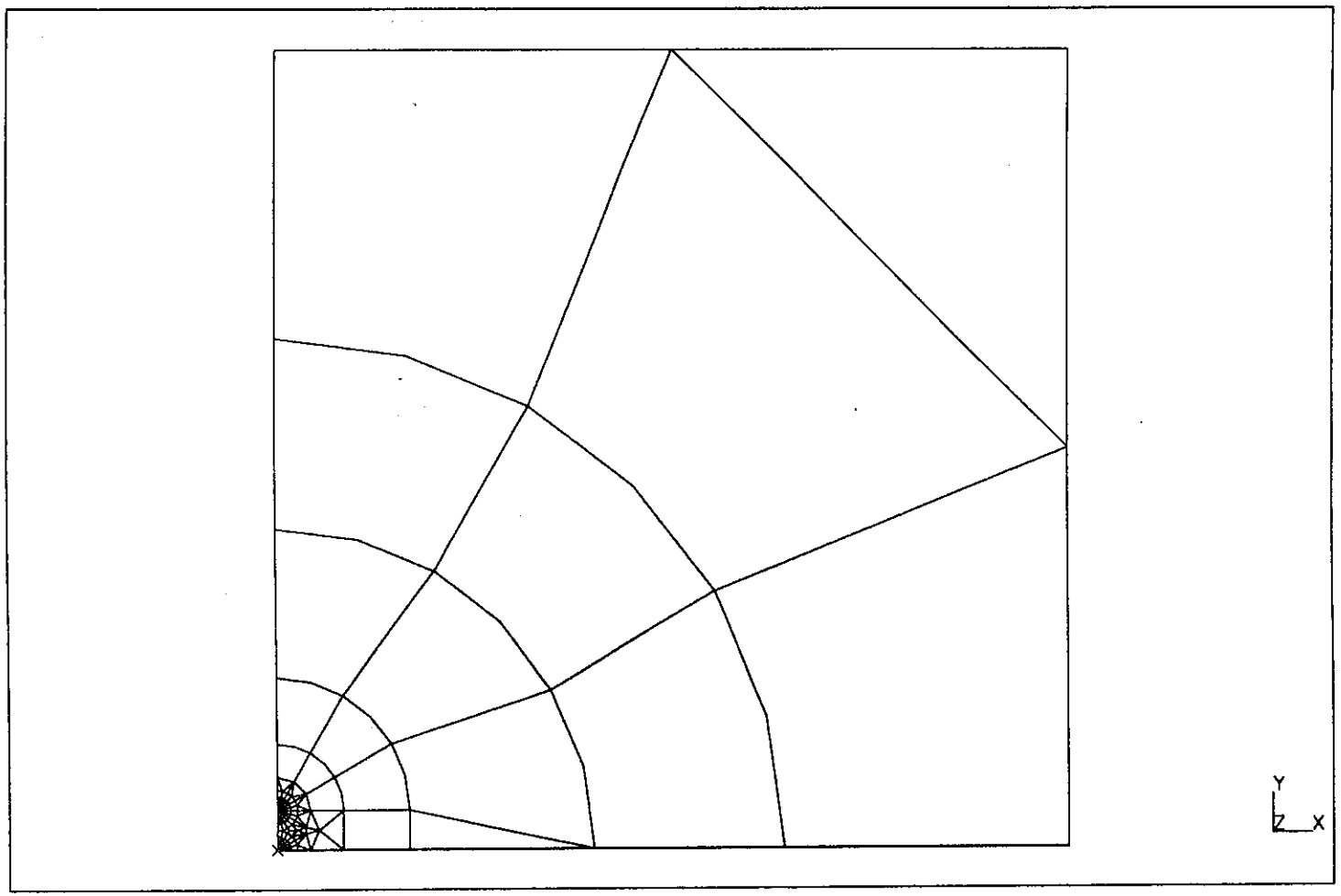

fig. 3c - Crack length 0.5 m : mesh zoom near the crack

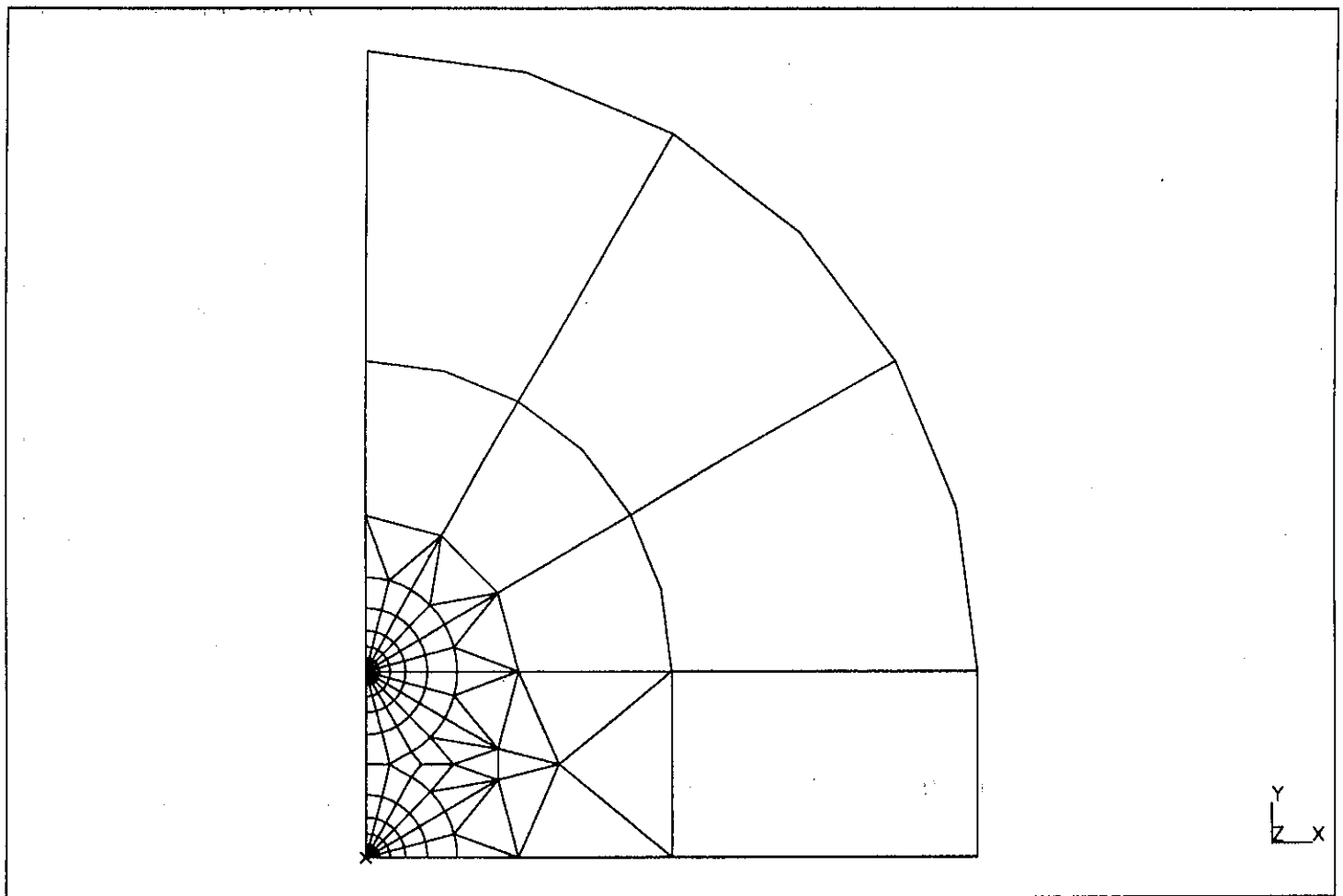

fig. 4 - Crack length 2.0 m : Dam and Foundation mesh

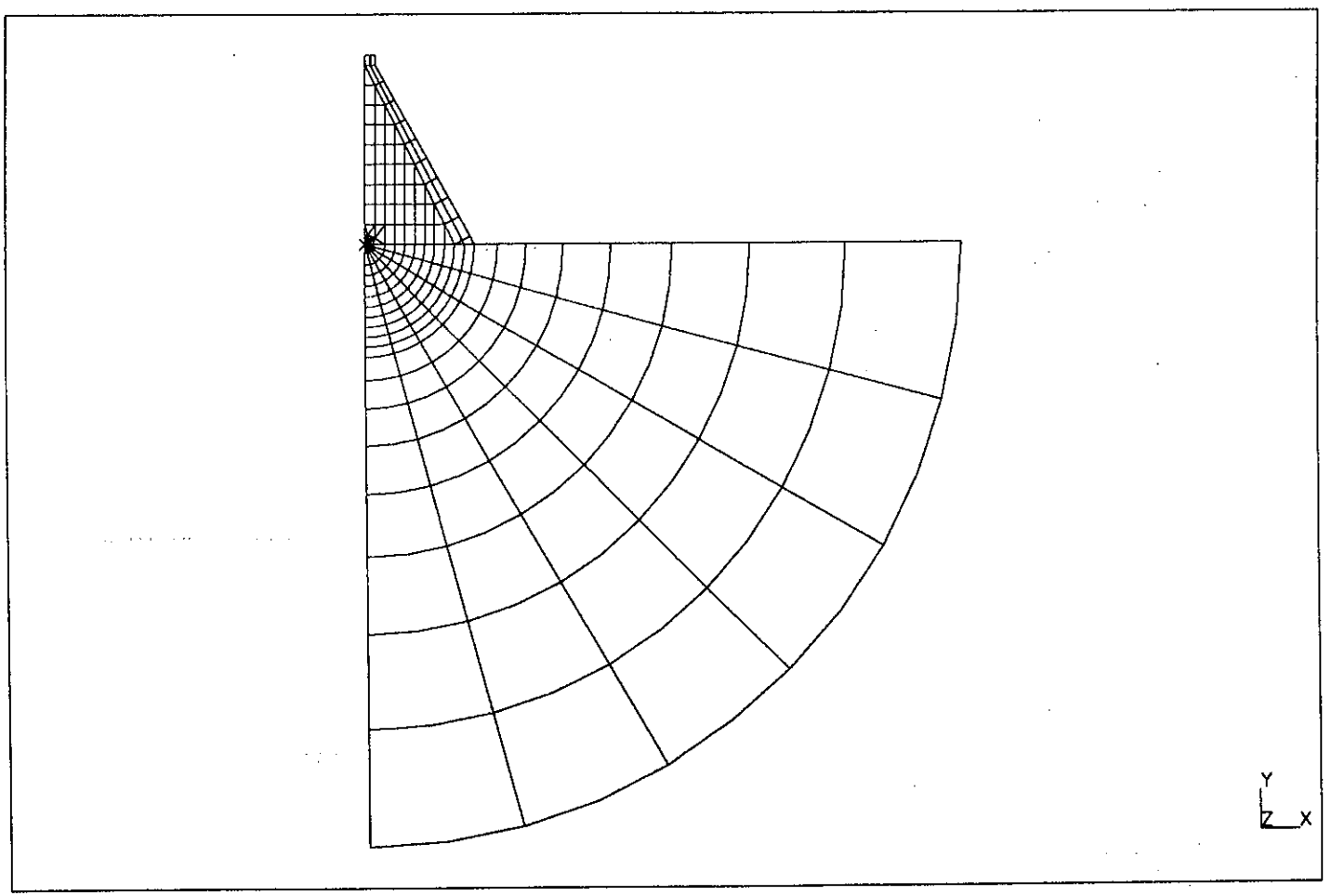

fig. 5a - Crack length 2.0 m : Dam mesh

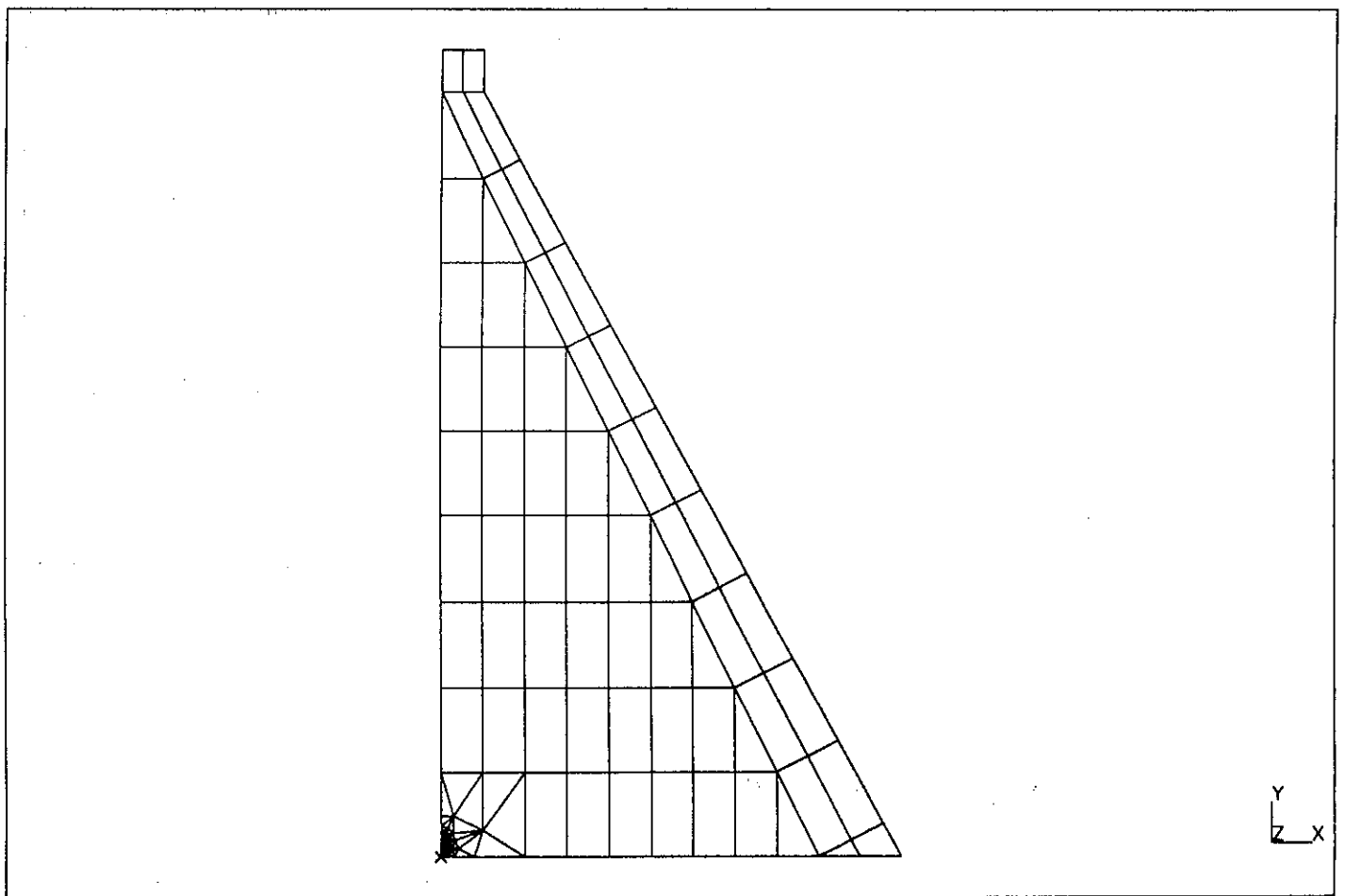

fig. 5b - Crack length 2.0 m : mesh zoom near the crack

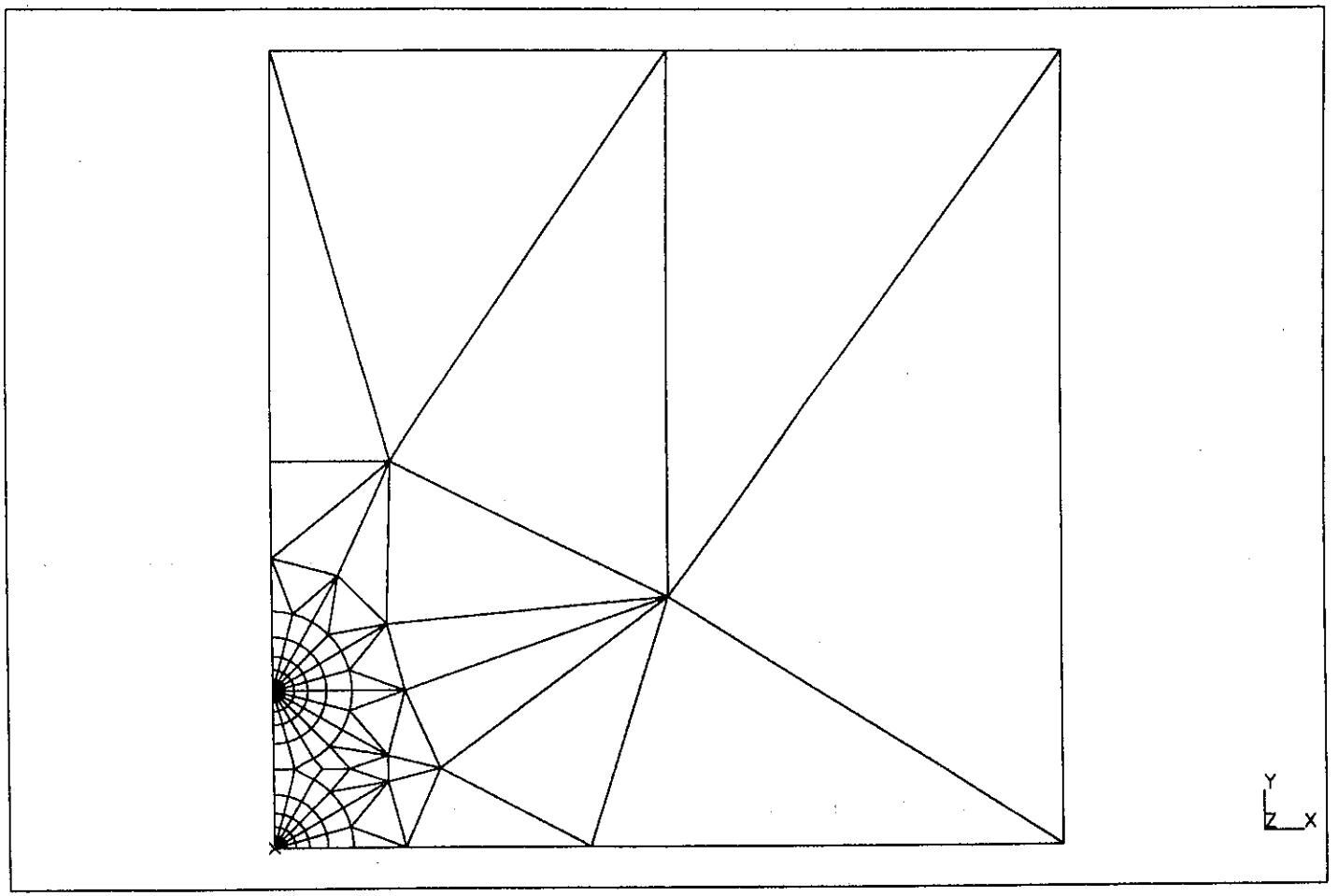

fig. 6 - Crack length 10.0 m : Dam and Foundation mesh

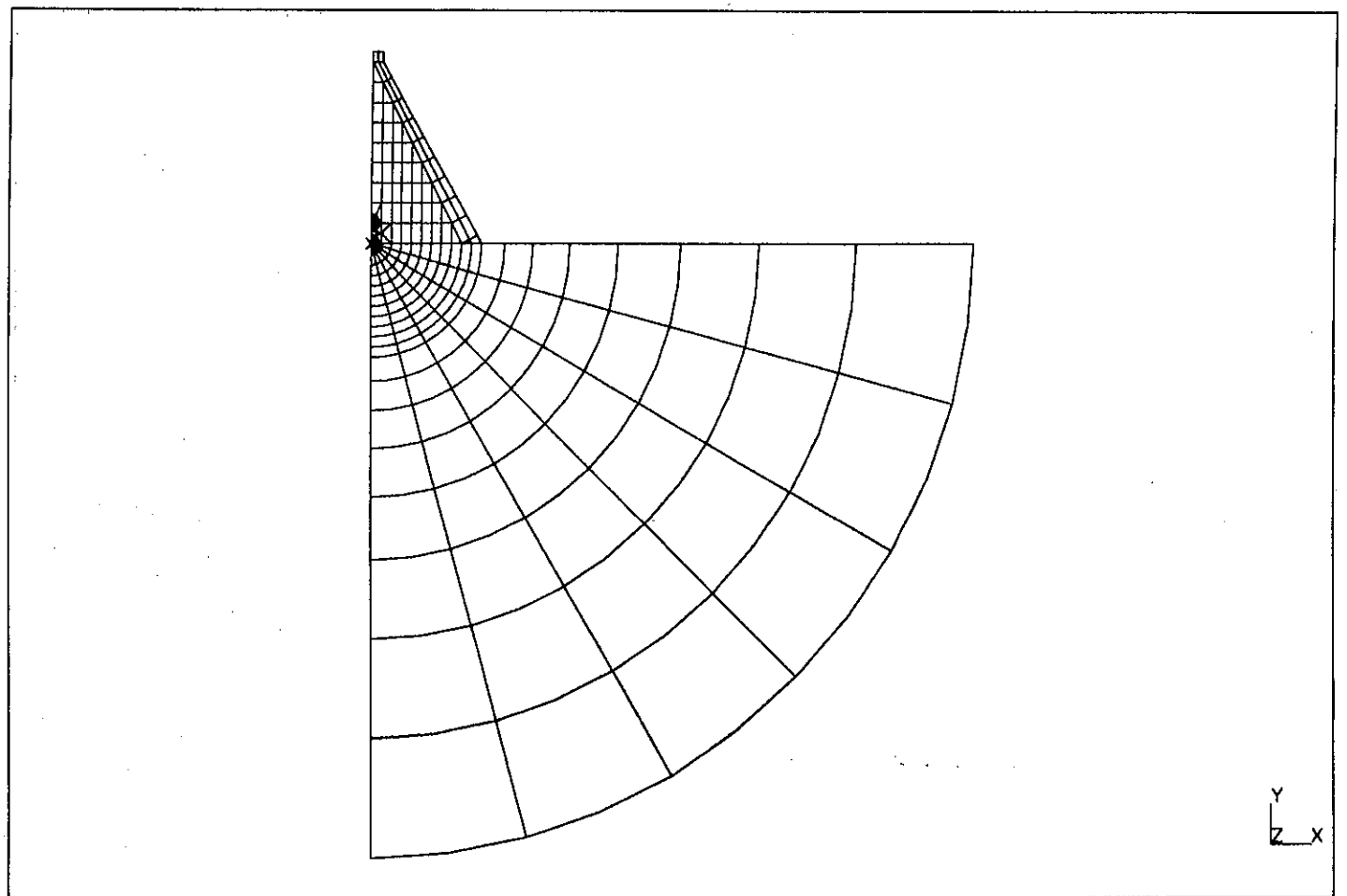

fig. 7a - Crack length 10.0 m : Dam mesh

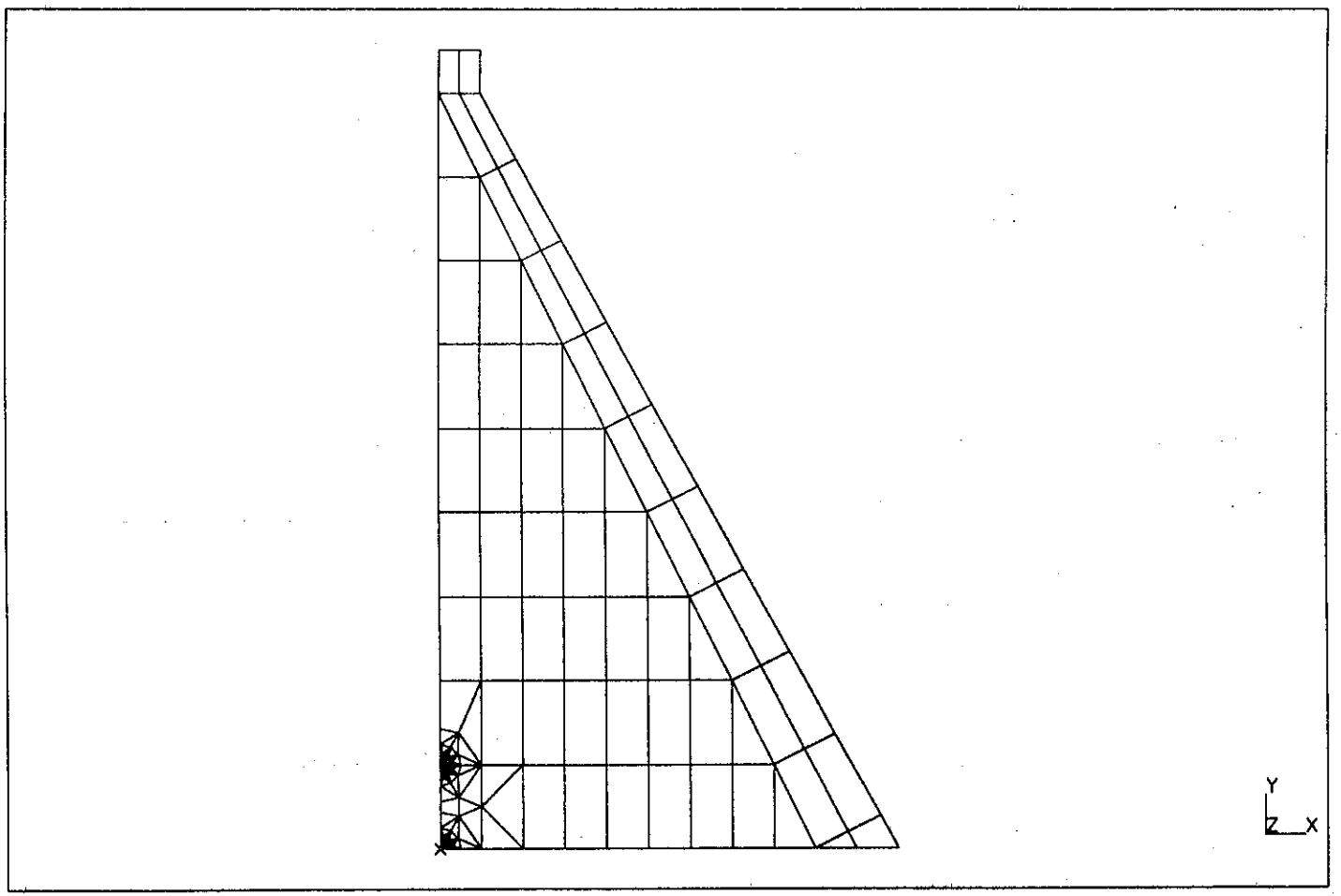

fig. 7b - Crack length 10.0 m : mesh zoom near the crack

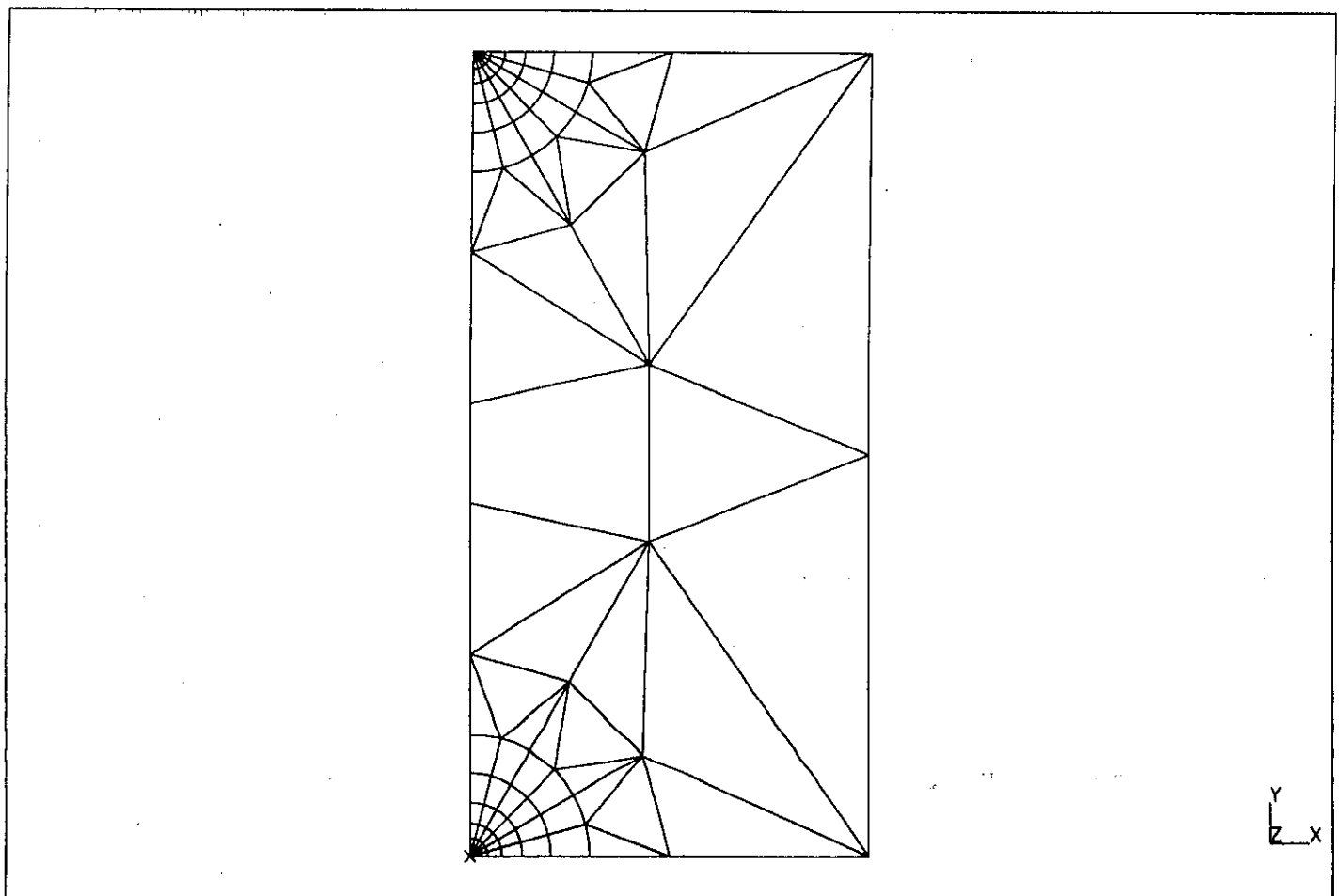

fig. 8 - Crack length 20.0 m : Dam and Foundation mesh

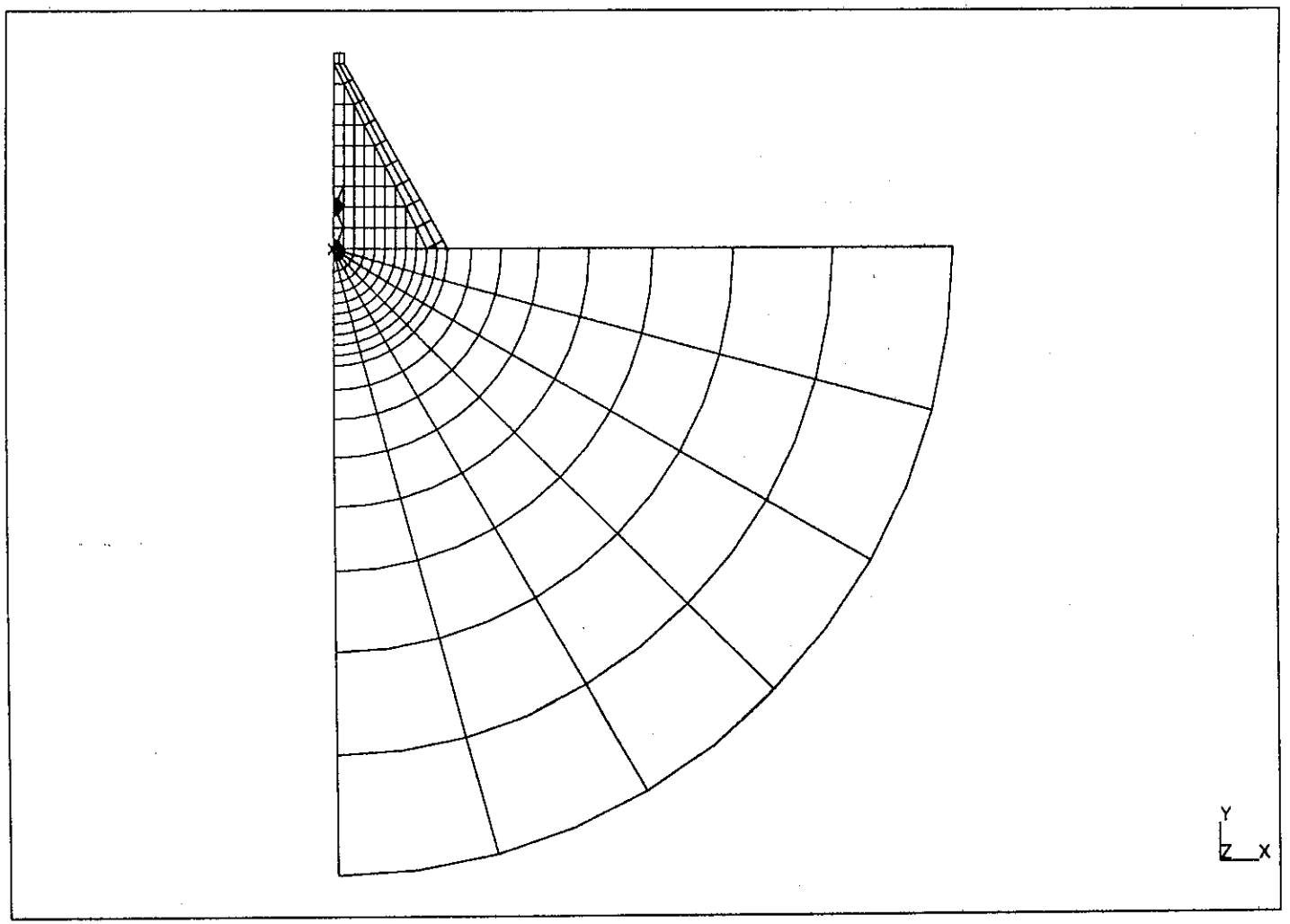

fig. 9a - Crack length 20.0 m : Dam mesh

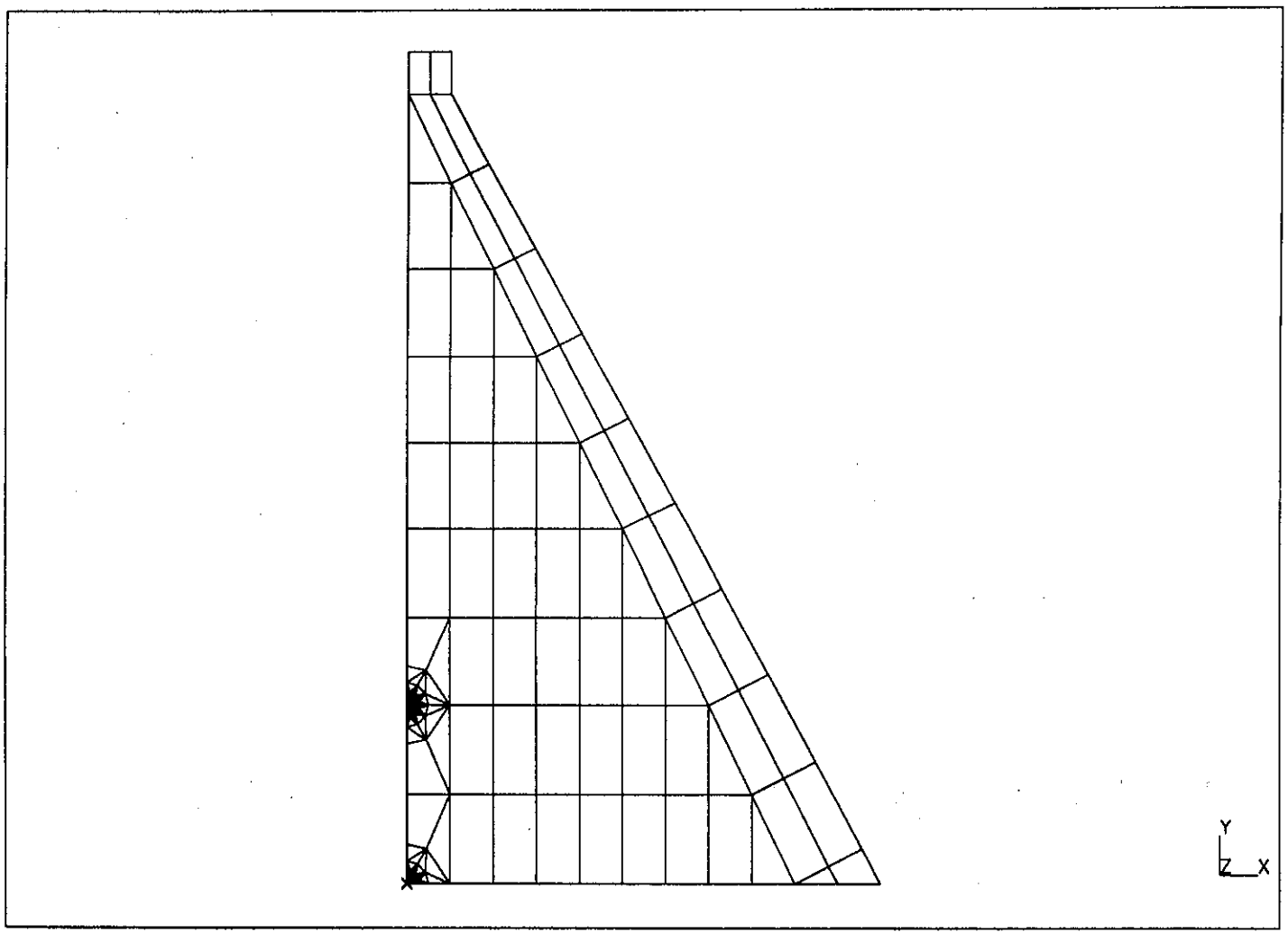

fig. 9b - Crack length 20.0 m and 40.0 m : mesh zoom near the crack tip

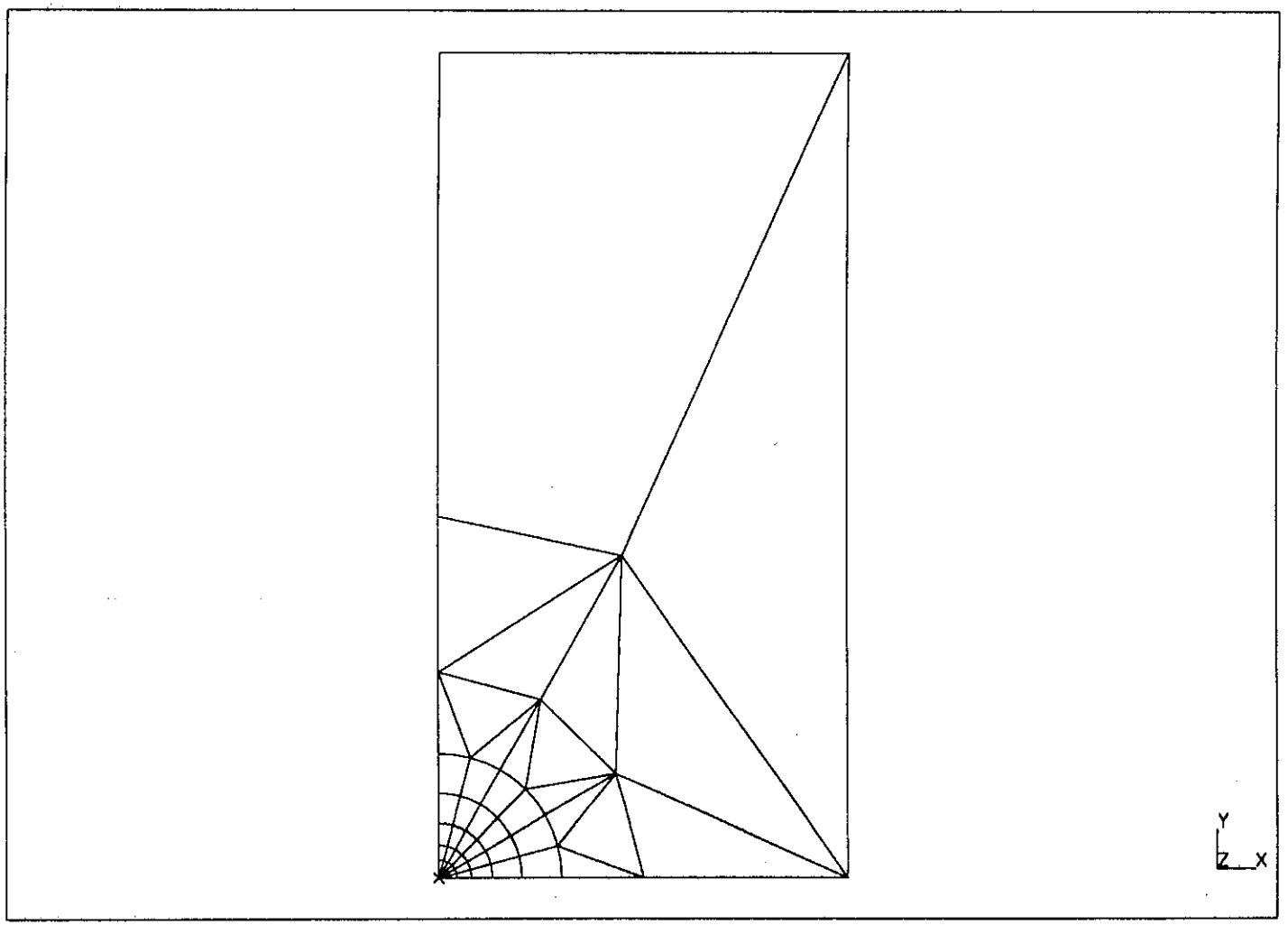

fig. 10 - Crack length 40.0 m : Dam and Foundation mesh

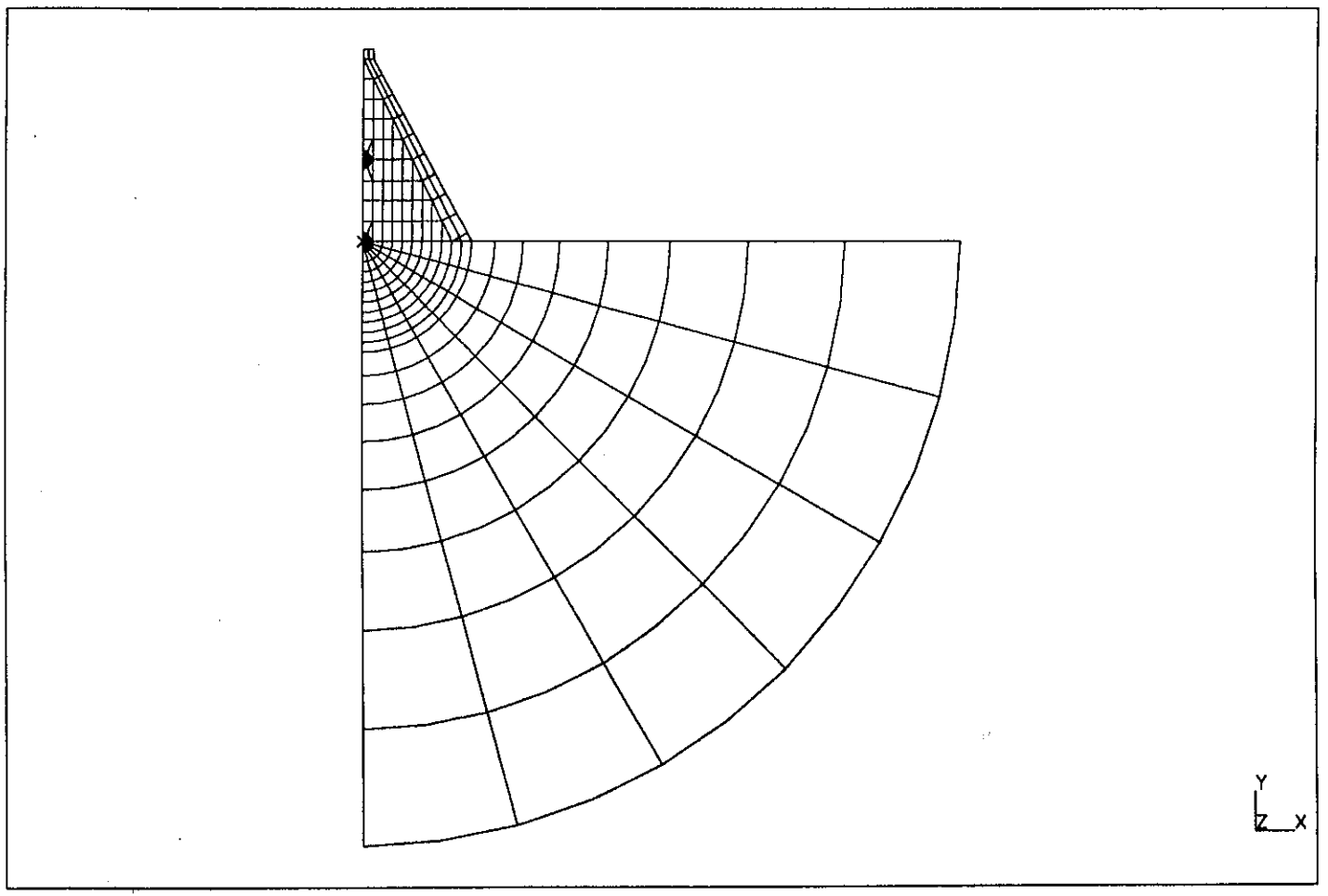

fig. 11 - Crack length 40.0 m : Dam mesh

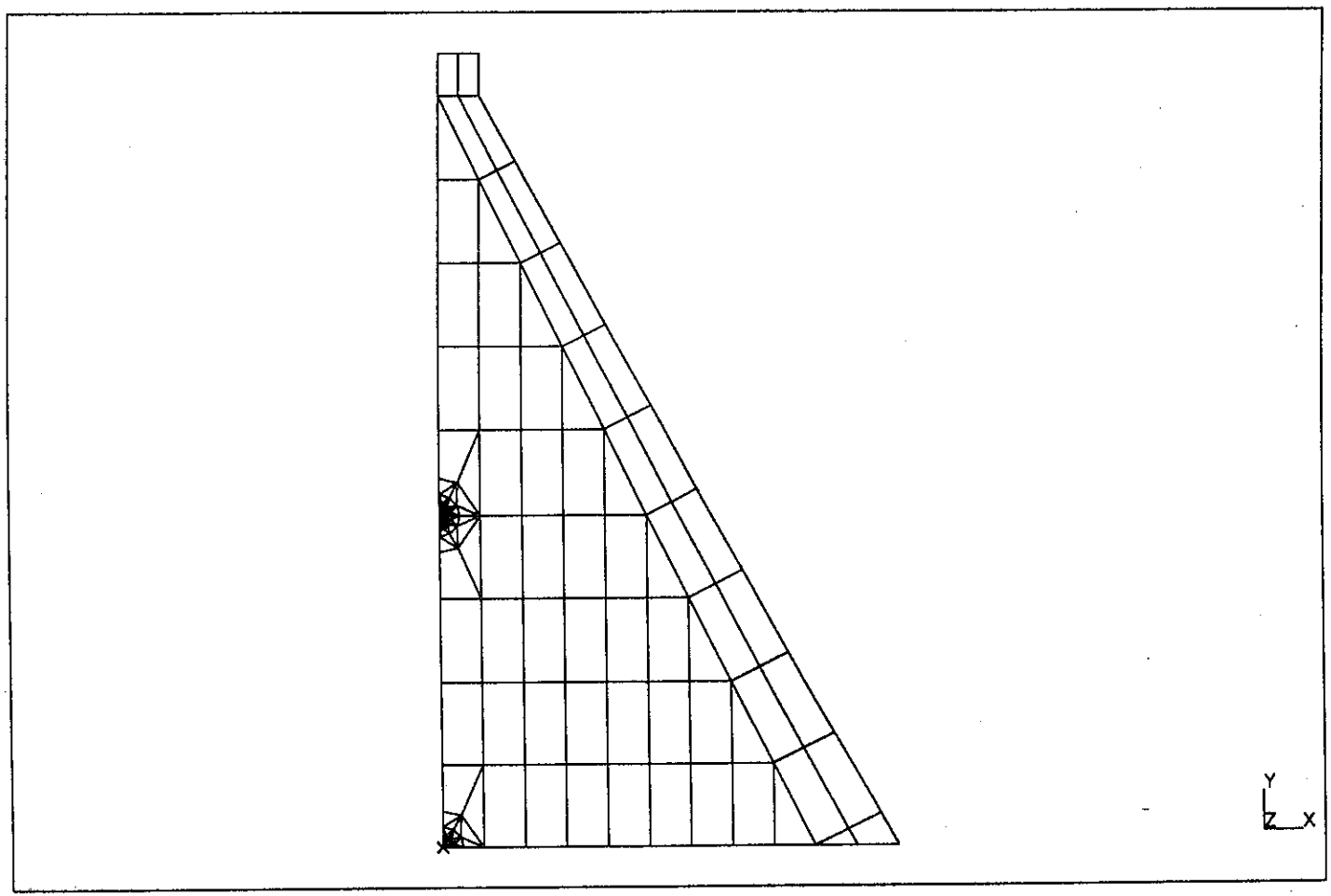

Third Benchmark Workshop on
NUMERICAL ANALYSIS OF DAMS
Gennevilliers, France, September 29-30, 1994

THEME A2

Evaluation of critical uniform temperature decrease for a cracked buttress dam

SYNTHESIS

&

COMPARISON OF RESULTS

NOTES

Third Benchmark Workshop on Numerical Analysis of Dams
Gennevilliers (France) - September 29-30, 1994

Theme A2 :

EVALUATION OF CRITICAL UNIFORM TEMPERATURE DECREASE FOR A CRACKED BUTTRESS DAM

SYNTHESIS REPORT

G.MAZZA', F.CHILLÉ

ENEL S.p.a. DSR/CRIS

PARTICIPANTS

The numerical evaluation of crack propagation induced by uniform temperature decrease has collected 7 participants from 4 countries. To solve the assigned theme they have used 7 different finite element codes. Authors and main computations aspects are listed in the following table:

	Authors	*Company*	*Code*	*MESH*
P01	Menga, Dalmagioni, Mazzá, Pellegrini	ISMES, ENEL	DIANA 5.1	BW with quarter points
P02	Bhattacharjee, Leger Tinawi	Dept. of Civil Engineering, Ecole Polytechnique de Montreal	FRAC_DAM	BW without midside nodes
P03	Chillé, Giuseppetti, Mazzá	ENEL	ABAQUS	BW with quarter points
P04	Shinmura, Cervenka, Boggs, Plizzari, Saouma	Dept. of Civil Engineering University of Colorado	MERLIN	- Whole dam modelled - Completely revised mesh
P05	Ilie, Stematiu	ADDL	ANSYS	Completely revised mesh composed by triangular 6-node elements
P06	Valente, Barpi	Politecnico di Torino	CCRAP	Completely revised mesh composed by triangular 6-node elements
P07	Linsbauer, Promper	University of Technology, Vienna	SOLVIA	BW with quarter points

Among all participants, 4 have used the mesh proposed by Benchmark Workshop specifications

while the others have set up different meshes composed by triangular elements.

COMPARISON OF RESULTS

Results presented by all the participants show a general good agreement; the observed discrepancies can be attribuited to the use of different meshes and interpolations used to evaluate requested displacements bewteen nodal points. In the following, results for both rigid and flexible foundation are briefly examined.

RESULTS FOR RIGID FOUNDATION

A first comparison of results can be made observing graphs showing the relationship bewteen crack lenght and the associated critical temperature. The agreement is completely satisfactory except for participant P06 who slightly overestimates the critical temperature.

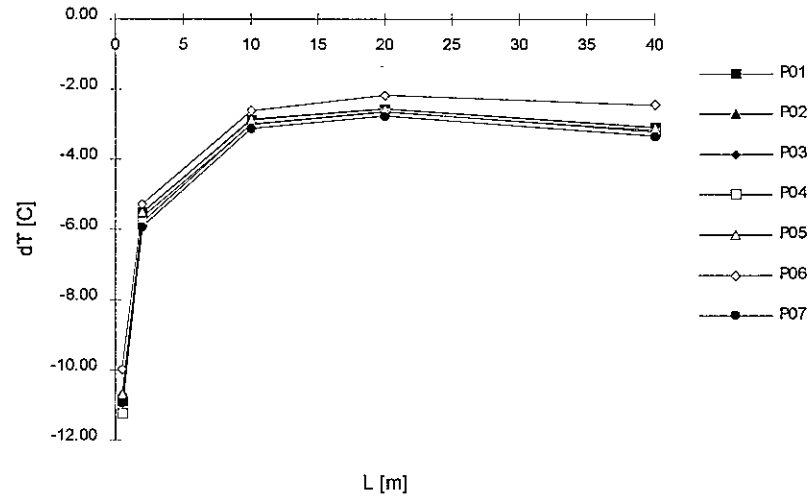

Graph of maximum openings related to different crack lenght is also reported; again participant P06 lies outside the common trend.

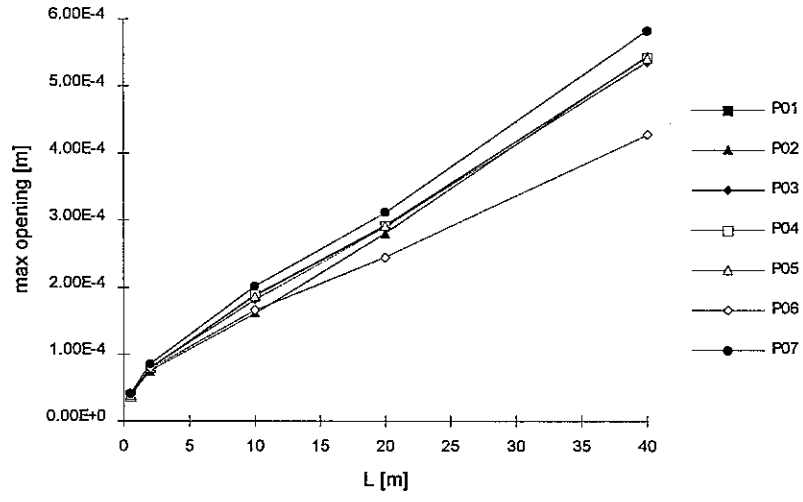

Positions of maximum openings along the crack are reported in the following graph; as it can be noted, for the maximum crack lenght considered (40 m) scatterring of results is particularly evident. This fact can be explained noting that the mesh assigned for this crack lenght is the coarsest, so that evaluation of maximum opening position is strongly dependent on the kind of interpolation used between nodal displacements, moreover it remains important the influence of different meshes used by participants.

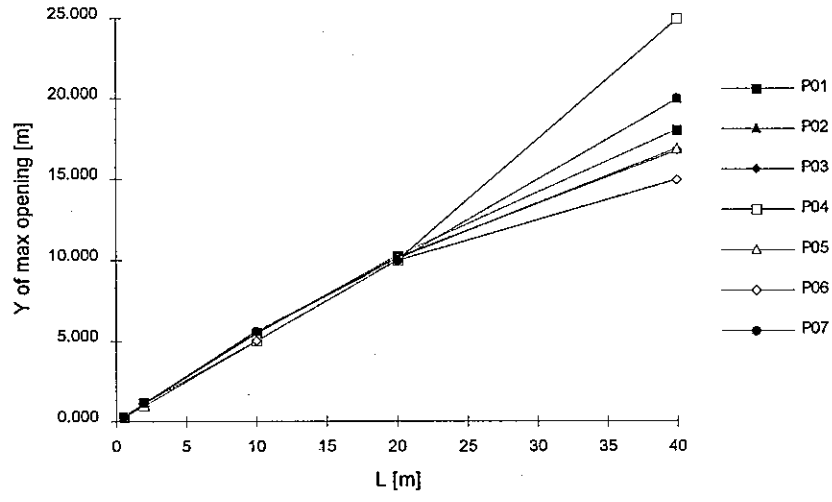

Benchmark Workshop specifications requested also distribution of openings along the crack and distribution of displacements normal to the crack (for all the different crack lenghts, from 0.5 to 40 m). Graphs relevant to these results are not reported here and can be found in the complete set of results.

RESULTS FOR FLEXIBLE FOUNDATION

As for the rigid foundation case, graphs showing the relationship bewteen crack lenght and the associated critical temperature present a satisfactory agreement.

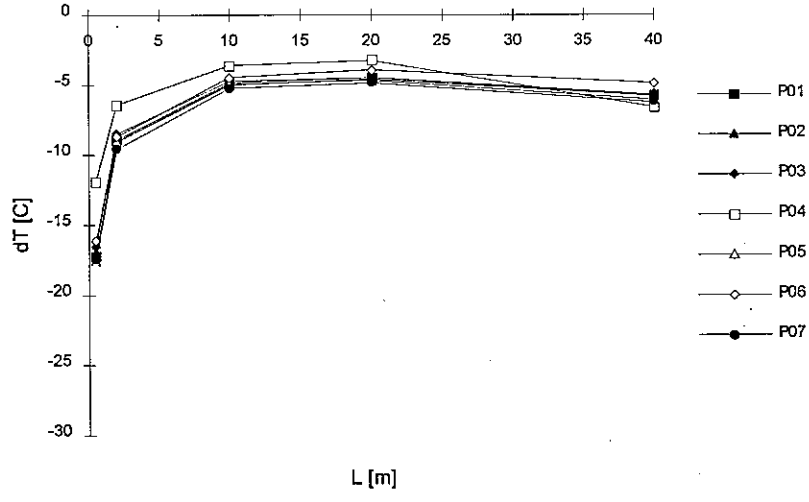

Maximum openings and their position along the crack are reported respectively in the following two graphs; the agreement is always good, except for a crack lenght of 40 m, when participant P04 overestimates both results. This is likely due to the particular mesh adopted.

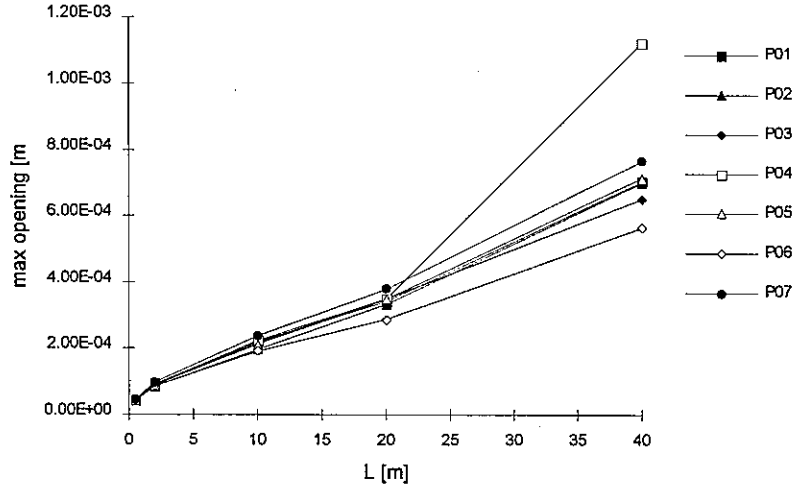

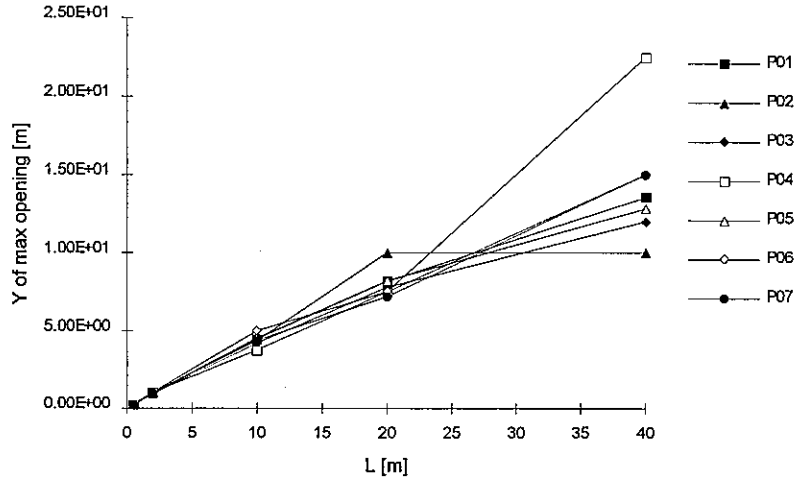

Also for the flexible foundation case, the requested distributions of openings and displacements normal to the crack are reported in the complete set of comparisons.

Third Benchmark Workshop on
NUMERICAL ANALYSIS OF DAMS
Gennevilliers, France, September 29-30, 1994

THEME A2

Evaluation of critical uniform temperature decrease for a cracked buttress dam

ANNEX:

COMPARISON OF RESULTS

THEME A2

	Authors	Company	Code	Hardware	CPU	MESH	METHOD	NOTE
P01	Menga Dalmagioni Mazzá Pellegrini	ISMES ENEL	DIANA 5.1	CONVEX C3	50 sec	BW with quarter points	Virtual extension of the crack	
P02	Bhattacharjee Leger Tinawi	Dept. of Civil Engineering, Ecole Polytechnique de Montreal	FRAC_DAM	RISC 6000	5 sec	BW without midside nodes	Energy release method	Also smeared crack
P03	Chillé Giuseppetti Mazzá	ENEL	ABAQUS	IBM RISK 6000	13 sec	BW with quarter points	J-integral	
P04	Shinmura Cervenka Boggs Plizzari Saouma	Dept. of Civil Engineering, University of Colorado	MERLIN			- Whole dam modelled - Completely revised mesh composed by triangular linear elements		
P05	Ilie Stematiu	ADDL	ANSYS	COMPAQ 486 PENTIUM	380 sec max	Completely revised mesh composed by triangular 6-node elements		
P06	Valente Barpi	Politecnico, Torino	CCRAP for cohesive model	HP720	90 sec each step	Completely revised mesh composed by triangular 6-node elements		Also cohesive computation
P07	Linsbauer Promper	University of Technology, Vienna	SOLVIA	486 DX2/66 EISA	50 sec max	BW with quarter points		

RIGID FOUNDATION

	dT [C]						
L [m]	**P01**	**P02**	**P03**	**P04**	**P05**	**P06**	**P07**
0.5	-10.88	-10.76	-10.71	-11.23	-10.69	-9.98	-10.94
2	-5.51	-5.64	-5.52	-5.79	-5.50	-5.27	-5.92
10	-2.89	-3.02	-2.86	-3.00	-2.88	-2.62	-3.13
20	-2.56	-2.66	-2.56	-2.64	-2.58	-2.18	-2.77
40	-3.09	-3.17	-3.08	-3.22	-3.10	-2.46	-3.34

	dmax [m]						
L [m]	**P01**	**P02**	**P03**	**P04**	**P05**	**P06**	**P07**
0.5	3.94E-5	3.70E-5	3.94E-5	3.65E-5	3.93E-5	4.05E-5	4.07E-5
2	7.95E-5	7.51E-5	7.95E-5	7.90E-5	7.93E-5	7.82E-5	8.50E-5
10	1.87E-4	1.61E-4	1.82E-4	1.89E-4	1.87E-4	1.66E-4	2.02E-4
20	2.92E-4	2.81E-4	2.90E-4	2.93E-4	2.91E-4	2.45E-4	3.11E-4
40	5.43E-4	5.45E-4	5.36E-4	5.43E-4	5.43E-4	4.27E-4	5.83E-4

	Y dmax [m]						
L [m]	**P01**	**P02**	**P03**	**P04**	**P05**	**P06**	**P07**
0.5	0.285	0.250	0.290	0.292	0.286	0.312	0.290
2	1.137	1.000	1.140	1.000	1.141	1.172	1.160
10	5.468	5.000	5.500	5.000	5.463	5.000	5.620
20	10.312	10.000	10.200	10.000	10.143	10.000	10.000
40	18.107	20.000	16.800	25.000	16.947	15.000	20.000

RIGID FOUNDATION

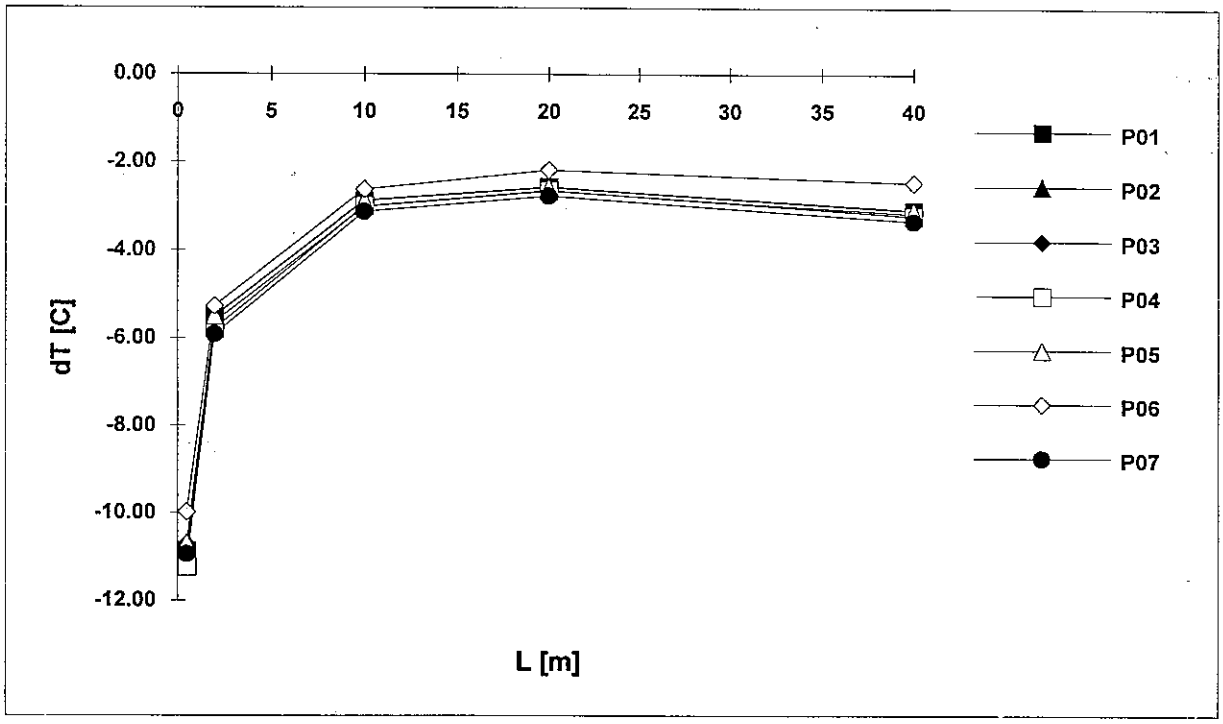

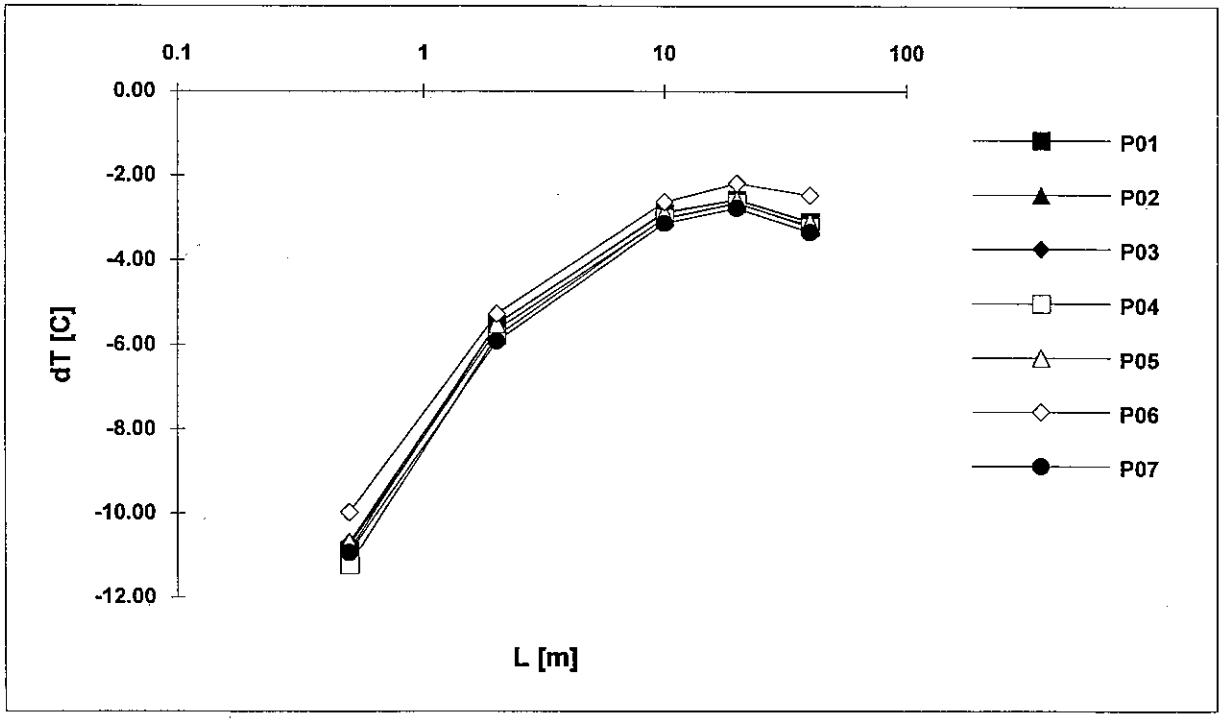

RIGID FOUNDATION

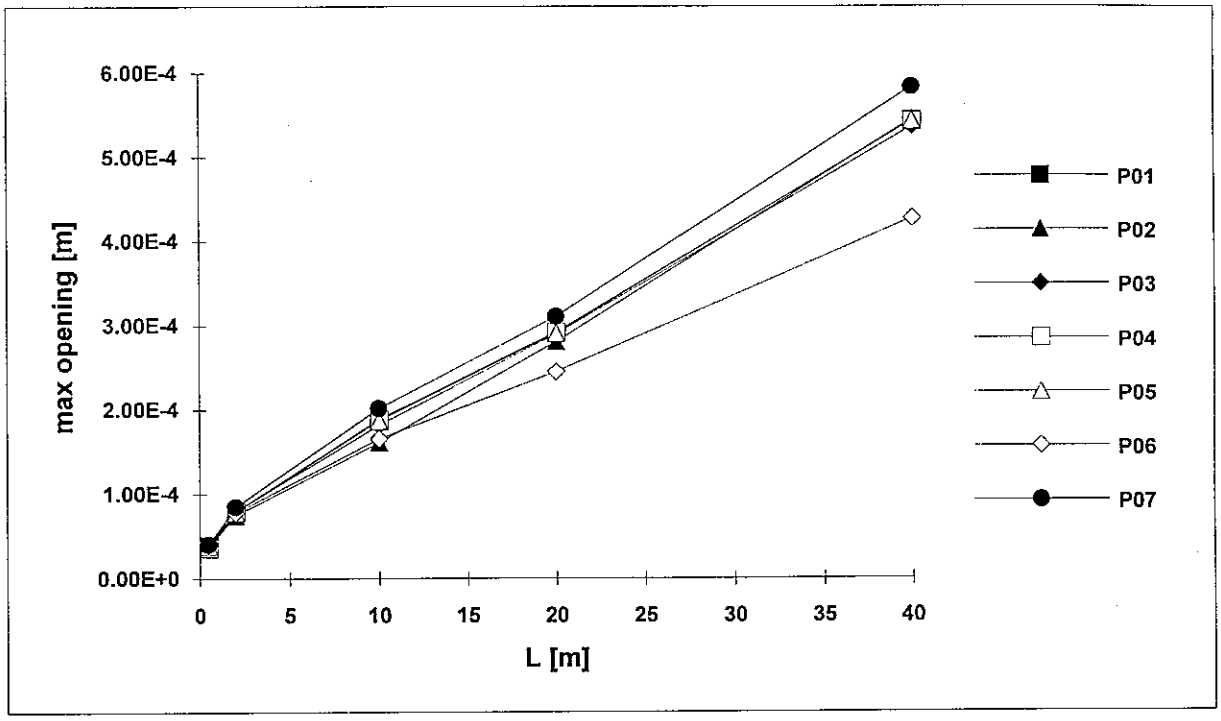

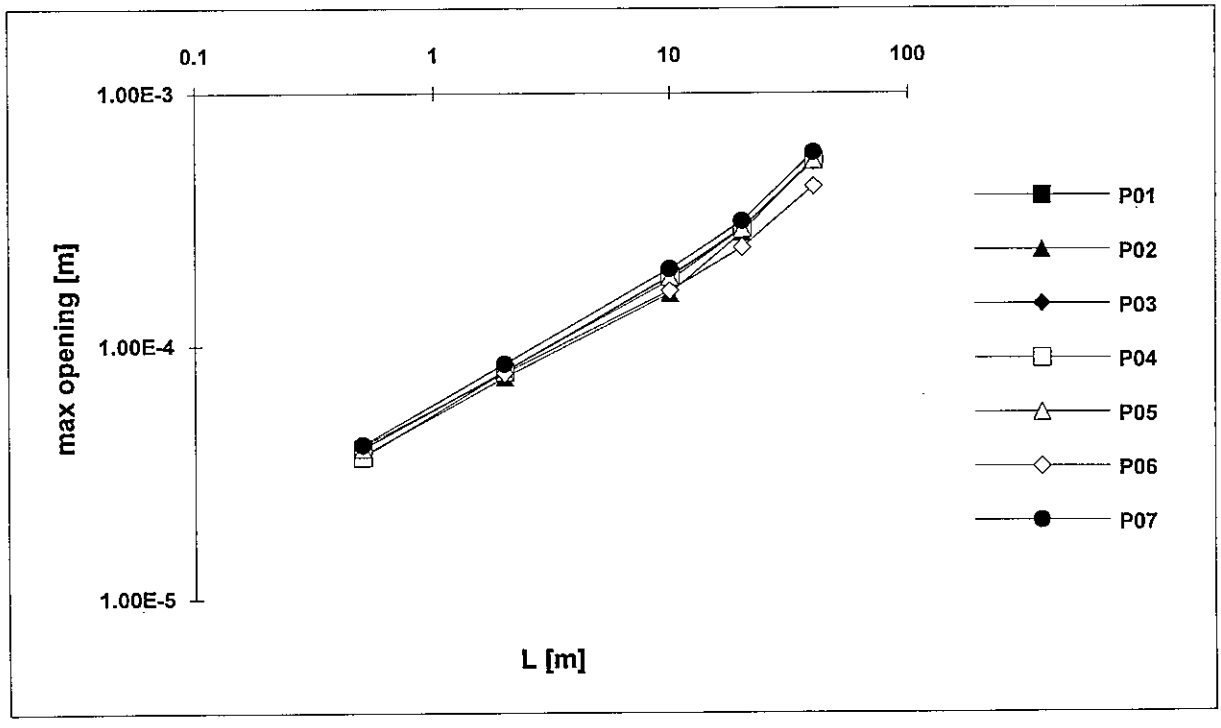

RIGID FOUNDATION

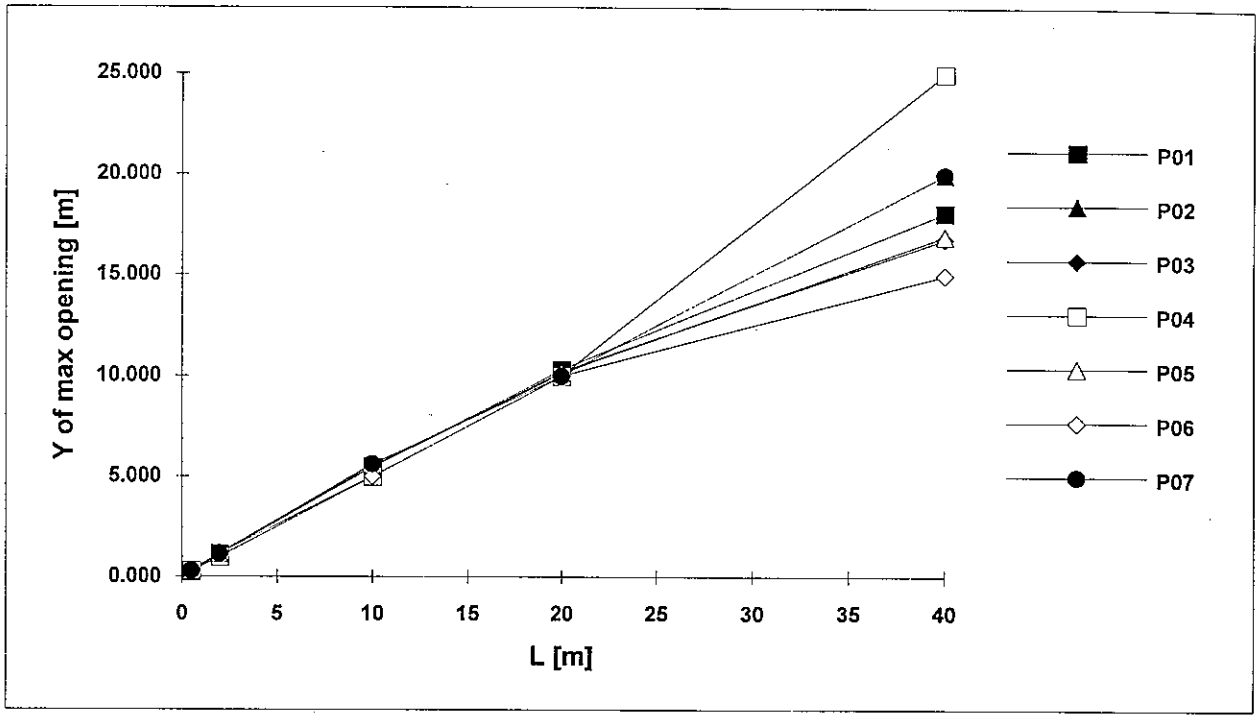

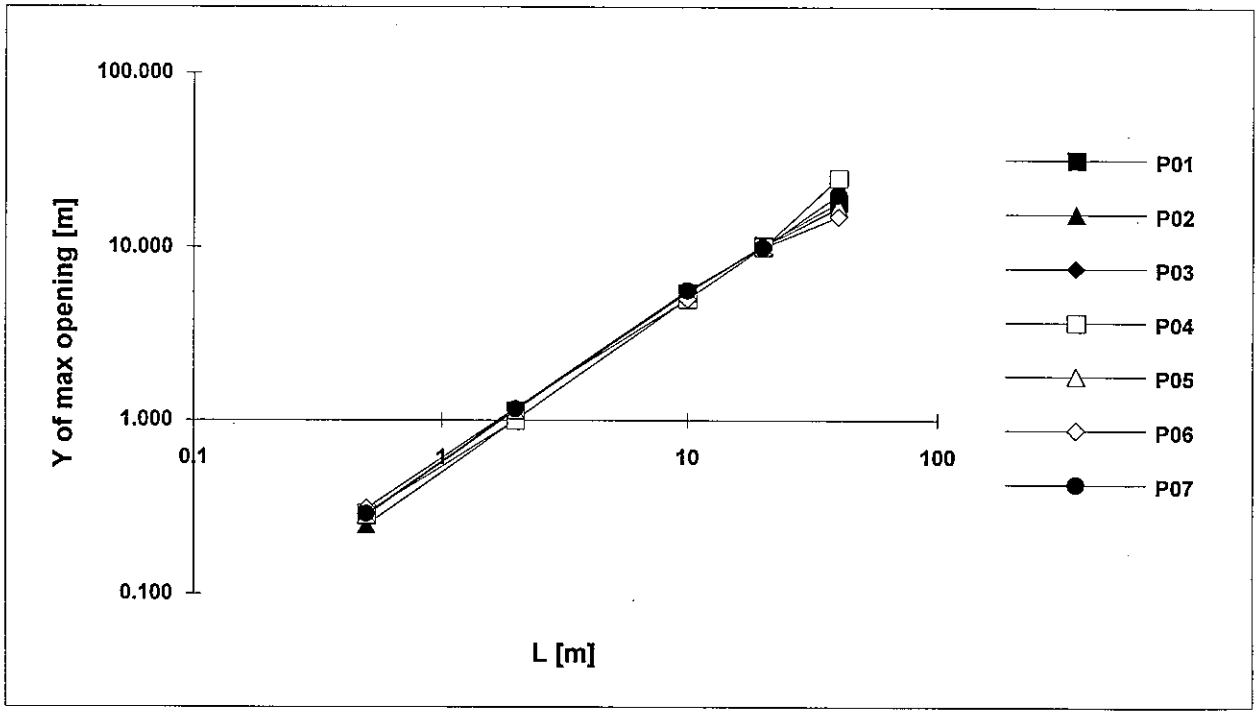

RIGID FOUNDATION

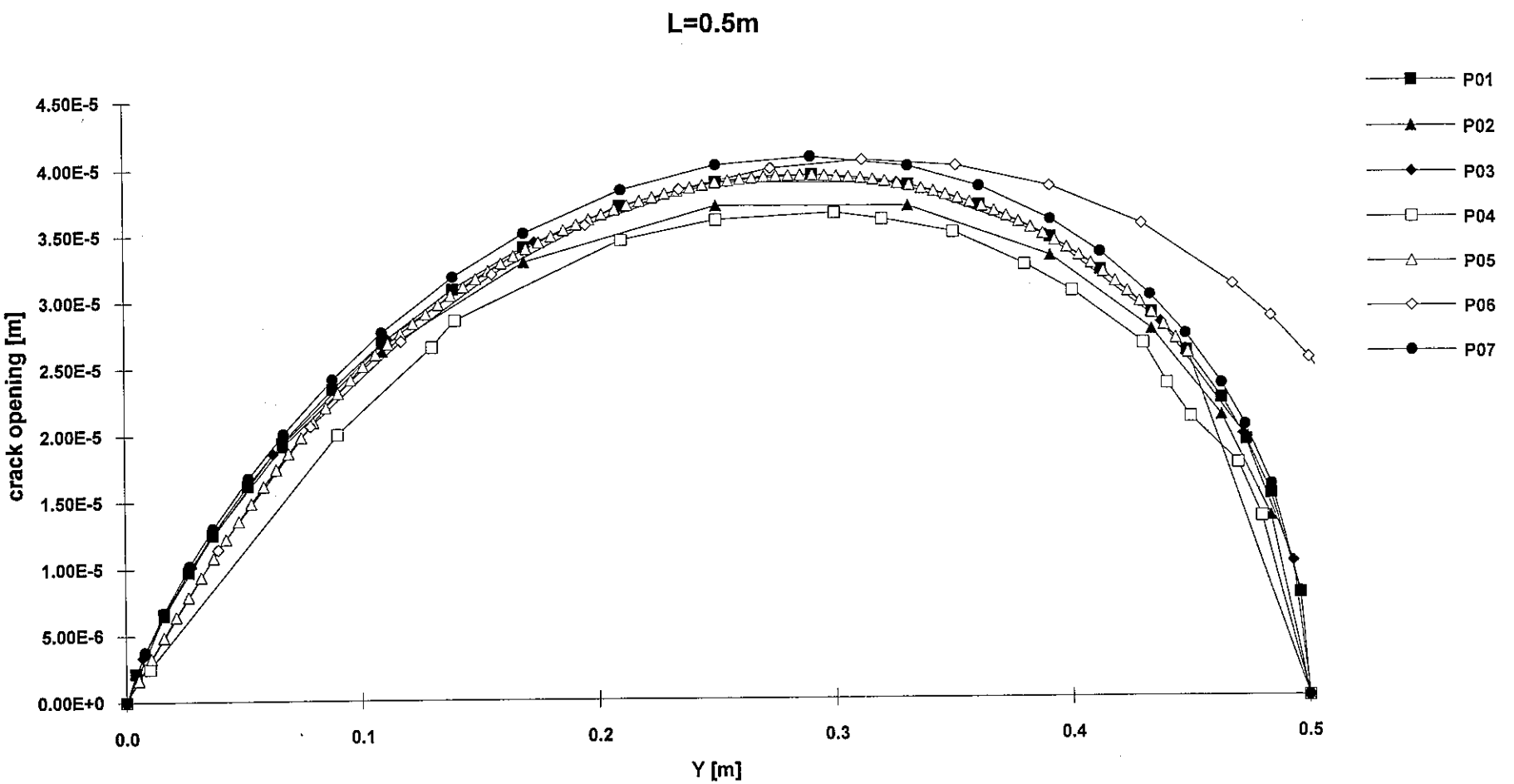

RIGID FOUNDATION

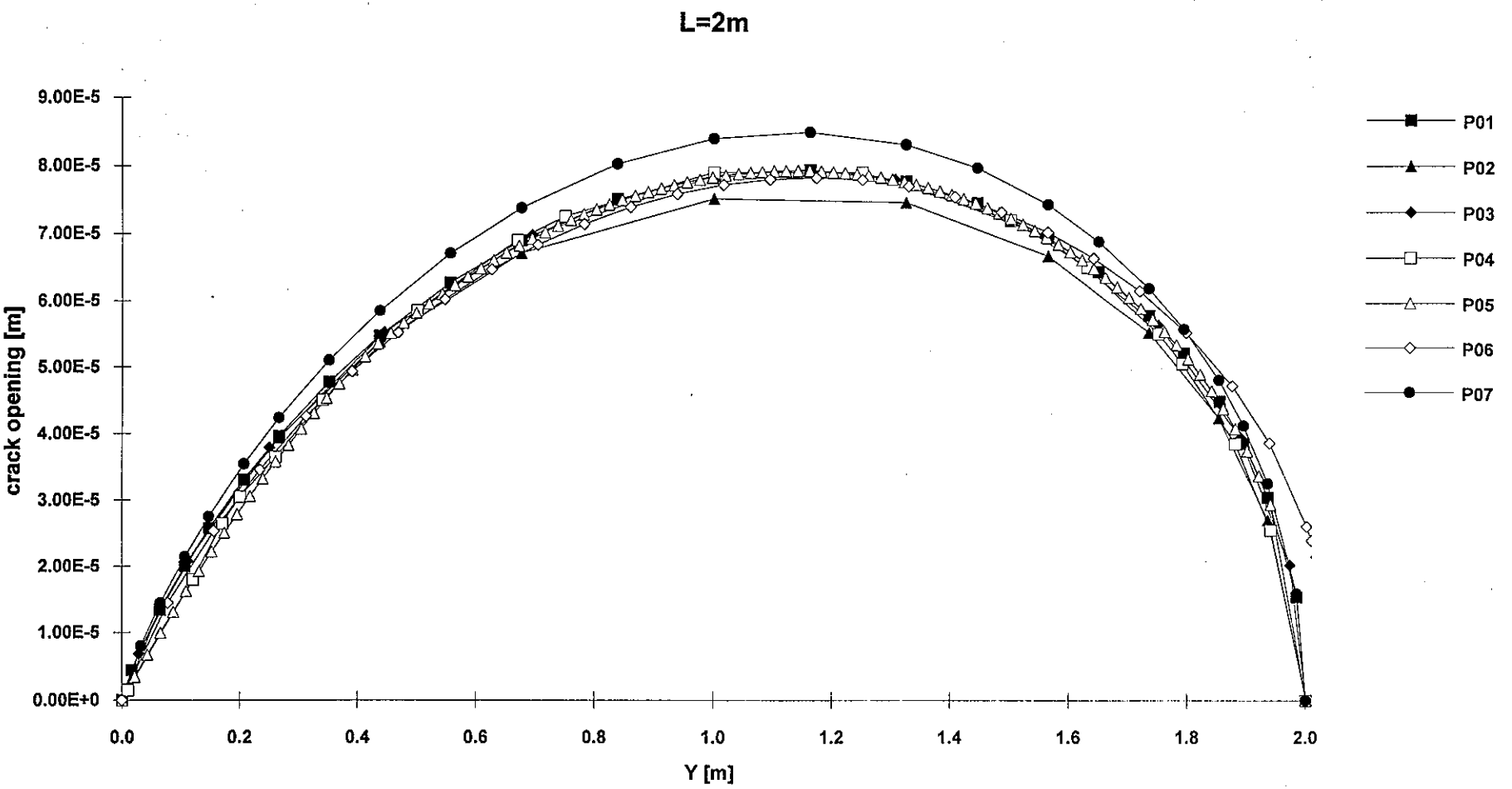

RIGID FOUNDATION

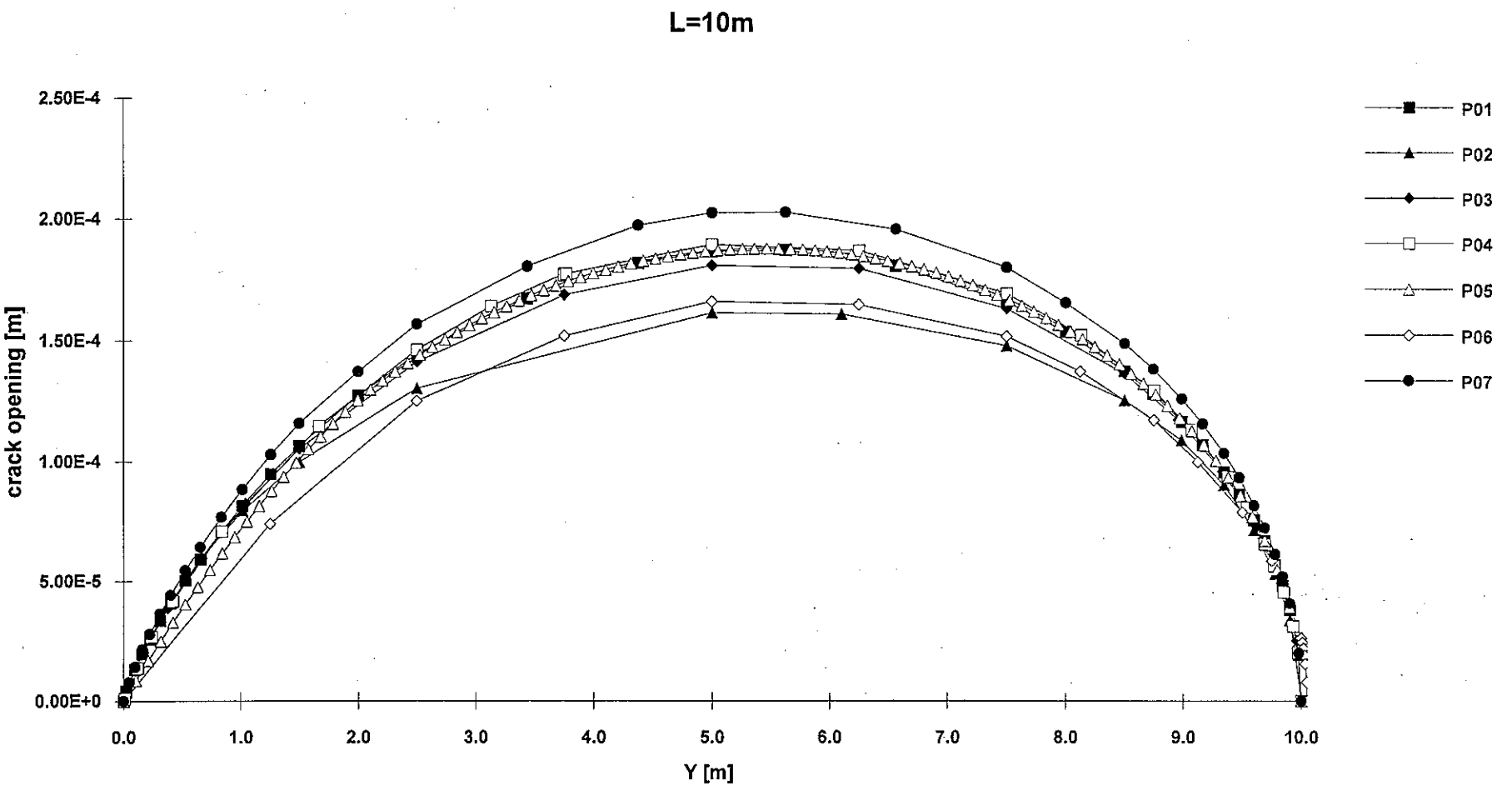

RIGID FOUNDATION

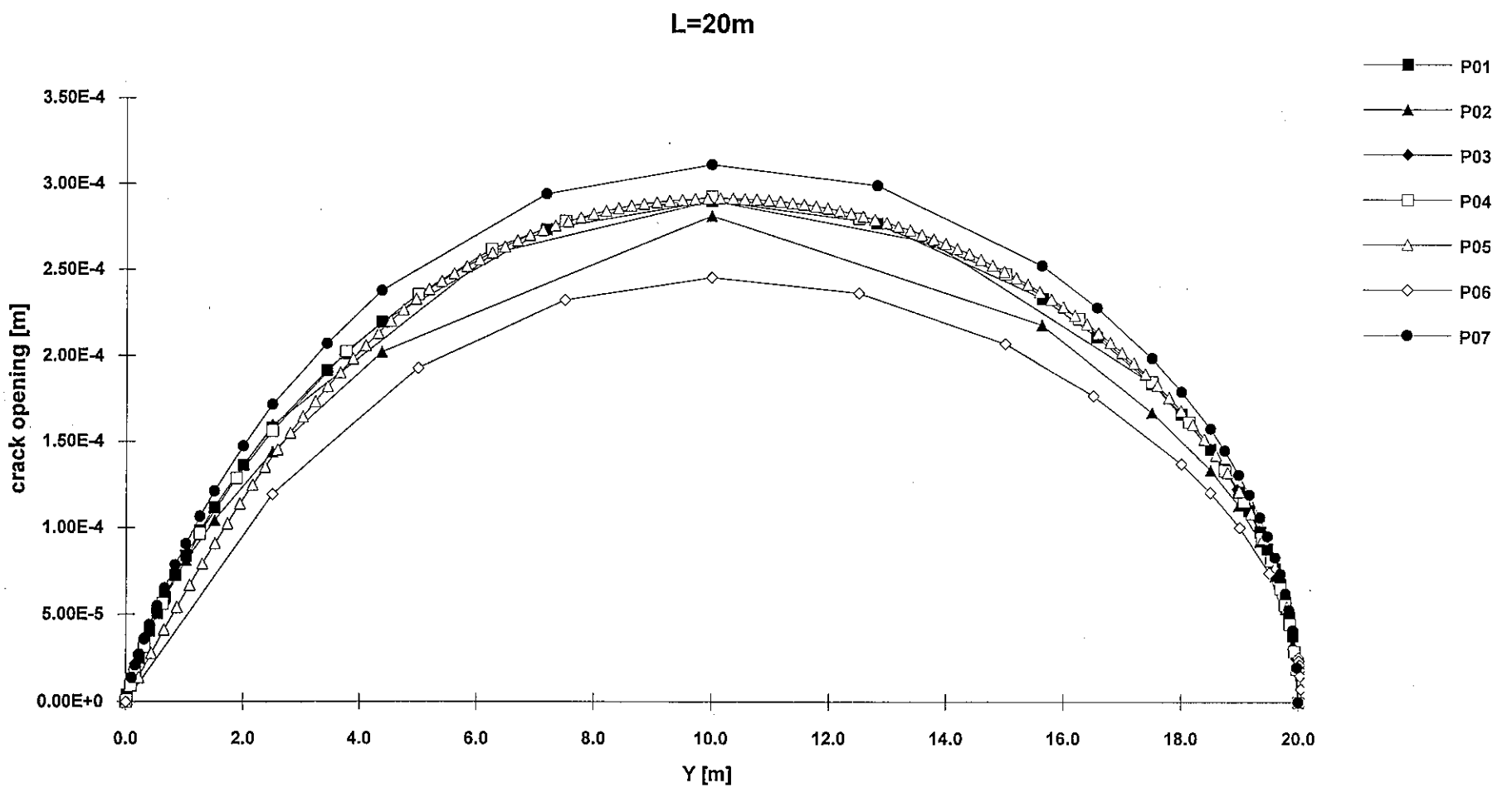

RIGID FOUNDATION

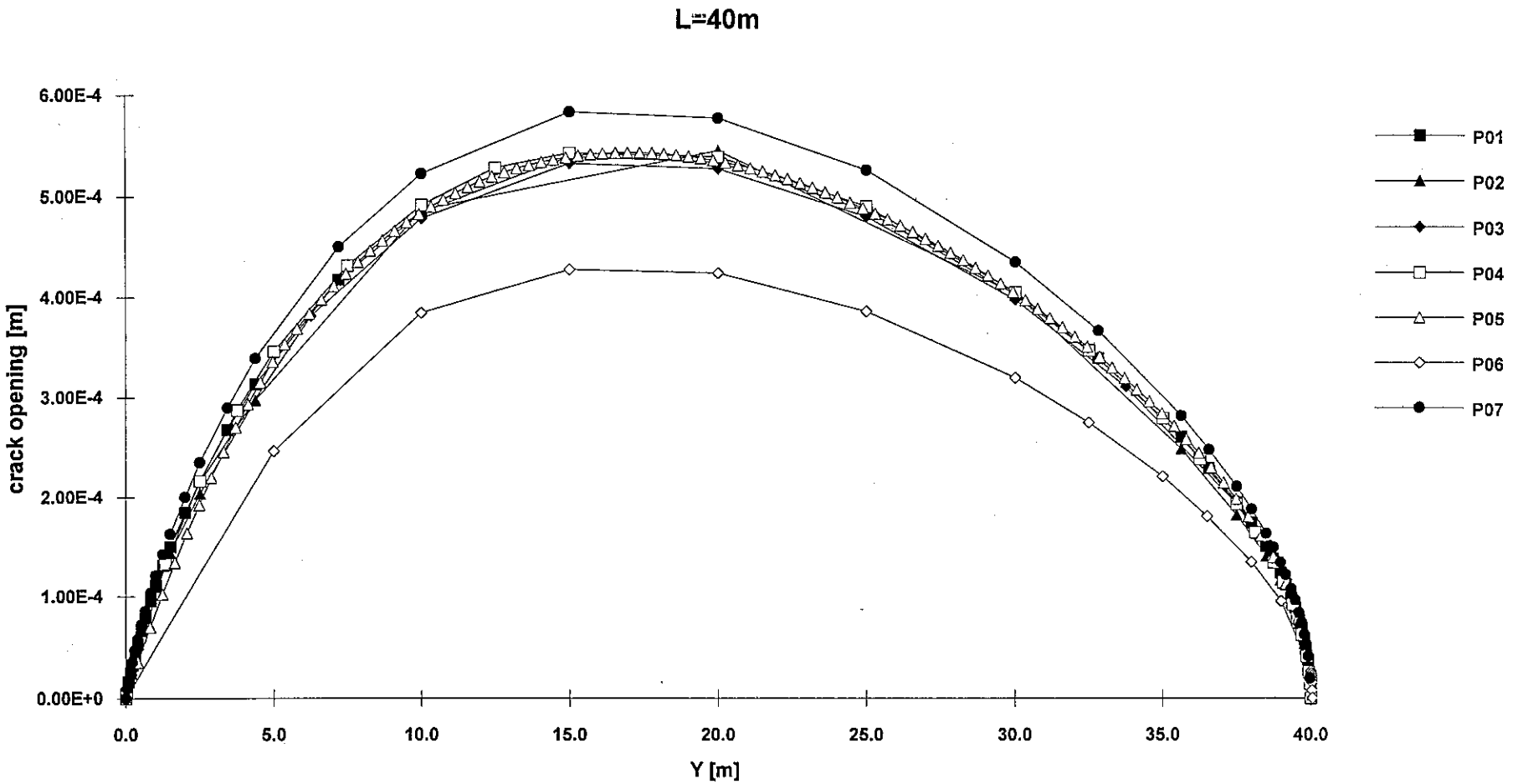

RIGID FOUNDATION

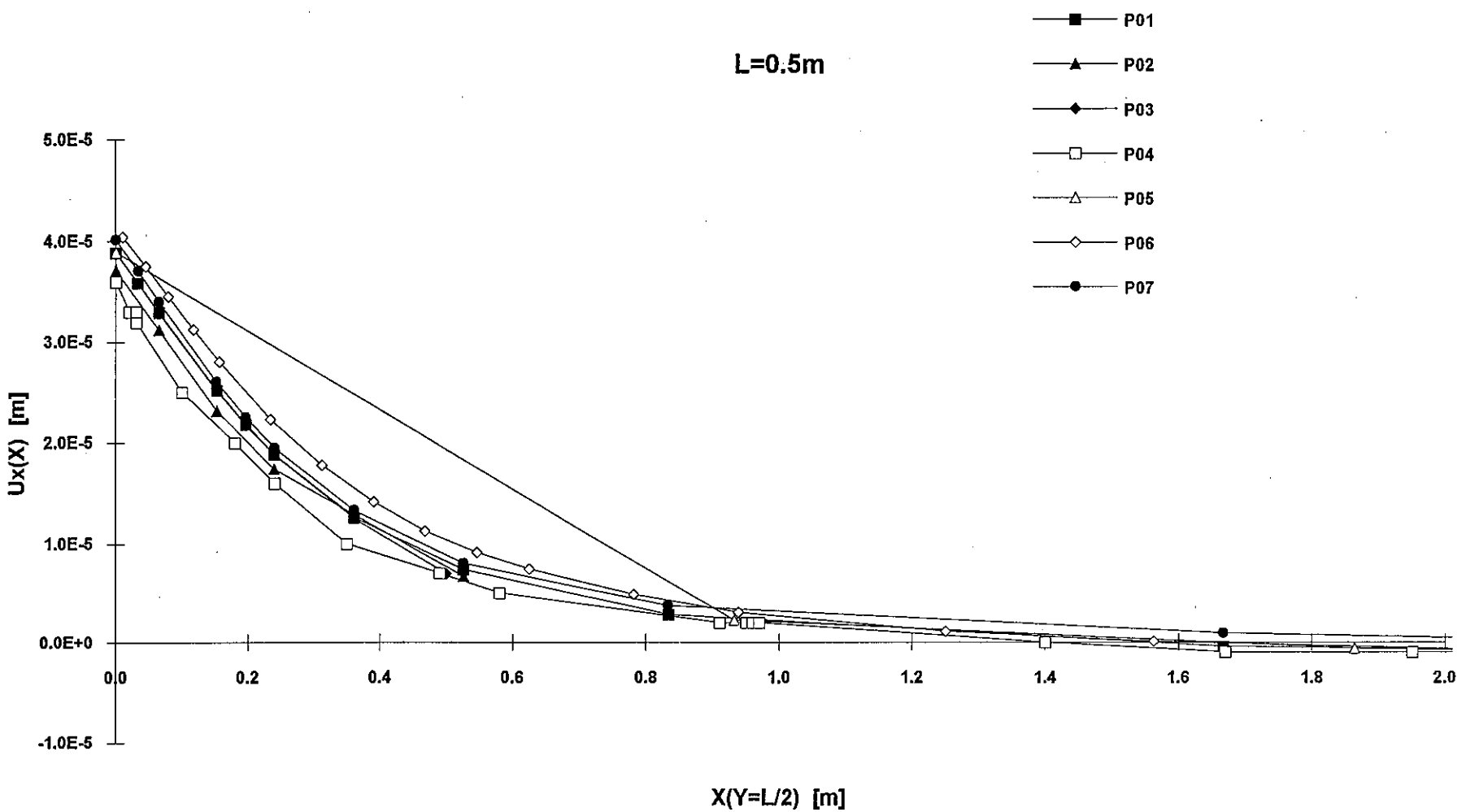

RIGID FOUNDATION

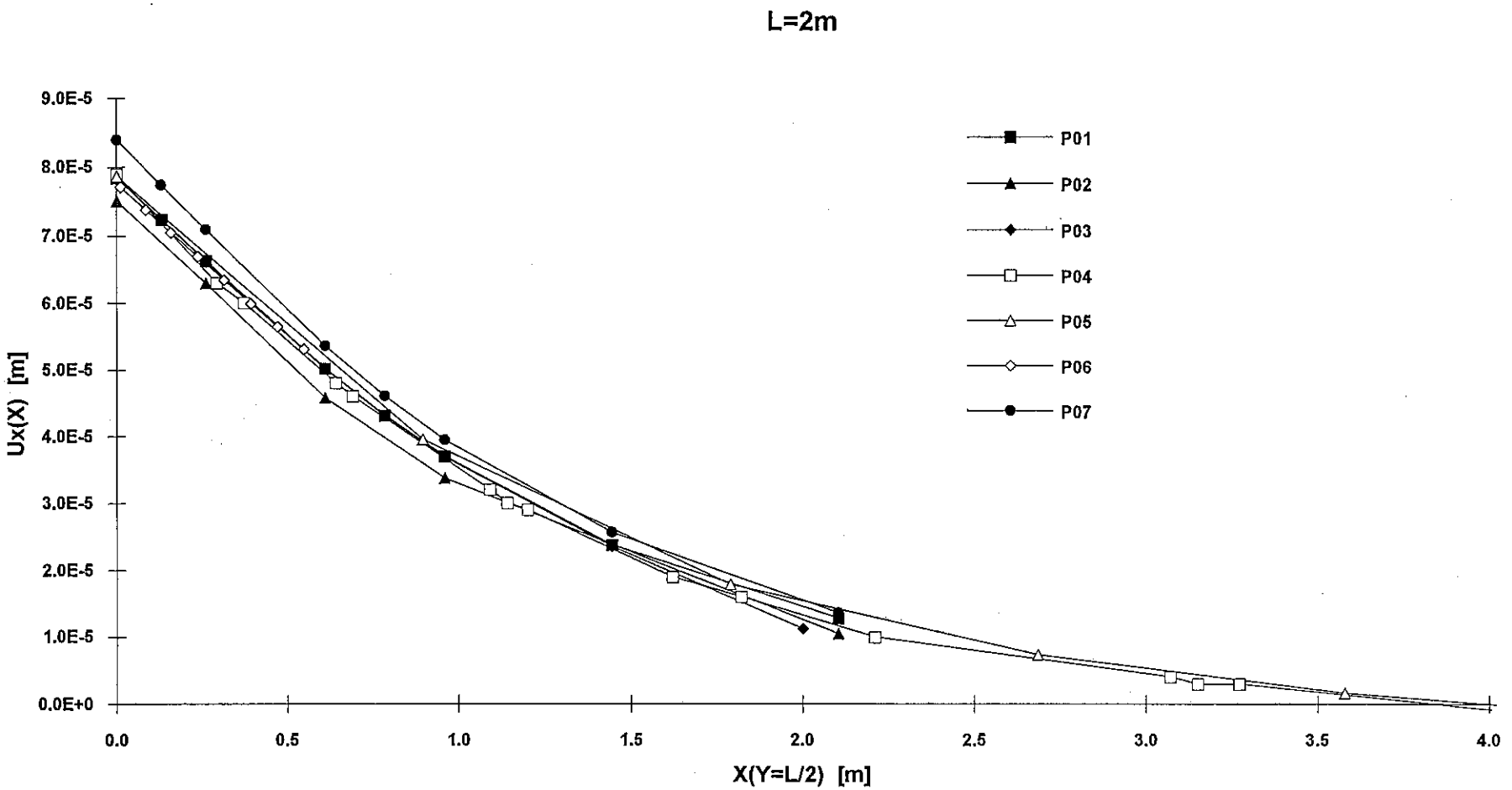

RIGID FOUNDATION

L=10m

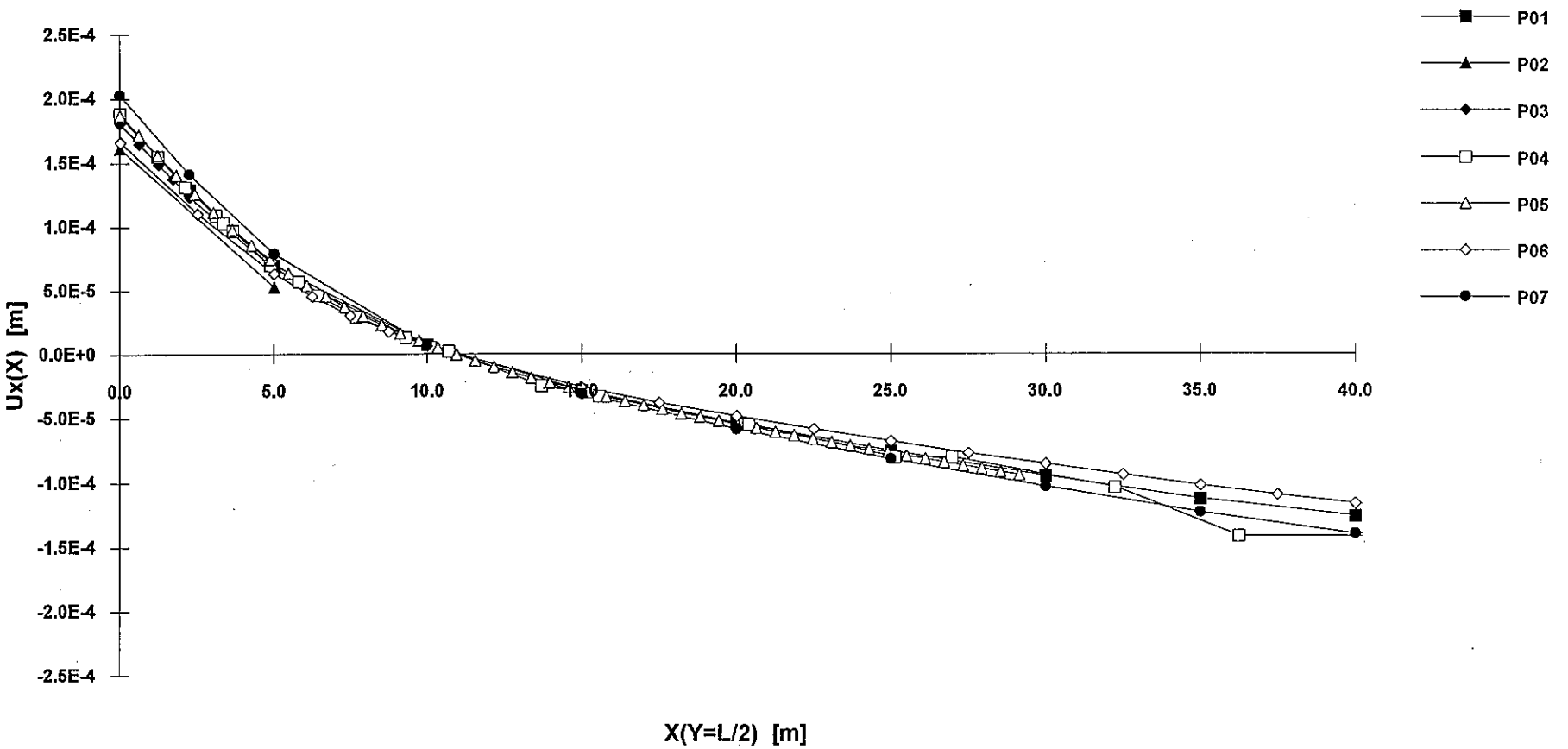

RIGID FOUNDATION

L=20m

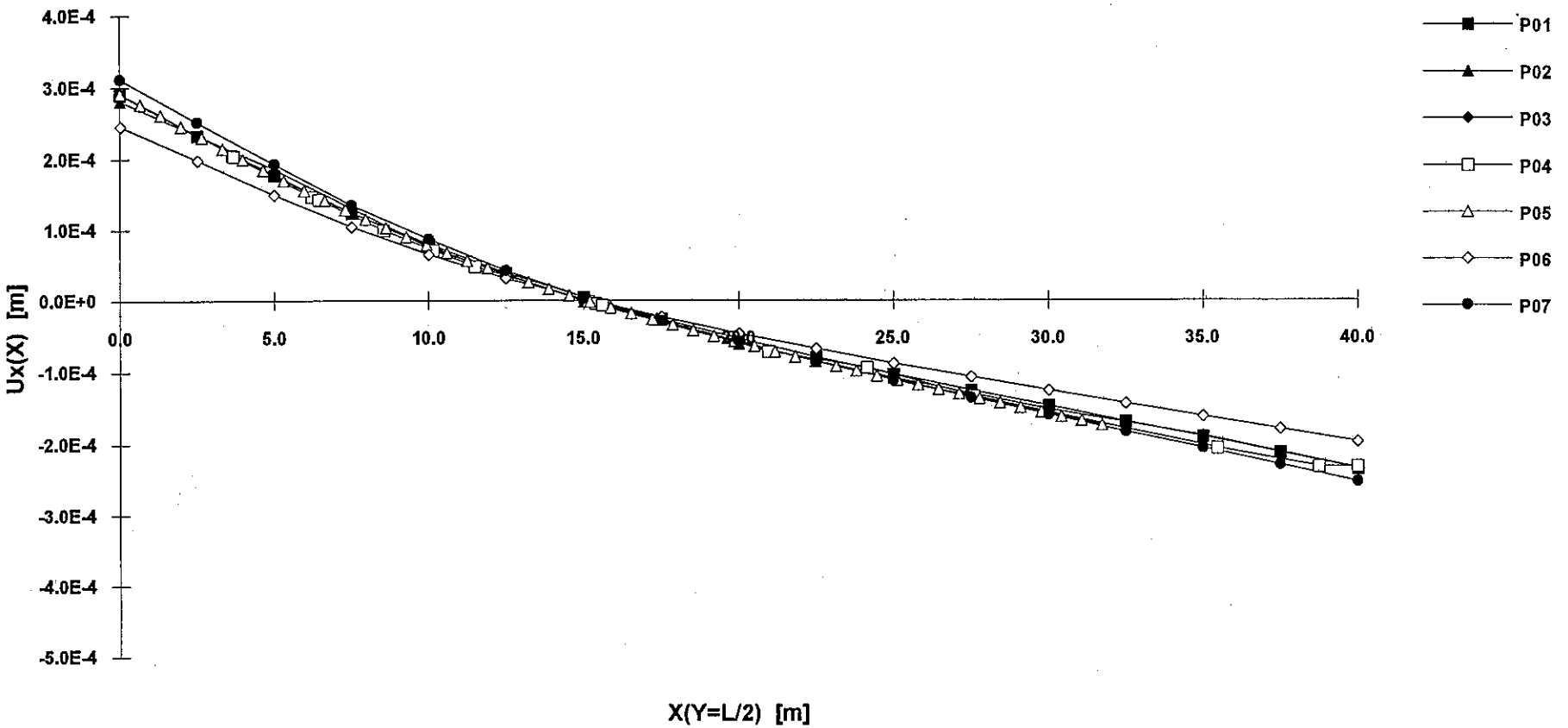

RIGID FOUNDATION

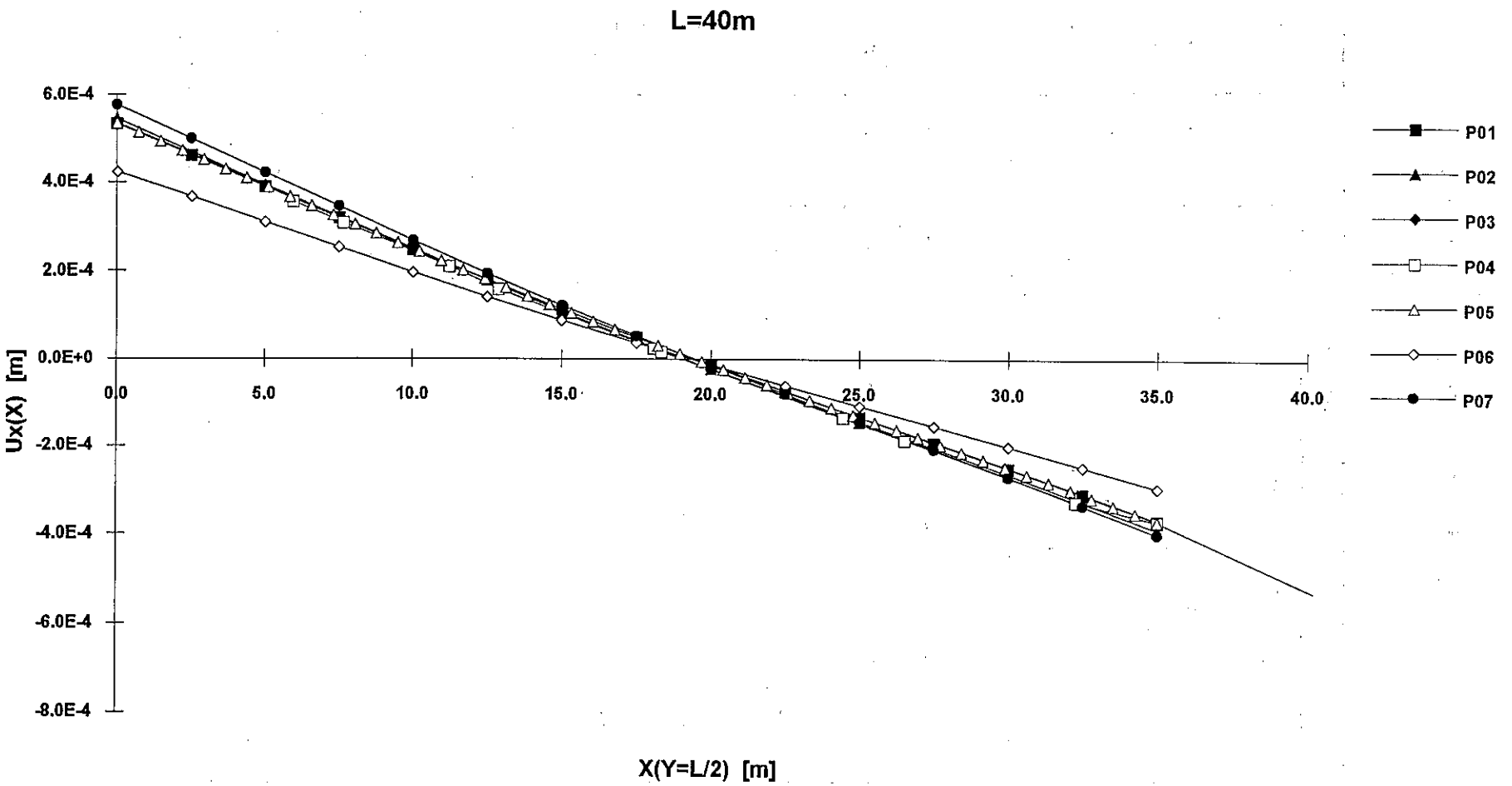

FLEXIBLE FOUNDATION

	dT [C]						
L [m]	**P01**	**P02**	**P03**	**P04**	**P05**	**P06**	**P07**
0.5	-17.19	-21.39	-16.51	-11.90	-17.50	-16.16	-17.39
2	-8.92	-11.34	-8.50	-6.42	-9.07	-8.71	-9.59
10	-4.84	-6.25	-4.75	-3.59	-4.94	-4.45	-5.25
20	-4.49	-5.80	-4.48	-3.26	-4.69	-3.92	-4.87
40	-5.77	-7.59	-5.73	-6.62	-6.10	-4.89	-6.28

	dmax [m]						
L [m]	**P01**	**P02**	**P03**	**P04**	**P05**	**P06**	**P07**
0.5	4.45E-5	4.39E-5	4.47E-5	4.10E-5	4.37E-5	4.43E-5	4.59E-5
2	9.00E-5	8.87E-5	9.08E-5	9.10E-5	8.85E-5	8.62E-5	9.62E-5
10	2.18E-4	2.07E-4	2.13E-4	2.21E-4	2.11E-4	1.89E-4	2.36E-4
20	3.42E-4	3.52E-4	3.49E-4	3.49E-4	3.48E-4	2.88E-4	3.79E-4
40	7.04E-4	8.03E-4	6.52E-4	1.12E-3	7.15E-4	5.66E-4	7.67E-4

	Y dmax [m]						
L [m]	**P01**	**P02**	**P03**	**P04**	**P05**	**P06**	**P07**
0.5	0.241	0.250	0.235	0.250	0.250	0.276	0.250
2	0.952	1.000	0.920	1.000	0.976	1.017	1.000
10	4.461	4.375	4.200	3.750	4.524	5.005	4.380
20	8.176	10.000	7.800	7.500	8.201	7.504	7.190
40	13.534	10.000	12.000	22.500	12.814	15.002	15.000

FLEXIBLE FOUNDATION

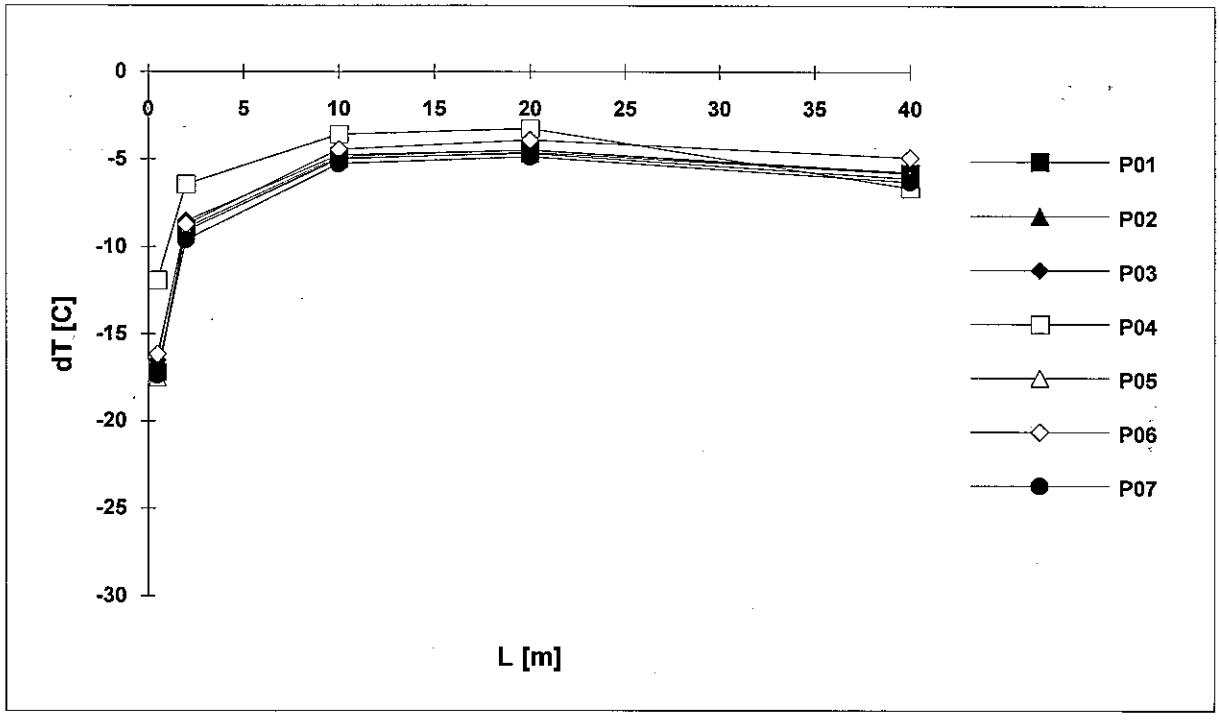

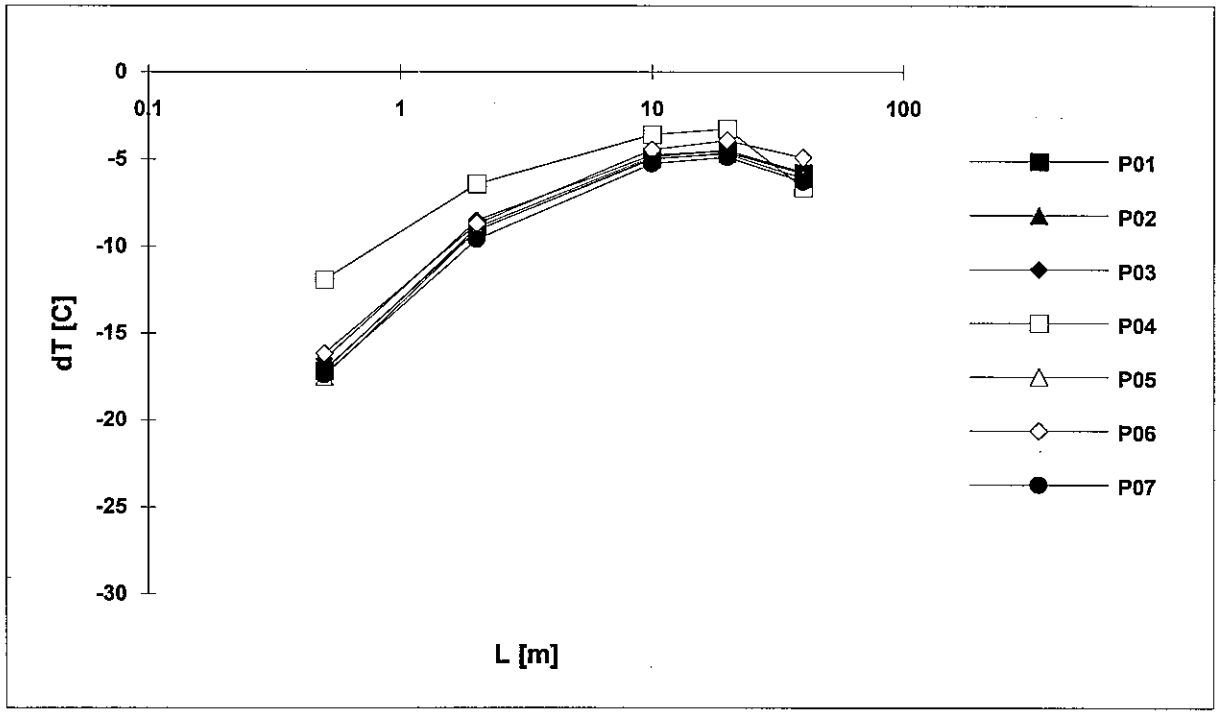

FLEXIBLE FOUNDATION

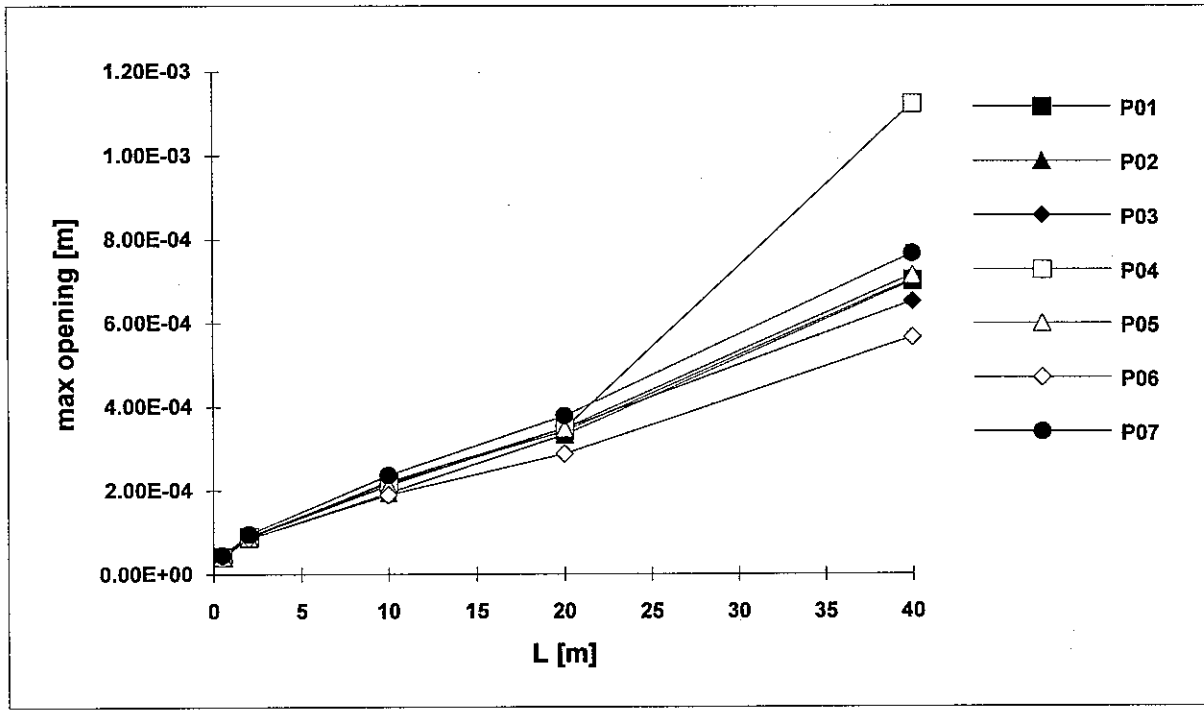

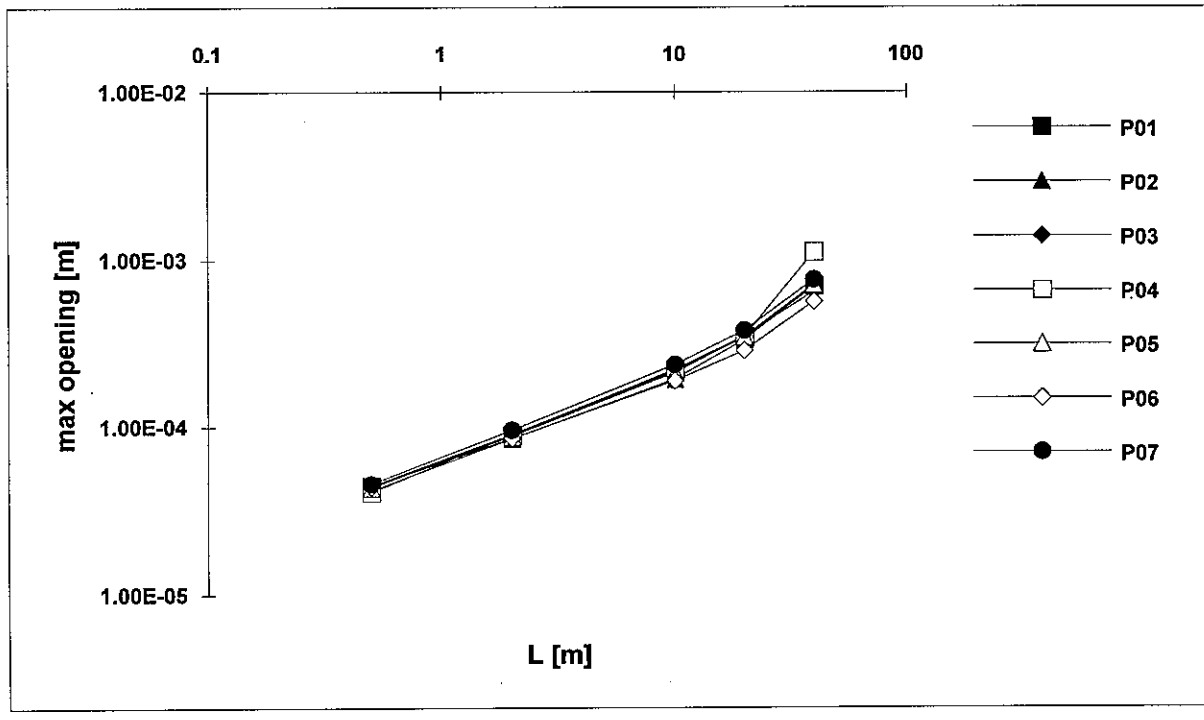

FLEXIBLE FOUNDATION

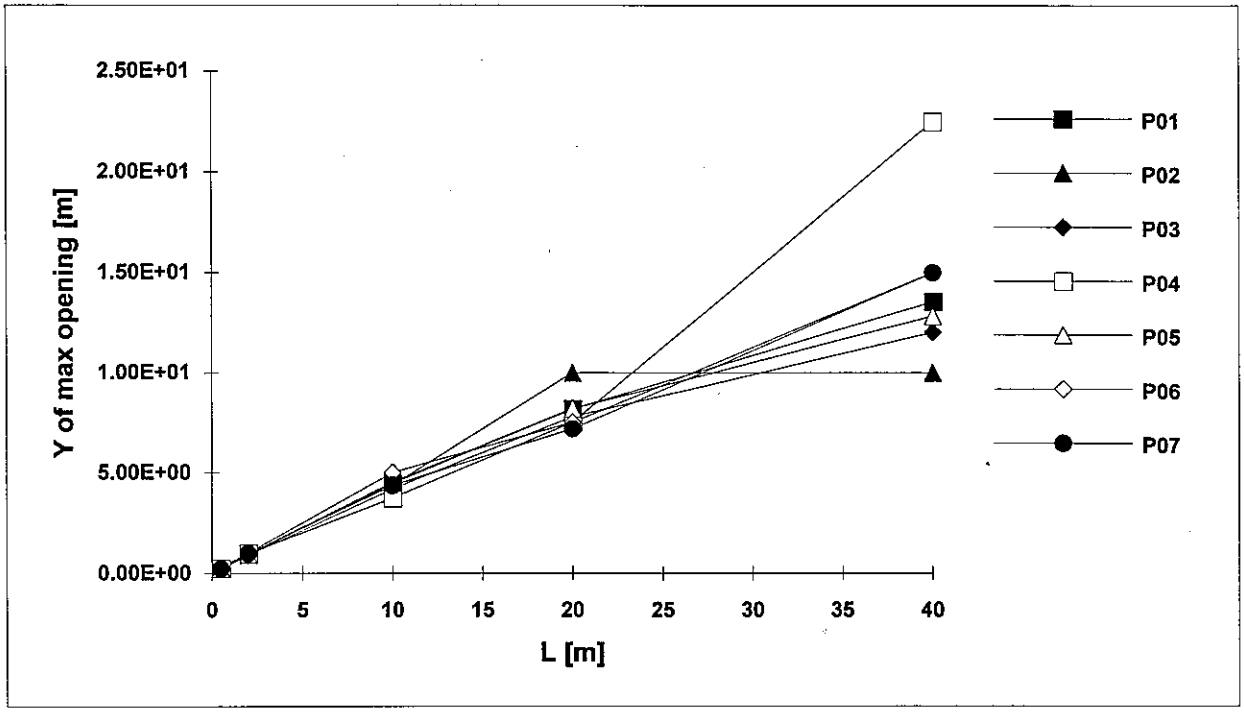

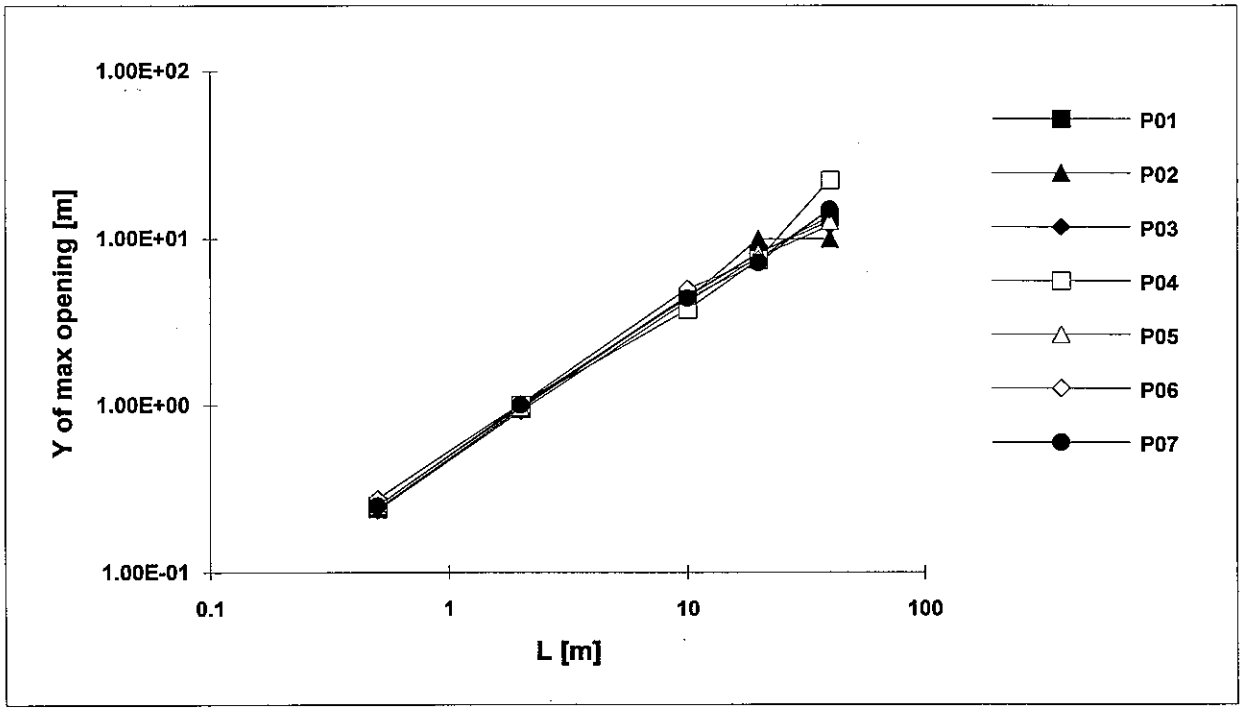

FLEXIBLE FOUNDATION

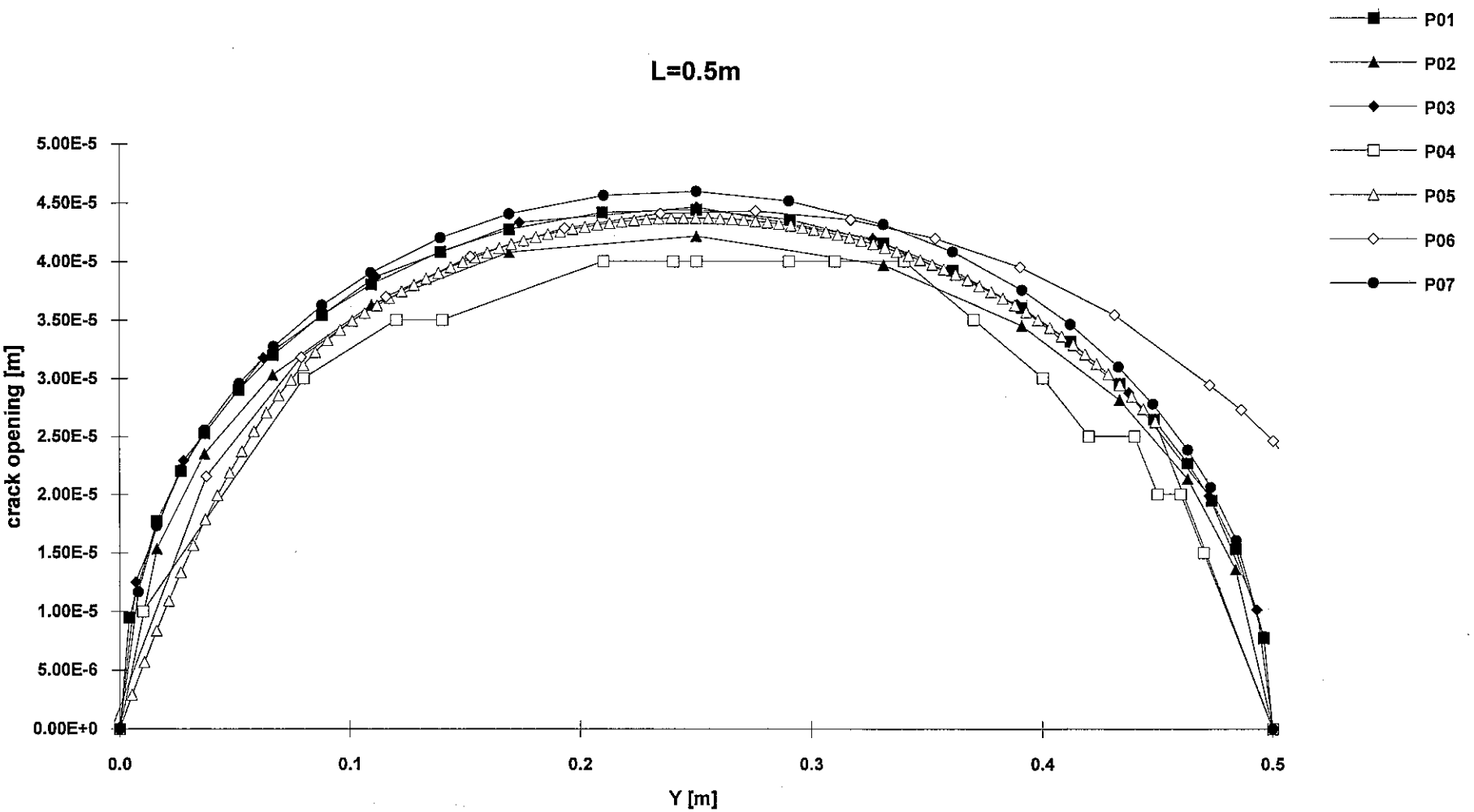

FLEXIBLE FOUNDATION

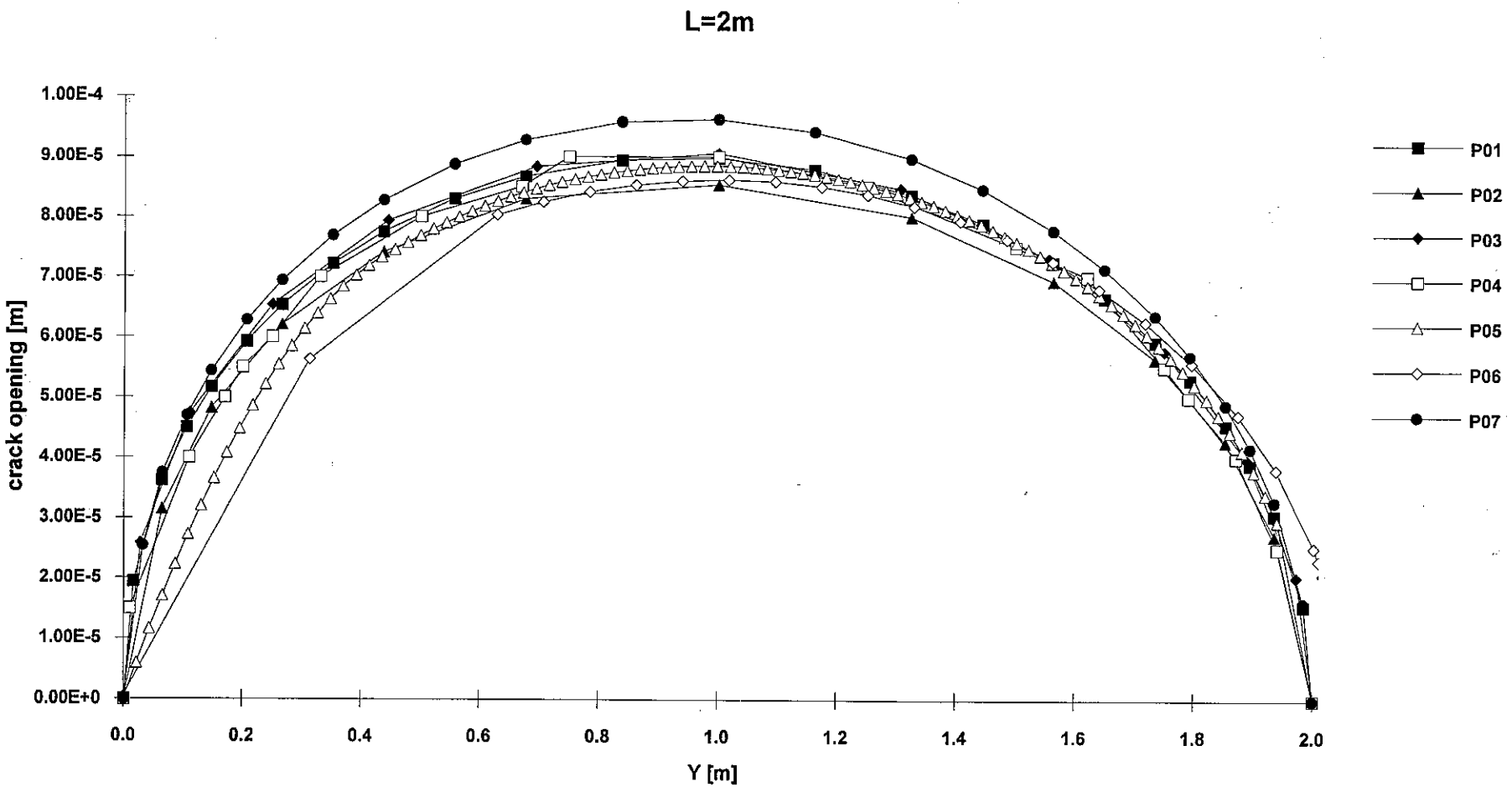

FLEXIBLE FOUNDATION

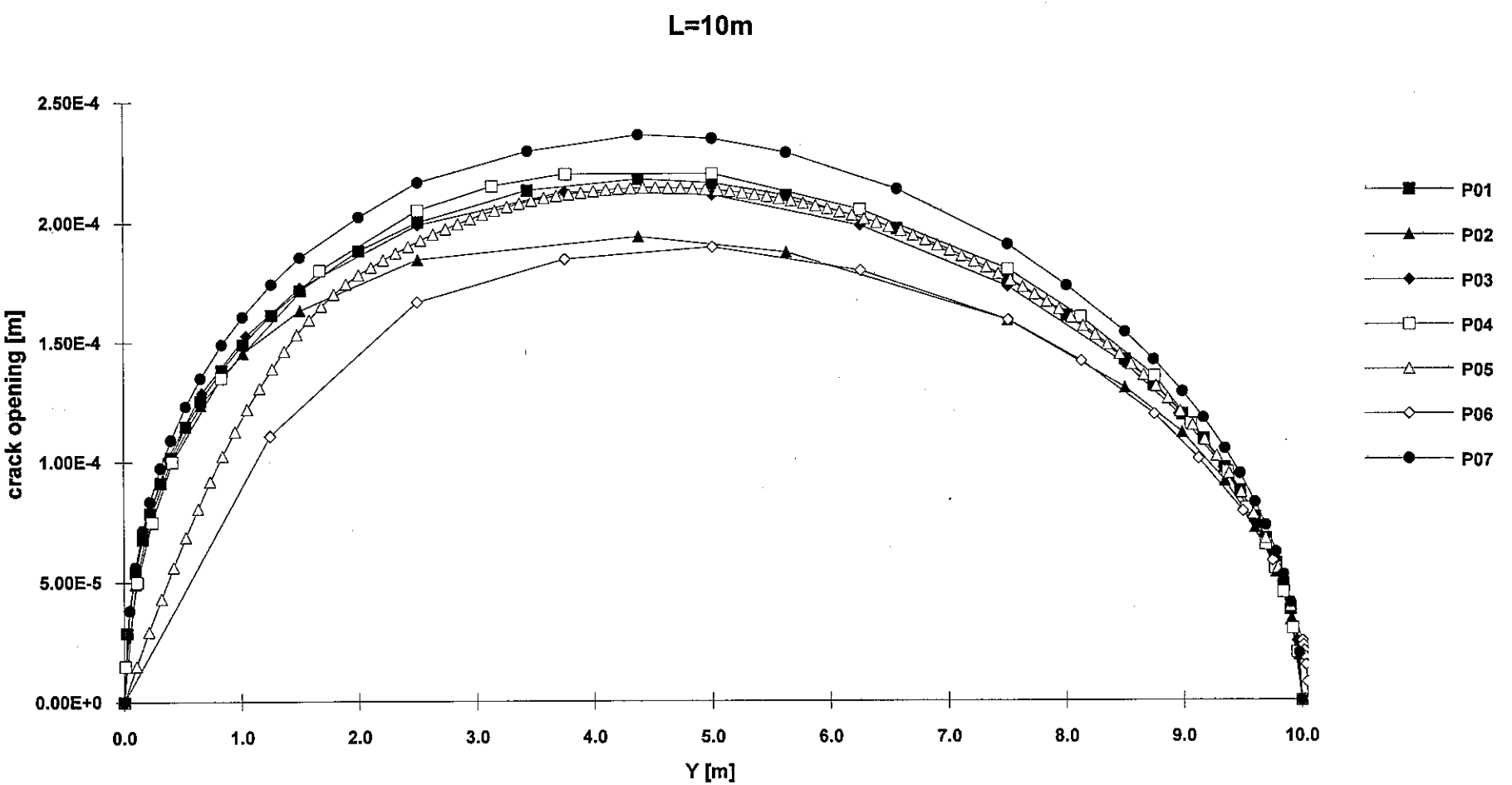

FLEXIBLE FOUNDATION

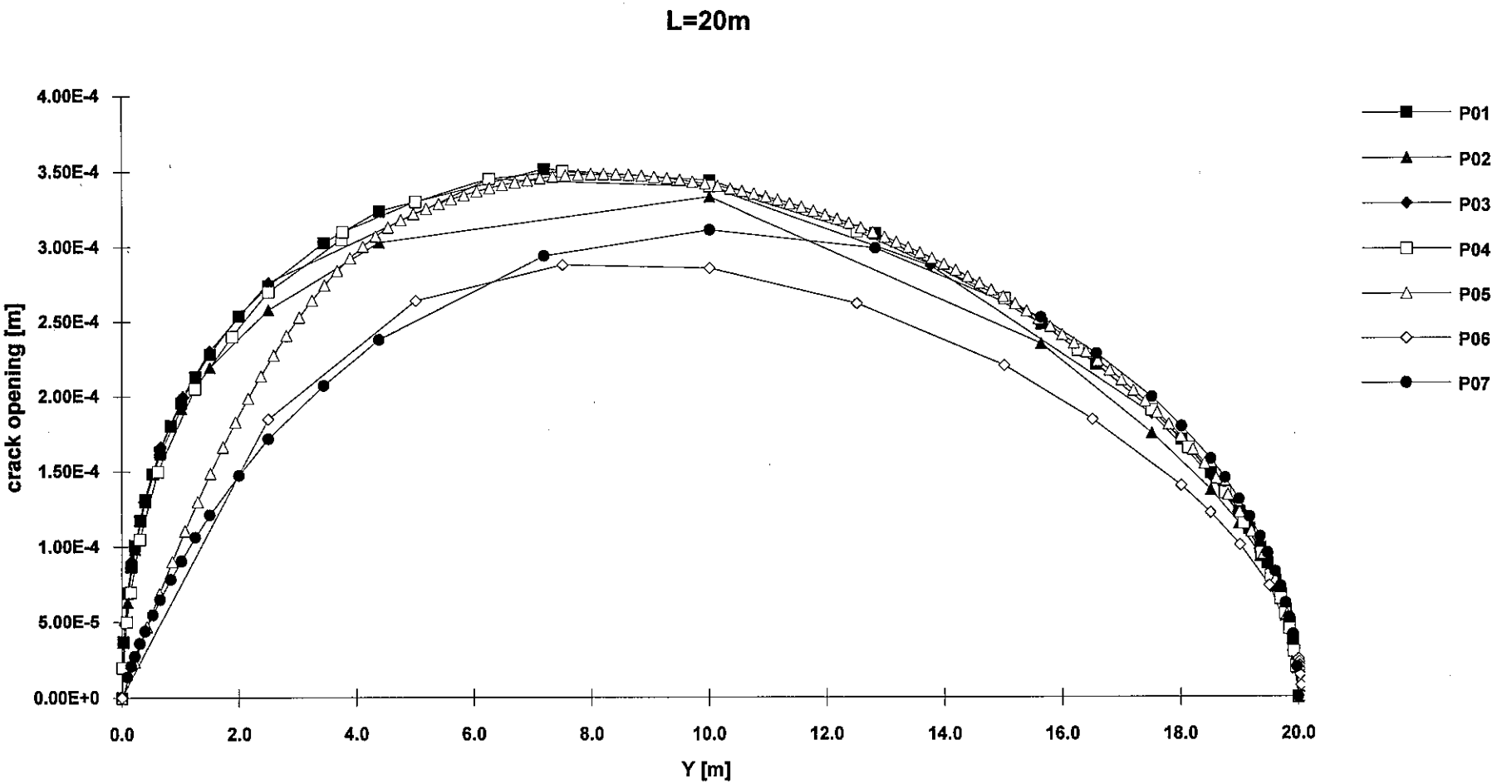

FLEXIBLE FOUNDATION

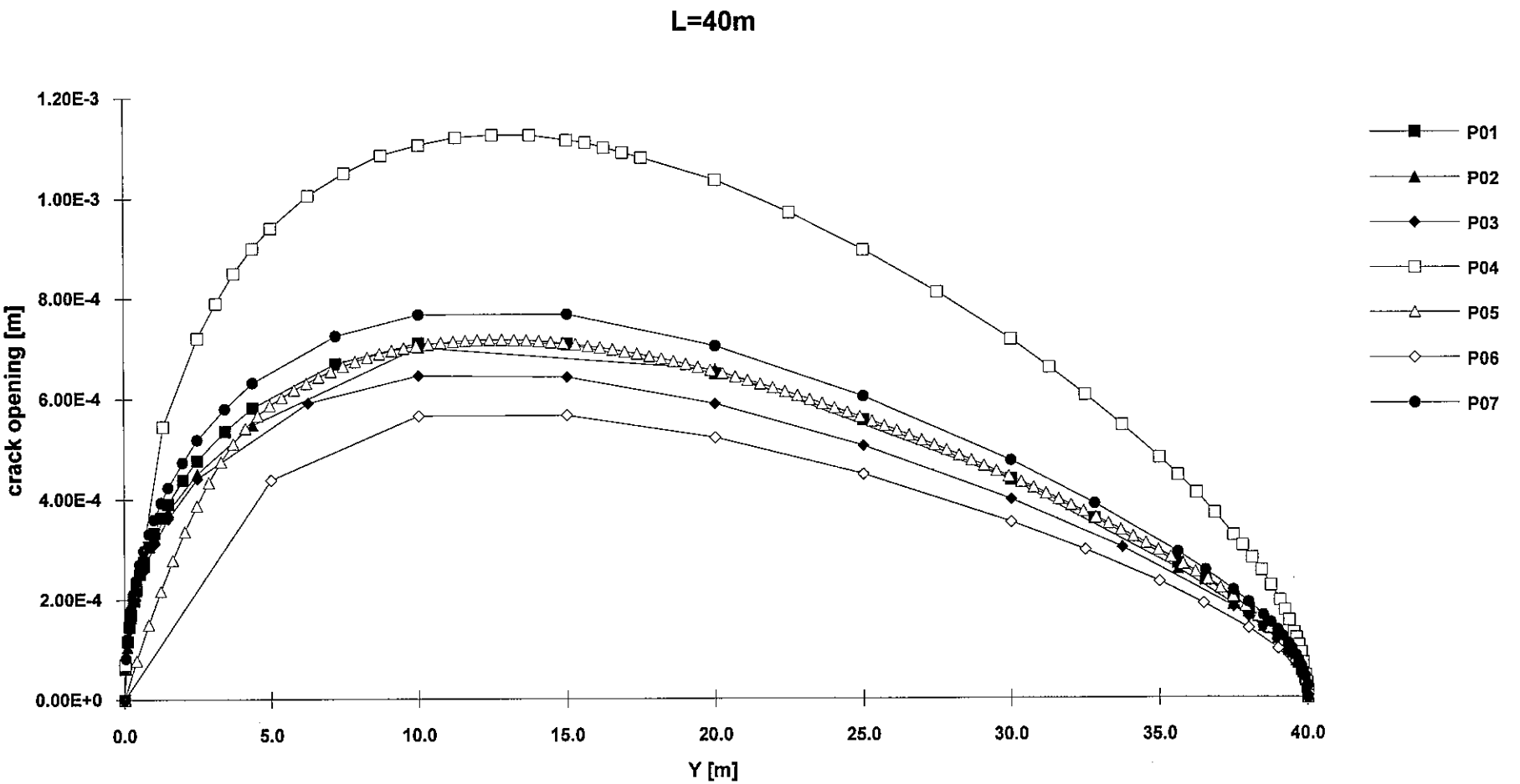

FLEXIBLE FOUNDATION

L=0.5m

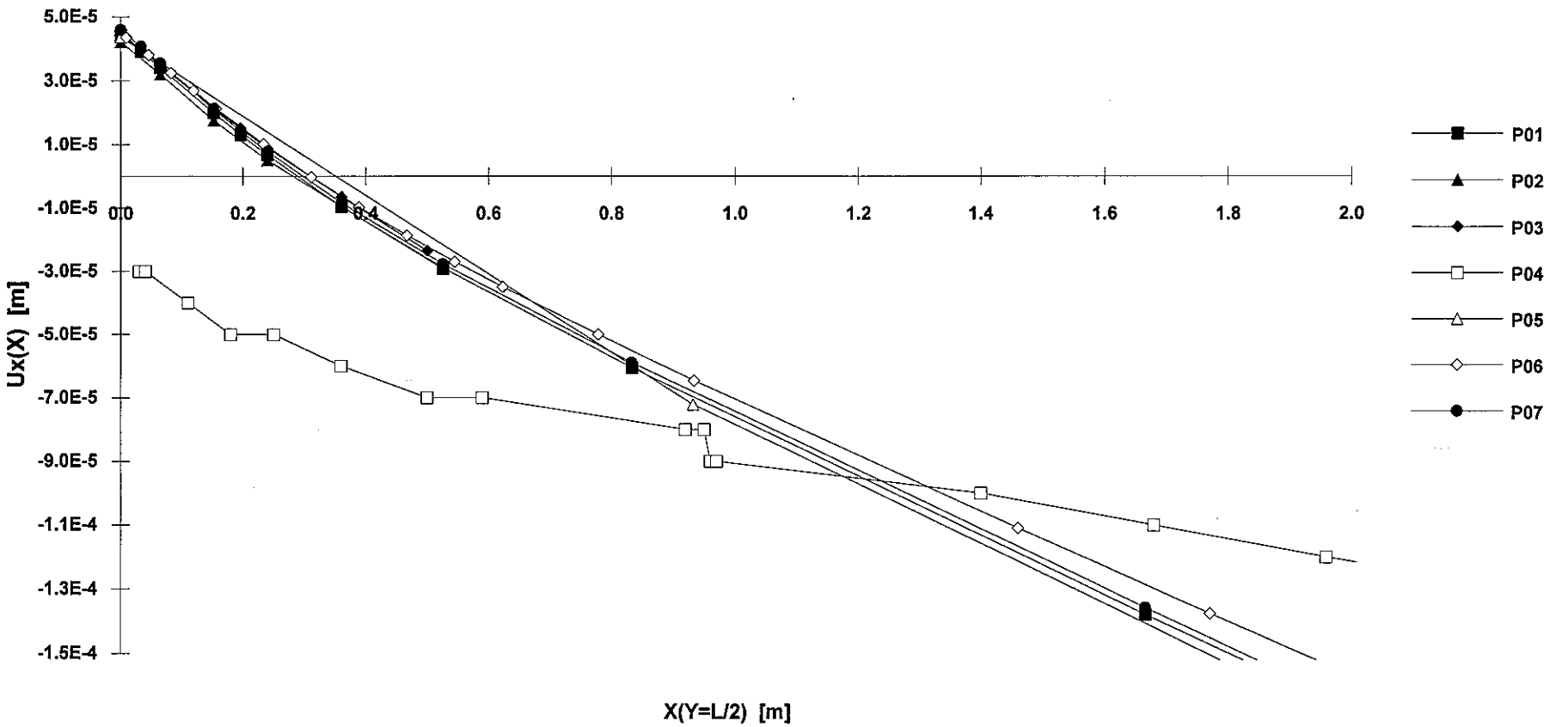

FLEXIBLE FOUNDATION

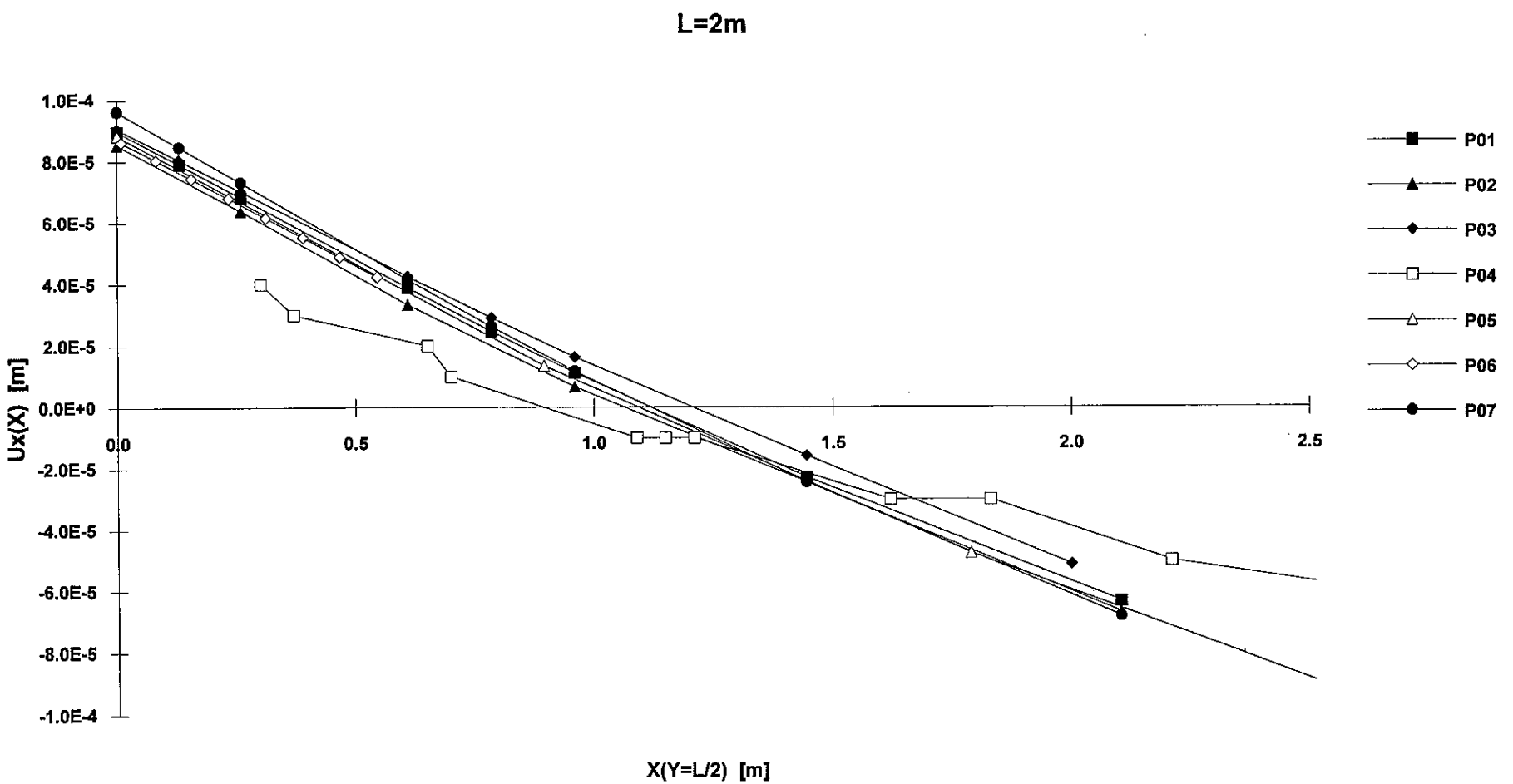

FLEXIBLE FOUNDATION

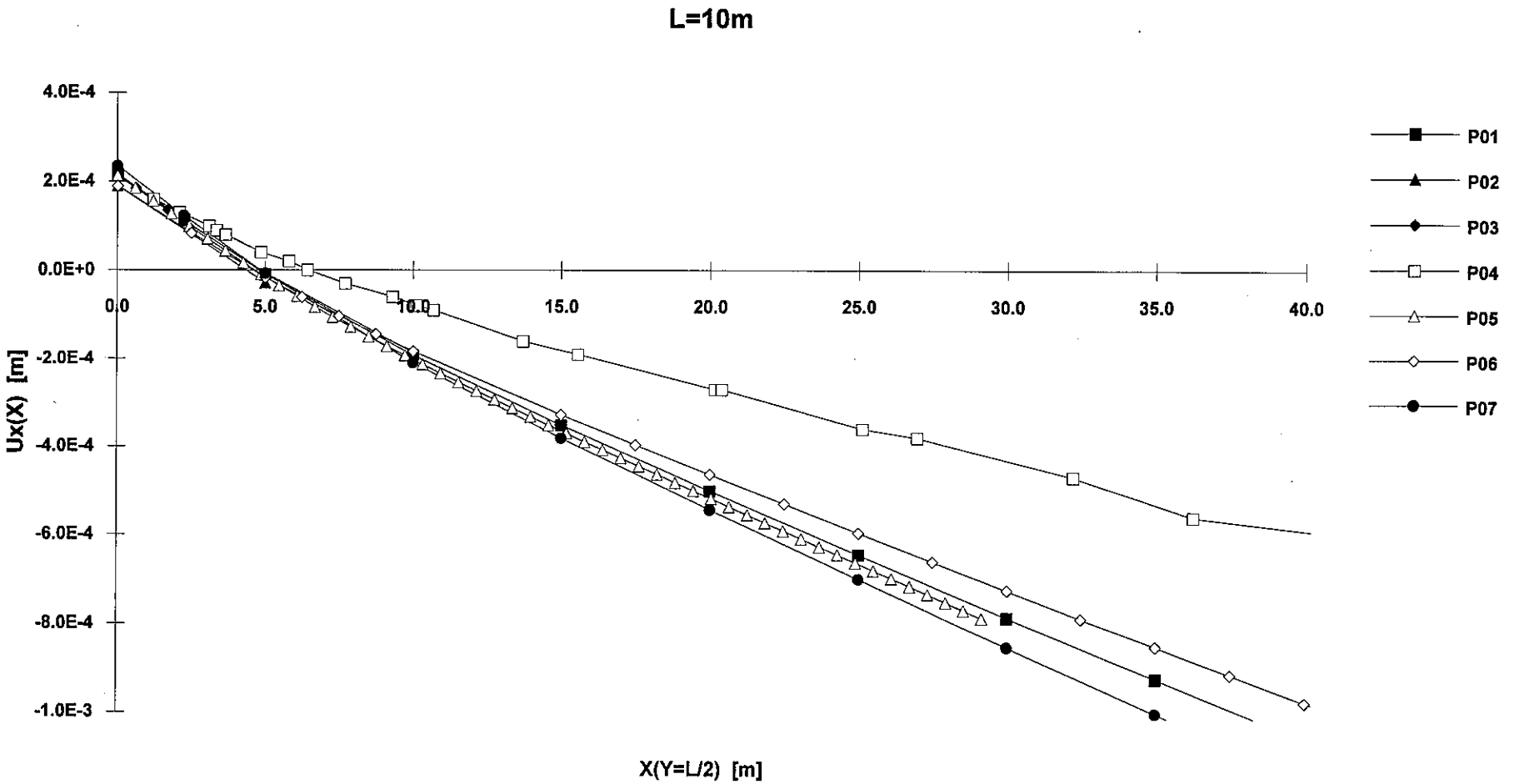

FLEXIBLE FOUNDATION

L=20m

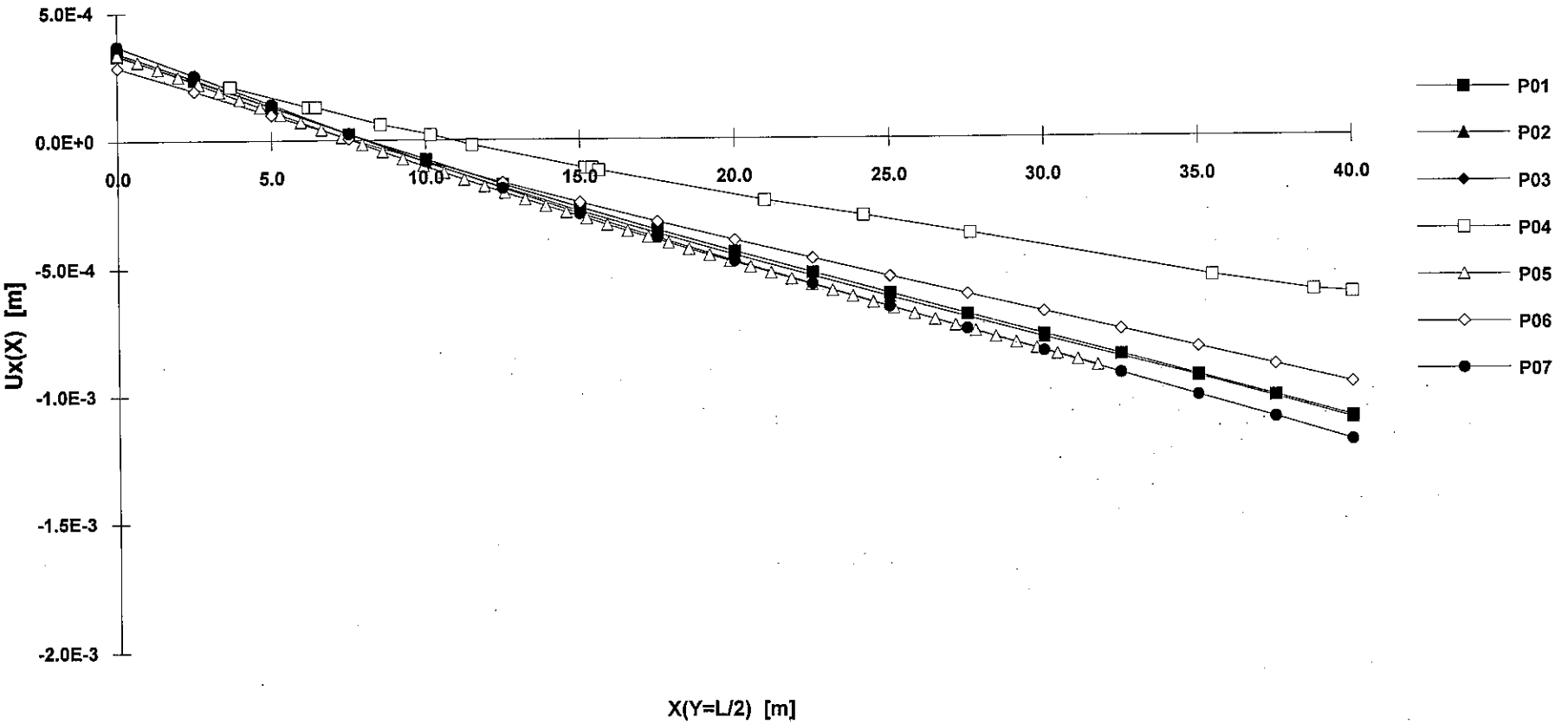

FLEXIBLE FOUNDATION

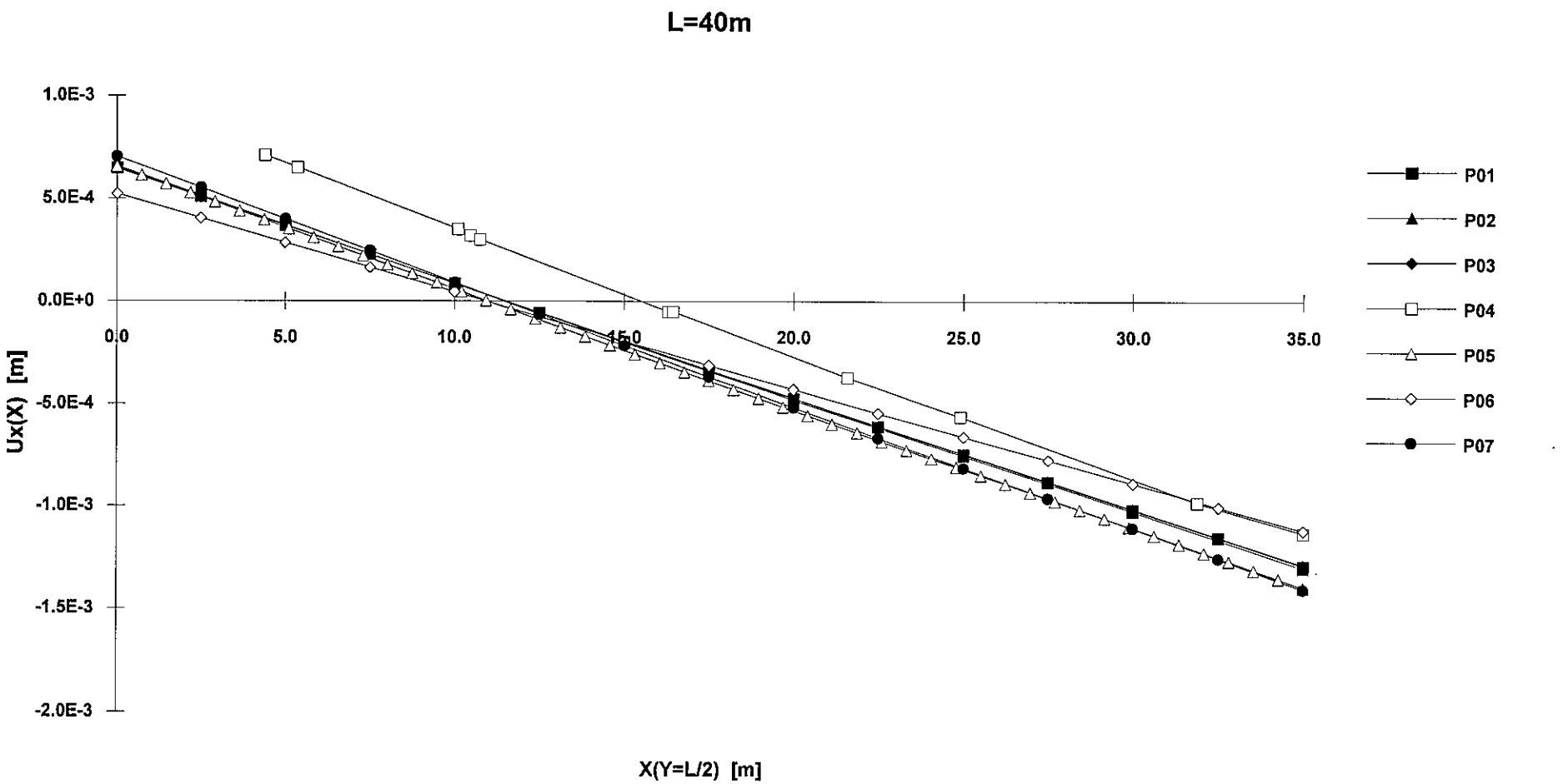

NOTES

NOTES

NOTES

Third Benchmark Workshop on
NUMERICAL ANALYSIS OF DAMS
Gennevilliers, France, September 29-30, 1994

THEME A2

Evaluation of critical uniform temperature decrease for a cracked buttress dam

PAPERS

- ABAQUS: F. Chillè, G. Giuseppetti, G. Mazzà, ENEL SpA DSR-CRIS, Italy
- ANSYS : L. Ilie, D. Stematiu, ADDL, France and Civil Engineering Institute of Bucharest, Romania
- CCRAP & LEFM : S. Valente, F. Barpi, Politecnico di Torino, Italy
- DIANA : R. Menga, P. Dalmagioni, G. Mazzà, R. Pellegrini, ISMES SpA and ENEL SpA DSR-CRIS, Italy
- FRAC_DAM : S.S. Bhattacharjee, P. Léger, R. Tinawi, Ecole Polytechnique de Montréal, Canada
- MERLIN : A. Shinmura, J. Cervenka, H. Boggs, G. Plizzari, V. Saouma, University of Colorado at Boulder, USA
- SOLVIA : H.N. Linsbauer, R. Promper, University of Technology, Vienna, and Österreichische Tauernkraftwerke AG, Salzburg, Austria

Third Benchmark Workshop on
NUMERICAL ANALYSIS OF DAMS
Paris, France, September 29-30, 1994

Theme A2: Evaluation of critical uniform temperature decrease of a cracked buttress dam

Linear analyses of a Cracked Buttress Dam

F. Chillè, G. Giuseppetti, G. Mazzà
ENEL S.p.A. CRIS, Milan, Italy

1. Introduction

In this paper the numerical results regarding the evaluation of the critical temperature decrease of a cracked buttress dam, as proposed by the ICOLD "ad hoc" Committee on Computational Aspects of Dam Analysis and Design, are presented. The input data are considered to be known, and have not been reported here.

The analyses have been carried out using the general purpose Finite Element Code ABAQUS [1].

2. Method of analysis

The critical temperature decrease for the dam can be obtained imposing the equivalence between the value of the stress intensity factor K_I at the crack tip for a certain value ΔT_{crit} and the experimental toughness of the material K_c.

The problem is solved with an energetic approach evaluating the J-integral value around the crack tip and using the relationship between the J-integral and the stress intensity factor K_I . For plane stress conditions

$$K_I = \sqrt{JE}$$

where E is the Young's modulus of the material. The critical temperature decrease is then obtained from the expression

$$\Delta T_{crit} = \frac{K_c}{\sqrt{J_1 E}}$$

where J_1 is the value of the J -integral for unitary temperature decrease.

3. Presentation of the requested results

Several meshes with different crack lengths have been considered. For all of them, the J-integral and the stress intensity factor have been evaluated. In figg. 1 and 2 these values are reported as function of the crack length.

Fig. 3 shows the critical temperature decrease as function of the crack length; the numerical values are listed in the table below.

L (m)	ΔT_{crit} (°C)	
	deformable found.	rigid found.
0.5	16.51	10.71
1.0	11.56	7.65
2.0	8.50	5.52
3.0	7.15	4.58
4.0	6.39	4.04
5.0	5.87	3.68
7.5	5.12	3.14
10.	4.75	2.86
15.	4.47	2.62
20.	4.48	2.56
25.	4.67	2.61
30.	4.96	2.72
35.	5.32	2.88
40.	5.73	3.08

In fig. 4 the same curves are reported in a log-scale: for small values of L, the solution tends to approach the theoretical curve referred to the infinite cracked plate subjected to uniform temperature decrease [2], while a minimum is found for a crack length of about 15m for rigid foundation and 20m for deformable foundation.

The openings along the crack line for the five crack length values proposed in the Benchmark theme are compared in fig.5 for the case of rigid foundation, and fig.6 for the case of deformable foundation; the nodal displacement values obtained from the analyses have been interpolated with cubic splines in order to have smooth and regular curves, and have been normalized with respect to the maximum crack opening value; the vertical coordinate along the crack has been normalized with respect to the current crack length.

The maximum opening displacements, normalized with respect to the current crack length, are reported as function of the crack length in fig.7.

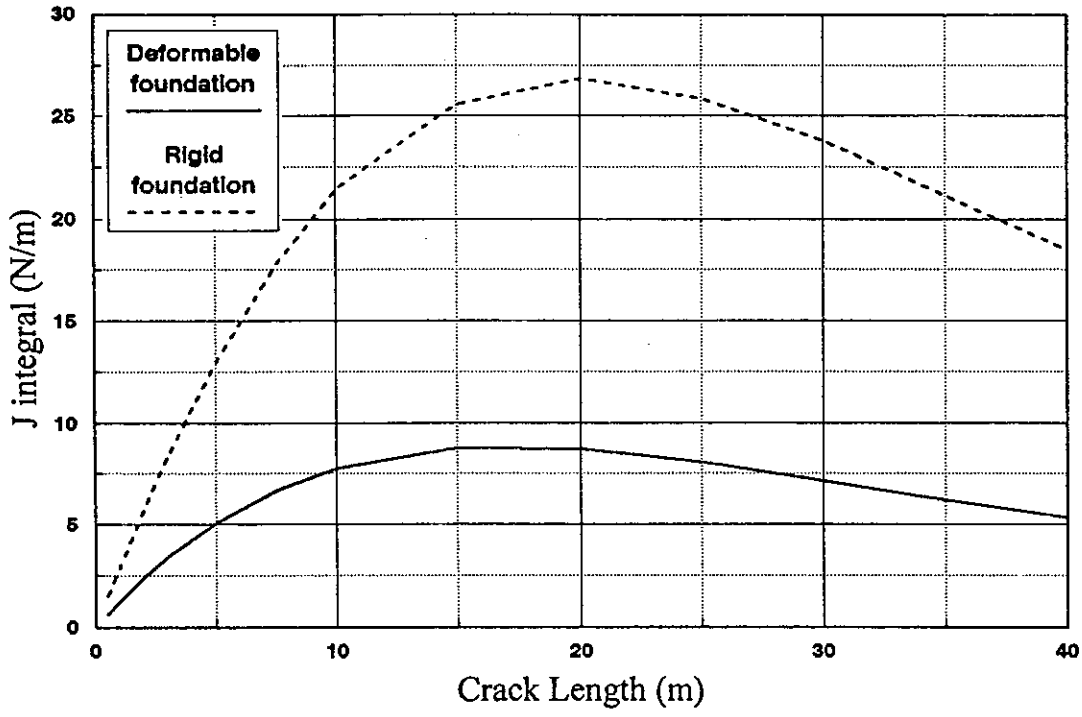

Fig. 1- J integral versus Crack Length

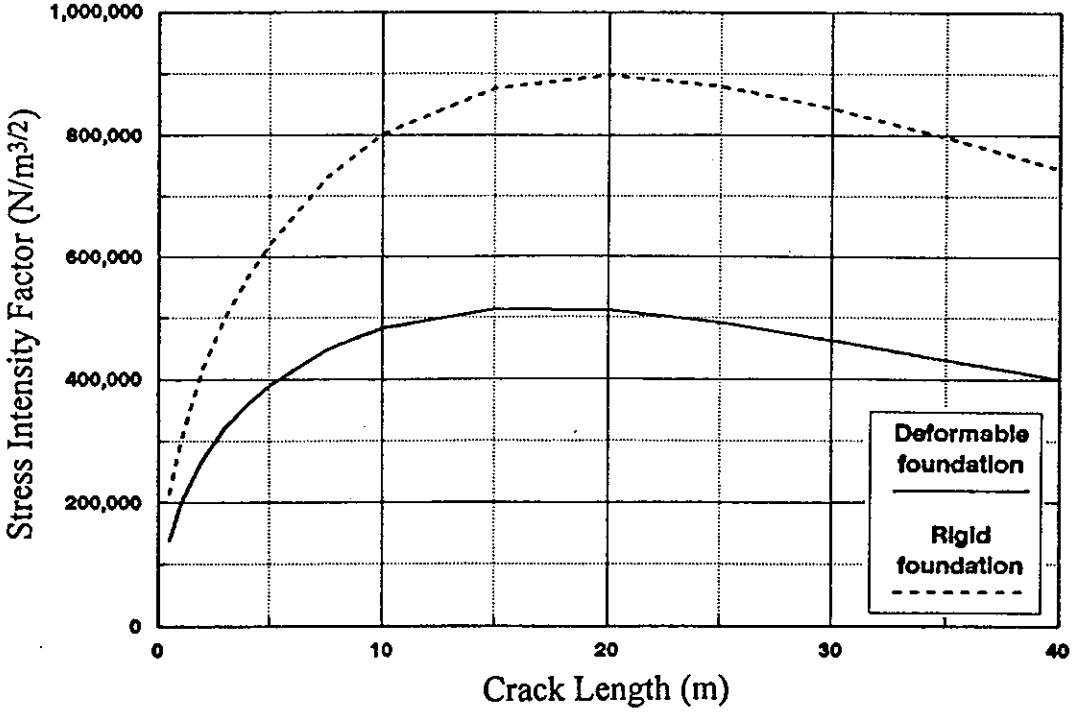

Fig. 2- Stress Intensity Factor K_I versus Crack Length

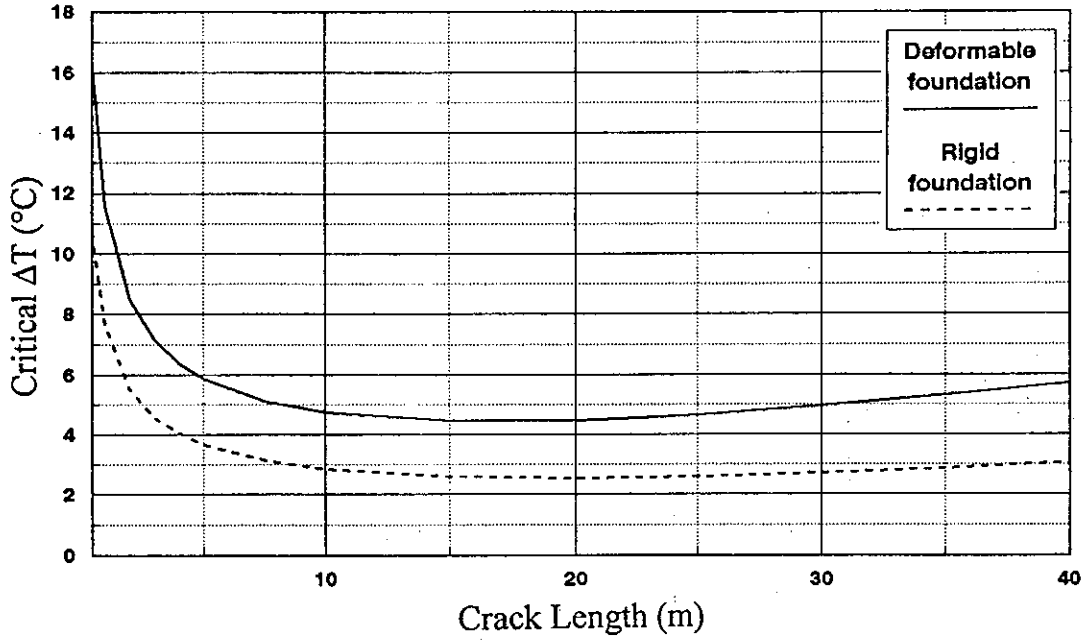

Fig. 3- Critical Temperature Decrease versus Crack Length

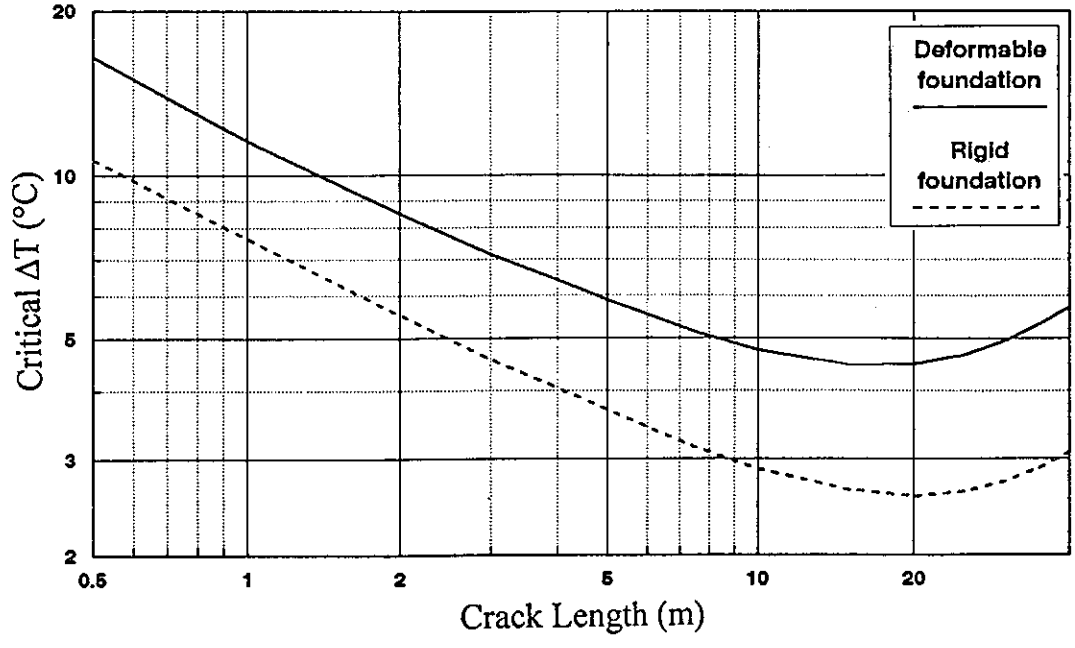

Fig. 4- Critical Temperature Decrease versus Crack Length (log-scale)

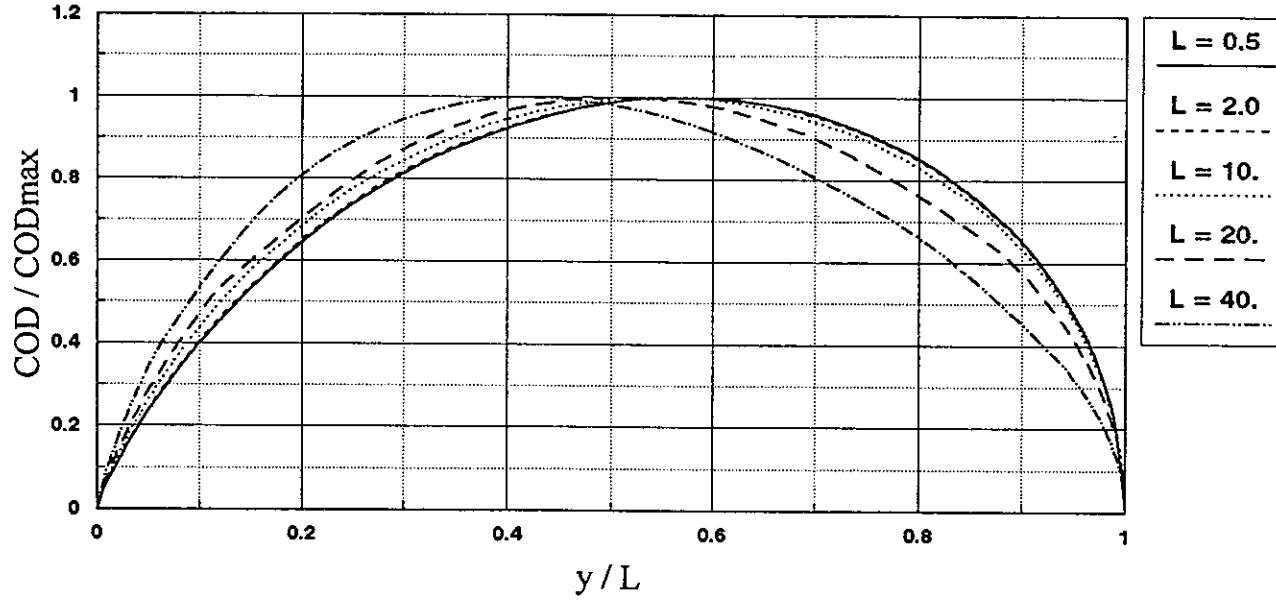

Fig. 5- Openings along the crack line (rigid foundation)

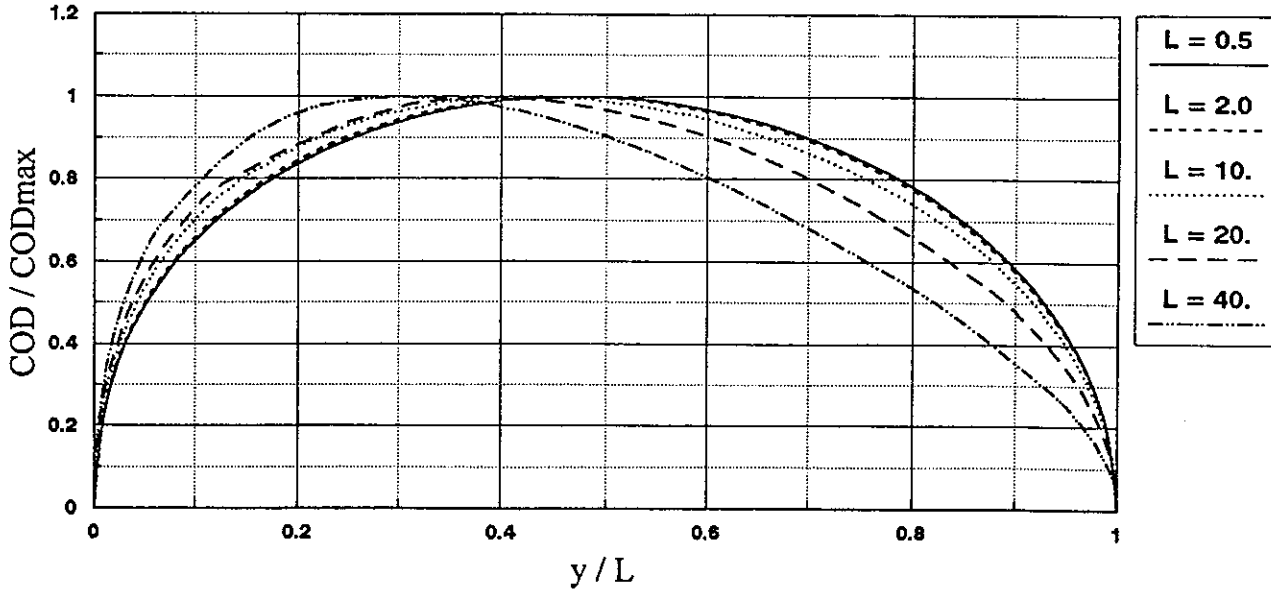

Fig. 6- Openings along the crack line (deformable foundation)

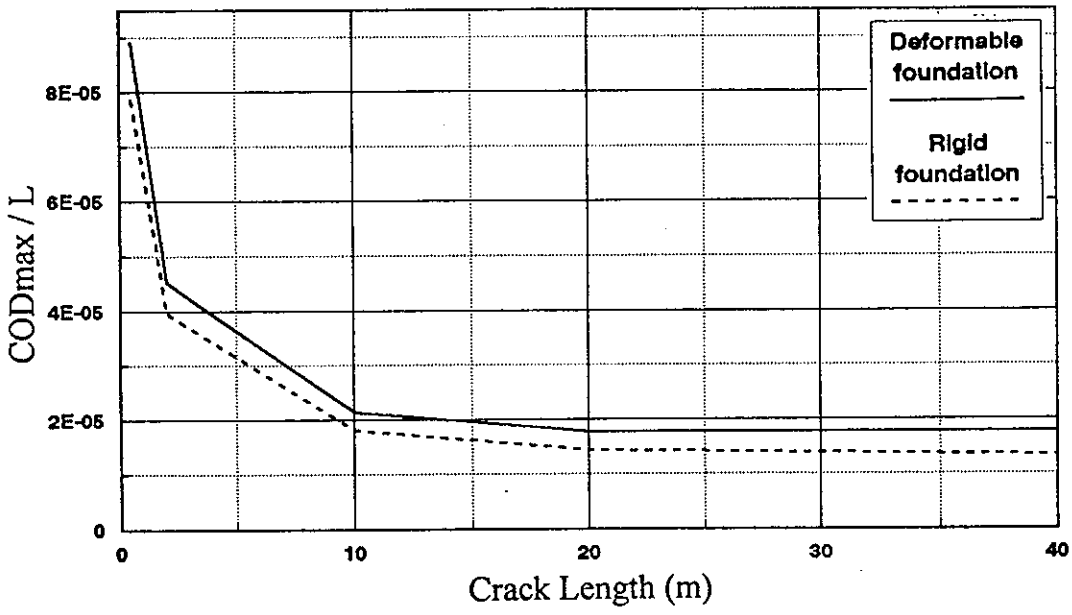

Fig. 7- Maximum Opening Displacement versus Crack Length

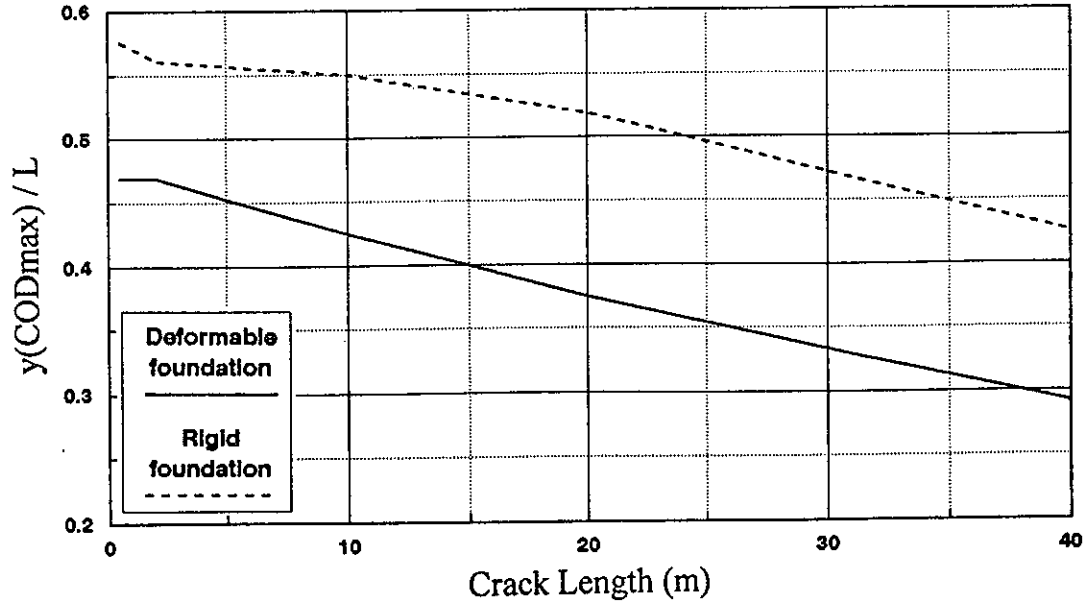

Fig. 8- Maximum Opening Displacement Level versus Crack Length

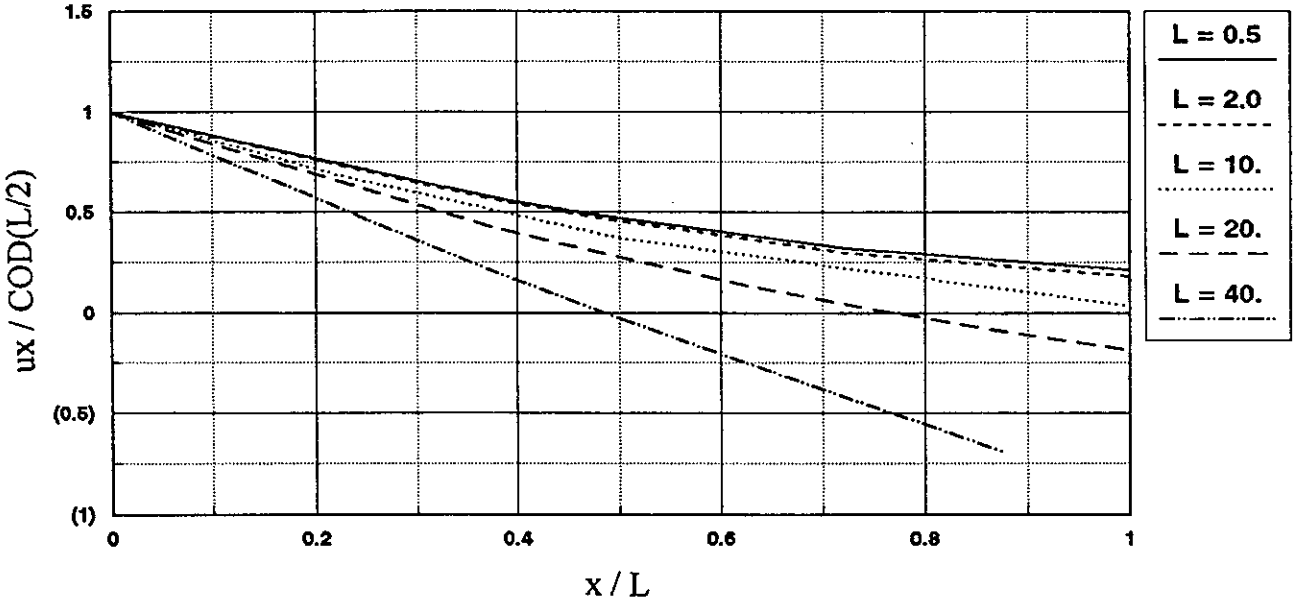

Fig. 9- Horizontal Displacements along the Crack Axis (rigid foundation)

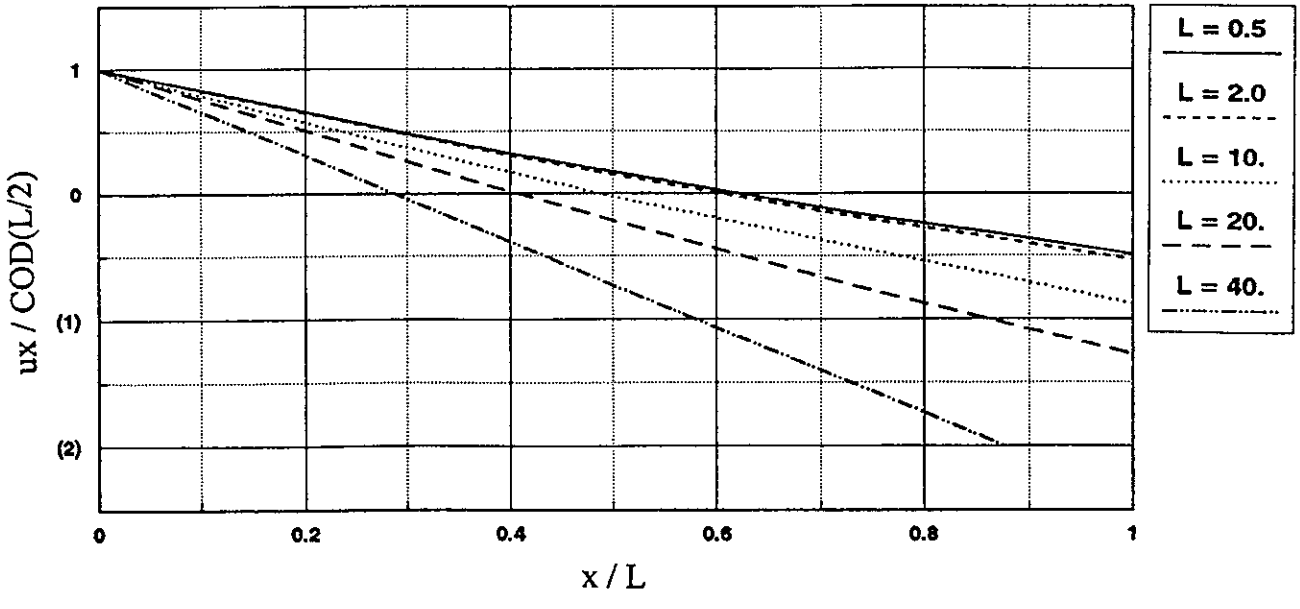

Fig. 10- Horizontal Displacements along the Crack Axis (deformable foundation)

The spline interpolation on the nodal displacement plots in figg. 5-6 led to the identification of a maximum opening displacement level which is independent from the nodal vertical coordinates in the mesh. The level corresponding to the maximum opening, normalized with respect to the current crack length, is reported as function of the crack length in fig.8.

The horizontal displacements along the crack axis (horizontal straight line at level y=L/2) for the five crack length values, normalized with respect to the crack opening displacement at midside crack length, are compared in fig.9 and 10 for the cases of rigid and deformable foundation respectively; the horizontal coordinate along the axis has been normalized with respect to the current crack length.

Numerical results, regarding nodal values without spline interpolation, are reported in tabb. 1-6 as requested by the benchmark theme A2.

4. F.E.M. discretization of the crack tip

The J-integral is an non-local energy measure; for this reason accurate J values can be obtained even with coarse meshes if the material behaves elastically. If a good description of local stress and strain field is required, i.e. for local approach, a more refined mesh is needed, and the singularity of these fields at the crack tip must be modeled. This can be done using 8-node isoparametric elements (fig. 11a), with one side collapsed on the crack tip, and the midside nodes shifted at 1/4 point on the sides connected with the tip (fig.11b). For this element the strain field near the collapsed side has the form

$$\varepsilon = \frac{A}{r} + \frac{B}{\sqrt{r}}$$

If the side of the element is not collapsed but the midside nodes are shifted to the 1/4 points (fig.11c), the strain is square root singular along the edges, but not in the interior of the element: this leads to worse results than the previous case.

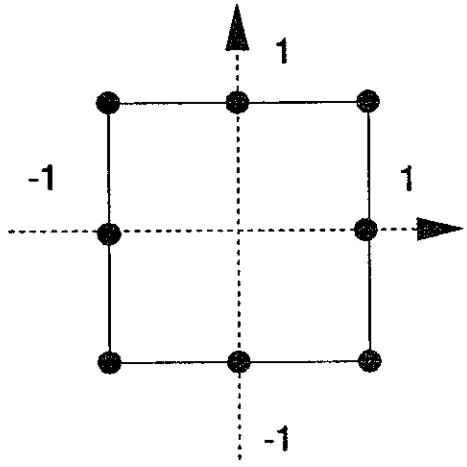

fig. 11a

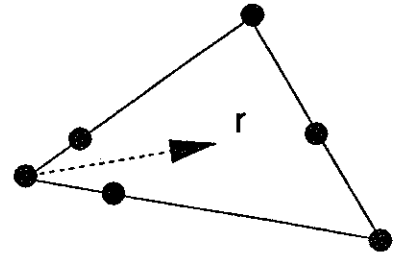

fig. 11b

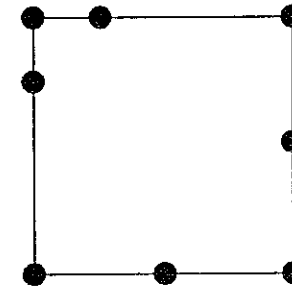

fig.11c

5. Comparison between different discretizations

The case of crack length of 10m and rigid foundation has been solved with different discretizations near the crack tip.

At first, the proposed mesh has been used; in fig. 12a the detail of this mesh near the crack is reported. Then the semicircular zone around the tip has been divided into meshes of 3x6, 3x3 and 3x1 elements; the latter is reported in fig.12b. Finally the mesh in figg.12c-d, with no collapsed element, has been used. The values of J-integral obtained with these meshes, with and without the quarter-point technique, are reported below:

MESH	1/4 point	J-integral
6x6	yes	21.42
6x6	no	21.43
3x6	yes	21.42
3x6	no	21.43
3x3	yes	21.42
3x3	no	21.43
3x1	yes	21.42
3x1	no	21.45
quad	yes	21.37
quad	no	20.90

The horizontal displacements obtained with 6x6, 3x1 and quad mesh are reported in fig.13a-b-c respectively. Even the coarse mesh gives quite good results: this means that, expecially for 3D cases, the J-integral approach, with degenerated elements at the crack tip, allows to considerably less refined meshes and shorter CPU times than a local approach.

6. References

[1] D.H. Hibbit, B.I. Karlsson, E.P. Sorensen: ABAQUS manuals (1993); Hibbit,Karlsson & Sorensen Inc., Pawtucket, Rhode Island.

[2] M. Fanelli: Dilatazioni termiche impedite in una lastra piana indefinita con fessura rettilinea (1985); ENEL-DSR-CRIS Internal Report n°3262, Milan, Italy.

[3] D. Broek: Elementary engineering fracture mechanics (1986); Martinus Nijhoff Publishers, Drodrecht, The Netherlands.

[4] J.R. Rice: A path independent integral and the approximate analysis of strain concentration by notches and cracks (1968); Journal of Applied Mechanics n°35.

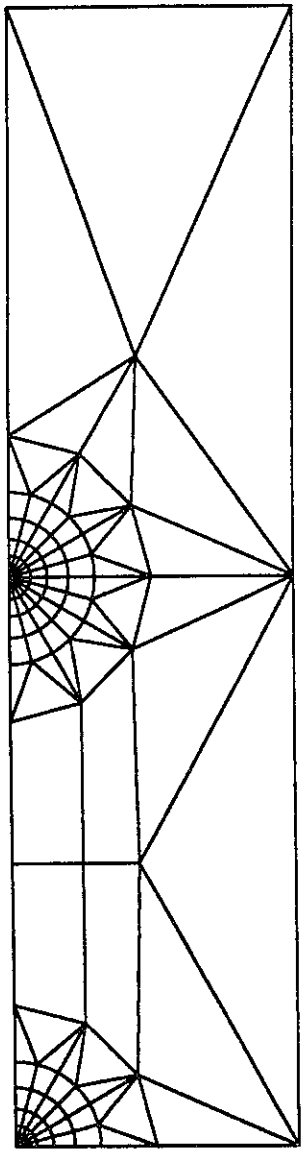

Fig. 12a- Mesh 6x6 (detail)

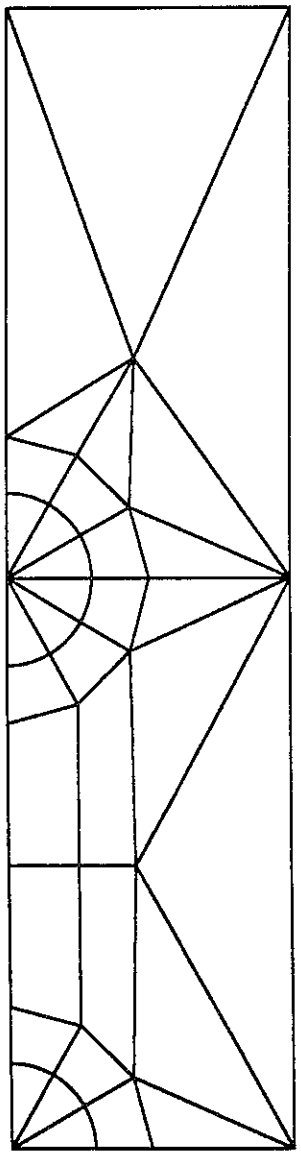

Fig. 12b- Mesh 3x1 (detail)

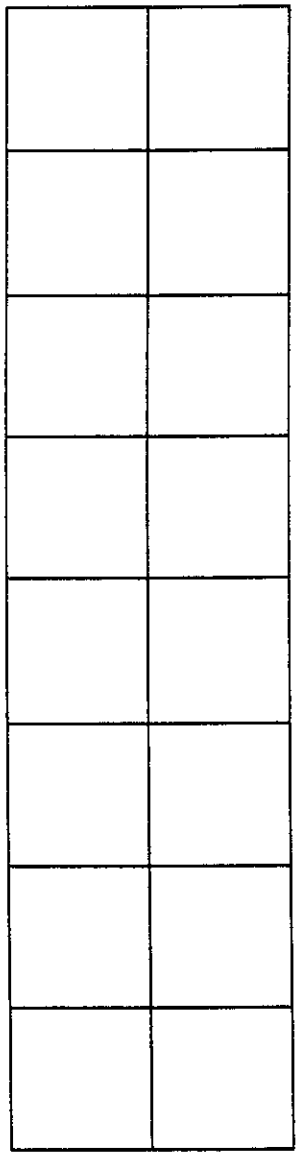

Fig. 12c- Mesh quad (detail)

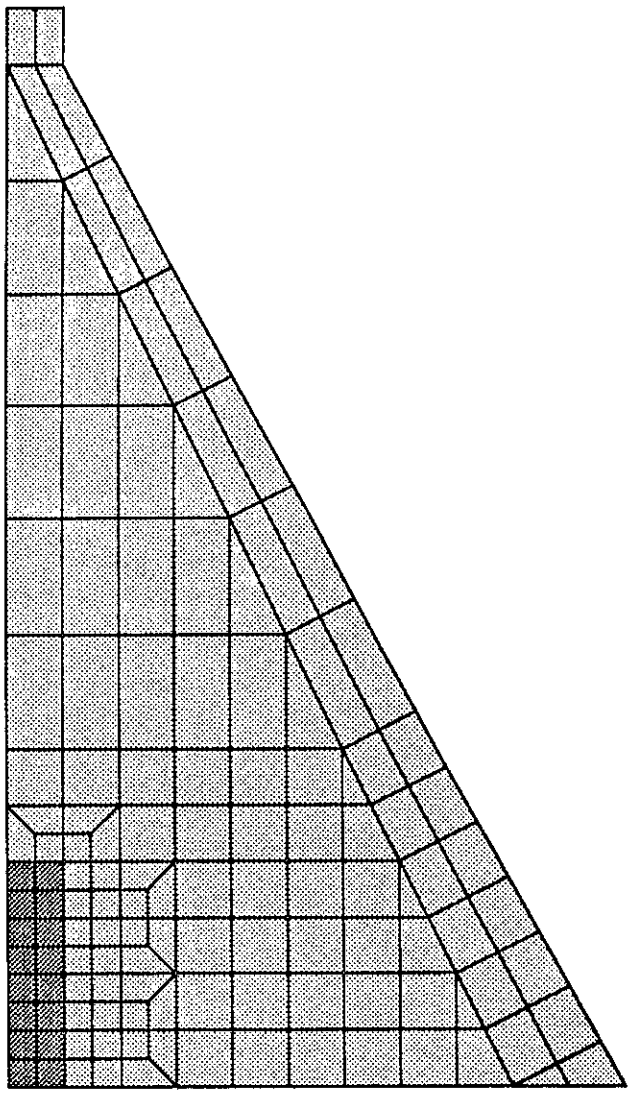

Fig. 12d- Mesh quad

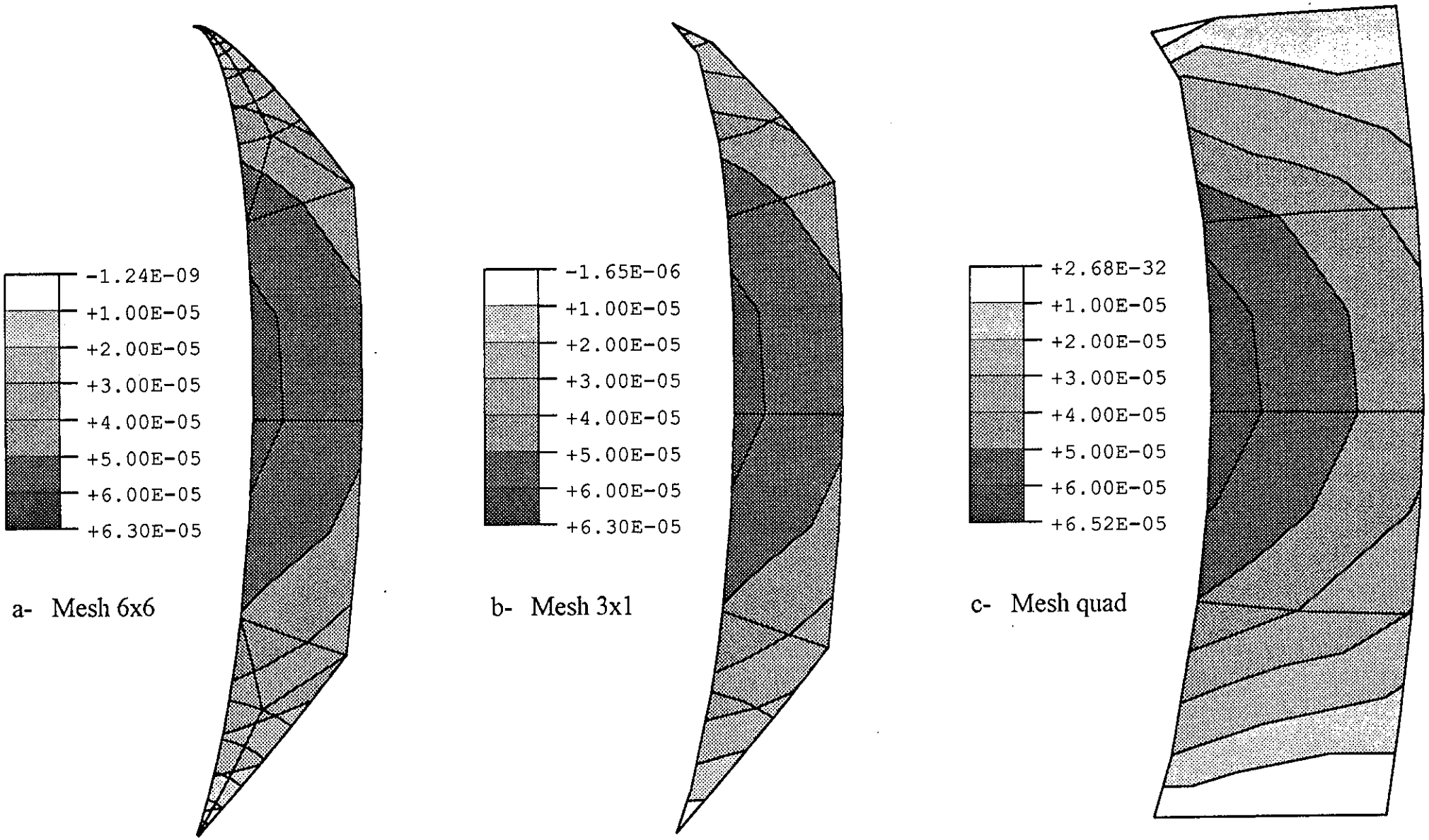

Fig. 13- Horizontal displacement on deformed geometry for different meshes (detail along the crack), L = 10m.

Tab. 1a (nodal values)

L (m)	ΔT (°C)	dmax (mm)	y(dmax) (m)	dmax/L	y(dmax)/L
0.50	10.7	0.0388	0.25	7.76E-5	0.500
2.00	5.52	0.0784	1.00	3.92E-5	0.500
10.0	2.86	0.1804	5.00	1.80E-5	0.500
20.0	2.56	0.2899	10.0	1.45E-5	0.500
40.0	3.08	0.5321	15.0	1.33E-5	3.750

Tab. 1b (interpolated values)

L (m)	ΔT (°C)	dmax (mm)	y(dmax) (m)	dmax/L	y(dmax)/L
0.50	10.7	0.0394	0.29	7.88E-5	0.580
2.00	5.52	0.0794	1.14	3.97E-5	0.570
10.0	2.86	0.1815	5.50	1.81E-5	0.550
20.0	2.56	0.2899	10.2	1.45E-5	0.510
40.0	3.08	0.5357	16.8	1.34E-5	0.420

Tab. 2a (nodal values)

L (m)	ΔT (°C)	dmax (mm)	y(dmax) (m)	dmax/L	y(dmax)/L
0.50	16.5	0.0446	0.25	8.92E-5	0.500
2.00	8.50	0.0905	1.00	4.53E-5	0.500
10.0	4.75	0.2125	3.75	2.12E-5	0.375
20.0	4.48	0.3449	6.25	1.72E-5	0.312
40.0	5.73	0.6446	10.0	1.61E-5	0.250

Tab. 2b (interpolated values)

L (m)	ΔT (°C)	dmax (mm)	y(dmax) (m)	dmax/L	y(dmax)/L
0.50	16.5	0.0447	0.24	8.93E-5	0.470
2.00	8.50	0.0908	0.92	4.54E-5	0.460
10.0	4.75	0.2134	4.20	2.13E-5	0.420
20.0	4.48	0.3488	7.80	1.74E-5	0.390
40.0	5.73	0.6519	12.0	1.63E-5	0.300

Tab. 3

Y (m)	UX (m)
L=0.5	
0.000000E+00	-7.845182E-08
6.944500E-03	3.354772E-06
2.777800E-02	1.015117E-05
6.250000E-02	1.857217E-05
1.111100E-01	2.712907E-05
1.736100E-01	3.440931E-05
2.500000E-01	3.882793E-05
3.263900E-01	3.871028E-05
3.888900E-01	3.471760E-05
4.375000E-01	2.808346E-05
4.722200E-01	1.965392E-05
4.930550E-01	1.010963E-05
5.000000E-01	-4.566552E-09
L=2.0	
0.000000E+00	-1.614891E-07
2.777800E-02	6.877661E-06
1.111120E-01	2.076592E-05
2.500000E-01	3.788968E-05
4.444400E-01	5.518049E-05
6.944400E-01	6.975459E-05
1.000000E+00	7.842705E-05
1.305560E+00	7.793375E-05
1.555560E+00	6.972871E-05
1.750000E+00	5.630749E-05
1.888900E+00	3.936254E-05
1.972220E+00	2.023418E-05
2.000000E+00	-8.953233E-09
L=10.0	
0.000000E+00	-1.476849E-07
4.166700E-02	6.458765E-06
1.666700E-01	2.009185E-05
3.750000E-01	3.842459E-05
6.666700E-01	5.972707E-05
1.041700E+00	8.246572E-05
1.500000E+00	1.051502E-04
2.500000E+00	1.409713E-04
3.750000E+00	1.685706E-04
5.000000E+00	1.804225E-04
6.250000E+00	1.791145E-04
7.500000E+00	1.628115E-04
8.500000E+00	1.359917E-04
8.958300E+00	1.169806E-04
9.333300E+00	9.583863E-05
9.625000E+00	7.312706E-05
9.833301E+00	4.932391E-05
9.958300E+00	2.486583E-05
1.000000E+01	-3.573088E-09
L=20.0	
0.000000E+00	-1.446349E-07
4.166600E-02	6.375785E-06
1.666680E-01	1.995317E-05
3.750000E-01	3.855733E-05
6.666600E-01	6.081286E-05
1.041660E+00	8.556990E-05
1.500000E+00	1.117501E-04
2.500000E+00	1.590932E-04
6.250000E+00	2.585474E-04
1.000000E+01	2.898611E-04
1.375000E+01	2.651997E-04
1.750000E+01	1.841169E-04
1.850000E+01	1.453508E-04
1.895840E+01	1.222866E-04
1.933320E+01	9.854698E-05
1.962500E+01	7.430300E-05
1.983340E+01	4.971697E-05
1.995820E+01	2.494747E-05
2.000000E+01	-2.296772E-09
L=40.0	
0.000000E+00	-1.856159E-07
4.166800E-02	8.213118E-06
1.666680E-01	2.577488E-05
3.750000E-01	5.003644E-05
6.666800E-01	7.941210E-05
1.041680E+00	1.126211E-04
1.500000E+00	1.484693E-04
2.500000E+00	2.156908E-04
6.250000E+00	3.814111E-04
1.000000E+01	4.780795E-04
1.500000E+01	5.321100E-04
2.000000E+01	5.265442E-04
2.500000E+01	4.793247E-04
3.000000E+01	3.966029E-04
3.375000E+01	3.101403E-04
3.750000E+01	1.926558E-04
3.800000E+01	1.717651E-04
3.850000E+01	1.484374E-04
3.895840E+01	1.235666E-04
3.933320E+01	9.874898E-05
3.962520E+01	7.398990E-05
3.983320E+01	4.928775E-05
3.995840E+01	2.466649E-05
4.000000E+01	-1.412858E-09

Tab. 4

Y (m)	UX (m)
L=0.5	
0.000000E+00	1.777715E-07
6.944500E-03	1.251307E-05
2.777800E-02	2.293691E-05
6.250000E-02	3.175927E-05
1.111100E-01	3.870240E-05
1.736100E-01	4.326696E-05
2.500000E-01	4.458443E-05
3.263900E-01	4.190580E-05
3.888900E-01	3.630466E-05
4.375000E-01	2.874002E-05
4.722200E-01	1.984943E-05
4.930550E-01	1.013672E-05
5.000000E-01	-3.570455E-09
L=2.0	
0.000000E+00	3.668555E-07
2.777800E-02	2.584466E-05
1.111120E-01	4.730463E-05
2.500000E-01	6.534049E-05
4.444400E-01	7.935288E-05
6.944400E-01	8.832418E-05
1.000000E+00	9.053690E-05
1.305560E+00	8.466830E-05
1.555560E+00	7.306509E-05
1.750000E+00	5.767382E-05
1.888900E+00	3.975294E-05
1.972220E+00	2.027755E-05
2.000000E+00	-6.820325E-09
L=10.0	
0.000000E+00	5.481421E-07
4.166700E-02	3.827093E-05
1.666700E-01	7.138085E-05
3.750000E-01	1.015629E-04
6.666700E-01	1.287575E-04
1.041700E+00	1.526588E-04
1.500000E+00	1.728481E-04
2.500000E+00	1.989421E-04
3.750000E+00	2.124746E-04
5.000000E+00	2.111127E-04
6.250000E+00	1.983620E-04
7.500000E+00	1.727079E-04
8.500000E+00	1.401568E-04
8.958300E+00	1.191430E-04
9.333300E+00	9.673120E-05
9.625000E+00	7.331862E-05
9.833301E+00	4.922825E-05
9.958300E+00	2.474904E-05
1.000000E+01	-2.654233E-09
L=20.0	
0.000000E+00	6.931841E-07
4.166600E-02	4.836080E-05
1.666680E-01	9.065882E-05
3.750000E-01	1.299565E-04
6.666600E-01	1.664194E-04
1.041660E+00	1.999267E-04
1.500000E+00	2.302785E-04
2.500000E+00	2.761908E-04
6.250000E+00	3.448677E-04
1.000000E+01	3.395567E-04
1.375000E+01	2.868851E-04
1.750000E+01	1.872942E-04
1.850000E+01	1.458135E-04
1.895840E+01	1.219176E-04
1.933320E+01	9.776309E-05
1.962500E+01	7.343613E-05
1.983340E+01	4.900570E-05
1.995820E+01	2.455148E-05
2.000000E+01	-1.737340E-09
L=40.0	
0.000000E+00	1.064240E-06
4.166800E-02	7.423700E-05
1.666680E-01	1.395328E-04
3.750000E-01	2.007609E-04

6.666800E-01	2.583275E-04
1.041680E+00	3.121938E-04
1.500000E+00	3.621793E-04
2.500000E+00	4.413220E-04
6.250000E+00	5.908597E-04
1.000000E+01	6.446422E-04
1.500000E+01	6.418058E-04
2.000000E+01	5.883134E-04
2.500000E+01	5.047484E-04
3.000000E+01	3.976798E-04
3.375000E+01	3.011317E-04
3.750000E+01	1.814990E-04
3.800000E+01	1.612057E-04
3.850000E+01	1.387786E-04
3.895840E+01	1.151267E-04
3.933320E+01	9.174549E-05
3.962520E+01	6.859638E-05
3.983320E+01	4.562390E-05
3.995840E+01	2.281195E-05
4.000000E+01	-1.030074E-09

Tab. 5

X (m)	UX (m)
L=0.5	
0.000000E+00	3.882793E-05
3.232400E-02	3.588555E-05
6.465000E-02	3.288298E-05
1.522200E-01	2.511584E-05
1.960000E-01	2.170559E-05
2.397900E-01	1.877136E-05
3.610200E-01	1.249522E-05
5.000000E-01	6.956023E-06
L=2.0	
0.000000E+00	7.842705E-05
1.293000E-01	7.233719E-05
2.586000E-01	6.612655E-05
6.088800E-01	5.003803E-05
7.840200E-01	4.294744E-05
9.591600E-01	3.681680E-05
1.444100E+00	2.356262E-05
2.000000E+00	1.117664E-05
L=10.0	
0.000000E+00	1.804225E-04
6.240900E-01	1.647456E-04
1.248200E+00	1.487530E-04
1.707100E+00	1.370219E-04
2.246700E+00	1.229724E-04
5.000000E+00	6.700171E-05
1.000000E+01	5.867701E-06
L=20.0	
0.000000E+00	2.898611E-04
2.500000E+00	2.330802E-04
5.000000E+00	1.775080E-04
7.500000E+00	1.237098E-04
1.000000E+01	7.987992E-05
1.250000E+01	3.902110E-05
1.500000E+01	4.610821E-06
1.750000E+01	-2.646722E-05
2.000000E+01	-5.385909E-05
L=40.0	
0.000000E+00	5.321100E-04
2.500000E+00	4.613980E-04
5.000000E+00	3.892651E-04
7.500000E+00	3.185477E-04
1.000000E+01	2.469948E-04
1.250000E+01	1.785708E-04
1.500000E+01	1.118389E-04
1.750000E+01	4.759671E-05
2.000000E+01	-1.452394E-05
2.250000E+01	-7.494769E-05
2.500000E+01	-1.339693E-04
2.750000E+01	-1.921343E-04
3.000000E+01	-2.500598E-04
3.250000E+01	-3.086558E-04
3.500000E+01	-3.685979E-04

Tab. 6

X (m)	UX (m)
L=0.5	
0.000000E+00	4.458443E-05
3.232400E-02	3.974523E-05
6.465000E-02	3.481286E-05
1.522200E-01	2.142059E-05
1.960000E-01	1.497591E-05
2.397900E-01	8.892810E-06
3.610200E-01	-6.528944E-06
5.000000E-01	-2.349733E-05
L=2.0	
0.000000E+00	9.053690E-05
1.293000E-01	8.048368E-05
2.586000E-01	7.024396E-05
6.088800E-01	4.243645E-05
7.840200E-01	2.904152E-05
9.591600E-01	1.638265E-05
1.444100E+00	-1.578692E-05
2.000000E+00	-5.118413E-05
L=10.0	
0.000000E+00	2.124746E-04
6.240900E-01	1.846681E-04
1.248200E+00	1.565067E-04
1.707100E+00	1.356544E-04
2.246700E+00	1.105888E-04
5.000000E+00	-6.344068E-06
1.000000E+01	-1.863041E-04
L=20.0	
0.000000E+00	3.448677E-04
2.500000E+00	2.391899E-04
5.000000E+00	1.321361E-04
7.500000E+00	2.479357E-05
1.000000E+01	-7.435348E-05
1.250000E+01	-1.723304E-04
1.500000E+01	-2.648066E-04
1.750000E+01	-3.544205E-04
2.000000E+01	-4.411892E-04
L=40.0	
0.000000E+00	6.446422E-04
2.500000E+00	5.064051E-04
5.000000E+00	3.667627E-04
7.500000E+00	2.271977E-04
1.000000E+01	8.515079E-05
1.250000E+01	-5.498153E-05
1.500000E+01	-1.949462E-04
1.750000E+01	-3.333252E-04
2.000000E+01	-4.705308E-04
2.250000E+01	-6.067566E-04
2.500000E+01	-7.421121E-04
2.750000E+01	-8.771002E-04
3.000000E+01	-1.012153E-03
3.250000E+01	-1.147979E-03
3.500000E+01	-1.284965E-03

THIRD BENCHMARK WARKSHOP ON NUMERICAL ANALYSIS OF DAMS

THEME A2 : Buttres dam

RAPPORT D'ETUDE

"Evaluation of critical uniform temperature decrease for a cracked buttres dam"

(Modifications for RAPPORT of 1 JUILLET 1994)

Date : 28 october 1994

Auteur : Dr Ing. Lucian ILIE,
Prof. Dr. Ing. Dan STEMATIU

Référence document : ICOLD/Buttres dam/03 rapport

SOMMAIRE

1 OBJET ET HYPOTHESES GENERALES

L'objet de cette étude est de déterminer la baisse critique de température pour la fissuration d'un barrage à contreforts.

Voir les spécifications techniques de l'étude dans le document ICOLD définissant le thème A2.

2 METHODOLOGIE

La modélisation et les calculs sont effectués par la méthode des éléments finis en utilisant le progiciel ANSYS version 5.0A en statique linéaire et petits déplacements.

Les matériaux du barrage et de la fondation sont élastiques linéaires et isotropes.

Le système d'unité utilisé est le suivant :

- m pour les distances,
- Newton pour les efforts,
- Pascal (N/m2) pour les contraintes,
- kg/m3 pour la densité,
- m/s2 pour l'accélération.

2-1 Modélisation

Les modèles sont entièrement construits en éléments bidimensionnels à 6 noeuds (PLANE2) avec une formulation :
- en contraintes planes pour le barrage,
- en déformations planes pour la fondation.

Chaque modèle correspond à une demi-section transversale du barrage (conditions de symétrie dans l'axe).

Les éléments de fond de fissure ont leurs noeuds milieux placés à une distance du fond de fissure égale à 25% de la longueur du côté pour créer une singularité en fond de fissure (contrainte infinie). La longueur de l'élément en fond de fissure est de 5 cm.

Les 10 modèles étudiés correspondent à 5 longueurs différentes de la fissure et 2 configurations de la fondation :
- rigide,
- élastique.

La taille des modèles varie de 1909 à 6034 éléments.

Voir dans les figures A, B et C suivantes des vues du modèle du barrage avec fondation élastique et longueur de fissure 40 m.

2-2 Calculs

On a calculé la différence de température du barrage générant le facteur critique d'intensité de contraintes demandé.

Les temps d'exécution, sur COMPAQ486 Pentium, des calculs pour les 5 modèles à fondation rigide et les 5 modèles à fondation élastique sont les suivants :

longueur fissure (m)	type de fondation	nombre d'éléments	temps CPU
0,5	rigide	3755	237
2	rigide	3036	222
10	rigide	3323	229
20	rigide	2534	174
40	rigide	1909	157
0,5	élastique	6034	380
2	élastique	4446	279
10	élastique	4208	270
20	élastique	3291	215
40	élastique	2666	175

2-2 Résultats

Le facteur d'intensité de contraintes KI a été calculé à partir des résultats en déplacements (mesure de l'ouverture de la fissure).

Voir dans les tableaux 1 à 6 suivants les résultats demandés.

Fig. 4

1
ANSYS 5.0 A
JUN 7 1994
15:30:54
PLOT NO. 1
ELEMENTS
TYPE NUM
U
ZV =1
DIST=217.25
XF =150
YF =-102.5
PRECISE HIDDEN

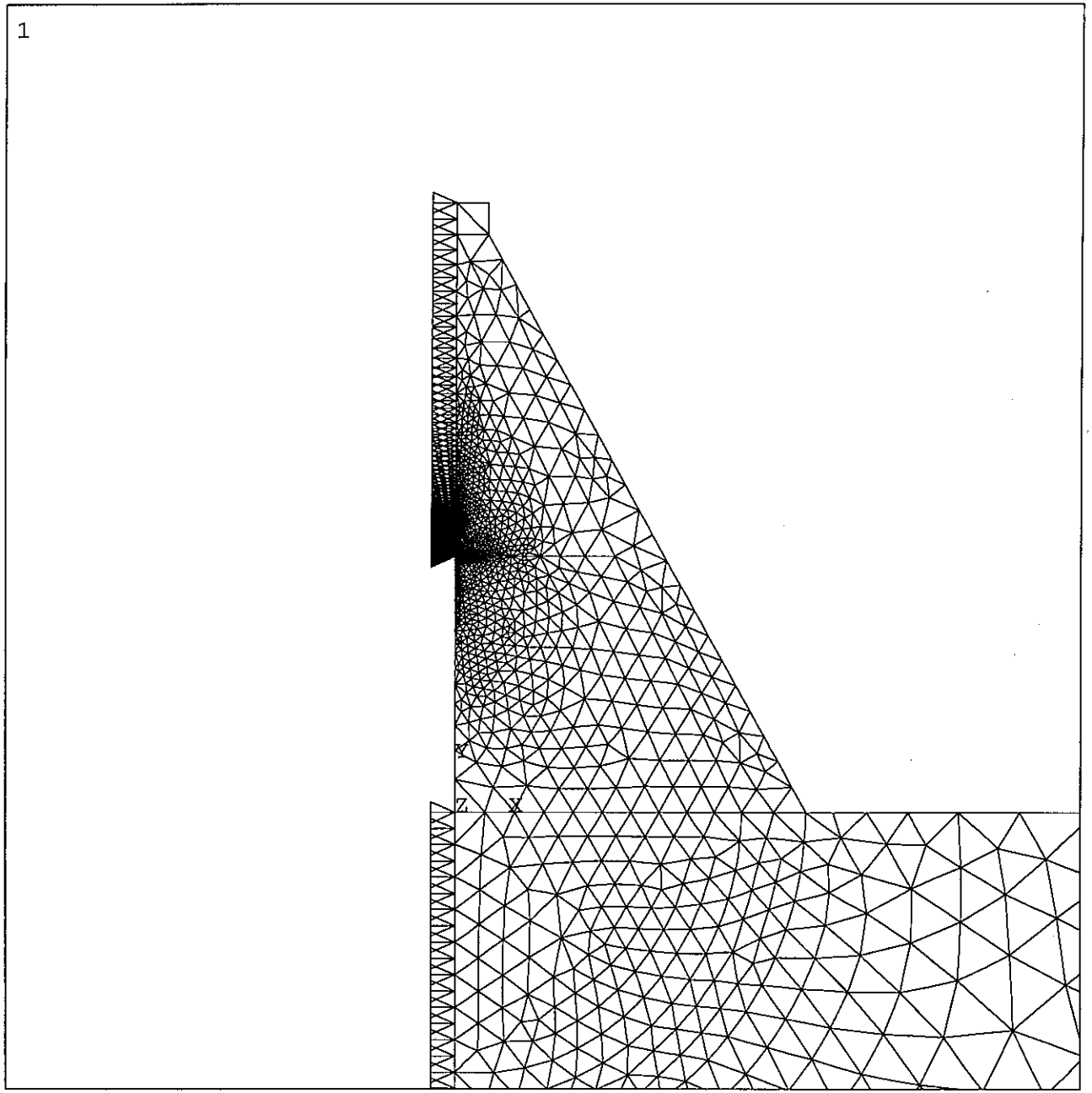
1
ANSYS 5.0 A
JUN 7 1994
15:31:48
PLOT NO. 3
ELEMENTS
TYPE NUM
U
ZV =1
*DIST=84.263
*XF =13.765
*YF =41.577
PRECISE HIDDEN
Y
Z
X

Fig. 8

Fig. c.

1
ANSYS 5.0 A
JUN 7 1994
15:32:29
PLOT NO. 4
ELEMENTS
TYPE NUM
U
ZV =1
*DIST=0.34778
*XF =0.098025
*YF =39.986
PRECISE HIDDEN

TABLE 1

RIGID FONDATION

L (m)	ΔT (°C)	d_{max} (m)	Y_{dmin} (m)
0.5	-10.69	$.3934E^{-04}$	.28574
2.0	- 5.50	$.7926E^{-04}$	1.1409
10.0	- 2.88	$.1874E^{-03}$	5.4625
20.0	- 2.58	$.2912E^{-03}$	10.1430
40.0	- 3.10	$.5429E^{-03}$	16.9470

TABLE 2
(12 october 1994)

DEFORMABLE FONDATION

L (m)	ΔT (°C)	d_{max} (m)	Y_{dmin} (m)
0.5	-17.50	$.4367E^{-04}$	.2498
2.0	- 9.07	$.8847E^{-04}$	.9759
10.0	- 4.94	$.2114E^{-03}$	4.5239
20.0	- 4.69	$.3481E^{-03}$	8.2005
40.0	- 6.10	$.7154E^{-03}$	12.8140

CONCRETE: Ex $=3.0E^{10}$ Nm^{-2}
NUXY =0.16
ALPXY $=1.0E^{-5}$
Kc $=2.3E^{6}$ **$Nm^{-3/2}$**

ROCK: Ex $=1.0E^{10}$ Nm^{-2}
NUXY =0.20

!
! TABLE 3
!
CRACKED BUTTRESS DAM L=0.5m Rig.fund. (ADDL-1994)

***** PATH VARIABLE SUMMARY *****

Y (m)	UX (m)
0.00000E+00	0.00000E+00
0.53153E-02	0.16526E-05
0.10631E-01	0.32685E-05
0.15946E-01	0.48475E-05
0.21261E-01	0.63897E-05
0.26576E-01	0.78951E-05
0.31892E-01	0.93637E-05
0.37207E-01	0.10796E-04
0.42522E-01	0.12191E-04
0.47837E-01	0.13549E-04
0.53153E-01	0.14870E-04
0.58468E-01	0.16155E-04
0.63783E-01	0.17402E-04
0.69099E-01	0.18613E-04
0.74414E-01	0.19788E-04
0.79729E-01	0.20925E-04
0.85044E-01	0.22026E-04
0.90360E-01	0.23089E-04
0.95675E-01	0.24116E-04
0.10099	0.25106E-04
0.10631	0.25969E-04
0.11162	0.26764E-04
0.11694	0.27533E-04
0.12225	0.28278E-04
0.12757	0.28998E-04
0.13288	0.29693E-04
0.13820	0.30363E-04
0.14351	0.31009E-04
0.14883	0.31629E-04
0.15414	0.32225E-04
0.15946	0.32796E-04
0.16477	0.33342E-04
0.17009	0.33863E-04
0.17540	0.34359E-04
0.18072	0.34831E-04
0.18603	0.35277E-04
0.19135	0.35692E-04
0.19667	0.36083E-04
0.20198	0.36452E-04
0.20730	0.36799E-04
0.21261	0.37125E-04
0.21793	0.37428E-04
0.22324	0.37709E-04
0.22856	0.37969E-04
0.23387	0.38206E-04
0.23919	0.38422E-04
0.24450	0.38616E-04
0.24982	0.38787E-04
0.25513	0.38937E-04
0.26023	0.39054E-04
0.26534	0.39151E-04
0.27044	0.39227E-04
0.27554	0.39284E-04
0.28064	0.39320E-04
0.28574	0.39336E-04
0.29084	0.39332E-04
0.29594	0.39307E-04
0.30105	0.39262E-04
0.30615	0.39198E-04
0.31125	0.39113E-04
0.31635	0.39000E-04
0.32145	0.38865E-04
0.32655	0.38706E-04
0.33165	0.38524E-04
0.33676	0.38318E-04
0.34186	0.38090E-04
0.34696	0.37838E-04
0.35206	0.37562E-04
0.35716	0.37264E-04
0.36226	0.36937E-04
0.36736	0.36578E-04
0.37247	0.36189E-04
0.37757	0.35770E-04
0.38267	0.35319E-04
0.38777	0.34838E-04
0.39287	0.34326E-04
0.39797	0.33779E-04
0.40307	0.33192E-04
0.40817	0.32565E-04
0.41328	0.31897E-04
0.41838	0.31190E-04
0.42348	0.30442E-04
0.42858	0.29649E-04
0.43368	0.28788E-04
0.43878	0.27857E-04
0.44388	0.26856E-04
0.44899	0.25785E-04
0.50000	0.41895E-09

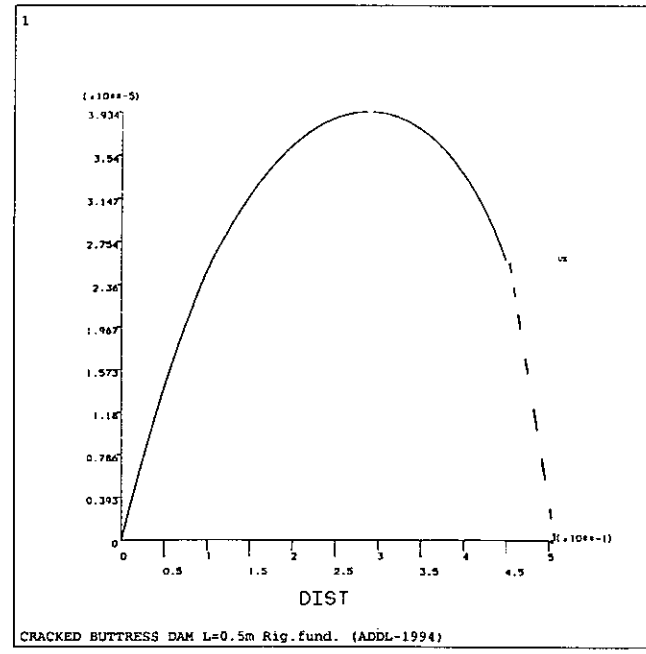

TABLE 4
(12 october 1994)

CRACKED BUTTRESS DAM L=0.5m Def.fund. (ADDL-1994)

***** PATH VARIABLE SUMMARY *****

S	UX
0.00000E+00	0.00000E+00
0.53153E-02	0.29042E-05
0.10631E-01	0.56900E-05
0.15946E-01	0.83572E-05
0.21261E-01	0.10906E-04
0.26576E-01	0.13336E-04
0.31892E-01	0.15648E-04
0.37207E-01	0.17841E-04
0.42522E-01	0.19916E-04
0.47837E-01	0.21872E-04
0.53153E-01	0.23710E-04
0.58468E-01	0.25430E-04
0.63783E-01	0.27030E-04
0.69099E-01	0.28513E-04
0.74414E-01	0.29877E-04
0.79729E-01	0.31122E-04
0.85044E-01	0.32249E-04
0.90360E-01	0.33257E-04
0.95675E-01	0.34147E-04
0.10099	0.34918E-04
0.10631	0.35590E-04
0.11162	0.36228E-04
0.11694	0.36838E-04
0.12225	0.37421E-04
0.12757	0.37977E-04
0.13288	0.38506E-04
0.13820	0.39007E-04
0.14351	0.39481E-04
0.14883	0.39928E-04
0.15414	0.40347E-04
0.15946	0.40739E-04
0.16477	0.41104E-04
0.17009	0.41441E-04
0.17540	0.41751E-04
0.18072	0.42034E-04
0.18603	0.42289E-04
0.19135	0.42517E-04
0.19667	0.42723E-04
0.20198	0.42910E-04
0.20730	0.43076E-04
0.21261	0.43222E-04
0.21793	0.43347E-04
0.22324	0.43452E-04
0.22856	0.43537E-04
0.23387	0.43601E-04
0.23919	0.43645E-04
0.24450	0.43668E-04
0.24982	0.43672E-04
0.25513	0.43654E-04
0.26023	0.43617E-04
0.26534	0.43562E-04
0.27044	0.43488E-04
0.27554	0.43396E-04
0.28064	0.43285E-04
0.28574	0.43156E-04
0.29084	0.43009E-04
0.29594	0.42843E-04
0.30105	0.42659E-04
0.30615	0.42456E-04
0.31125	0.42236E-04
0.31635	0.41992E-04
0.32145	0.41727E-04
0.32655	0.41442E-04
0.33165	0.41134E-04
0.33676	0.40806E-04
0.34186	0.40457E-04
0.34696	0.40086E-04
0.35206	0.39695E-04
0.35716	0.39282E-04
0.36226	0.38843E-04
0.36736	0.38376E-04
0.37247	0.37881E-04
0.37757	0.37358E-04
0.38267	0.36806E-04
0.38777	0.36227E-04
0.39287	0.35618E-04
0.39797	0.34978E-04
0.40307	0.34300E-04
0.40817	0.33585E-04
0.41328	0.32832E-04
0.41838	0.32041E-04
0.42348	0.31213E-04
0.42858	0.30342E-04
0.43368	0.29408E-04
0.43878	0.28406E-04
0.44388	0.27339E-04
0.44899	0.26204E-04
0.50000	0.41903E-09

TABLE 5

CRACKED BUTTRESS DAM L=0.5m Rig.fund. (ADDL-1994)

***** PATH VARIABLE SUMMARY *****

Y (m)	UX (m)
0.00000E+00	0.38937E-04
0.93231	0.22382E-05
1.8646	-0.63318E-06
2.7969	-0.16009E-05
3.7292	-0.23349E-05
4.6615	-0.30310E-05
5.5938	-0.37299E-05
6.5261	-0.44435E-05
7.4584	-0.51762E-05
8.3908	-0.59299E-05
9.3231	-0.67055E-05
10.255	-0.75034E-05
11.188	-0.83241E-05
12.120	-0.91676E-05
13.052	-0.10034E-04
13.985	-0.10924E-04
14.917	-0.11837E-04
15.849	-0.12773E-04
16.782	-0.13732E-04
17.714	-0.14715E-04
18.646	-0.15721E-04
19.578	-0.16750E-04
20.511	-0.17802E-04
21.443	-0.18877E-04
22.375	-0.19975E-04
23.308	-0.21093E-04
24.240	-0.22234E-04
25.172	-0.23395E-04
26.105	-0.24574E-04
27.037	-0.25776E-04
27.969	-0.26991E-04
28.901	-0.28218E-04
29.834	-0.29467E-04
30.766	-0.30713E-04
31.698	-0.31956E-04
32.631	-0.33221E-04
33.563	-0.34475E-04
34.495	-0.35675E-04
35.428	-0.36821E-04
36.360	-0.38046E-04
37.292	-0.39228E-04
38.225	-0.40142E-04
39.157	-0.40786E-04
40.089	-0.41201E-04
41.021	-0.43181E-04
41.954	-0.41721E-04
42.886	-0.36634E-04
43.818	-0.27919E-04
44.751	-0.15577E-04

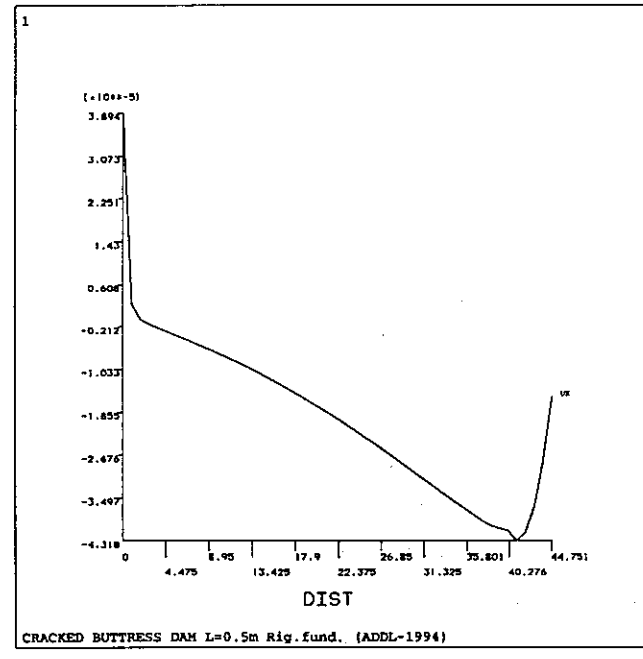

ANSYS 5.0 A
JUN 7 1994
14:24:49
PLOT NO. 2
POST1
PATH PLOT
NOD1=8
NOD2=96

ZV =1
DIST=0.75
XF =0.5
YF =0.5
ZF =0.5
CENTROID HIDDEN

TABLE 6
(12 october 1994)

CRACKED BUTTRESS DAM L=0.5m Def.fund. (ADDL-1994)

***** PATH VARIABLE SUMMARY *****

S	UX
0.00000E+00	0.43654E-04
0.93231	-0.72203E-04
1.8646	-0.15892E-03
2.7969	-0.24276E-03
3.7292	-0.32575E-03
4.6615	-0.40836E-03
5.5938	-0.49075E-03
6.5261	-0.57297E-03
7.4584	-0.65504E-03
8.3908	-0.73697E-03
9.3231	-0.81877E-03
10.255	-0.90041E-03
11.188	-0.98189E-03
12.120	-0.10632E-02
13.052	-0.11443E-02
13.985	-0.12253E-02
14.917	-0.13060E-02
15.849	-0.13865E-02
16.782	-0.14667E-02
17.714	-0.15466E-02
18.646	-0.16263E-02
19.578	-0.17057E-02
20.511	-0.17847E-02
21.443	-0.18635E-02
22.375	-0.19418E-02
23.308	-0.20197E-02
24.240	-0.20973E-02
25.172	-0.21744E-02
26.105	-0.22510E-02
27.037	-0.23272E-02
27.969	-0.24028E-02
28.901	-0.24780E-02
29.834	-0.25525E-02
30.766	-0.26264E-02
31.698	-0.26997E-02
32.631	-0.27724E-02
33.563	-0.28443E-02
34.495	-0.29154E-02
35.428	-0.29857E-02
36.360	-0.30552E-02
37.292	-0.31238E-02
38.225	-0.31915E-02
39.157	-0.32581E-02
40.089	-0.33239E-02
41.021	-0.33892E-02
41.954	-0.34527E-02
42.886	-0.35145E-02
43.818	-0.35745E-02
44.751	-0.36327E-02

TABLE 4
(12 october 1994)

CRACKED BUTTRESS DAM L=2.0m Def.fund. (ADDL-1994)

***** PATH VARIABLE SUMMARY *****

S	UX
0.00000E+00	0.00000E+00
0.21688E-01	0.59380E-05
0.43375E-01	0.11637E-04
0.65063E-01	0.17095E-04
0.86750E-01	0.22315E-04
0.10844	0.27295E-04
0.13013	0.32035E-04
0.15181	0.36536E-04
0.17350	0.40797E-04
0.19519	0.44818E-04
0.21688	0.48600E-04
0.23856	0.52143E-04
0.26025	0.55446E-04
0.28194	0.58509E-04
0.30363	0.61333E-04
0.32531	0.63917E-04
0.34700	0.66262E-04
0.36869	0.68367E-04
0.39038	0.70232E-04
0.41206	0.71858E-04
0.43375	0.73246E-04
0.45544	0.74506E-04
0.47713	0.75710E-04
0.49881	0.76858E-04
0.52050	0.77949E-04
0.54219	0.78984E-04
0.56388	0.79962E-04
0.58556	0.80884E-04
0.60725	0.81750E-04
0.62894	0.82559E-04
0.65063	0.83311E-04
0.67231	0.84007E-04
0.69400	0.84647E-04
0.71569	0.85230E-04
0.73738	0.85757E-04
0.75906	0.86227E-04
0.78075	0.86644E-04
0.80244	0.87019E-04
0.82413	0.87351E-04
0.84582	0.87640E-04
0.86750	0.87886E-04
0.88919	0.88089E-04
0.91088	0.88249E-04
0.93257	0.88366E-04
0.95425	0.88440E-04
0.97594	0.88471E-04
0.99763	0.88459E-04
1.0193	0.88404E-04
1.0410	0.88306E-04
1.0610	0.88182E-04
1.0810	0.88021E-04
1.1009	0.87823E-04
1.1209	0.87589E-04
1.1409	0.87319E-04
1.1609	0.87013E-04
1.1809	0.86670E-04
1.2008	0.86291E-04
1.2208	0.85875E-04
1.2408	0.85423E-04
1.2608	0.84935E-04
1.2808	0.84407E-04
1.3007	0.83836E-04
1.3207	0.83225E-04
1.3407	0.82572E-04
1.3607	0.81877E-04
1.3806	0.81141E-04
1.4006	0.80364E-04
1.4206	0.79545E-04
1.4406	0.78678E-04
1.4606	0.77761E-04
1.4805	0.76792E-04
1.5005	0.75771E-04
1.5205	0.74699E-04
1.5405	0.73576E-04
1.5605	0.72398E-04
1.5804	0.71155E-04
1.6004	0.69844E-04
1.6204	0.68466E-04
1.6404	0.67021E-04
1.6604	0.65506E-04
1.6803	0.63903E-04
1.7003	0.62209E-04
1.7203	0.60423E-04
1.7403	0.58544E-04
1.7603	0.56544E-04
1.7802	0.54412E-04
1.8002	0.52150E-04
1.8202	0.49727E-04
1.8402	0.47112E-04
1.8601	0.44299E-04
1.8801	0.41206E-04
1.9001	0.37795E-04
1.9201	0.33959E-04
1.9401	0.29557E-04
2.0000	0.41857E-09

!
! TABLE 5
!
CRACKED BUTTRESS DAM L=2.0m Rig.fund. (ADDL-1994)

***** PATH VARIABLE SUMMARY *****

Y (m)	UX (m)
0.00000E+00	0.78756E-04
0.89467	0.39483E-04
1.7893	0.17832E-04
2.6840	0.73587E-05
3.5787	0.16596E-05
4.4734	-0.18747E-05
5.3680	-0.43583E-05
6.2627	-0.63003E-05
7.1574	-0.79477E-05
8.0520	-0.94271E-05
8.9467	-0.10807E-04
9.8414	-0.12126E-04
10.736	-0.13407E-04
11.631	-0.14665E-04
12.525	-0.15907E-04
13.420	-0.17141E-04
14.315	-0.18370E-04
15.209	-0.19596E-04
16.104	-0.20822E-04
16.999	-0.22048E-04
17.893	-0.23277E-04
18.788	-0.24507E-04
19.683	-0.25741E-04
20.577	-0.26977E-04
21.472	-0.28216E-04
22.367	-0.29458E-04
23.261	-0.30702E-04
24.156	-0.31949E-04
25.051	-0.33195E-04
25.945	-0.34443E-04
26.840	-0.35690E-04
27.735	-0.36934E-04
28.629	-0.38174E-04
29.524	-0.39409E-04
30.419	-0.40626E-04
31.313	-0.41833E-04
32.208	-0.43027E-04
33.103	-0.44192E-04
33.997	-0.45329E-04
34.892	-0.46422E-04
35.787	-0.47475E-04
36.681	-0.48449E-04
37.576	-0.49275E-04
38.471	-0.49900E-04
39.365	-0.50284E-04
40.260	-0.50146E-04
41.155	-0.49525E-04
42.049	-0.47676E-04
42.944	-0.44277E-04

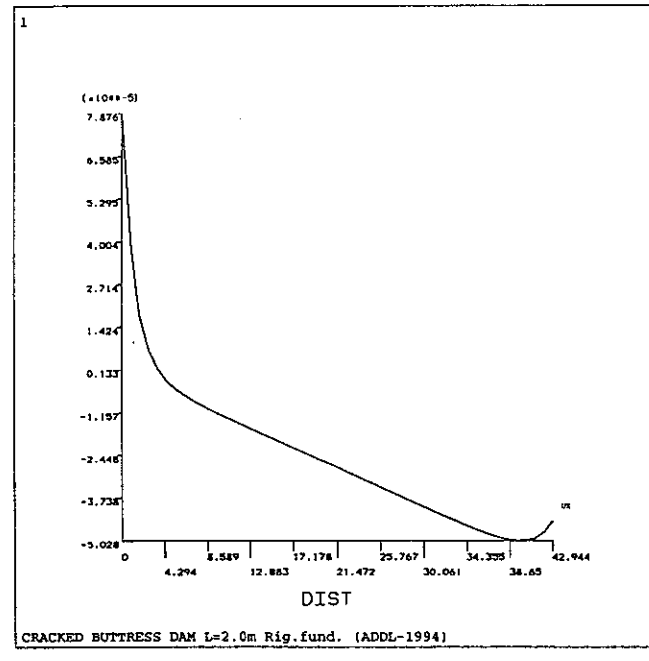

ANSYS 5.0 A
JUN 7 1994
14:25:23
PLOT NO. 2
POST1
PATH PLOT
NOD1=8
NOD2=238

ZV =1
DIST=0.75
XF =0.5
YF =0.5
ZF =0.5
CENTROID HIDDEN

TABLE 6
(12 october 1994)

CRACKED BUTTRESS DAM L=2.0m Def.fund. (ADDL-1994)

***** PATH VARIABLE SUMMARY *****

S	UX
0.00000E+00	0.88306E-04
0.89467	0.13499E-04
1.7893	-0.47605E-04
2.6840	-0.98974E-04
3.5787	-0.14626E-03
4.4734	-0.19161E-03
5.3680	-0.23586E-03
6.2627	-0.27943E-03
7.1574	-0.32253E-03
8.0520	-0.36528E-03
8.9467	-0.40776E-03
9.8414	-0.45002E-03
10.736	-0.49210E-03
11.631	-0.53400E-03
12.525	-0.57574E-03
13.420	-0.61734E-03
14.315	-0.65880E-03
15.209	-0.70011E-03
16.104	-0.74128E-03
16.999	-0.78230E-03
17.893	-0.82318E-03
18.788	-0.86391E-03
19.683	-0.90448E-03
20.577	-0.94488E-03
21.472	-0.98512E-03
22.367	-0.10252E-02
23.261	-0.10651E-02
24.156	-0.11048E-02
25.051	-0.11442E-02
25.945	-0.11835E-02
26.840	-0.12226E-02
27.735	-0.12614E-02
28.629	-0.13000E-02
29.524	-0.13383E-02
30.419	-0.13764E-02
31.313	-0.14142E-02
32.208	-0.14517E-02
33.103	-0.14889E-02
33.997	-0.15258E-02
34.892	-0.15624E-02
35.787	-0.15986E-02
36.681	-0.16344E-02
37.576	-0.16698E-02
38.471	-0.17048E-02
39.365	-0.17393E-02
40.260	-0.17733E-02
41.155	-0.18068E-02
42.049	-0.18396E-02
42.944	-0.18718E-02

TABLE 3

CRACKED BUTTRESS DAM L=10.0m Rig.fund. (ADDL-1994)

***** PATH VARIABLE SUMMARY *****

Y (m)	UX (m)		
0.00000E+00	0.00000E+00	7.3187	0.17052E-03
0.10521	0.84387E-05	7.4219	0.16850E-03
0.21042	0.16671E-04	7.5250	0.16635E-03
0.31562	0.24698E-04	7.6281	0.16407E-03
0.42083	0.32519E-04	7.7312	0.16163E-03
0.52604	0.40133E-04	7.8344	0.15904E-03
0.63125	0.47542E-04	7.9375	0.15629E-03
0.73646	0.54744E-04	8.0406	0.15339E-03
0.84166	0.61741E-04	8.1437	0.15032E-03
0.94687	0.68531E-04	8.2469	0.14706E-03
1.0521	0.75115E-04	8.3500	0.14360E-03
1.1573	0.81494E-04	8.4531	0.13993E-03
1.2625	0.87666E-04	8.5562	0.13605E-03
1.3677	0.93632E-04	8.6594	0.13191E-03
1.4729	0.99392E-04	8.7625	0.12750E-03
1.5781	0.10495E-03	8.8656	0.12282E-03
1.6833	0.11029E-03	8.9687	0.11778E-03
1.7885	0.11544E-03	9.0719	0.11239E-03
1.8937	0.12037E-03	9.1750	0.10656E-03
1.9990	0.12510E-03	9.2781	0.10025E-03
2.1042	0.12953E-03	9.3812	0.93316E-04
2.2094	0.13333E-03	9.4844	0.85642E-04
2.3146	0.13699E-03	9.5875	0.77021E-04
2.4198	0.14051E-03	9.6906	0.67045E-04
2.5250	0.14390E-03	9.7937	0.55015E-04
2.6302	0.14716E-03	9.8969	0.39055E-04
2.7354	0.15028E-03	10.0000	0.41851E-09
2.8406	0.15327E-03		
2.9458	0.15612E-03		
3.0510	0.15884E-03		
3.1562	0.16143E-03		
3.2614	0.16388E-03		
3.3667	0.16620E-03		
3.4719	0.16838E-03		
3.5771	0.17043E-03		
3.6823	0.17235E-03		
3.7875	0.17410E-03		
3.8927	0.17572E-03		
3.9979	0.17723E-03		
4.1031	0.17863E-03		
4.2083	0.17993E-03		
4.3135	0.18112E-03		
4.4187	0.18221E-03		
4.5239	0.18320E-03		
4.6292	0.18408E-03		
4.7344	0.18485E-03		
4.8396	0.18552E-03		
4.9448	0.18609E-03		
5.0500	0.18655E-03		
5.1531	0.18690E-03		
5.2562	0.18715E-03		
5.3594	0.18730E-03		
5.4625	0.18735E-03		
5.5656	0.18730E-03		
5.6687	0.18715E-03		
5.7719	0.18690E-03		
5.8750	0.18656E-03		
5.9781	0.18611E-03		
6.0812	0.18556E-03		
6.1844	0.18492E-03		
6.2875	0.18416E-03		
6.3906	0.18329E-03		
6.4937	0.18232E-03		
6.5969	0.18124E-03		
6.7000	0.18006E-03		
6.8031	0.17876E-03		
6.9062	0.17736E-03		
7.0094	0.17584E-03		
7.1125	0.17419E-03		
7.2156	0.17242E-03		

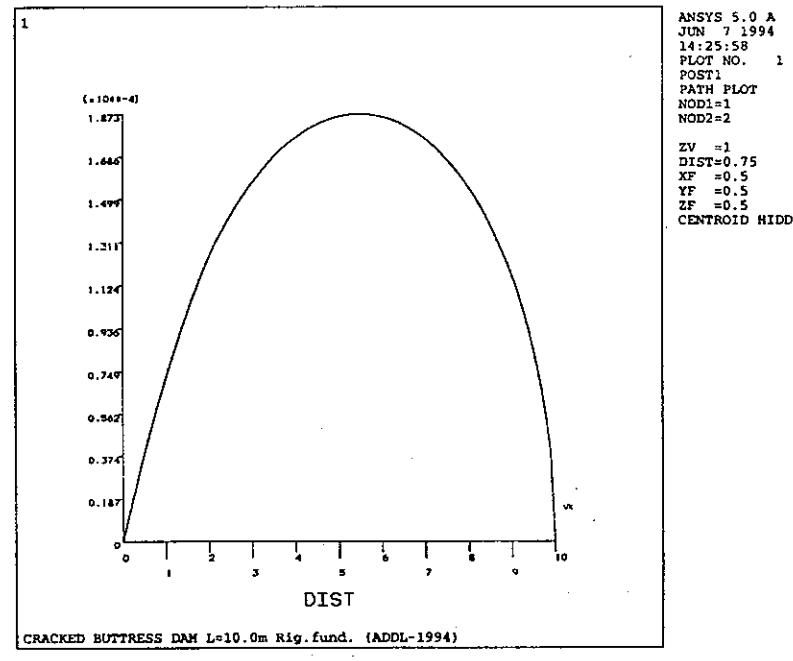

TABLE 4
(12 october 1994)

CRACKED BUTTRESS DAM L=10.0m Def.fund. (ADDL-1994)

***** PATH VARIABLE SUMMARY *****

S	UX
0.00000E+00	0.00000E+00
0.10521	0.15009E-04
0.21042	0.29392E-04
0.31562	0.43149E-04
0.42083	0.56278E-04
0.52604	0.68782E-04
0.63125	0.80659E-04
0.73646	0.91910E-04
0.84166	0.10253E-03
0.94687	0.11253E-03
1.0521	0.12190E-03
1.1573	0.13065E-03
1.2625	0.13877E-03
1.3677	0.14626E-03
1.4729	0.15312E-03
1.5781	0.15936E-03
1.6833	0.16497E-03
1.7885	0.16996E-03
1.8937	0.17432E-03
1.9990	0.17805E-03
2.1042	0.18121E-03
2.2094	0.18427E-03
2.3146	0.18718E-03
2.4198	0.18993E-03
2.5250	0.19253E-03
2.6302	0.19497E-03
2.7354	0.19725E-03
2.8406	0.19938E-03
2.9458	0.20135E-03
3.0510	0.20317E-03
3.1562	0.20483E-03
3.2614	0.20634E-03
3.3667	0.20769E-03
3.4719	0.20888E-03
3.5771	0.20992E-03
3.6823	0.21080E-03
3.7875	0.21155E-03
3.8927	0.21221E-03
3.9979	0.21278E-03
4.1031	0.21325E-03
4.2083	0.21362E-03
4.3135	0.21389E-03
4.4187	0.21406E-03
4.5239	0.21413E-03
4.6292	0.21411E-03
4.7344	0.21398E-03
4.8396	0.21376E-03
4.9448	0.21344E-03
5.0500	0.21302E-03
5.1531	0.21253E-03
5.2562	0.21194E-03
5.3594	0.21127E-03
5.4625	0.21050E-03
5.5656	0.20965E-03
5.6687	0.20871E-03
5.7719	0.20767E-03
5.8750	0.20655E-03
5.9781	0.20533E-03
6.0812	0.20403E-03
6.1844	0.20263E-03
6.2875	0.20114E-03
6.3906	0.19956E-03
6.4937	0.19787E-03
6.5969	0.19609E-03
6.7000	0.19422E-03
6.8031	0.19225E-03
6.9062	0.19018E-03
7.0094	0.18801E-03
7.1125	0.18572E-03
7.2156	0.18332E-03
7.3187	0.18081E-03
7.4219	0.17818E-03
7.5250	0.17544E-03
7.6281	0.17258E-03
7.7312	0.16959E-03
7.8344	0.16645E-03
7.9375	0.16317E-03
8.0406	0.15975E-03
8.1437	0.15618E-03
8.2469	0.15242E-03
8.3500	0.14848E-03
8.4531	0.14436E-03
8.5562	0.14004E-03
8.6594	0.13547E-03
8.7625	0.13066E-03
8.8656	0.12558E-03
8.9687	0.12017E-03
9.0719	0.11442E-03
9.1750	0.10826E-03
9.2781	0.10164E-03
9.3812	0.94419E-04
9.4844	0.86479E-04
9.5875	0.77618E-04
9.6906	0.67432E-04
9.7937	0.55224E-04
9.8969	0.39128E-04
10.0000	0.41848E-09

!
! TABLE 5
!
CRACKED BUTTRESS DAM L=10.0m Rig.fund. (ADDL-1994)

***** PATH VARIABLE SUMMARY *****

Y (m)	UX (m)
0.00000E+00	0.18655E-03
0.60734	0.17137E-03
1.2147	0.15589E-03
1.8220	0.14051E-03
2.4293	0.12553E-03
3.0367	0.11123E-03
3.6440	0.97829E-04
4.2514	0.85440E-04
4.8587	0.73981E-04
5.4660	0.63485E-04
6.0734	0.53875E-04
6.6807	0.45033E-04
7.2880	0.36924E-04
7.8954	0.29467E-04
8.5027	0.22554E-04
9.1100	0.16153E-04
9.7174	0.10211E-04
10.325	0.46455E-05
10.932	-0.55989E-06
11.539	-0.54540E-05
12.147	-0.10077E-04
12.754	-0.14450E-04
13.361	-0.18611E-04
13.969	-0.22574E-04
14.576	-0.26364E-04
15.183	-0.30004E-04
15.791	-0.33504E-04
16.398	-0.36879E-04
17.005	-0.40146E-04
17.613	-0.43314E-04
18.220	-0.46397E-04
18.827	-0.49398E-04
19.435	-0.52322E-04
20.042	-0.55190E-04
20.649	-0.58002E-04
21.257	-0.60760E-04
21.864	-0.63472E-04
22.471	-0.66142E-04
23.079	-0.68776E-04
23.686	-0.71374E-04
24.293	-0.73944E-04
24.901	-0.76486E-04
25.508	-0.79001E-04
26.115	-0.81493E-04
26.723	-0.83964E-04
27.330	-0.86415E-04
27.937	-0.88847E-04
28.545	-0.91259E-04
29.152	-0.93653E-04

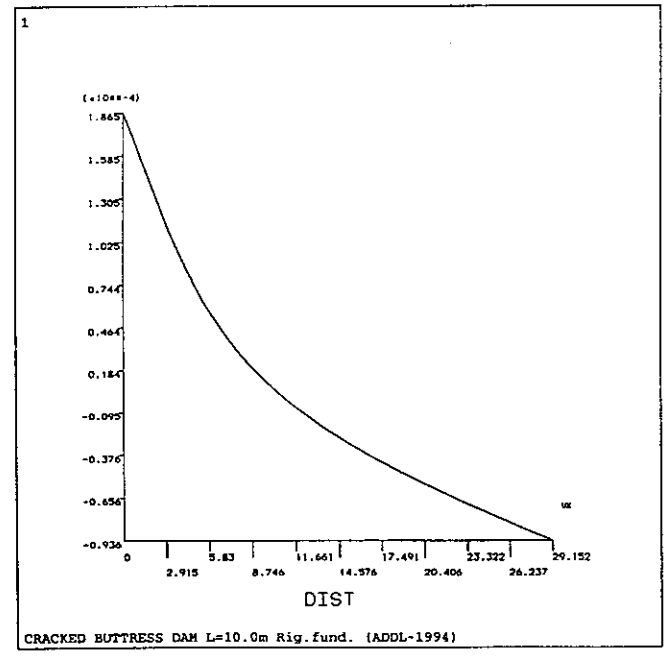

ANSYS 5.0 A
JUN 7 1994
14:26:00
PLOT NO. 2
POST1
PATH PLOT
NOD1=8
NOD2=289

ZV =1
DIST=0.75
XF =0.5
YF =0.5
ZF =0.5
CENTROID HIDDEN

TABLE 6
(12 october 1994)

CRACKED BUTTRESS DAM L=10.0m Def.fund. (ADDL-1994)

***** PATH VARIABLE SUMMARY *****

S	UX
0.00000E+00	0.21302E-03
0.60734	0.18501E-03
1.2147	0.15657E-03
1.8220	0.12790E-03
2.4293	0.99292E-04
3.0367	0.71075E-04
3.6440	0.43494E-04
4.2514	0.16720E-04
4.8587	-0.92840E-05
5.4660	-0.34446E-04
6.0734	-0.58828E-04
6.6807	-0.82528E-04
7.2880	-0.10557E-03
7.8954	-0.12802E-03
8.5027	-0.14998E-03
9.1100	-0.17149E-03
9.7174	-0.19259E-03
10.325	-0.21335E-03
10.932	-0.23379E-03
11.539	-0.25395E-03
12.147	-0.27387E-03
12.754	-0.29357E-03
13.361	-0.31308E-03
13.969	-0.33240E-03
14.576	-0.35157E-03
15.183	-0.37059E-03
15.791	-0.38948E-03
16.398	-0.40825E-03
17.005	-0.42691E-03
17.613	-0.44547E-03
18.220	-0.46393E-03
18.827	-0.48231E-03
19.435	-0.50061E-03
20.042	-0.51883E-03
20.649	-0.53699E-03
21.257	-0.55508E-03
21.864	-0.57310E-03
22.471	-0.59107E-03
23.079	-0.60899E-03
23.686	-0.62685E-03
24.293	-0.64467E-03
24.901	-0.66243E-03
25.508	-0.68016E-03
26.115	-0.69785E-03
26.723	-0.71549E-03
27.330	-0.73310E-03
27.937	-0.75068E-03
28.545	-0.76822E-03
29.152	-0.78573E-03

TABLE 3

CRACKED BUTTRESS DAM L=20.0m Rig.fund. (ADDL-1994)

***** PATH VARIABLE SUMMARY *****

Y (m)	UX (m)		
0.00000E+00	0.00000E+00	14.778	0.25236E-03
0.21580	0.14057E-04	14.978	0.24879E-03
0.43160	0.27755E-04	15.179	0.24505E-03
0.64741	0.41095E-04	15.380	0.24113E-03
0.86321	0.54076E-04	15.581	0.23703E-03
1.0790	0.66699E-04	15.782	0.23271E-03
1.2948	0.78963E-04	15.983	0.22817E-03
1.5106	0.90869E-04	16.184	0.22341E-03
1.7264	0.10242E-03	16.384	0.21842E-03
1.9422	0.11361E-03	16.585	0.21321E-03
2.1580	0.12444E-03	16.786	0.20774E-03
2.3738	0.13491E-03	16.987	0.20197E-03
2.5896	0.14502E-03	17.188	0.19590E-03
2.8054	0.15478E-03	17.389	0.18951E-03
3.0212	0.16418E-03	17.590	0.18281E-03
3.2370	0.17321E-03	17.790	0.17567E-03
3.4528	0.18189E-03	17.991	0.16808E-03
3.6686	0.19022E-03	18.192	0.16004E-03
3.8844	0.19818E-03	18.393	0.15139E-03
4.1002	0.20578E-03	18.594	0.14208E-03
4.3160	0.21303E-03	18.795	0.13198E-03
4.5318	0.21992E-03	18.996	0.12085E-03
4.7476	0.22645E-03	19.197	0.10840E-03
4.9634	0.23262E-03	19.397	0.94160E-04
5.1792	0.23822E-03	19.598	0.77148E-04
5.3950	0.24290E-03	19.799	0.54566E-04
5.6108	0.24736E-03	20.000	0.41830E-09
5.8266	0.25160E-03		
6.0425	0.25563E-03		
6.2583	0.25944E-03		
6.4741	0.26303E-03		
6.6899	0.26640E-03		
6.9057	0.26955E-03		
7.1215	0.27249E-03		
7.3373	0.27521E-03		
7.5531	0.27771E-03		
7.7689	0.27999E-03		
7.9847	0.28205E-03		
8.2005	0.28390E-03		
8.4163	0.28552E-03		
8.6321	0.28693E-03		
8.8479	0.28812E-03		
9.0637	0.28908E-03		
9.2795	0.28984E-03		
9.4953	0.29044E-03		
9.7111	0.29087E-03		
9.9269	0.29114E-03		
10.143	0.29123E-03		
10.358	0.29116E-03		
10.559	0.29095E-03		
10.760	0.29058E-03		
10.961	0.29008E-03		
11.162	0.28942E-03		
11.363	0.28863E-03		
11.564	0.28768E-03		
11.765	0.28660E-03		
11.965	0.28537E-03		
12.166	0.28399E-03		
12.367	0.28247E-03		
12.568	0.28079E-03		
12.769	0.27897E-03		
12.970	0.27700E-03		
13.171	0.27488E-03		
13.371	0.27262E-03		
13.572	0.27020E-03		
13.773	0.26764E-03		
13.974	0.26492E-03		
14.175	0.26204E-03		
14.376	0.25899E-03		
14.577	0.25576E-03		

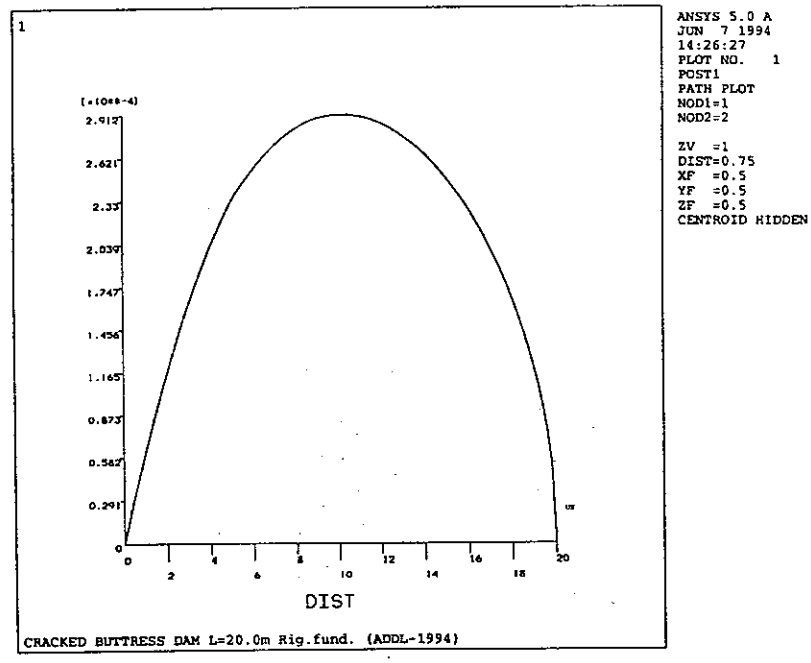

TABLE 4
(12 october 1994)

CRACKED BUTTRESS DAM L=20.0m Def.fund. (ADDL-1994)

***** PATH VARIABLE SUMMARY *****

S	UX		
0.00000E+00	0.00000E+00		
0.21580	0.23910E-04		
0.43160	0.46920E-04		
0.64741	0.69028E-04		
0.86321	0.90235E-04		
1.0790	0.11054E-03		
1.2948	0.12995E-03		
1.5106	0.14845E-03		
1.7264	0.16606E-03	14.978	0.26625E-03
1.9422	0.18276E-03	15.179	0.26145E-03
2.1580	0.19856E-03	15.380	0.25649E-03
2.3738	0.21346E-03	15.581	0.25138E-03
2.5896	0.22746E-03	15.782	0.24608E-03
2.8054	0.24056E-03	15.983	0.24058E-03
3.0212	0.25276E-03	16.184	0.23488E-03
3.2370	0.26406E-03	16.384	0.22899E-03
3.4528	0.27445E-03	16.585	0.22289E-03
3.6686	0.28395E-03	16.786	0.21657E-03
3.8844	0.29254E-03	16.987	0.20997E-03
4.1002	0.30024E-03	17.188	0.20310E-03
4.3160	0.30703E-03	17.389	0.19595E-03
4.5318	0.31292E-03	17.590	0.18850E-03
4.7476	0.31791E-03	17.790	0.18066E-03
4.9634	0.32200E-03	17.991	0.17240E-03
5.1792	0.32531E-03	18.192	0.16372E-03
5.3950	0.32849E-03	18.393	0.15447E-03
5.6108	0.33143E-03	18.594	0.14460E-03
5.8266	0.33413E-03	18.795	0.13397E-03
6.0425	0.33660E-03	18.996	0.12236E-03
6.2583	0.33882E-03	19.197	0.10948E-03
6.4741	0.34081E-03	19.397	0.94861E-04
6.6899	0.34255E-03	19.598	0.77528E-04
6.9057	0.34406E-03	19.799	0.54700E-04
7.1215	0.34533E-03	20.000	0.41828E-09
7.3373	0.34636E-03		
7.5531	0.34715E-03		
7.7689	0.34771E-03		
7.9847	0.34802E-03		
8.2005	0.34810E-03		
8.4163	0.34794E-03		
8.6321	0.34754E-03		
8.8479	0.34690E-03		
9.0637	0.34610E-03		
9.2795	0.34520E-03		
9.4953	0.34414E-03		
9.7111	0.34293E-03		
9.9269	0.34156E-03		
10.143	0.34004E-03		
10.358	0.33837E-03		
10.559	0.33668E-03		
10.760	0.33486E-03		
10.961	0.33290E-03		
11.162	0.33081E-03		
11.363	0.32859E-03		
11.564	0.32623E-03		
11.765	0.32375E-03		
11.965	0.32115E-03		
12.166	0.31842E-03		
12.367	0.31556E-03		
12.568	0.31257E-03		
12.769	0.30945E-03		
12.970	0.30620E-03		
13.171	0.30282E-03		
13.371	0.29931E-03		
13.572	0.29567E-03		
13.773	0.29189E-03		
13.974	0.28799E-03		
14.175	0.28394E-03		
14.376	0.27974E-03		
14.577	0.27540E-03		
14.778	0.27090E-03		

!
! TABLE 5
!
CRACKED BUTTRESS DAM L=20.0m Rig.fund. (ADDL-1994)

***** PATH VARIABLE SUMMARY *****

Y (m)	UX (m)
0.00000E+00	0.29116E-03
0.66132	0.27615E-03
1.3226	0.26083E-03
1.9840	0.24545E-03
2.6453	0.23002E-03
3.3066	0.21467E-03
3.9679	0.19939E-03
4.6292	0.18435E-03
5.2906	0.16967E-03
5.9519	0.15537E-03
6.6132	0.14149E-03
7.2745	0.12802E-03
7.9358	0.11495E-03
8.5972	0.10231E-03
9.2585	0.90157E-04
9.9198	0.78461E-04
10.581	0.67223E-04
11.242	0.56371E-04
11.904	0.45882E-04
12.565	0.35728E-04
13.226	0.25967E-04
13.888	0.16516E-04
14.549	0.73604E-05
15.210	-0.15482E-05
15.872	-0.10161E-04
16.533	-0.18529E-04
17.194	-0.26670E-04
17.856	-0.34621E-04
18.517	-0.42384E-04
19.178	-0.49952E-04
19.840	-0.57354E-04
20.501	-0.64598E-04
21.162	-0.71708E-04
21.824	-0.78686E-04
22.485	-0.85551E-04
23.146	-0.92319E-04
23.808	-0.98978E-04
24.469	-0.10554E-03
25.130	-0.11202E-03
25.792	-0.11842E-03
26.453	-0.12477E-03
27.114	-0.13107E-03
27.775	-0.13732E-03
28.437	-0.14351E-03
29.098	-0.14964E-03
29.759	-0.15576E-03
30.421	-0.16187E-03
31.082	-0.16796E-03
31.743	-0.17404E-03

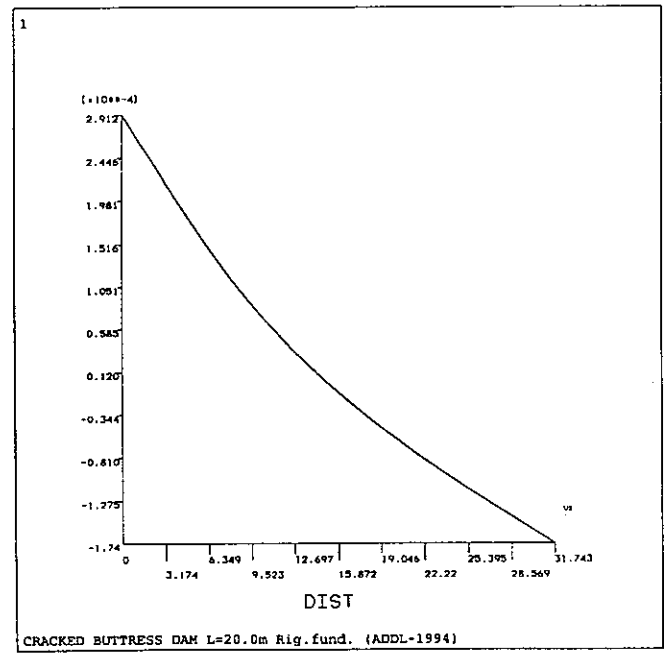

TABLE 6
(12 october 1994)

CRACKED BUTTRESS DAM L=20.0m Def.fund. (ADDL-1994)

***** PATH VARIABLE SUMMARY *****

S	UX
0.00000E+00	0.33837E-03
0.66132	0.30906E-03
1.3226	0.27946E-03
1.9840	0.24968E-03
2.6453	0.21971E-03
3.3066	0.18965E-03
3.9679	0.15953E-03
4.6292	0.12950E-03
5.2906	0.99674E-04
5.9519	0.70101E-04
6.6132	0.40824E-04
7.2745	0.11859E-04
7.9358	-0.16796E-04
8.5972	-0.45098E-04
9.2585	-0.72962E-04
9.9198	-0.10042E-03
10.581	-0.12748E-03
11.242	-0.15419E-03
11.904	-0.18058E-03
12.565	-0.20668E-03
13.226	-0.23241E-03
13.888	-0.25787E-03
14.549	-0.28306E-03
15.210	-0.30804E-03
15.872	-0.33274E-03
16.533	-0.35723E-03
17.194	-0.38152E-03
17.856	-0.40565E-03
18.517	-0.42962E-03
19.178	-0.45342E-03
19.840	-0.47708E-03
20.501	-0.50062E-03
21.162	-0.52404E-03
21.824	-0.54736E-03
22.485	-0.57060E-03
23.146	-0.59377E-03
23.808	-0.61686E-03
24.469	-0.63988E-03
25.130	-0.66285E-03
25.792	-0.68575E-03
26.453	-0.70865E-03
27.114	-0.73155E-03
27.775	-0.75442E-03
28.437	-0.77726E-03
29.098	-0.80009E-03
29.759	-0.82294E-03
30.421	-0.84582E-03
31.082	-0.86875E-03
31.743	-0.89171E-03

TABLE 3

CRACKED BUTTRESS DAM L=40.0m Rig.fund. (ADDL-1994)

***** PATH VARIABLE SUMMARY *****

Y (m)	UX (m)
0.00000E+00	0.00000E+00
0.41335	0.35515E-04
0.82669	0.69658E-04
1.2400	0.10243E-03
1.6534	0.13383E-03
2.0667	0.16385E-03
2.4801	0.19250E-03
2.8934	0.21978E-03
3.3068	0.24569E-03
3.7201	0.27022E-03
4.1335	0.29339E-03
4.5468	0.31518E-03
4.9601	0.33559E-03
5.3735	0.35302E-03
5.7868	0.36859E-03
6.2002	0.38339E-03
6.6135	0.39744E-03
7.0269	0.41073E-03
7.4402	0.42326E-03
7.8536	0.43503E-03
8.2669	0.44604E-03
8.6803	0.45629E-03
9.0936	0.46578E-03
9.5069	0.47452E-03
9.9203	0.48246E-03
10.334	0.48986E-03
10.747	0.49674E-03
11.160	0.50311E-03
11.574	0.50897E-03
11.987	0.51431E-03
12.400	0.51914E-03
12.814	0.52345E-03
13.227	0.52725E-03
13.640	0.53056E-03
14.054	0.53346E-03
14.467	0.53597E-03
14.880	0.53809E-03
15.294	0.53982E-03
15.707	0.54117E-03
16.120	0.54212E-03
16.534	0.54268E-03
16.947	0.54286E-03
17.361	0.54271E-03
17.774	0.54223E-03
18.187	0.54144E-03
18.601	0.54033E-03
19.014	0.53890E-03
19.427	0.53715E-03
19.841	0.53508E-03
20.261	0.53269E-03
20.681	0.53001E-03
21.101	0.52704E-03
21.521	0.52379E-03
21.941	0.52026E-03
22.361	0.51644E-03
22.781	0.51236E-03
23.200	0.50802E-03
23.620	0.50342E-03
24.040	0.49856E-03
24.460	0.49345E-03
24.880	0.48809E-03
25.300	0.48248E-03
25.720	0.47664E-03
26.140	0.47055E-03
26.560	0.46422E-03
26.980	0.45765E-03
27.400	0.45084E-03
27.820	0.44380E-03
28.240	0.43652E-03
28.660	0.42900E-03
29.080	0.42123E-03
29.500	0.41322E-03
29.920	0.40497E-03
30.340	0.39647E-03
30.760	0.38770E-03
31.180	0.37868E-03
31.600	0.36938E-03
32.020	0.35979E-03
32.440	0.34992E-03
32.860	0.33973E-03
33.280	0.32922E-03
33.700	0.31836E-03
34.120	0.30712E-03
34.540	0.29548E-03
34.960	0.28340E-03
35.380	0.27082E-03
35.800	0.25770E-03
36.220	0.24395E-03
36.640	0.22947E-03
37.060	0.21412E-03
37.480	0.19772E-03
37.900	0.18000E-03
38.320	0.16053E-03
38.740	0.13861E-03
39.160	0.11282E-03
39.580	0.79485E-04
40.000	0.41822E-09

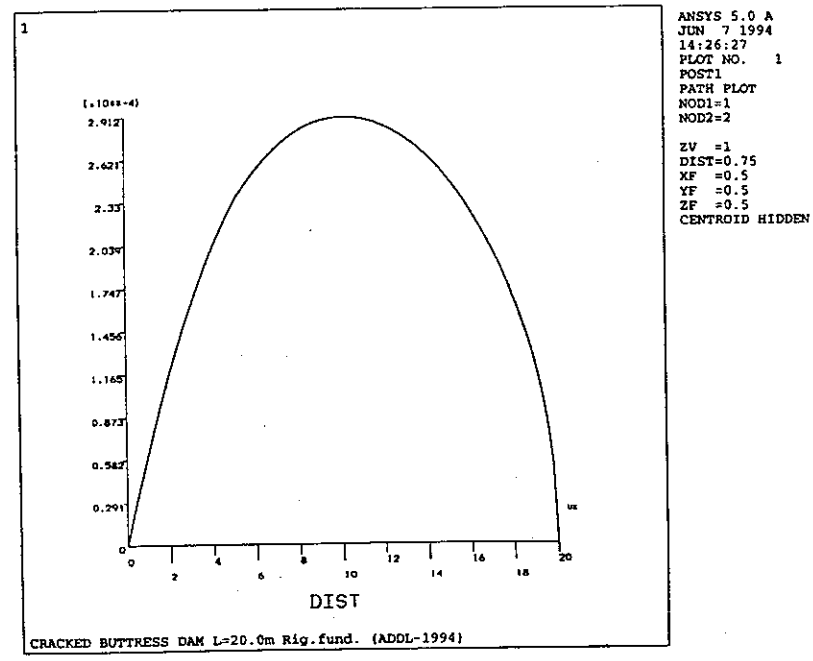

TABLE 4
(12 october 1994)

CRACKED BUTTRESS DAM L=40.0m Def.fund. (ADDL-1994)

***** PATH VARIABLE SUMMARY *****

S	UX
0.00000E+00	0.00000E+00
0.41335	0.77669E-04
0.82669	0.15010E-03
1.2400	0.21729E-03
1.6534	0.27925E-03
2.0667	0.33596E-03
2.4801	0.38744E-03
2.8934	0.43368E-03
3.3068	0.47468E-03
3.7201	0.51044E-03
4.1335	0.54097E-03
4.5468	0.56625E-03
4.9601	0.58630E-03
5.3735	0.60206E-03
5.7868	0.61654E-03
6.2002	0.62995E-03
6.6135	0.64230E-03
7.0269	0.65359E-03
7.4402	0.66381E-03
7.8536	0.67297E-03
8.2669	0.68107E-03
8.6803	0.68810E-03
9.0936	0.69407E-03
9.5069	0.69898E-03
9.9203	0.70303E-03
10.334	0.70651E-03
10.747	0.70942E-03
11.160	0.71176E-03
11.574	0.71354E-03
11.987	0.71474E-03
12.400	0.71538E-03
12.814	0.71544E-03
13.227	0.71494E-03
13.640	0.71391E-03
14.054	0.71252E-03
14.467	0.71073E-03
14.880	0.70855E-03
15.294	0.70598E-03
15.707	0.70301E-03
16.120	0.69966E-03
16.534	0.69591E-03
16.947	0.69178E-03
17.361	0.68738E-03
17.774	0.68269E-03
18.187	0.67771E-03
18.601	0.67244E-03
19.014	0.66689E-03
19.427	0.66104E-03
19.841	0.65490E-03
20.261	0.64844E-03
20.681	0.64173E-03
21.101	0.63480E-03
21.521	0.62762E-03
21.941	0.62022E-03
22.361	0.61257E-03
22.781	0.60472E-03
23.200	0.59668E-03
23.620	0.58844E-03
24.040	0.58000E-03
24.460	0.57136E-03
24.880	0.56254E-03
25.300	0.55354E-03
25.720	0.54436E-03
26.140	0.53501E-03
26.560	0.52548E-03
26.980	0.51578E-03
27.400	0.50591E-03
27.820	0.49587E-03
28.240	0.48567E-03
28.660	0.47530E-03
29.080	0.46476E-03
29.500	0.45404E-03
29.920	0.44316E-03
30.340	0.43210E-03
30.760	0.42085E-03
31.180	0.40941E-03
31.600	0.39778E-03
32.020	0.38594E-03
32.440	0.37389E-03
32.860	0.36160E-03
33.280	0.34907E-03
33.700	0.33627E-03
34.120	0.32317E-03
34.540	0.30975E-03
34.960	0.29598E-03
35.380	0.28179E-03
35.800	0.26715E-03
36.220	0.25196E-03
36.640	0.23614E-03
37.060	0.21954E-03
37.480	0.20200E-03
37.900	0.18323E-03
38.320	0.16283E-03
38.740	0.14009E-03
39.160	0.11362E-03
39.580	0.79766E-04
40.000	0.41821E-09

!
! TABLE 5
!
CRACKED BUTTRESS DAM L=40.0m Rig.fund. (ADDL-1994)

***** PATH VARIABLE SUMMARY *****

Y (m)	UX (m)
0.00000E+00	0.53508E-03
0.72917	0.51442E-03
1.4583	0.49363E-03
2.1875	0.47272E-03
2.9167	0.45172E-03
3.6459	0.43066E-03
4.3750	0.40957E-03
5.1042	0.38846E-03
5.8334	0.36736E-03
6.5626	0.34631E-03
7.2917	0.32533E-03
8.0209	0.30444E-03
8.7501	0.28366E-03
9.4793	0.26303E-03
10.208	0.24253E-03
10.938	0.22219E-03
11.667	0.20205E-03
12.396	0.18210E-03
13.125	0.16234E-03
13.854	0.14276E-03
14.583	0.12340E-03
15.313	0.10423E-03
16.042	0.85246E-04
16.771	0.66442E-04
17.500	0.47833E-04
18.229	0.29387E-04
18.959	0.11139E-04
19.688	-0.69084E-05
20.417	-0.24770E-04
21.146	-0.42521E-04
21.875	-0.60173E-04
22.604	-0.77731E-04
23.334	-0.95152E-04
24.063	-0.11242E-03
24.792	-0.12962E-03
25.521	-0.14677E-03
26.250	-0.16388E-03
26.979	-0.18101E-03
27.709	-0.19799E-03
28.438	-0.21499E-03
29.167	-0.23200E-03
29.896	-0.24904E-03
30.625	-0.26612E-03
31.354	-0.28326E-03
32.084	-0.30043E-03
32.813	-0.31772E-03
33.542	-0.33512E-03
34.271	-0.35264E-03
35.000	-0.37028E-03

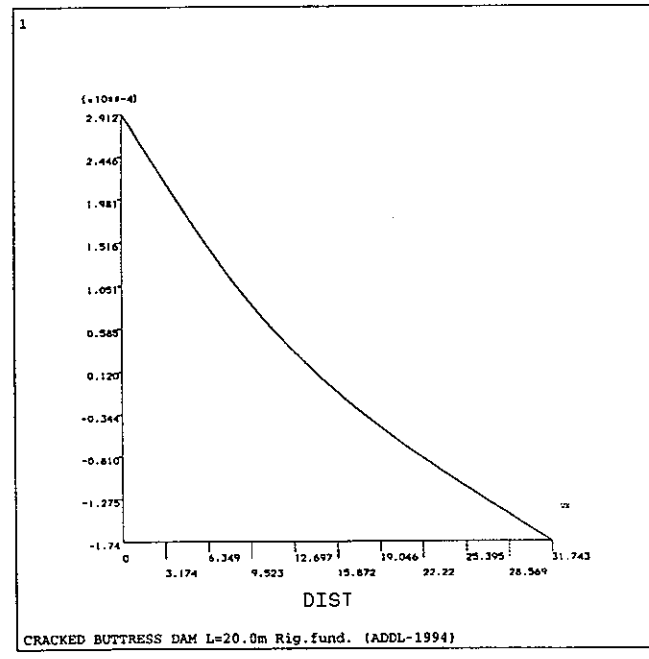

TABLE 6
(12 october 1994)

CRACKED BUTTRESS DAM L=40.0m Def.fund. (ADDL-1994)

***** PATH VARIABLE SUMMARY *****

S	UX
0.00000E+00	0.65490E-03
0.72917	0.61210E-03
1.4583	0.56915E-03
2.1875	0.52606E-03
2.9167	0.48282E-03
3.6459	0.43946E-03
4.3750	0.39597E-03
5.1042	0.35237E-03
5.8334	0.30869E-03
6.5626	0.26493E-03
7.2917	0.22114E-03
8.0209	0.17731E-03
8.7501	0.13349E-03
9.4793	0.89691E-04
10.208	0.45925E-04
10.938	0.22212E-05
11.667	-0.41386E-04
12.396	-0.84893E-04
13.125	-0.12829E-03
13.854	-0.17160E-03
14.583	-0.21476E-03
15.313	-0.25780E-03
16.042	-0.30073E-03
16.771	-0.34355E-03
17.500	-0.38622E-03
18.229	-0.42879E-03
18.959	-0.47121E-03
19.688	-0.51347E-03
20.417	-0.55559E-03
21.146	-0.59765E-03
21.875	-0.63965E-03
22.604	-0.68162E-03
23.334	-0.72348E-03
24.063	-0.76522E-03
24.792	-0.80693E-03
25.521	-0.84863E-03
26.250	-0.89032E-03
26.979	-0.93209E-03
27.709	-0.97374E-03
28.438	-0.10154E-02
29.167	-0.10571E-02
29.896	-0.10989E-02
30.625	-0.11408E-02
31.354	-0.11827E-02
32.084	-0.12247E-02
32.813	-0.12668E-02
33.542	-0.13090E-02
34.271	-0.13514E-02
35.000	-0.13939E-02

EVALUATION OF THE CRITICAL TEMPERATURE DECREASE IN A CRACKED BUTTRESS DAM THROUGH THE COHESIVE CRACK MODEL (*)

F. BARPI and S. VALENTE, *Politecnico di Torino, 10129 Torino, Italy*

INTRODUCTION

The numerical analyses described in this paper are carried out on problems proposed by ICOLD (International Committee on Large Dams), "ad hoc" Committee on Computational Aspects of Dam Analysis and Design. A uniform temperature decrease is assumed to be critical when it causes the propagation of a pre-existing (stress free) crack. Two different models are considered for the crack behaviour: the linear elastic fracture mechanics (abbreviated as LEFM) and the cohesive (or fictitious) crack model. The second model was first proposed by Barenblatt [1] and, independently, by Dugdale [2] for metals. Later on it was applied to concrete by Hillerborg [3] and Carpinteri [4] in order to solve Mode I crack propagation problems. Recently it was extended to Mixed-Mode problems (Mode I and II) by Carpinteri and Valente [5, 6]. Applications of the cohesive crack model to dam were presented by Carpinteri et al. [7] and Valente et al. [8]. Two different foundation schemes are considered: the rigid one and the deformable one.

1.0 GEOMETRICAL DATA AND BOUNDARY CONDITIONS

The main geometrical data are reported in figure 1. The analyses are carried out with reference to the following pre-existing (stress free) crack lengths L:

0.5 m, 2 m, 10 m , 20 m, 40 m.

With reference to the deformable foundation scheme, a semicircular rock zone with a radius of 300 m is taken into account. On the semicircular border of the rock zone a fixed boundary condition is applied. A plane stress condition is assumed for the buttress and a plane strain condition for the foundation. The elements are linear-strain six-node triangles. In order to use the cohesive model the mesh originally proposed by ICOLD has been changed (see for example figure 5).

2.0 PHYSICAL-MECHANICAL PARAMETERS

The following data are assumed in the numerical analyses:

2.1 Concrete:

Young's elastic modulus	E_c	=	30,000	MPa
Poisson's ratio	ν	=	0.16	
Thermal dilatation coefficient	α	=	10^{-5}	$°C^{-1}$
Fracture energy	$\mathcal{G}_F$	=	176.33	N/m
Toughness	K_{IC}	=	$2.3\ 10^6$	$Nm^{-3/2}$
Ultimate tensile strength	σ_u	=	2.4	MPa

(*) Paper submitted for publication in the proceeding of the: "Third ICOLD Benchmark Workshop on Numerical Analysis of Dams", Paris (France), September 29-30, 1994

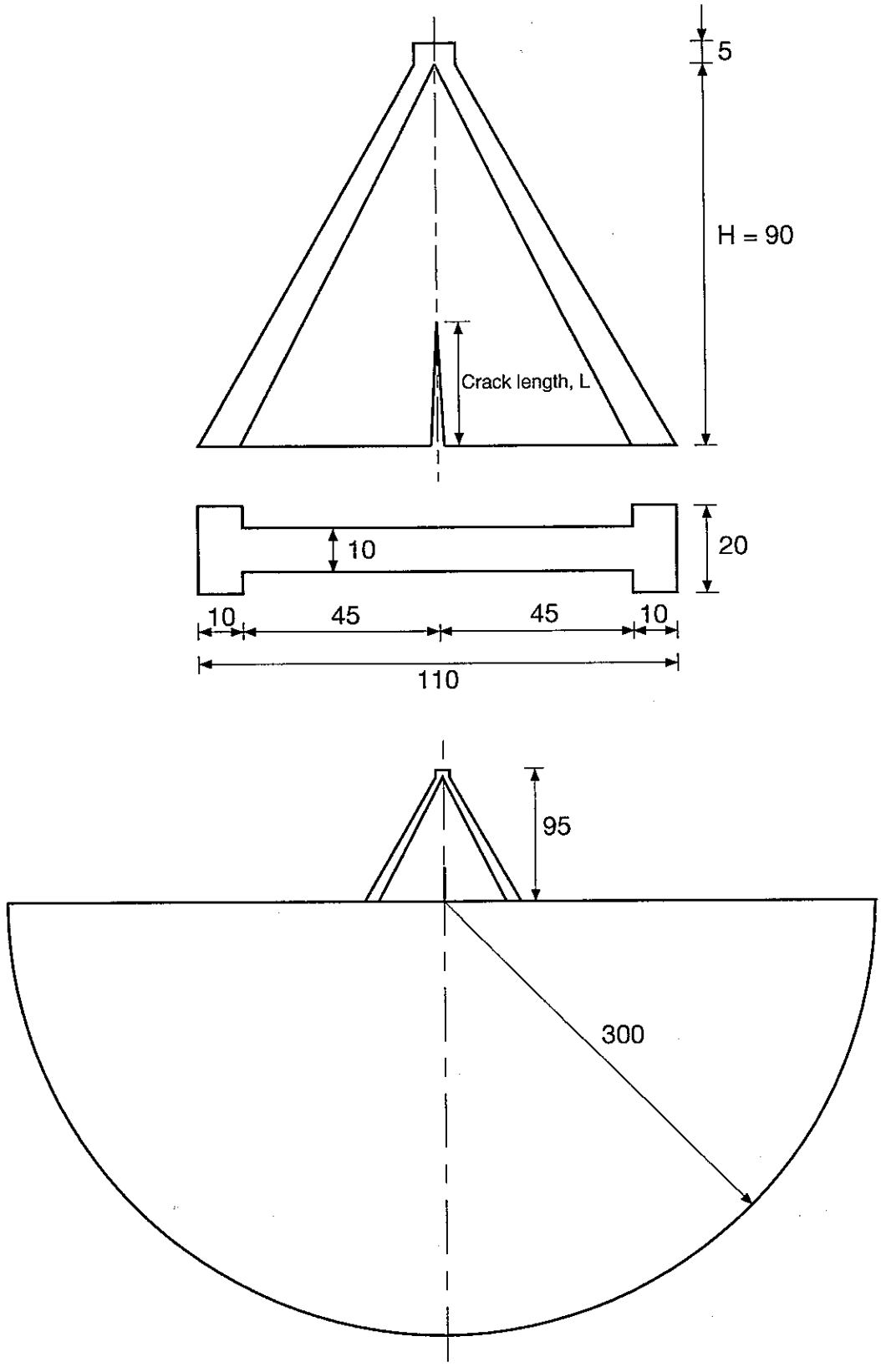

Fig. 1 - Geometrical data, rigid and deformable foundation.

2.2 Rock :

Young's elastic modulus	E_r	=	10,000 MPa
Poisson's ratio	ν	=	0.2

3.0 LOADING CONDITION

A uniform thermal distribution in the dam (both slab and web) is assumed. This is to be intended as a variation with reference to the average (unstressed) state, which is assumed conventionally to correspond to a uniform temperature of 0 °C.
The foundation is assumed to remain at constant average (0 °C) temperature.

4.0 LINEAR ELASTIC FRACTURE MECHANICS

For the analysis executed according to the Linear Elastic Fracture Mechanics (LEFM) hypotheses the so called "Quarter Point Displacement Technique" (QPDT) is used [9, 10]. With reference to symbols indicated in figure 2b, it results:

$$K_I = \frac{G}{k+1}\sqrt{\frac{8\pi}{\ell}}(v_{B2} - v_{B1}), \qquad (1)$$

where:

K_I : Mode I stress intensity factor,

$G = \frac{E_c}{1+\nu}$: tangential elastic modulus,

$k = \frac{3-\nu}{1+\nu}$: for plane stress condition.

According to LEFM, $K_I = K_{IC}$ is assumed as the critical condition.

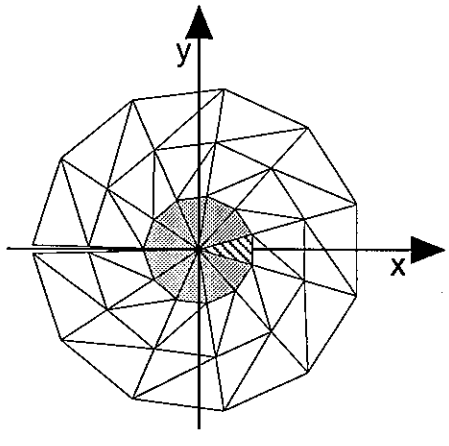

Fig. 2a - The centre of dashed element is taken as the tip of the fictitious crack.

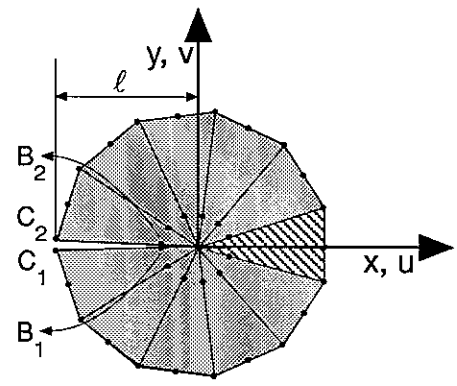

Fig. 2b - Quarter-point elements around the crack tip.

5.0 THE COHESIVE CRACK MODEL

The cohesive model rests on assumption that as an extension of the real crack a fictitious crack (also referred to as process zone) is formed where the material, albeit damaged, is still able to transfer stresses which are decreasing functions of the relative displacement discontinuity (COD) as shown in figures 3, 4. The fictitious crack grows perpendicularly to the principal tensile stress at the point where the latter reaches the material tensile strength, σ_u. Figure 3 introduce the concepts and symbols (ℓ_f, ℓ_r) that are typical of the cohesive crack model [3 to 8, 11, 12].

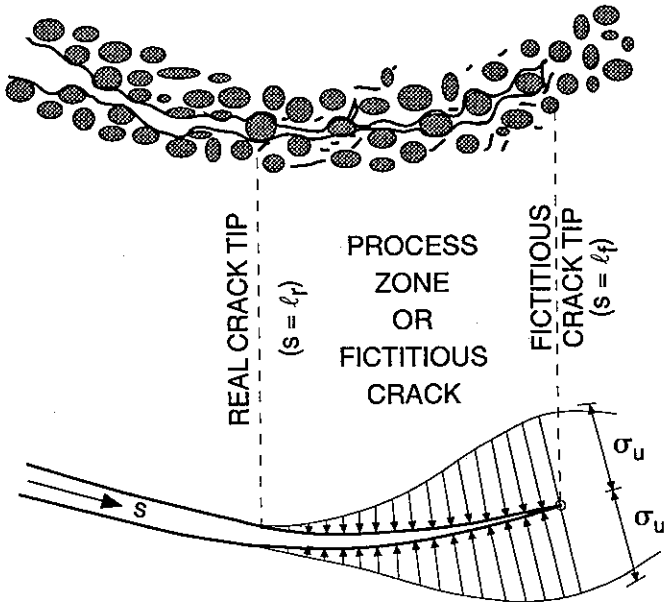

Fig. 3 - The cohesive model represents the process zone as a fictitious extension of the real crack.

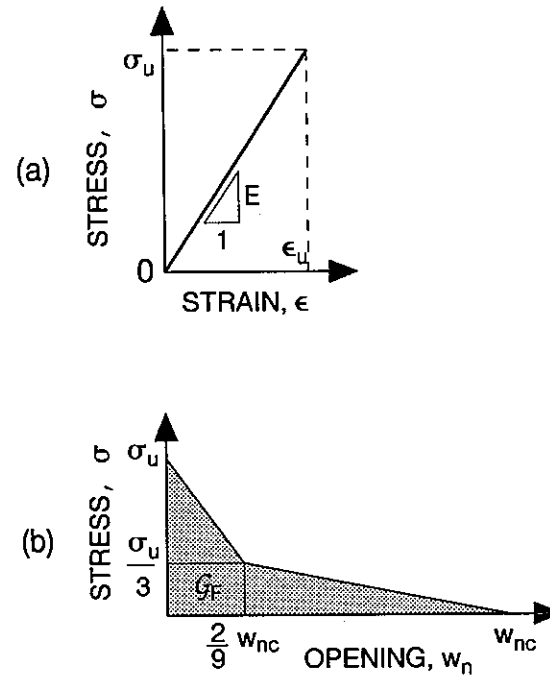

Fig. 4 - Double constitutive law: (a) for the undamaged material; b) for the fictitious crack.

According to the finite element method, keeping in mind that both constitutive laws are linear, by taking the unknowns to be the n nodal displacements, **u**, it is possible to write the equilibrium conditions through the virtual work equation as follows [5, 6]:

$$\mathbf{Lu} = \mathbf{F}_1 + T\,\mathbf{F}_2, \tag{2}$$

where:

L: symmetrical (n x n) matrix assembled by bringing together contributions from both constitutive laws,
$\mathbf{F}_1$: vector depending on σ_u, ℓ_f and ℓ_r,
$\mathbf{F}_2$: external load vector corresponding to $T = 1$,
T : decrease in temperature, defined in section 3.0.

During the evolutionary process, matrix **L** remains always definite positive, and ∞^1 equilibrated and congruent configurations, **u**, are obtained, one for each value of T:

$$\mathbf{u}_1 = \mathbf{L}^{-1}\mathbf{F}_1,\ \mathbf{u}_2 = \mathbf{L}^{-1}\mathbf{F}_2,\ \mathbf{u}_1 + T\mathbf{u}_2,\ \mathbf{u} = \mathbf{u}\,(T, \ell_r, \ell_f). \tag{3}$$

By denoting with σ_{x1} and σ_{x2} the horizontal stresses at the fictitious crack tip related to $\mathbf{u}_1$ and $\mathbf{u}_2$ respectively, the fictitious crack growth condition turns out to be:

$$\sigma_x = \sigma_{x1} + T\,\sigma_{x2} = \sigma_u\,. \tag{4}$$

The length of the fictitious crack (ℓ_f) is surely an increasing monotone function of time during the irreversible cracking process, and, for this reason, as suggested by Carpinteri and Valente [5, 6], it is assumed as the control variable for numerical simulations. Therefore, all the remaining unknowns (**u**, T, ℓ_r) are regarded as dependent variables, which are determined through eqs. (3), (4), and the bilinear softening law shown in fig. 4. Since $\mathbf{L} = \mathbf{L}(T, \ell_r)$ the solution is achieved through an iterative cycle on eqs. (3) and (4).
At each step of the evolutionary process, the crack opening displacement (COD) turns out to be a monotonic increasing function of time. Consequently, the softening law requires no unloading hypotheses.
The centre of the dashed element in figure 2a is taken to coincide with the fictitious crack tip. At the beginning of the fictitious crack propagation process, the real crack is absent. It begins to grow later on, when the decrease in temperature reaches the value T_{c1}. During the evolutionary process, the decrease in temperature can reach a peak value T_{c2}.
For each value of L, the following temperature has been assumed as the critical value:

$$T_c = \min\,(T_{c1},\ T_{c2})\,. \tag{5}$$

The values of T_c, obtained according to eq. (5), are listed in tables 1, 2, 3, 4 together with the maximum half-value of the crack opening displacements (dmax) and the level (ydmax) at which it occurs. According to the heuristic conclusions published in [10] since σ_x tends to σ_u when L tends to 40 m it is possible that a bifurcation of the equilibrium path by break down of symmetry occurs. Therefore the case L = 40 m requires further analyses.
Evolutionary analyses were carried out with a program (CCRAP, Cohesive CRAck Program) specially developed by the Authors to study the propagation of a fictitious crack in Mixed-Mode conditions. This program uses a re-meshing technique which is based on the rotary-translation of a finite element rosette [5 to 8, 11, 12] (see figure 2). In this case, to ensure symmetrical conditions, the crack's vertical growth has been imposed *a priori.*
The simulations, based on LEFM, were also carried out with the CCRAP program, by setting $\ell_r = \ell_f$, arranging the nodes around the tip of the crack as shown in figure 2b, and using eq. (1). Since both models are based on the same initial mesh, the length of the crack taken into account in LEFM analyses is seen to correspond to the nominal length L plus the radius of the rosette. Since the latter is 3 cm, it may be concluded that this error decreases by increasing L.
For each case being considered, figures 8, 9, 10, 11 and 12 show the diagrams relating to the semi-openings of the crack and the horizontal displacements measured on a given horizontal alignment (displacements referred to half the model).

6.0 HARDWARE USED

The analyses were performed without taking advantage of the structure's symmetrical configuration. The degrees of freedom considered were ca 6,600 for problems with a rigid foundation and ca 9,200 for those with a deformable foundation. Each single step performed for LEFM analyses required 30 sec. on a HP 720 computer for the problems with 6,600 d.o.f.'s and about 90 sec. for those with 9,200 d.o.f.'s.

7.0 CONCLUSIONS

- The cohesive crack model is more conservative than the linear elastic fracture mechanics, when $\frac{\partial K_I}{\partial L} > 0$, the opposite occurs when $\frac{\partial K_I}{\partial L} < 0$.

  In the case analysed the first condition occurs for small value of L, the second for large value of L.
- As shown in [4], the differences between the two models tends to zero when the brittleness number $s_E = \frac{\mathcal{G}_F}{\sigma_u H}$ tends to zero.
- In case of rigid foundation with L = 0.5, the value of T_c, predicted according to the cohesive crack model, is 20 % less than the same value predicted according to LEFM.
- In the case of rigid foundation T_c is lower than in case of deformable foundation.
- Further analyses are necessary in order to compute the T_c reduction due to the following phenomena:
  - creep ,
  - size-effect on σ_u,
  - bifurcation by break down of symmetry [12],

  and T_c increment due to the following phenomena :
  - size-effect on $\mathcal{G}_F$.
- Horizontal displacements determined on the basis of the cohesive crack model are always higher than those worked out from LEFM.
- It has been observed numerically that the length of the process zone:
  - increases with increasing notch depth (L),
  - when the deformable foundation is taken into account it decreases with constant notch depth.

Table 1 - Cohesive crack model

RIGID FOUNDATIONS			
L m	T_c °C	dmax mm	ydmax m
0.5	8.04	0.03645	0.351
2	4.63	0.08543	1.406
10	2.83	0.19974	6.249
20	2.58	0.30386	10.000
40	3.19	0.56171	15.000

Table 2 - LEFM

RIGID FOUNDATIONS			
L m	T_c °C	dmax mm	ydmax m
0.5	9.98	0.00405	0.311
2	5.27	0.01483	1.172
10	2.62	0.06329	4.999
20	2.18	0.11243	10.000
40	2.46	0.17347	15.000

Table 3 - Cohesive crack model

DEFORMABLE FOUNDATIONS			
L m	T_c °C	dmax mm	ydmax m
0.5	13.76	0.04238	0.275
2	8.44	0.10239	1.250
10	5.00	0.23693	5.004
20	4.80	0.36906	10.003
40	6.41	0.75679	15.002

Table 4 - LEFM

DEFORMABLE FOUNDATIONS			
L m	T_c °C	dmax mm	ydmax m
0.5	16.16	0.00273	0.275
2	8.71	0.00989	1.017
10	4.45	0.04254	5.004
20	3.91	0.07341	7.503
40	4.89	0.11568	15.002

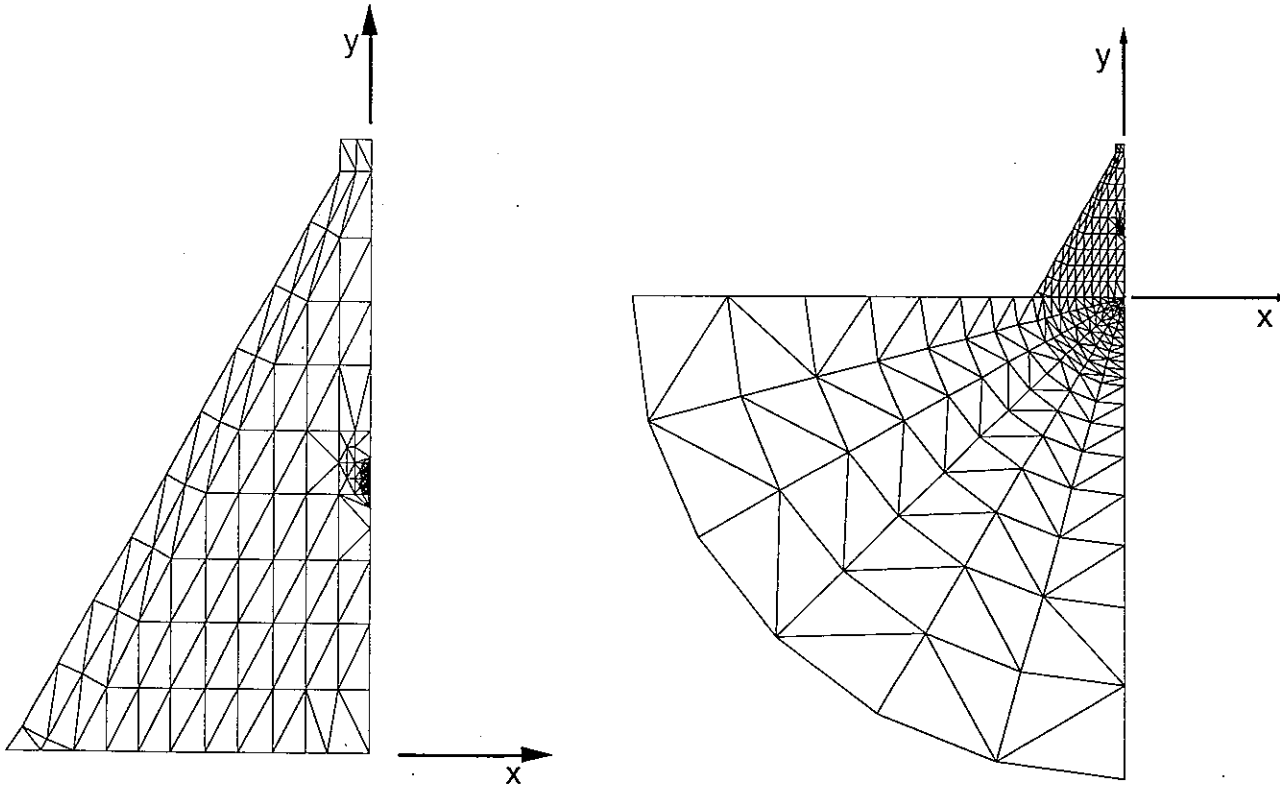

Fig. 5 - Finite element mesh used for L = 40m in the case of rigid and deformable foundation (referred to half the model).

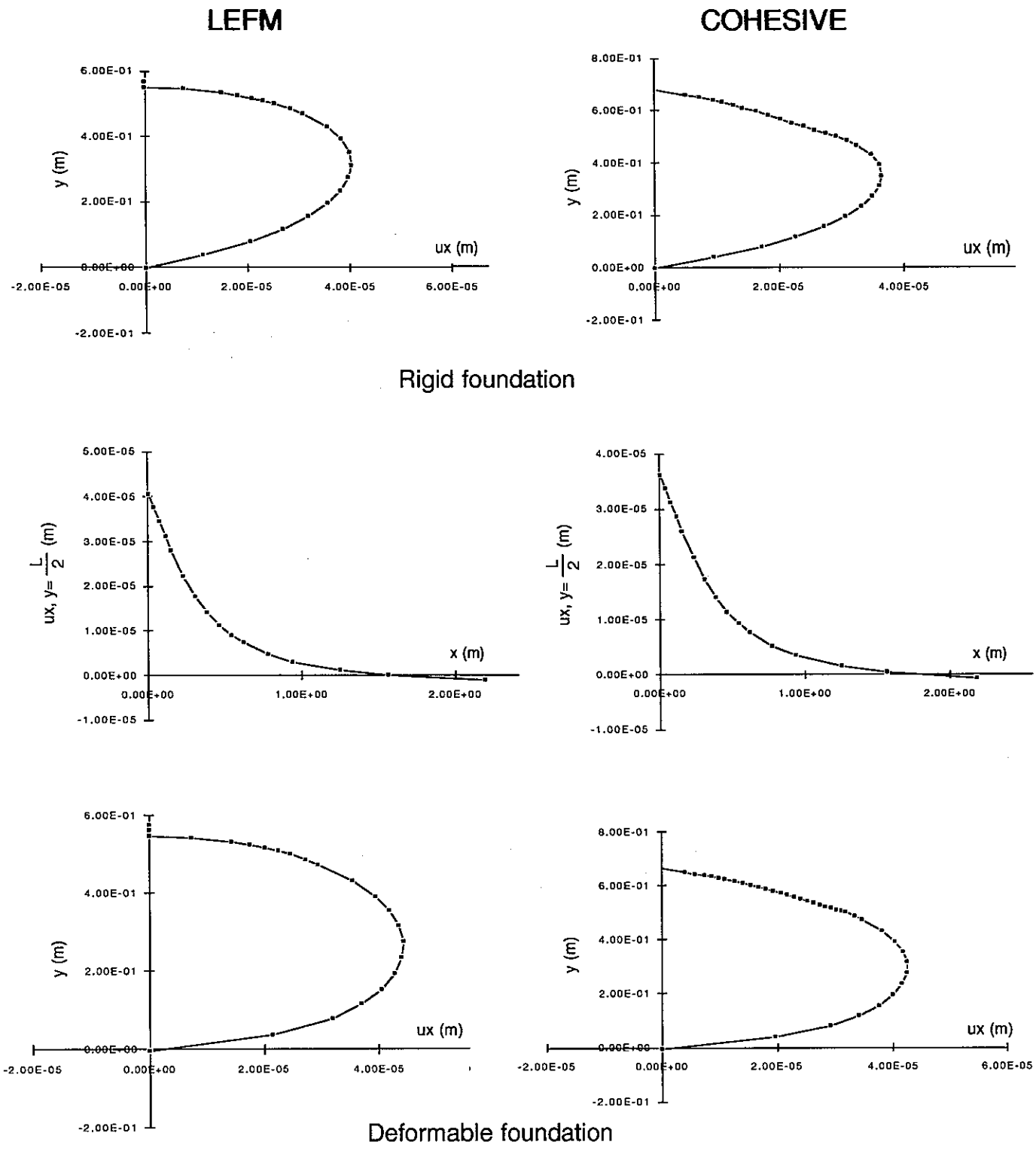

Fig. 8 - Crack length 0.5m.

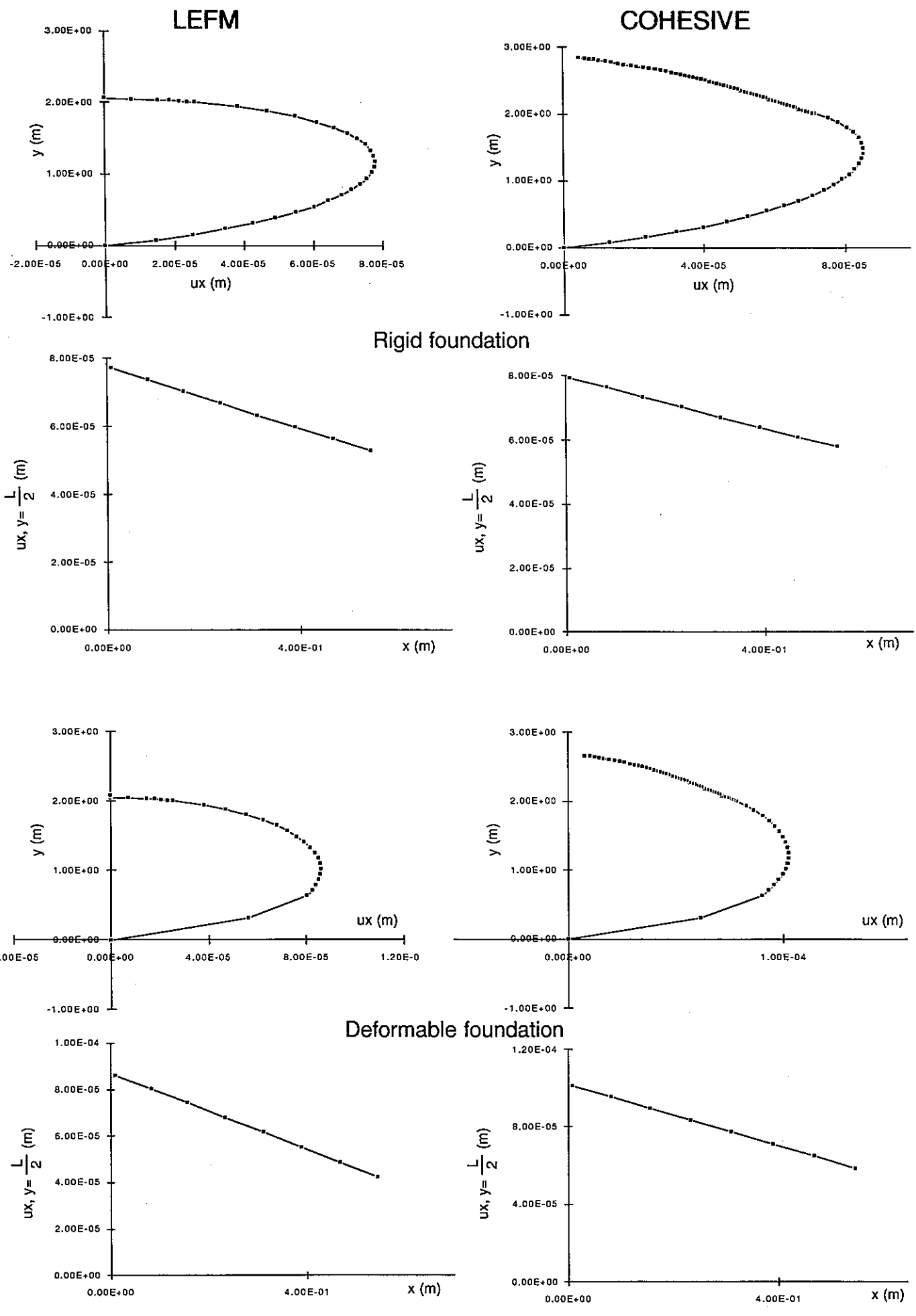

Fig. 9 - Crack length 2m.

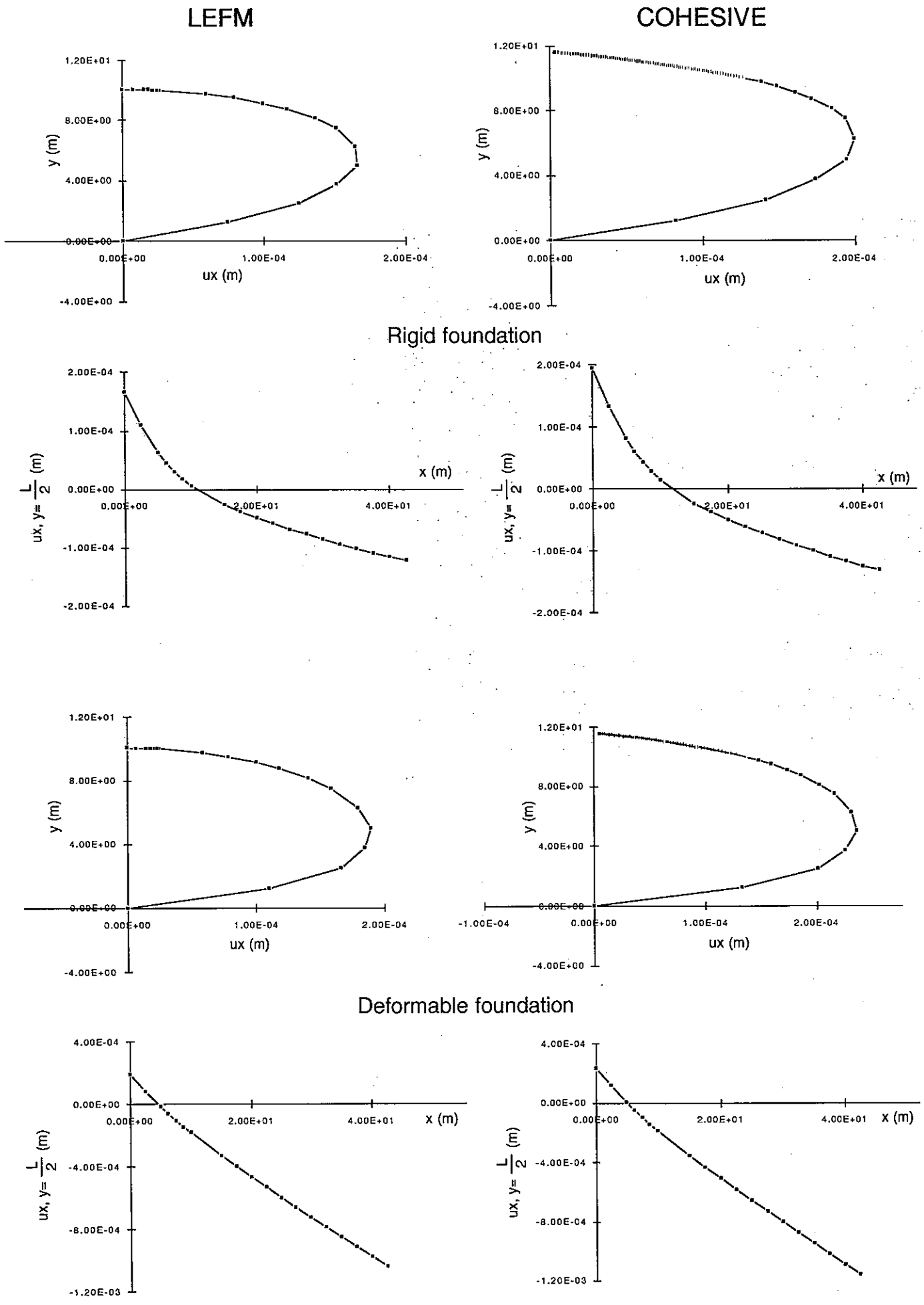

Fig. 10 - Crack length 10m.

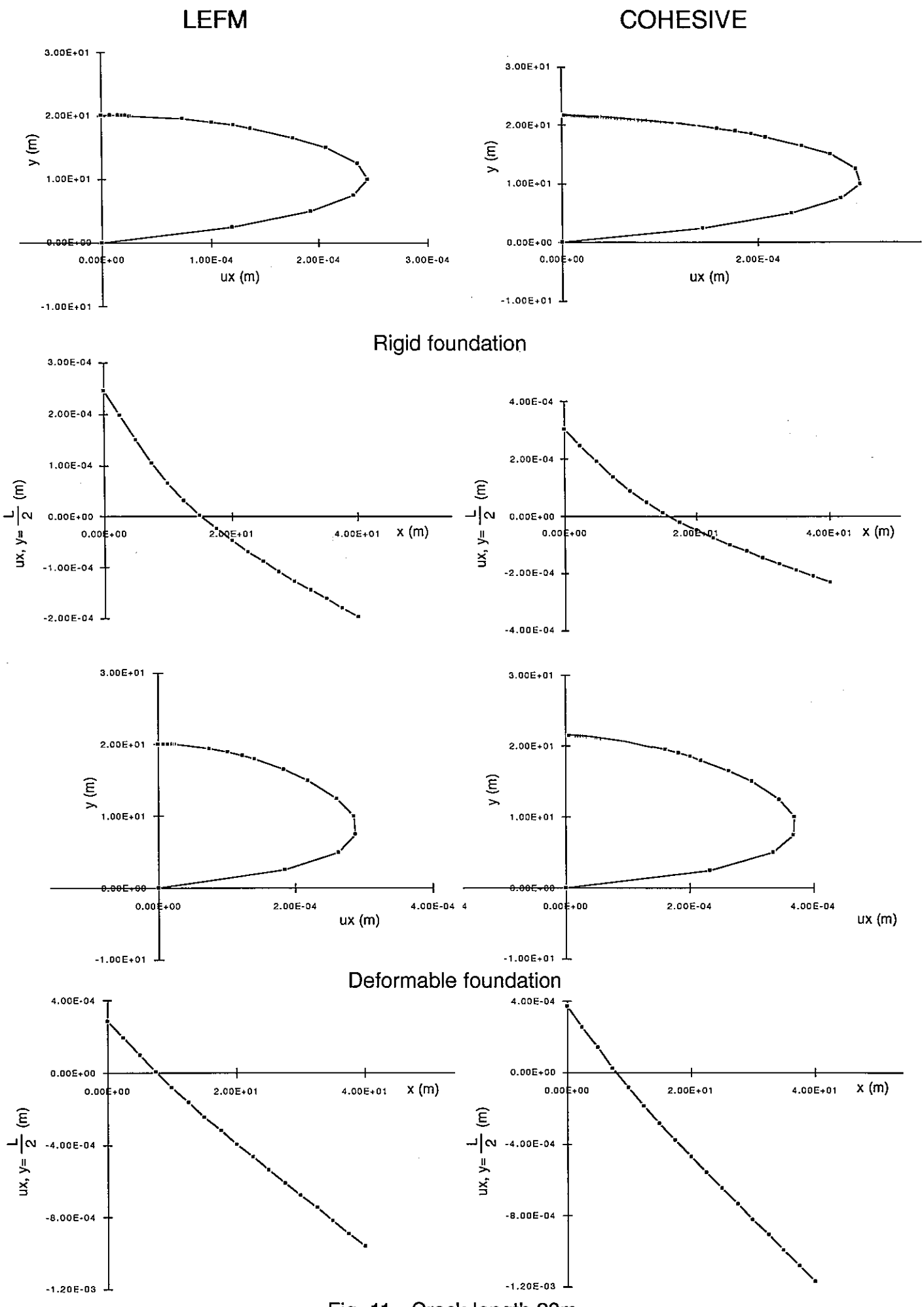

Fig. 11 - Crack length 20m.

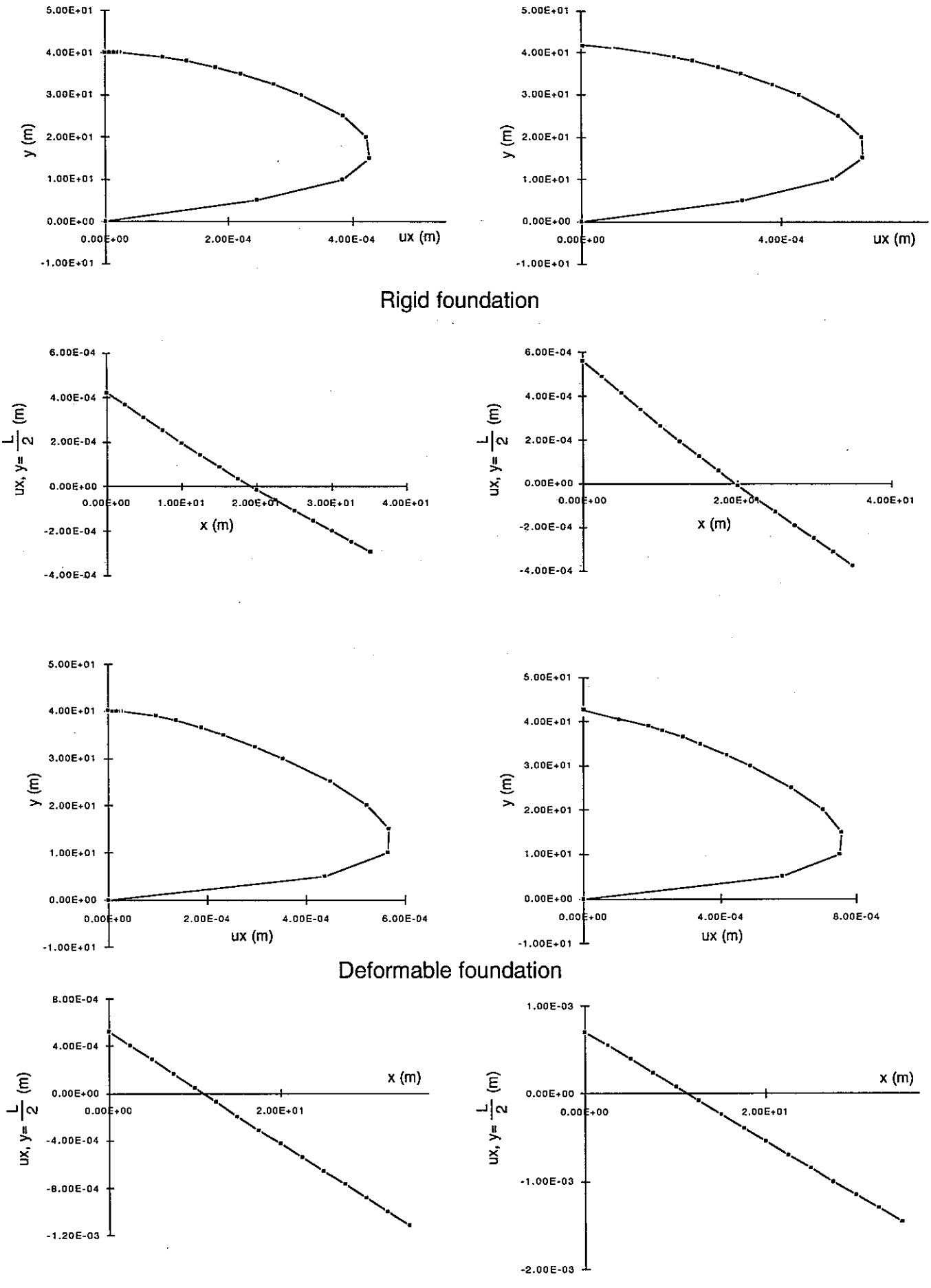

Fig. 12 - Crack length 40m.

REFERENCES

[1] Barenblatt, G.I. 'The formation of equilibrium cracks during brittle fracture: general ideas and hypotheses. Axially-symmetric cracks' *J. Appl. Math. Mech.*, vol. 23, pp. 622-636, 1959.

[2] Dugdale, D.S. 'Yielding of steel sheets containing slits' *J. Mech. Phys. Solids*, Vol. 8, pp. 100-104, 1960.

[3] Hillerborg, A., Modeer, M. and Petersson, P.E. 'Analysis of crack formation and crack growth in concrete by means of fracture mechanics and finite elements' *Cement Concrete Res.*, Vol. 6, pp. 773-782, 1976.

[4] Carpinteri, A., 'Post-peak and post-bifurcation analysis of cohesive crack propagation' *Eng. Fract. Mech.* , Vol. 32-2, pp. 265-278, 1989.

[5] Carpinteri, A., Valente, S. 'Size scale transition from ductile to brittle failure: a dimensional analysis approach' in *Proc. of France-U.S. Workshop on Strain Localisation and Size Effect due to Cracking and Damage*, Mazars J., Bazant Z.P., (eds.), France, pp. 477-490, 1988.

[6] Bocca, P., Carpinteri A., and Valente S. 'Mixed mode fracture of concrete' *Int. J. Solids Structures*, Vol. 27, pp. 1139-1153, 1991.

[7] Carpinteri, A., Valente, S., Ferrara, G., Imperato, L. 'Experimental and numerical fracture modelling of a gravity dam' *Fracture Mechanics of Concrete Structures*, Bazant Z.P., (ed.), Elsevier Applied Science, pp. 351-360, 1992.

[8] Valente, S., Barpi, F., Ferrara, G., Giuseppetti , G. 'Numerical simulation of centrifuge tests on prenotched gravity dam models' in *Dam Fracture and Damage*, Boudardot, Mazars & Saouma (eds.), Balkema, Rotterdam, pp. 111-119, 1994.

[9] Henshell, R. D., Shaw, K. G. 'Crack tip elements are unnecessary' *Int. J. for Num. Meth. in Eng.*, Vol. 9, pp. 495-509, 1975.

[10] Barsoum, R. S., 'On the use of isoparametrics finite elements in linear fracture mechanics' *Int. J. for Num. Meth. in Eng.*, Vol. 10, pp. 25-38, 1976.

[11] Valente, S. 'Heuristic softening strip model in the prediction of crack trajectories' *Theor. Appl. Fract. Mech.*, Vol. 19, pp. 119-125, 1993.

[12] Valente, S. 'Bifurcation phenomena in cohesive crack propagation' *Computers and Structures*, Vol. 44 1/2, pp. 55-62, 1992.

NOTES

THIRD ICOLD BENCHMARK WORKSHOP ON NUMERICAL ANALYSIS OF DAMS

Paris, France

September 29-30, 1994

Theme A2

Evaluation of critical uniform temperature decrease of a cracked buttress dam: application of the Virtual Crack Extension method

by

R.Menga (**), P.Dalmagioni (**), G.Mazzà(*), R.Pellegrini(**)

(*) ENEL S.p.A.-DSR/CRIS Via Ornato 90/14 Milano (Italy)

(**) ISMES S.p.A. Viale Giulio Cesare 29, Bergamo (Italy)

Abstract

The analyses specified by the Organizing Committee have been performed with a plane finite element model of the pre-cracked concrete buttress, run with the code DIANA, version 5.1. The code, developed at TNO (Delft), allows for the evaluation of the stress intensity factor within a Linear Elastic Fracture Mechanics approach to be compared with Mode I toughness factor: the virtual crack extension method is implemented for this evaluation. The structure is subjected to an uniform temperature decrease. The performance of different types of quarter point finite elements has been verified, throughout the exercise.

Introduction

In this paper the results obtained solving the exercise proposed in the Theme A2 of the Third Benchmark Workshop on Numerical Analysis of Dams are described, together with the theoretical background of the mathematical model used.

Scope of the analyses is that of evaluating the value of the uniform temperature decrease at which instability

of a vertical crack already present in a concrete dam buttress occurs.

The analyses have been carried out under two different assumptions on foundation modelling, one being that of rigid foundation, the other that of deformable foundation.

The pre-cracked dam buttress and its foundation have been studied with the finite element computer code DIANA (developed at TNO Delft) 5.1 Version, installed at ISMES on a Convex C3 computer. Conditions making the crack unstable have been evaluated applying Linear Elastic Fracture Mechanics (TNO, 1993), under the assumption of mode I crack opening, through the evaluation of the stress intensity factor at the upper crack tip. By comparison with the toughness factor, given here as temperature independent, the temperature decrease (ΔT) that makes the crack propagating is calculated.

The structural problem is characterised by a stress-strain singularity at the crack tips, which is represented here by purposedly defined finite elements (quarter point elements).

Theoretical and implementation framework

The DIANA code calculates the linear elastic fracture mechanics (LEFM) energy release rate and stress intensity factor by means of the Virtual Crack Extension Method (Parks 1974, Hellen 1975). The virtual extension of the crack always takes place in the plane of the crack itself.

The stress intensity factor is derived from the energy release rate as if the loading of the crack is purely mode-I (opening) load. This method is implemented in the code for quadratic plane stress (membrane), plane strain and solid elements. The method performs best when the midpoint nodes of the quadratic elements that are near the crack tip are at quarter point position (quarter point elements) (Barsoum 1976, Henshell 1975).

The implementation of the virtual crack extension method of Version 5.1 is valid if no external loading is directly applied on the elements surrounding the crack tip. Thermal loading on those particular elements is allowed.

The stress intensity factor can be calculated from the energy release rate, G. The energy release rate equals the release of the elastic energy W_{in} minus the external potential P_{ext} when the cracked area, A_c, increases of one unit:

$$G = -\frac{\partial W_{in}}{\partial A_c} + \frac{\partial P_{ext}}{\partial A_c}$$

For a two dimensional problem, the concept can be expressed in terms of crack length a. If W_{in} is the elastic energy and t is the thickness of a plate, then the energy release rate, at constant displacements ($P_{ext}=0$) , is defined as:

$$G = -\frac{1}{t}\frac{\partial W_{in}}{\partial A_c}$$

In the implementation of the method in DIANA release 5.1 a numerical differentiation is made to find out the difference of potential energy in two situations characterised by a small crack size difference.

$$\Delta P = P(a_2) - P(a_1)$$

where a is the crack length (for a two dimensional problem) and $\Delta a = a_2 - a_1$ is the crack extension. In a linear static analysis the potential energy, expressed in the FE framework, is calculated as:

$$P = \frac{1}{2}\mathbf{u}^T\mathbf{K}\mathbf{u} - \mathbf{u}^T\mathbf{b}$$

In this equation $\mathbf{u}$ represents the displacement vector, $\mathbf{K}$ the stiffness matrix and $\mathbf{b}$ the load vector. The increment in potential energy due to a crack extension Δa, applying the equilibrium condition $\mathbf{Ku}=\mathbf{b}$ is:

$$\Delta P = \frac{1}{2}\mathbf{u}^T\Delta\mathbf{K}\mathbf{u} - \mathbf{u}^T\mathbf{b}$$

This procedure requires the calculation of $\mathbf{K}$ and $\mathbf{b}$ for each crack opening rate Δa.

The crack opening rate can be considered as the displacement along the crack direction of all the nodes of the finite element grid which belong to the contour Γ_0 identified by the elements surrounding the crack tip. The remaining elements (Γ_1) do not displace. The matrix $\mathbf{K}$ does change only for the elements belonging to both Γ_0 e Γ_1.

Since the stiffness matrix of the structure, $\mathbf{K}$, is the sum of the element matrices, then its rate is the sum of the rates of the elementar matrices of the elements involved in the geometrical change Δa:

$$-\frac{1}{2}\mathbf{u}^T\mathbf{K}\mathbf{u} = -\frac{1}{2}\mathbf{u}^T\sum_{i=1}^{N_c}\mathbf{K}_i^c\mathbf{u}$$

where $\mathbf{K}_i^c$ is the stiffness matrix of an element between the contours Γ_0 and Γ_1, and N_c is the number of such elements.

The same holds true for the nodal loads vector. When the load is not directly applied against the crack face, the load vector does not depend on Δa. Under mode I crack opening and plane stress conditions, G for unit width can be written as follows:

$$G = K_I^2\frac{1}{E} = -\frac{1}{2}\mathbf{u}^T\frac{\Delta\mathbf{K}}{\Delta a}\mathbf{u}$$

When the load depends on crack opening, i.e. when it is applied directly on the elements adjacent to the crack, the external potential contribution must be included. One can demonstrate that the external potential contribution to the energy release rate can be evaluated in this case again, only for the elements belonging to both Γ_0 and Γ_1.

The nodal loads vector for each element is written as follows for the thermal load:

$$\mathbf{b}^e = -\int_{V_e} \mathbf{B}\,\mathbf{D}\,\alpha\,\Delta T\,\mathbf{i}\,dV_e$$

where $\mathbf{i}^T = [1,1,1,0,0,0]$, V_e is the elementar volume, D is the elasticity matrix and B is the strain-displacement matrix.

In this case, under the same assumptions as before (mode I crack opening, plane stress conditions) the energy release rate for unit width is given by the following expression:

$$G = K_I^2 \frac{1}{E} = -\frac{1}{2}\mathbf{u}^T \frac{\Delta \mathbf{K}}{\Delta a}\mathbf{u} + \mathbf{u}^T \frac{\Delta \mathbf{b}}{\Delta a}$$

As stated in the introduction, the stresses and strains at the crack tip are singular at the crack tip. In the vicinity of the crack tip the stress singularity can be described by the following expression:

$$\sigma = \frac{K_I}{\sqrt{2\pi r}} f(\vartheta)$$

where r e ϑ are the polar coordinates of a system having the crack tip as its centre.

To model this singularity in a finite element approach with the usual elements, would require a considerably refined mesh near the crack tip (Zienkiewicz, 1978). It can be shown however that e.g. for two dimensional quadratic elements, when the 'mid'-nodes on the edges adjacent to the crack tip, have a position at a quarter distance from the crack tip node, the element can describe this $1/\sqrt{r}$ singularity. Elements conceived this way are called 'quarter point' elements.

Validation of the code and of the modelling methodology

Some validation tests have been carried out to assess the accuracy of the solution obtained by the code for the case of thermal load with the finite elements and the mesh refinement actually adopted for the analyses performed for the Benchmark. The performance of two different types of finite elements surrounding the crack , i.e. triangles and collapsed quadrangles, has also been verified.

The test problem is made of a pre-cracked concrete slab 10m thick: the crack direction is normal to the major dimension of the structure.

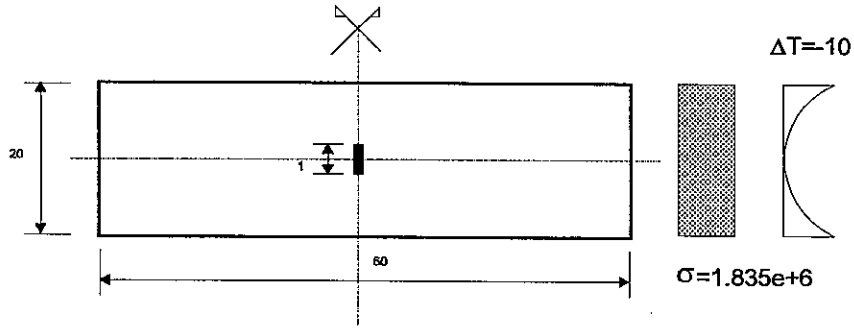

The loads considered in this exercise consist of a uniform stress and of a parabolically distributed temperature decrease along the smaller side of the slab. The finite element mesh is the same as that used for the dam buttress in the case of rigid foundation and 0.5 m crack length. Triangles and quadrangles collapsed at the crack tip have been used as suggested by Harrop, 1978.

Test case 1: uniform traction

A σ=1.835e6 Nm^{-2} uniform traction is applied against the 20m long slab faces. Concrete elastic parameters are E=3.e10 Nm^{-2} e υ=0.16. The results (mode I stress intensity factor K_I, energy release rate G, crack opening ρ) obtained by the FE solutions are compared in the following table with the exact solution (Tada, 1973):

	K_I [$Nm^{-3/2}$]	G [Nm^{-1}]	$\rho/2$ [m]
DIANA triangles	2302000	176.6	6.1160e-5
DIANA quadrangles	2299000	176.1	6.1130e-5
exact (Tada, 1973)	2303000	176.8	6.1335e-5

Test case 2: thermal load:

A uniform temperature distribution has been applied along the slab thickness along its major sides and one variable following a quadratic law along the minor sides (the maximum value at the side's edges is 10°C and the minimum at the slab's centre is 0°C). The comparison of the results obtained with the FE solutions and the exact one (Hellen et al., 1978) is given in the following table:

	K_I [$Nm^{-3/2}$]	G [Nm^{-1}]
DIANA triangles	1253000	52.30
DIANA quadrangles	1251000	52.15
exact (Hellen, 1978)	1248600	51.97

The results obtained allow to consider suitable the proposed mesh and the elements adopted.

There is no clear indication about the excellence of one type of finite element respect to the other:

quadrangles appear to perform better than triangles for the thermal case. The opposite occurs for the athermal case. The obtained results are however close to each other. The sensitivity of this result in terms of critical temperature and crack displacements will be given in the following sections for the pre-cracked dam buttress case.

The dam buttress case: the models.

The meshes provided by the Organizing Committee have been used for the discretization of the structure. The buttress has been discretized by isoparametric plane stress finite elements, namely CQ16M quadrilateral with 8 nodes and CT12M with 6 nodes. The foundation, when modelled (deformable foundation), has been discretized by plane strain finite elements (CQ16E, CT12E).

The mid side nodes of the elements at the crack tip have been moved to the "quarter point" position for a more effective description of the crack tip singularity
As for the validation tests, and with the same purpose, also eight node isoparametric quarter point elements collapsed at the crack tip have been used following (Harrop, 1978).

Half structure has been discretized, taking advantage of the symmetry boundary condition of no horizontal displacement of the mid-side section of the buttress. The nodes at the buttress basement (rigid foundation) as well as those at the foundation base (deformable foundation) have been restrained in the plane of the model.

The material model parameters have been provided by the Organizing Committee:

- **Concrete:**

- Young's elastic modulus $E_c = 3.0e^{+10}\ Nm^{-2}$
- Poisson ratio coefficient $\upsilon = 0.16$
- Thermal dilatation coefficient $\alpha = 1.0e^{-5}\ °C^{-1}$
- Toughness $K_c = 2.3e^{+6}\ Nm^{-3/2}$

- **Rock (deformable foundation):**

- Young's elastic modulus $E_r = 1.0e^{+10}\ Nm^{-2}$
- Poisson ratio coefficient $\upsilon = 0.2$

The analyses have been run on a Convex C3 computer. Each load case has been solved for a unit temperature decrease (run I). Taking advantage of the linearity of the stress and stress intensity factors with temperature in the model, the critical temperature decrease has been calculated analytically. Finally, the critical temperature decrease has been applied as a load (run II), obtaining from the finite element run the critical stress intensity factor (toughness factor) and the corresponding stress and displacement fields.

The computing time (relative to runs I) is about 50 sec each.

Results of the benchmark cases.

The results required for the dam buttress case are grouped in tables 1-6. Two sets of results are given, one obtained with triangular isoparametric 6 nodes elements around the crack tip, the other with quadrilateral 8 nodes elements collapsed at the crack tip.

The predicted temperature decrease for crack instability (initiation) for different crack lengths is depicted in the following graph, considering the two prescribed assumptions for the stiffness contribution of the foundation.

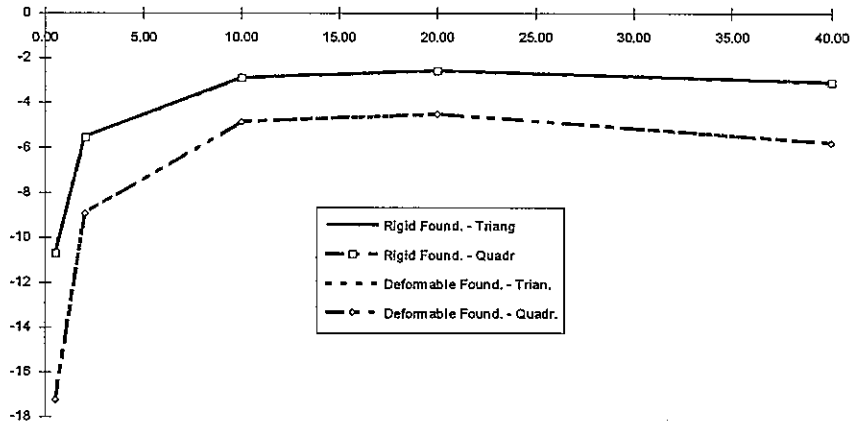

Comments to the results

The biggest critical ΔT for both structural cases, Rigid Foundation or Deformable Foundation, has been found for the smallest crack length (0.5m). The critical temperature sharply decreases with crack length: the more deformable is the foundation, the sharper is the ΔT decrease. For lengths bigger than 10m, ΔT is nearly constant for the rigid foundation case, whereas it shows a more marked, but still slight increase, for the deformable foundation case, when the crack length is bigger than 20m.

The rigid foundation enhances crack instability occurrence, showing smaller critical ΔT (of about 33%) respect to the deformable foundation case.

The sensitivity of the results to the selected types of isoparametric finite elements is small and irrelevant for practical purposes, at least for mesh refinements like those proposed for the dam buttress case.

Acknowledgements

DIANA Analysis b.v. provided technical literature regarding the LEFM model implemented in DIANA. Their contribution is gratefully acknowledged.

References

1. Barsoum R.S.: "On the use of Isoparametric Finite Elements in Linear Fracture Mechanics." *Int.J Num.Methods in Eng.*, **10** 25-37 (1976).

2. Harrop L.P.: "Linear Elastic Intensity Factor using a distorted Isoparametric Finite Element", Proceedings of the First International Conference, Swansea, 1978.

3. Hellen T.K.: "On the method of virtual crack extension." *Int.J.Num.Methods in Eng.*, **9** 187-207 (1975)

4. Hellen T.K., Cesari F.: "Soluzione Mediante il Metodo Degli Elementi Finiti di una Lastra Fessurata al Centro in Presenza di un Gradiente Termico", 5th Congresso Aimeta, Florence, 25-28 October 1978, in Italian.

5. Henshell R.D., Shaw K.G.: "Crack Tip Finite Elements are Unnecessary." *Int.J.Num.Methods in Eng.*, **9** 495-507 (1975).

6. Parks D.M.: "A stiffness derivative finite element technique for determination of crack tip stress intensity factors." *Int.J.of Fracture*, **10**(4) 487-502 (1974).

7. Tada H., Paris P.C., Irwin G.R.: *The stress analysis of crack handbook*, Del.Research Corporation, Hellertown, Pennsylvania, U.S.A. (1973).

8. TNO Building and Construction Research: "DIANA 5.1 Verification Report", 1993

9. Zienkiewicz O.C., Taylor R.L.: "The Finite Element Method, Volume 1, Basic Formulation and Linear Problems", 4th ed. pp 189-191, 1978.

TABLE 1.a

RIGID FOUNDATION Δ

L [m]	DT [°C]	dmax [m]	ydmax [m]
0.50	-10.877	7.89E-05	0.285
2.00	-5.513	1.59E-04	1.137
10.00	-2.886	3.75E-04	5.468
20.00	-2.562	5.84E-04	10.312
40.00	-3.087	1.09E-03	18.107

TABLE 1.b

RIGID FOUNDATION □

L [m]	DT [°C]	dmax [m]	ydmax [m]
0.50	-10.703	7.88E-05	0.244
2.00	-5.521	1.59E-04	1.137
10.00	-2.891	3.75E-04	5.468
20.00	-2.564	5.84E-04	10.312
40.00	-3.088	1.09E-03	18.107

TABLE 2.a

DEFORMABLE FOUNDATION Δ

L [m]	DT [°C]	dmax [m]	ydmax [m]
0.50	-17.1898	8.90E-05	0.241
2.00	-8.9182	1.80E-04	0.952
10.00	-4.8421	4.36E-04	4.461
20.00	-4.4904	6.83E-04	8.176
40.00	-5.7745	1.41E-03	13.534

TABLE 2.b

DEFORMABLE FOUNDATION □

L [m]	DT [°C]	dmax [m]	ydmax [m]
0.50	-17.2285	8.91E-05	0.241
2.00	-8.9355	1.77E-04	0.949
10.00	-4.8452	4.36E-04	4.553
20.00	-4.4931	7.09E-04	8.657
40.00	-5.774	1.43E-03	15.094

TABLE 3.a

L=0.5 m - RIGID FOUNDATION

y [m]	ux(y) trian [m]	ux(y) quad [m]
0	0	0
0.004034	2.16E-06	2.15E-06
0.01614	6.6E-06	6.61E-06
0.02651	9.77E-06	9.78E-06
0.03688	1.26E-05	1.26E-05
0.05169	1.62E-05	1.62E-05
0.06651	1.94E-05	1.94E-05
0.08785	2.34E-05	2.34E-05
0.1092	2.69E-05	2.69E-05
0.1391	3.09E-05	3.09E-05
0.169	3.4E-05	3.41E-05
0.2095	3.71E-05	3.71E-05
0.25	3.89E-05	3.89E-05
0.2905	3.94E-05	3.94E-05
0.331	3.86E-05	3.86E-05
0.3609	3.71E-05	3.71E-05
0.3908	3.46E-05	3.46E-05
0.4121	3.21E-05	3.21E-05
0.4335	2.88E-05	2.88E-05
0.4483	2.6E-05	2.6E-05
0.4631	2.24E-05	2.24E-05
0.4735	1.93E-05	1.92E-05
0.4839	1.52E-05	1.51E-05
0.496	7.74E-06	7.41E-06
0.5	0	0

TABLE 3.b

L=2. m - RIGID FOUNDATION

y [m]	ux(y) trian [m]	ux(y) quad [m]
0	0	0
0.01614	4.43E-06	4.41E-06
0.06455	1.35E-05	1.35E-05
0.106	0.00002	2E-05
0.1475	2.58E-05	2.58E-05
0.2068	3.31E-05	3.31E-05
0.266	3.96E-05	3.96E-05
0.3514	4.77E-05	4.77E-05
0.4368	5.46E-05	5.47E-05
0.5564	6.27E-05	6.28E-05
0.6761	6.9E-05	6.91E-05
0.838	7.5E-05	7.51E-05
1	7.85E-05	7.86E-05
1.162	7.94E-05	7.95E-05
1.324	7.77E-05	7.77E-05
1.444	7.45E-05	7.45E-05
1.563	6.94E-05	6.94E-05
1.649	6.44E-05	6.44E-05
1.734	5.78E-05	5.78E-05
1.793	5.2E-05	0.000052
1.853	4.48E-05	4.48E-05
1.894	3.85E-05	3.84E-05
1.935	3.04E-05	3.02E-05
1.984	1.55E-05	1.48E-05
2	0	0

TABLE 3.c

L=10. m - RIGID FOUNDATION

y [m]	ux(y) trian [m]	ux(y) quad [m]
0	0	0
0.02421	4.19E-06	4.18E-06
0.09683	1.3E-05	1.3E-05
0.159	1.95E-05	1.95E-05
0.2213	2.54E-05	2.55E-05
0.3102	3.33E-05	3.34E-05
0.399	4.06E-05	4.07E-05
0.5271	5.04E-05	5.05E-05
0.6551	5.94E-05	5.95E-05
0.8346	7.1E-05	7.11E-05
1.014	8.16E-05	8.18E-05
1.257	9.47E-05	9.49E-05
1.5	0.000106	0.000107
2	0.000127	0.000127
2.5	0.000144	0.000144
3.437	0.000167	0.000167
4.375	0.000181	0.000182
5	0.000186	0.000186
5.625	0.000187	0.000187
6.562	0.00018	0.000181
7.5	0.000166	0.000166
8	0.000153	0.000154
8.5	0.000137	0.000137
8.743	0.000128	0.000128
8.986	0.000116	0.000117
9.165	0.000107	0.000107
9.345	9.55E-05	9.56E-05
9.473	8.63E-05	8.63E-05
9.601	7.56E-05	7.56E-05
9.69	6.7E-05	6.7E-05
9.779	5.69E-05	5.68E-05
9.841	4.84E-05	4.83E-05
9.903	3.78E-05	3.76E-05
9.976	1.9E-05	1.83E-05
10	0	0

TABLE 3.d

L=20. m - RIGID FOUNDATION

y [m]	ux(y) trian [m]	ux(y) quad [m]
0	0	0
0.02421	4.1E-06	4.08E-06
0.09683	1.28E-05	1.28E-05
0.159	1.92E-05	1.92E-05
0.2213	2.51E-05	2.52E-05
0.3102	3.31E-05	3.31E-05
0.399	4.05E-05	4.05E-05
0.5271	5.06E-05	5.06E-05
0.6551	6E-05	6E-05
0.8346	7.23E-05	7.23E-05
1.014	8.38E-05	8.38E-05
1.257	9.83E-05	9.83E-05
1.5	0.000112	0.000112
2	0.000136	0.000136
2.5	0.000158	0.000158
3.437	0.000191	0.000191
4.375	0.000219	0.00022
7.188	0.000273	0.000273
10	0.00029	0.00029
12.81	0.000277	0.000277
15.63	0.000233	0.000233
16.56	0.000211	0.000211
17.5	0.000184	0.000184
18	0.000166	0.000166
18.5	0.000145	0.000145
18.74	0.000134	0.000134
18.99	0.000121	0.000121
19.16	0.00011	0.00011
19.35	9.78E-05	9.77E-05
19.47	8.8E-05	8.79E-05
19.6	7.67E-05	7.66E-05
19.69	6.77E-05	6.76E-05
19.78	5.73E-05	5.71E-05
19.84	4.86E-05	4.84E-05
19.9	3.8E-05	3.77E-05
19.98	1.91E-05	1.81E-05
20	0	0

TABLE 3.e

L=40. m - RIGID FOUNDATION

y [m]	ux(y) trian [m]	ux(y) quad [m]
0	0	0
0.02421	5.34E-06	5.32E-06
0.09683	1.66E-05	1.66E-05
0.159	2.51E-05	2.51E-05
0.2213	3.29E-05	3.29E-05
0.3102	4.34E-05	4.34E-05
0.399	5.32E-05	5.33E-05
0.5271	6.66E-05	6.67E-05
0.6551	7.92E-05	7.93E-05
0.8346	9.59E-05	9.59E-05
1.014	0.000112	0.000112
1.257	0.000132	0.000132
1.5	0.00015	0.00015
2	0.000185	0.000185
2.5	0.000217	0.000217
3.437	0.000268	0.000268
4.375	0.000313	0.000313
7.188	0.000418	0.000418
10	0.000484	0.000484
15	0.000539	0.000539
20	0.000533	0.000534
25	0.000486	0.000486
30	0.000402	0.000402
32.81	0.000339	0.000339
35.62	0.00026	0.00026
36.56	0.000229	0.000229
37.5	0.000195	0.000195
38	0.000174	0.000174
38.5	0.00015	0.00015
38.74	0.000138	0.000138
38.99	0.000124	0.000123
39.17	0.000112	0.000112
39.34	9.92E-05	9.91E-05
39.47	8.89E-05	8.88E-05
39.6	7.74E-05	7.72E-05
39.69	6.82E-05	6.8E-05
39.78	5.76E-05	5.74E-05
39.84	4.88E-05	4.86E-05
39.9	3.81E-05	3.77E-05
39.98	1.91E-05	1.81E-05
40	0	0

TABLE 4.a

L=0.5 m - DEFORMABLE FOUNDATION

y [m]	ux(y) trian [m]	ux(y) quad [m]
0	0	0
0.004034	9.49E-06	8.99E-06
0.01614	1.77E-05	1.75E-05
0.02651	2.2E-05	2.19E-05
0.03688	2.53E-05	2.52E-05
0.05169	2.9E-05	2.9E-05
0.06651	3.2E-05	3.2E-05
0.08785	3.54E-05	3.54E-05
0.1092	3.81E-05	3.81E-05
0.1391	4.08E-05	4.08E-05
0.169	4.27E-05	4.27E-05
0.2095	4.41E-05	4.42E-05
0.25	4.44E-05	4.44E-05
0.2905	4.35E-05	4.36E-05
0.331	4.15E-05	4.16E-05
0.3609	3.92E-05	3.93E-05
0.3908	3.6E-05	3.61E-05
0.4121	3.31E-05	3.32E-05
0.4335	2.95E-05	2.95E-05
0.4483	2.64E-05	2.64E-05
0.4631	2.27E-05	2.27E-05
0.4735	1.94E-05	1.94E-05
0.4839	1.53E-05	1.52E-05
0.496	7.75E-06	7.43E-06
0.5	0	0

TABLE 4.b

L=2. m - DEFORMABLE FOUNDATION

y [m]	ux(y) trian [m]	ux(y) quad [m]
0	0	0
0.01614	1.94E-05	1.84E-05
0.06455	3.62E-05	3.58E-05
0.106	4.5E-05	4.48E-05
0.1475	5.17E-05	5.16E-05
0.2068	5.92E-05	5.91E-05
0.266	6.53E-05	6.52E-05
0.3514	7.22E-05	7.21E-05
0.4368	7.75E-05	7.75E-05
0.5564	0.000083	8.3E-05
0.6761	8.67E-05	8.67E-05
0.838	8.94E-05	8.94E-05
1	8.98E-05	8.98E-05
1.162	8.78E-05	8.79E-05
1.324	8.36E-05	8.37E-05
1.444	7.89E-05	7.89E-05
1.563	7.24E-05	7.24E-05
1.649	6.65E-05	6.65E-05
1.734	5.92E-05	5.92E-05
1.793	5.3E-05	5.29E-05
1.853	4.54E-05	4.54E-05
1.894	3.89E-05	3.88E-05
1.935	3.06E-05	3.04E-05
1.984	1.55E-05	1.48E-05
2	0	0

TABLE 4.c

L=10. m - DEFORMABLE FOUNDATION

y [m]	ux(y) trian [m]	ux(y) quad [m]
0	0	0
0.02421	2.88E-05	2.73E-05
0.09683	5.43E-05	5.37E-05
0.159	6.8E-05	6.76E-05
0.2213	7.88E-05	7.85E-05
0.3102	9.14E-05	9.11E-05
0.399	0.000102	0.000102
0.5271	0.000115	0.000115
0.6551	0.000126	0.000125
0.8346	0.000138	0.000138
1.014	0.000149	0.000149
1.257	0.000161	0.000161
1.5	0.000172	0.000172
2	0.000188	0.000188
2.5	0.0002	0.0002
3.437	0.000213	0.000213
4.375	0.000218	0.000218
5	0.000216	0.000216
5.625	0.000211	0.000211
6.562	0.000197	0.000197
7.5	0.000176	0.000176
8	0.000161	0.000161
8.5	0.000142	0.000142
8.743	0.000131	0.000131
8.986	0.000119	0.000119
9.165	0.000109	0.000109
9.345	9.69E-05	9.69E-05
9.473	8.73E-05	8.73E-05
9.601	7.63E-05	7.62E-05
9.69	6.75E-05	6.74E-05
9.779	5.72E-05	5.71E-05
9.841	4.86E-05	4.84E-05
9.903	3.8E-05	3.77E-05
9.976	1.91E-05	1.83E-05
10	0	0

TABLE 4.d

L=20. m - DEFORMABLE FOUNDATION

y [m]	ux(y) trian [m]	ux(y) quad [m]
0	0	0
0.02421	3.68E-05	3.48E-05
0.09683	6.94E-05	6.86E-05
0.159	8.7E-05	8.65E-05
0.2213	0.000101	0.000101
0.3102	0.000118	0.000117
0.399	0.000131	0.000131
0.5271	0.000148	0.000148
0.6551	0.000163	0.000163
0.8346	0.00018	0.00018
1.014	0.000196	0.000195
1.257	0.000213	0.000213
1.5	0.000228	0.000228
2	0.000254	0.000254
2.5	0.000274	0.000274
3.437	0.000303	0.000303
4.375	0.000324	0.000324
7.188	0.000351	0.000352
10	0.000344	0.000344
12.81	0.000309	0.000309
15.63	0.000248	0.000248
16.56	0.000221	0.000221
17.5	0.00019	0.00019
18	0.000171	0.000171
18.5	0.000148	0.000148
18.74	0.000136	0.000136
18.99	0.000122	0.000122
19.16	0.000111	0.000111
19.35	9.86E-05	9.85E-05
19.47	8.85E-05	8.84E-05
19.6	7.71E-05	7.7E-05
19.69	6.8E-05	6.79E-05
19.78	5.74E-05	5.73E-05
19.84	4.87E-05	4.85E-05
19.9	3.81E-05	3.77E-05
19.98	1.91E-05	1.81E-05
20	0	0

TABLE 4.e

L=40. m - DEFORMABLE FOUNDATION

y [m]	ux(y) trian [m]	ux(y) quad [m]
0	0	0
0.02421	6.17E-05	5.84E-05
0.09683	0.000117	0.000115
0.159	0.000146	0.000146
0.2213	0.00017	0.00017
0.3102	0.000198	0.000198
0.399	0.000222	0.000221
0.5271	0.000251	0.000251
0.6551	0.000276	0.000276
0.8346	0.000307	0.000306
1.014	0.000333	0.000333
1.257	0.000364	0.000364
1.5	0.000392	0.000391
2	0.000439	0.000439
2.5	0.000478	0.000478
3.437	0.000535	0.000536
4.375	0.000582	0.000582
7.188	0.000669	0.000669
10	0.000709	0.000709
15	0.000707	0.000708
20	0.000649	0.000649
25	0.000556	0.000557
30	0.000438	0.000438
32.81	0.00036	0.00036
35.62	0.00027	0.00027
36.56	0.000236	0.000236
37.5	0.000199	0.000199
38	0.000177	0.000177
38.5	0.000152	0.000152
38.74	0.000139	0.000139
38.99	0.000125	0.000124
39.17	0.000113	0.000113
39.34	9.97E-05	9.96E-05
39.47	8.93E-05	8.92E-05
39.6	7.76E-05	7.75E-05
39.69	6.84E-05	6.82E-05
39.78	5.77E-05	5.75E-05
39.84	4.89E-05	4.87E-05
39.9	3.81E-05	3.78E-05
39.98	1.91E-05	1.81E-05
40	0	0

TABLE 5.a

L=0.5 m - RIGID FOUNDATION

x(y=L/2) [m]	ux(x) trian [m]	ux(x) quad [m]
0	3.89E-05	3.89E-05
0.03262	3.59E-05	3.59E-05
0.06465	3.3E-05	3.3E-05
0.1522	2.52E-05	2.52E-05
0.196	2.18E-05	2.18E-05
0.2398	1.89E-05	1.89E-05
0.361	1.26E-05	1.26E-05
0.526	7.36E-06	7.36E-06
0.8333	2.81E-06	2.81E-06
1.667	-4.2E-07	-4.2E-07
2.833	-1.5E-06	-1.5E-06

TABLE 5.b

L=2. m - RIGID FOUNDATION

x(y=L/2) [m]	ux(x) trian [m]	ux(x) quad [m]
0	7.85E-05	7.86E-05
0.1305	7.24E-05	7.24E-05
0.2586	6.63E-05	6.64E-05
0.6089	5.01E-05	5.02E-05
0.784	4.31E-05	4.31E-05
0.9592	3.7E-05	3.7E-05
1.444	2.38E-05	2.38E-05
2.104	1.28E-05	1.28E-05

TABLE 5.c

L=10. m - RIGID FOUNDATION

x(y=L/2) [m]	ux(x) trian [m]	ux(x) quad [m]
0	0.000186	0.000186
2.247	0.000129	0.000129
5	6.93E-05	6.94E-05
10	7.07E-06	7.07E-06
15	-2.9E-05	-2.9E-05
20	-5.4E-05	-5.4E-05
25	-7.5E-05	-7.5E-05
30	-9.4E-05	-9.5E-05
35	-0.00011	-0.00011
40	-0.00013	-0.00013
42.5	-0.00013	-0.00013

TABLE 5.d

L=20. m - RIGID FOUNDATION

x(y=L/2) [m]	ux(x) trian [m]	ux(x) quad [m]
0	0.00029	0.00029
2.5	0.000233	0.000233
5	0.000178	0.000178
7.5	0.000124	0.000124
10	8E-05	8.01E-05
12.5	3.91E-05	3.91E-05
15	4.69E-06	4.68E-06
17.5	-2.6E-05	-2.6E-05
20	-5.4E-05	-5.4E-05
22.5	-8E-05	-8E-05
25	-0.0001	-0.0001
27.5	-0.00013	-0.00013
30	-0.00015	-0.00015
32.5	-0.00017	-0.00017
35	-0.00019	-0.00019
37.5	-0.00021	-0.00021
40	-0.00023	-0.00023

TABLE 5.e

L=40. m - RIGID FOUNDATION

x(y=L/2) [m]	ux(x) trian [m]	ux(x) quad [m]
0	0.000533	0.000534
2.5	0.000462	0.000463
5	0.00039	0.00039
7.5	0.000319	0.000319
10	0.000248	0.000248
12.5	0.000179	0.000179
15	0.000112	0.000112
17.5	4.78E-05	4.78E-05
20	-1.5E-05	-1.5E-05
22.5	-7.5E-05	-7.5E-05
25	-0.00013	-0.00013
27.5	-0.00019	-0.00019
30	-0.00025	-0.00025
32.5	-0.00031	-0.00031
35	-0.00037	-0.00037

TABLE 6.a

L=0.5 m - DEFORMABLE FOUNDATION

x(y=L/2) [m]	ux(x) trian [m]	ux(x) quad [m]
0	4.44E-05	4.44E-05
0.03262	3.92E-05	3.92E-05
0.06465	3.41E-05	3.41E-05
0.1522	1.99E-05	1.99E-05
0.196	1.31E-05	1.31E-05
0.2398	6.69E-06	6.65E-06
0.361	-9.6E-06	-9.7E-06
0.526	-2.9E-05	-2.9E-05
0.8333	-6.1E-05	-6.1E-05
1.667	-0.00014	-0.00014
2.833	-0.00024	-0.00024

TABLE 6.b

L=2. m - DEFORMABLE FOUNDATION

x(y=L/2) [m]	ux(x) trian [m]	ux(x) quad [m]
0	8.98E-05	8.98E-05
0.1305	7.9E-05	7.9E-05
0.2586	6.83E-05	6.83E-05
0.6089	3.88E-05	3.88E-05
0.784	2.47E-05	2.46E-05
0.9592	1.13E-05	1.12E-05
1.444	-2.3E-05	-2.3E-05
2.104	-6.3E-05	-6.4E-05

TABLE 6.c

L=10. m - DEFORMABLE FOUNDATION

x(y=L/2) [m]	ux(x) trian [m]	ux(x) quad [m]
0	0.000216	0.000216
2.247	0.000113	0.000113
5	-9.3E-06	-9.4E-06
10	-0.00019	-0.00019
15	-0.00035	-0.00035
20	-0.0005	-0.0005
25	-0.00064	-0.00065
30	-0.00079	-0.00079
35	-0.00092	-0.00092
40	-0.00106	-0.00106
42.5	-0.00113	-0.00113

TABLE 6.d

L=20. m - DEFORMABLE FOUNDATION

x(y=L/2) [m]	ux(x) trian [m]	ux(x) quad [m]
0	0.000344	0.000344
2.5	0.000237	0.000237
5	0.00013	0.00013
7.5	2.24E-05	2.23E-05
10	-7.6E-05	-7.7E-05
12.5	-0.00017	-0.00017
15	-0.00027	-0.00027
17.5	-0.00035	-0.00035
20	-0.00044	-0.00044
22.5	-0.00052	-0.00052
25	-0.00061	-0.00061
27.5	-0.00069	-0.00069
30	-0.00077	-0.00077
32.5	-0.00085	-0.00085
35	-0.00093	-0.00093
37.5	-0.00101	-0.00101
40	-0.0011	-0.0011

TABLE 6.e

L=40. m - DEFORMABLE FOUNDATION

x(y=L/2) [m]	ux(x) trian [m]	ux(x) quad [m]
0	0.000649	0.000649
2.5	0.00051	0.00051
5	0.000369	0.000369
7.5	0.000228	0.000228
10	8.5E-05	8.49E-05
12.5	-5.6E-05	-5.6E-05
15	-0.0002	-0.0002
17.5	-0.00034	-0.00034
20	-0.00047	-0.00047
22.5	-0.00061	-0.00061
25	-0.00074	-0.00075
27.5	-0.00088	-0.00088
30	-0.00102	-0.00102
32.5	-0.00115	-0.00115
35	-0.00129	-0.00129

THIRD ICOLD BENCHMARK WORKSHOP ON NUMERICAL ANALYSIS OF DAMS

Paris, France
September 29-30, 1994

Theme A2

Evaluation of critical uniform temperature decrease of a cracked buttress dam: application of non linear fracture mechanics and smeared crack approach

by
R.Menga (**), P.Dalmagioni (**), G.Mazzà(*), R.Pellegrini(**)

(*) ENEL S.p.A.-DSR/CRIS Via Ornato 90/14 Milano (Italy)
(**) ISMES S.p.A. Viale Giulio Cesare 29, Bergamo (Italy)

Abstract

The exercise proposed in Theme A2 has been solved by a non linear fracture mechanics model implemented in a smeared crack formulation. The critical temperature decrease, capable of activating a pre-existing crack in a concrete dam buttress has been evaluated. This exercise has been solved for the case of rigid foundation, considering all the initial pre-crack lengths proposed by the Organizing Committee.

The DIANA finite element code (Vs.5.1) has been used (TNO, 1993). The analyses have been run on a Convex C3 computer: each load case has required 50 minutes computing time.

THE MODEL

Concrete has been modelled as a linear elastic, fracturing material, cracking being activated when the tensile strength is reached along the direction of the maximum principal stress. The crack direction is perpendicular to that of the tensile strength. The process of crack opening is described by a decrease of stress carrying capacity normally to the crack (this stress will be called in the following residual strength): the resulting

residual strength - crack opening relationship is characterised by the energy spent in the process, which is considered a material property (Gf, specific fracture energy). From the attainment of the tensile strength to the loss of any residual stress the entire process of cracking, i.e. diffuse micro cracking, micro cracks coalescence to complete crack opening is phenomenologically reproduced by this so called softening law.

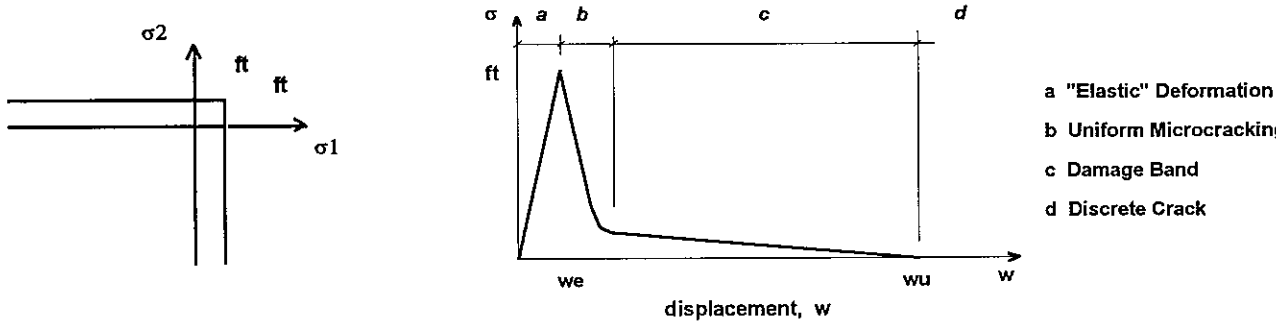

In the smeared crack approach the crack opening is translated into a crack strain, this translation implying a proper selection of a representative dimension of a cracked continuum. In the numerical applications mesh dependency effects can potentially arise due to it. In order to maintain the same specific fracture energy for the F.E. models, adequate scaling factors have been therefore adopted for the translation from displacements to strains.

Quadrilateral and triangular isoparametric elements with 8/6 nodes respectively and 9 Gauss points have been adopted for the finite element mesh.

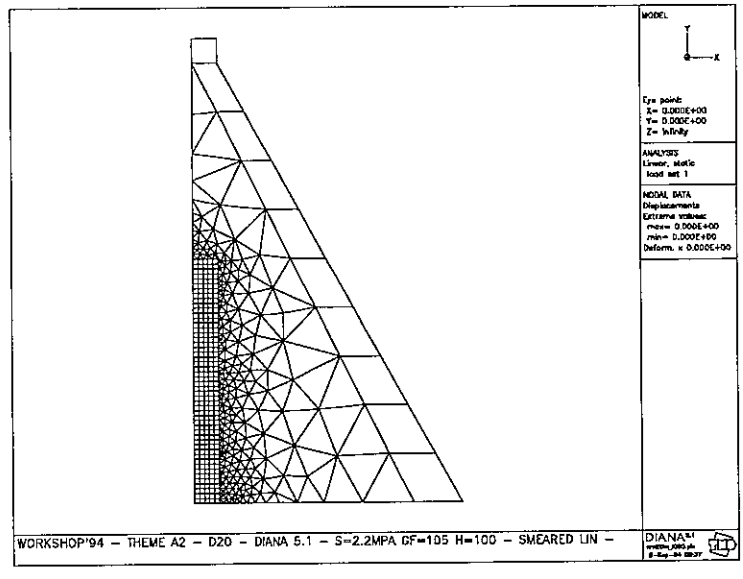

As quite customary with these models, also to avoid any preferential crack development, regularly spaced rows of quadrilateral elements of constant length, l, have been selected for describing the area nearby the crack. Two different element length values were used: 25 cm for the models with an initial crack length of 0.5 and 2 metres, 100 cm for those with 10, 20 and 40 meters initial crack length.

The crack is considered unstable when no stress carrying capacity is attained anymore at the crack tip, that

is when all the fracture energy has been spent. Potentially different results respect to the LEFM solution in terms of critical temperature decrease can arise, due to the still open problem of defining a possible general relationship linking the specific fracture energy to the energy release rate, as defined in LEFM (see later in this paper).

MODEL CALIBRATION

Model parameters are the following and have been given the values listed hereafter:

- Young's elastic modulus $E_c = 3.0e^{+10}$ Nm^{-2}
- Poisson ratio coefficient $\upsilon = 0.16$
- Thermal dilatation coefficient $\alpha = 1.0e^{-5}$ °C^{-1}
- Tensile strength $\sigma_t = 2.2e^{+6}$ Nm^{-2}
- Specific fracture energy $G_f = 105$ Nm^{-1}
- Ultimate crack width $w_u = 0.25$ mm

The calibration procedure has been based on describing as far as possible the same concrete as that indicated by the Organizing Committee (Menga et al., 1994) for the LEFM computations. To this purpose relationships proposed by the FIP/CEB Model Code (FIP/CEB MC, 1990) have been adopted, taking as a reference a Class 20 concrete and considering a maximum inert diameter of 32mm, the class being selected on the basis of the Young Modulus assigned by the Organizing Committee.

The values of fracture energy obtained this way are representative of a dam concrete (Bruhwiler,1991); the same holds for the selected ultimate crack width.

Attempts of translating in a general relationship the fracture toughness into specific fracture energy are not conclusive. Relationships between them have been obtained under limit conditions, which cannot be however reproduced in usual experiments (Elices et al., 1989; Planas et al., 1988). Correlations found in the literature (Jenq and Shah, 1985; Nallathambi and Karihaloo; Rice et al., 1973; Wittmann et al., 1988; Perdikaris and Romeo) are empirical and applicable only to specific structural typologies. In general they acknowledge that for a given concrete the specific fracture energy is bigger than the energy release rate (strictly related to the stress intensity factor in LEFM) but the values of the correlation factors (20, 33, 50) are highly variable and lead to inconsistent Gf values for the case considered.

The shape of the softening law is decisive for correctly describing the impact of cracking on the stress redistribution in a structure (Wittman et al., 1988). A bilinear softening law characterised by an intermediate crack width, w_l, (here 0.04 mm) corresponding to 15 % residual strength is proposed by the FIP/CEB recommendations. The influence of linear, bilinear (FIP/CEB MC, 1990) and non linear (Hordjik et al., 1987) softening laws characterised by the same specific fracture energy and tensile strength, has been evaluated in a preliminary validation of the procedure, described in the following section.

VALIDATION OF THE PROCEDURE

The procedural aspects of the non linear analysis as well as the impact of the different shapes of the softening law, at constant Gf and tensile strength, have been evaluated with Test case 1 (Menga et al., 1994), a centrally pre-cracked slab solved in closed form by Tada et al., 1973, also adopted for the validation of the LEFM approach (Menga et al., 1994). In the following Figure the different softening laws are depicted, the only difference between them being the crack opening associated to a given residual strength value.

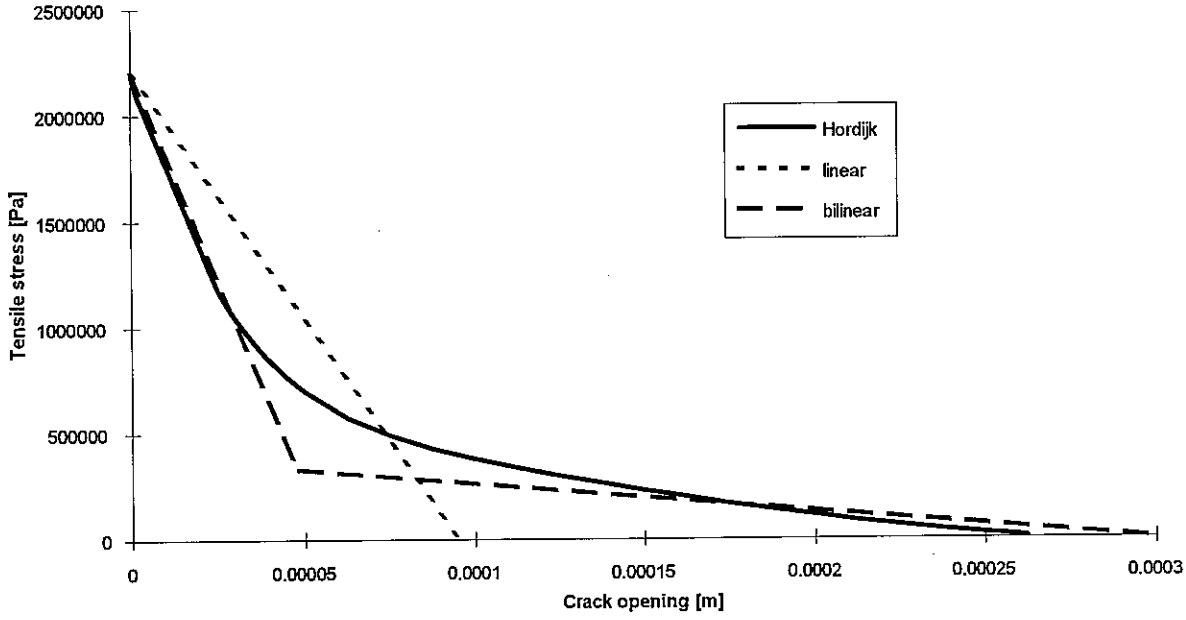

Taking b=10m (2b, slab width) and 2a, crack length, 4m and describing the body of the structure by quadrilateral plane stress elements, those adjacent to the crack faces being 25cm long, the following multiplying factors of the limit load have been obtained:

linear softening law	1.018
bilinear softening law (MC 90)	1.045
non linear softening law (Hordjik et al., 1987)	1.037.

The differences found respect to the exact solution and between numerical solutions are consistently due to a bigger amount of tensile residual strength carrying capacity allowed by the introduction of the softening and by the bilinear and non-linear laws at a given strain respectively. The limited possibility of stress re-distribution allowed by this structure restrains the scatter between different softening laws and, primarily, between them and the LEFM solution.

This result allows to consider the procedure adequate for the analysis of the dam; being the dam problem characterised by a higher capability of stress redistribution, the different assumptions on the softening law

shapes are expected to play a major role on the critical temperature evaluation.

THE DAM CASE: RESULTS

The problem of determining the critical temperature decrease capable of making a crack unstable has been addressed with the procedure and the model outlined here above. The results refer to the case of the buttress resting on a rigid foundation.

The post crack behaviour is characterised by a linear softening law. The criterion for crack instability is that of zero residual strength achievement.

The resulting critical temperature variations are given in the following Figure together with those obtained with LEFM (Menga et al., 1994).

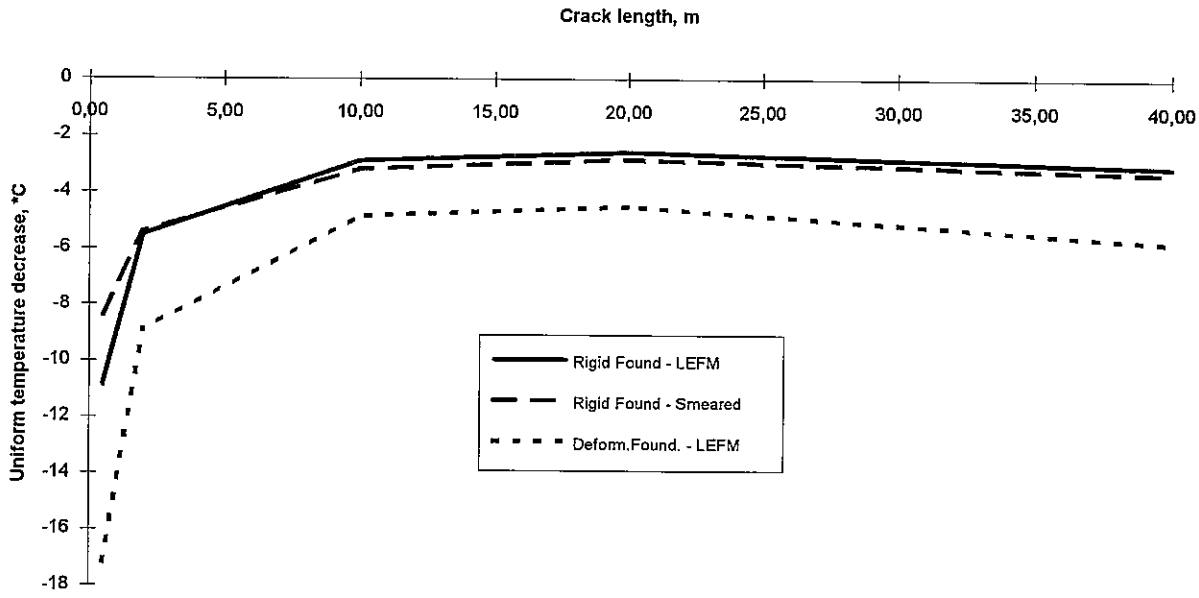

A satisfactory agreement has been achieved. As expected, bigger temperature variations are needed to make the crack unstable according to the non linear approach. This result accounts on the higher 'ductility' of the concrete as described by the non linear model. This effect is reversed for the smallest pre-crack length: in this case the solution is significantly affected by crack diffusion along the dam foundation interface.

Increasing the ultimate crack width, which is unavoidable when the softening law is changed into bilinear and non-linear keeping Gf and tensile strength values, the predicted temperature values grow significantly. The numerical solution was found in this case difficult to achieve, specifically for the smaller pre-cracked lengths.

References

1. Bruhwiler E., "Determination of fracture properties of dam concrete from core samples", Proc. International Conference on "Dam Fracture", EPRI, Sept.11-13 1991, Boulder, Colorado, USA.

2. Elices, M. and Planas J., "Material Models" in Fracture Mechanics of Concrete Structures, L.Elfgren Editor, Chapman and Hall, 1989, Ch.3, pp.16-62.

3. FIP/CEB 1990: "Copy for the CMC-Meeting in Munich", March 1990

4. Hordjik D.A., Reinhardt H.W., Cornelissen H.A.W., "Fracture mechanics parameters of concrete from uniaxial tests as influenced by specimen length", Proc. SEM-RILEM Int. Conference on Fracture of Concrete and Rock, Shah S.P. Swartz S.E. Editors, SEM, Bethel, 13, 149, 1987.

5. Jenq Y.S., and Shah S.P., "A Fracture Toughness Criterion for Concrete", *Engineering Fracture Mechanics*, Vol.21, No.5, 1985, pp.1055-1069.

6. Menga R., Dalmagioni P., Mazza' G. And Pellegrini R. "Evaluation of critical uniform temperature decrease of a cracked buttress dam", this Benchmark, 1994.

7. Nallathambi P. and Karihaloo B.L., "Determination of specimen-size independent fracture Toughness of plain concrete", *Magazine of Concrete Research*, Vol.38, No.135, pp.67-76.

8. Perdikaris P.C. and Romeo A., "Size Effect on the Fracture Energy of Plain Concrete and Stability Issues in 3-Point Bending Fracture Toughness Testing", to be published.

9. Planas J. and Elices M., "Conceptual and experimental problems in the determination of the fracture energy of concrete", *Fracture Toughness and Fracture Energy*, Mihashi et al. Editors, Balkema, 1988, Rotterdam, ISBN 90 619 1988 6, pp. 165-181.

10. Rice J.R., Paris P.C. and Merkle J.G., "Some Further Aspects of J-Integral Analysis and Estimates", *Progress in Flaw Growth and Fracture Toughness Testing*, ASTM, STP 536, 00.731-745, 1973.

11. Tada H., Paris P.C., Irwin G.R. The stress analysis of crack handbook, Del. Research Corporation, Hellertown, Pennsylvania, USA, 1973.

12. TNO Building and Construction Research: "DIANA 5.1 Verification Report."

13. Wittmann F.H., Rokugo K., Bruhwiler E., Mihashi H. and Simonin P., "Fracture energy and strain softening of concrete as determined by means of compact tension specimens", *Materials and Structures*, 1988, **21**, pp. 21-32.

NOTES

THIRD ICOLD BENCHMARK WORKSHOP ON NUMERICAL ANALYSIS OF DAMS

Theme A2

Evaluation of Critical Temperature State in a Cracked Buttress Dam using the Strain Energy Release Rate Concept

by

S.S. Bhattacharjee, P. Léger, and R. Tinawi

Department of Civil Engineering, Ecole Polytechnique de Montreal, Canada, H3C 3A7

ABSTRACT

This paper presents the results of the third ICOLD benchmark analysis of a cracked buttress dam, for a uniform temperature decrease in the structure. An existing crack is represented explicitly as an inter-element gap in the finite element model. A small increment to the existing crack length is provided by releasing the crack tip nodes, and the strain energy release rate is computed from two separate analyses. The stress intensity factor (SIF) is computed from the energy release rate using the standard linear elastic fracture mechanics (LEFM) relations. Two sets of analyses are conducted to obtain an extrapolated value of SIF for the original crack length. This value of SIF, calculated for a unit temperature decrease, is compared with the specified material fracture toughness value to determine the critical temperature state that corresponds to an impending propagation of the existing crack. The finite element analysis program FRAC_DAM, an 'in-house' development to conduct research on the cracking behaviour of concrete dams, has been used. Finite element meshes supplied for the benchmark analyses have been considered without the mid-side nodes in the quadrilateral and triangular elements. The buttress dam section has been analyzed for rigid and flexible foundation conditions using the material properties, as specified. The LEFM results obtained for the rigid foundation condition have also been compared with those obtained using a smeared crack analysis model.

INTRODUCTION

FRAC_DAM is a special purpose nonlinear finite element analysis program, that has been developed during the course of research activities on two-dimensional static and seismic crack responses of concrete dams. Figure 1 summarizes the main capabilities of this computer program. The initiation of new cracks and the propagation of localized cracks are simulated by modifying the stress-strain relationships of finite elements. The fracture energy conservation principle and the width of a crack band determine the evolution of damage in finite elements. The global stability of a finite element analysis is determined by checking the energy equilibrium. Theoretical background of this computer program, validation of the numerical implementations, and its applications to different

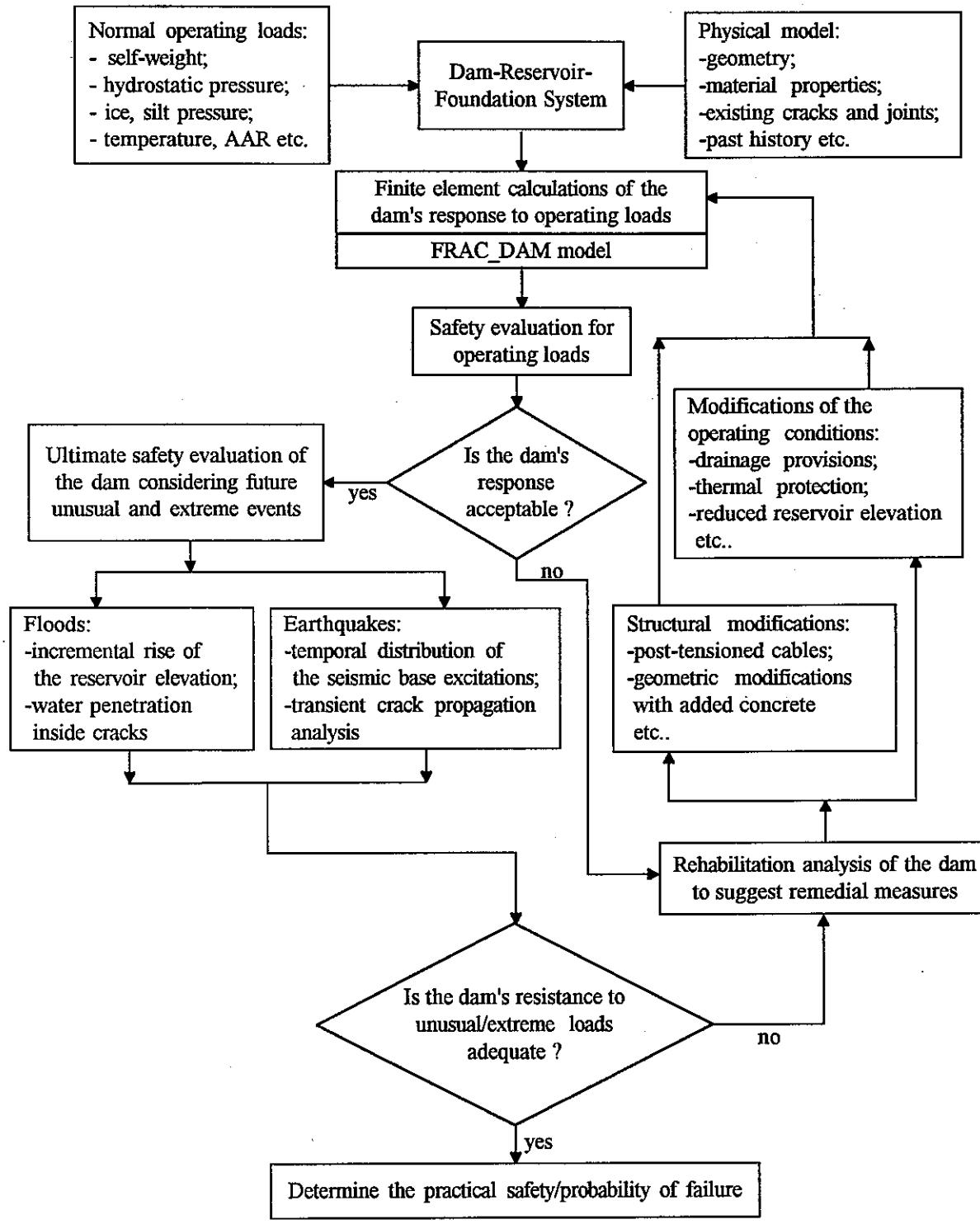

Figure 1 : Safety evaluation of concrete dams using finite element methods.

structural analysis problems have been presented in the literature [1-14]. Smeared crack analysis results obtained with this program have also been verified with an independently developed damage mechanics analysis computer program ALFABET (Ghrib[15]).

The stability of a discrete crack can be determined by post-processing the energy and displacement output created by the FRAC_DAM program (Bhattacharjee[2]). The purpose of this paper is to demonstrate the application of this package in the third ICOLD benchmark analysis of a cracked buttress dam for a uniform decrease of the internal temperature state. An existing crack is modelled as a discrete gap in the finite element model. The node release technique is used to determine the rate of energy release for a small increment of the crack length. A post-processing program FRAC_SIF is used to compute stress intensity factors from the energy response quantities obtained from FRAC_DAM finite element analyses.

The paper starts with a brief description of the temperature stress analysis algorithm, as implemented in the FRAC_DAM computer program, followed by a summary of the computational methodology adopted for the calculation of the stress intensity factors. Results and discussions are presented in the subsequent section. The data supplied for the benchmark analysis will not be repeated in this presentation. The paper concludes with an emphasis on the interpretation of finite element analysis results.

FINITE ELEMENT STRESS-STRAIN ANALYSIS OF TEMPERATURE CHANGES

The specified nodal temperature data are interpolated to the finite element Gauss integration points. In a two-dimensional plane stress analysis, the unrestrained thermal strain, ϵ^T, corresponding to a temperature change, DT, from the reference stress-free state is given as,

$$\{\epsilon^T\} = \begin{Bmatrix} \epsilon_x^T \\ \epsilon_y^T \\ \gamma_{xy}^T \end{Bmatrix} = \begin{Bmatrix} \alpha \\ \alpha \\ 0 \end{Bmatrix} DT \qquad (1)$$

where α is the coefficient of thermal dilation, which is assumed to be a constant material property. The unrestrained strain due to a temperature change, $\{\epsilon^T\}$, is modelled as a pseudo-load, $\{f^T\}$, applied to the structure,

$$\{f^T\} = \int [B]^T [D] \{\epsilon^T\} \, dV \qquad (2)$$

where [B] is the strain-displacement transformation matrix, [D] the constitutive relationship matrix, and dV is the volume associated with an integration point. The displacement vector, {u}, corresponding to this pseudo-load is obtained by solving the following equation:

$$[K]\{u\} = \{f^T\} \qquad (3)$$

where [K] is the structural stiffness matrix. Other load components, if required, can be assembled with $\{f^T\}$ in the right hand side vector of equation (3). Assuming that the creep effects have been explicitly considered by modifying the thermal expansion coefficient, the

mechanical strains, $\{\epsilon\}$, caused by external and internal restraints to the temperature induced volumetric changes, are obtained as follows:

$$\{\epsilon\} = [B]\ \{u\} - \{\epsilon^T\} \tag{4}$$

The mechanical stresses, $\{\sigma\}$, corresponding to the mechanical strains are determined using the standard constitutive relationship matrix. The mechanical strain energy in a system, U, is evaluated by summing the contributions of all Gauss integration points from all finite elements in the structure:

$$U = \frac{1}{2} \int \{\sigma\}^T \{\epsilon\}\ dV \tag{5}$$

FRAC_DAM computer program reports the internal strain energy, external work done, and other energy components including the dissipated fracture energy in a step-by-step static or seismic analysis (Bhattacharjee [2]).

FORMULATION OF THE STRESS INTENSITY FACTOR

The stress intensity factor is related to the rate of energy release, G, which is a measure of the energy available for an increment of crack length, dl, as follows:

$$G = -\frac{d\pi}{dl} \tag{6}$$

where π is the potential energy of the system. The crack length 'l' is replaced by the fracture area, A, in a three-dimensional analysis. The parameter π is defined as follows:

$$\pi = U - W \tag{7}$$

where W is the work done by external forces. In the present temperature stress analysis problem, with no external forces applied to the structure, the external work W is zero. Therefore, $\pi = U$, and this readily implies that,

$$G = -\frac{dU}{dl} \tag{8}$$

The energy release rate, G, can be obtained for different modes (opening, sliding or tearing) of crack extension. The stress intensity factor for a mode-I (opening) crack extension can be determined from the corresponding energy release rate, G_I, as follows:

$$K_I = \sqrt{\frac{8\mu G_I}{1+\kappa}} \tag{9}$$

where μ is the shear modulus of the material, and κ is an elastic constant defined for the plane stress condition, in terms of the Poisson's ratio, ν, as follows,

$$\kappa = \frac{3-\nu}{1+\nu} \tag{10}$$

FINITE ELEMENT EVALUATION OF THE STRESS INTENSITY FACTOR

An existing discrete crack is represented explicitly as an inter-element gap in the finite element model, and a uniform temperature decrease of 1° C is applied to the structure. For a given crack length, l, the first structural analysis is conducted to determine the total strain energy in the system $U(l)$. The crack length is increased by Δl in the subsequent analysis by releasing the crack tip nodes, and the corresponding strain energy $U(l+\Delta l)$ is determined. The rate of energy release for a mode I crack extension, G_I, is computed using the finite difference approximation:

$$G_I = -\frac{U(l+\Delta l) - U(l)}{\Delta l} \tag{11}$$

The computed value of G_I, as well as the stress intensity factor K_I, corresponds to an average crack length of $(l+\Delta l/2)$. A second set of analyses is conducted with a different value of Δl. The stress intensity factor corresponding to the original crack length, l, is computed from an extrapolation of the two values obtained for two different average crack lengths. This numerical strategy provides results within engineering accuracy (Owen and Fawkes[16]). A comparative evaluation of this technique with the displacement extrapolation method, and also with the fracture energy based smeared crack analysis results, are available in Bhattacharjee et al. [1].

The calculated stress intensity factor value is compared with the specified material fracture toughness to determine the critical temperature decrease for a given crack length. Only a mode I propagation of the upper crack-tip is considered to determine the critical temperature value. Propagation of the crack into the foundation and the uplifting of the dam along the dam-foundation interface have not been considered in the present investigations. Finite element meshes specifically refined at the crack tips, as suggested for the benchmark analyses, have been used with modifications of the element types. Mid-side nodes of the triangular and quadrilateral elements have been removed to conform with the FRAC_DAM element library. The meshes supplied for benchmark analyses, referred in the following presentation as benchmark meshes (BM), are not reproduced in this paper. A typical linear elastic temperature stress analysis of the dam-foundation model, using the FRAC_DAM computer program, takes about 5 sec in a RISC 6000 workstation.

RESULTS AND DISCUSSIONS

Figure 2(a) shows the critical temperature values for different crack lengths, obtained using the energy release rate method. The magnitudes of critical temperature value, DT_c, vary significantly depending on the foundation condition (rigid or flexible). However, the predicted responses for different crack lengths show a similar trend in both cases. The magnitude of DT_c decreases significantly as the crack length increases from 0.5 m to 10 m. The variation in critical value is relatively insignificant for crack lengths greater than

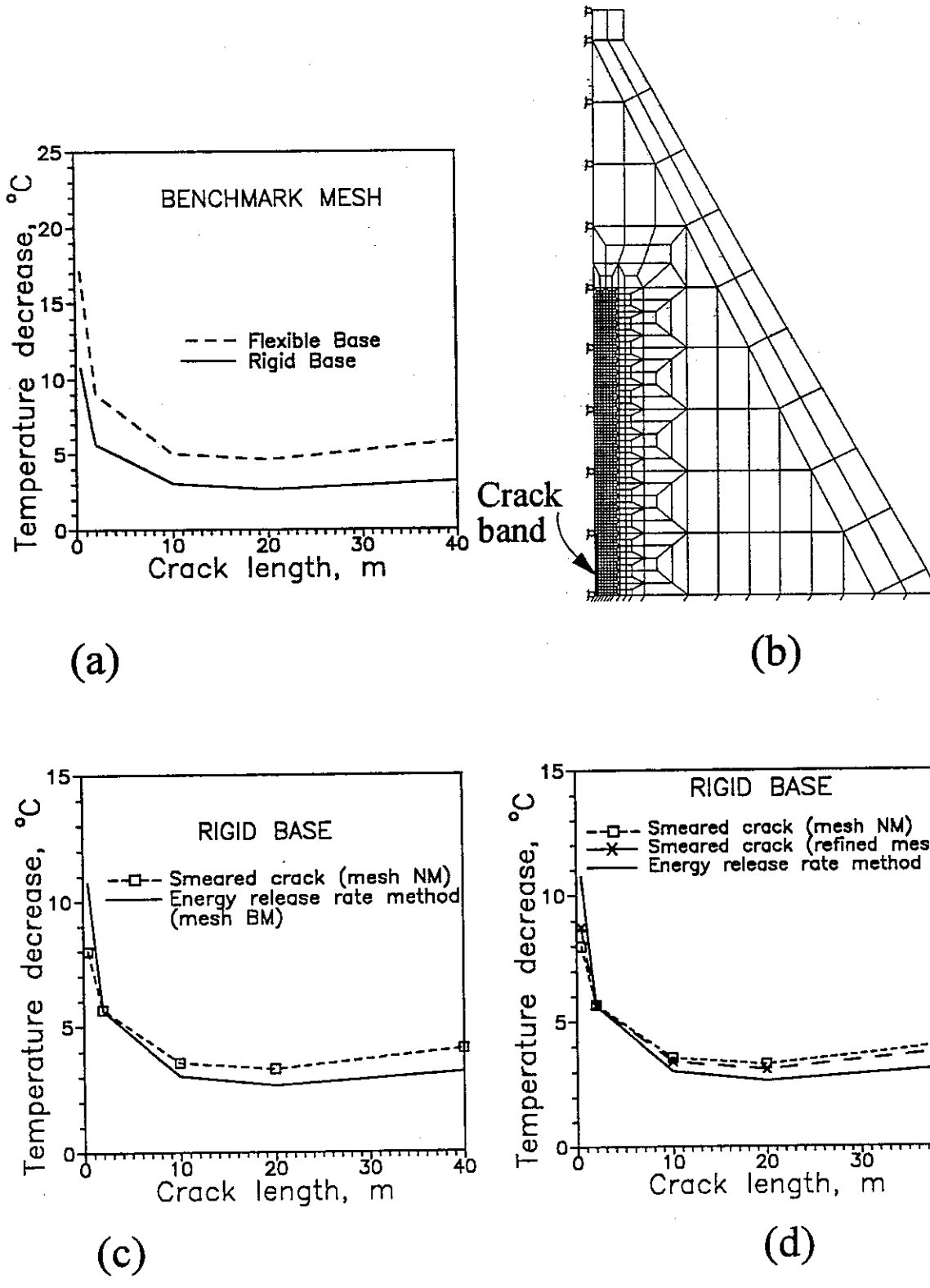

Figure 2: Critical temperature evaluation : (a) LEFM with discrete crack, (b) smeared crack analysis mesh (NM), (c) comparison between smeared crack and LEFM, and (d) effects of mesh refinement on smeared crack response.

than 10 m. However, this value increases slightly for a very long crack (>40 m), because of the confining effects of the webs in the narrow top part of the buttress dam.

Figure 2(b) shows a new finite element mesh (NM) for smeared crack analysis of the rigid base buttress dam. A pre-existing crack is embedded in a band of elements by assigning null stiffness and strength values (shown shaded in Fig. 2(b)). The bi-linear strain softening constitutive models for the crack-tip elements are adjusted to conserve the fracture energy (G_f=176 N/m) for unit length of crack propagation in the complete structure. Analyses with different crack lengths have shown that a pre-existing crack propagates instantly after the tensile stress in the crack-tip element reaches the assumed material tensile strength value. In order to conduct a comparative evaluation of the predicted responses, the tensile strength value in a smeared crack analysis with a 2 m long initial crack has been calibrated to provide a critical temperature decrease of 5.64 °C, which is identical to the response obtained using the LEFM energy release rate method. The calibrated tensile strength value (2.79 MPa) is retained constant, and the fracture energy based smeared crack model is used to determine the critical temperature values for other crack lengths. The width of the crack-band remains the same for all crack lengths, and the change in crack length is accommodated by modifying the stress-strain resistance of finite elements. However, the boundary conditions at the crack-lips are not exactly represented in the smeared crack model.

Figure 2(c) compares the critical temperature responses obtained using the LEFM energy release rate method (mesh BM) and the smeared crack model (mesh NM). Smeared crack results for different crack lengths show a trend similar to that obtained using the LEFM method. However, it is apparent that the calibration of the tensile strength for a certain crack length does not ensure a close match of predicted responses for other crack lengths. To investigate the effects of mesh refinement, another finite element mesh (not shown here) has also been considered, that provides a crack-band width equal to one-half of the size of the mesh in Fig. 2(b). Results obtained from the smeared crack analyses with this refined finite element mesh (calibrated tensile strength=3.57 MPa) are presented in Fig. 2(d), and compared with other results already shown in Fig. 2(c). The softening initiation criterion in the smeared crack model, that uses the principal tensile stress value, causes a mesh sensitive response prediction in this particular problem, where a crack propagates instantly after the initiation of softening at the crack-tip element. However, finite element mesh sensitivities of the LEFM energy release rate method are insignificant (Bhattacharjee et al.[1]). Application of the displacement extrapolation method provides stress intensity factors that are in excellent agreement with those predicted using the energy release rate method. The requested results of the benchmark analyses, obtained with the LEFM energy release rate method, are presented in Tables 1-6.

CONCLUSIONS

Stress intensity factors can be computed by a simple post-processing of the energy responses obtained from FRAC_DAM analyses. Existing linear elastic finite element

analysis computer programs, that compute the strain energy stored in a system, can also be used to compute the stress intensity factors. At least two linear elastic analyses are required to obtain the K_I value. The energy release rate method provides mesh objective responses, and it can be applied to asses the stability of an exiting crack tip with a very little computational effort. However, in many structural analyses, the propagation of a crack may be arrested due to the redistribution of internal resistance mechanisms; and the ultimate structural failure load may well exceed the load magnitude that corresponds to a brief instance of initial unstable crack growth (Bhattacharjee[6], Ghrib[15]). The application of energy release rate concept in a discrete crack propagation analysis with extensive remeshing may not be very efficient, particularly when a crack profile becomes curvilinear in a mixed-mode loading scenario.

In the present smeared crack analyses, the cracks propagated to a significant depth instantly after the tensile stress at the crack tip element had reached the assumed material tensile strength value. Local finite element stresses and strains at the crack tip are sensitive to the discretization of the finite element model, which caused a mesh sensitive prediction of the crack initiation temperature load. Moreover, the boundary conditions at the crack lips were not properly represented in smeared crack analyses. This fact probably contributed to the discrepancies between the smeared crack analysis results and the discrete crack results, obtained for different crack lengths, although the crack-band width and the calibrated tensile strength were maintained constant.

However, a crack induced local material failure is not always expected to cause the sudden global failure of a 3D dam structure. Moreover, a concrete dam in practice may not experience a uniform instantaneous decrease of internal temperature. Continuum mechanics models are efficient to approximately simulate the curvilinear propagation of a crack in the structure, and thereby determine the margin of safety that the structure possesses between the crack initiation load and the ultimate failure load. Many inherent limitations of the local smeared crack analysis model can be eliminated by using a 'non-local' averaging of the finite element strains at the crack tip.

This benchmark workshop on crack stability analysis of a buttress dam has provided a scope to compare the performances of different crack analysis models. Further investigations should be conducted to study the influences of creep, cyclic temperature change, etc. Experimental investigations may also be considered to corroborate the numerically predicted behaviour.

ACKNOWLEDGEMENT

The authors are thankful to the Natural Science and Engineering Research Council (NSERC) of Canada, Hydro-Quebec, and Alcan, for their support to conduct research on structural safety of concrete dams, at Ecole Polytechnique, Montreal. Thanks are also due to Mr. M. Leclerc for his help in preparation of supplementary finite element meshes.

BIBLIOGRAPHY

1. S.S. Bhattacharjee, P. Léger, and R. Tinawi, "Comparative analyses of LEFM and smeared fracture models for the safety evaluation of cracked concrete structures". ***Technical Report***, Dept. of Civil Engg, Ecole Poly., Montreal, 1994.
2. S.S. Bhattacharjee, "FRAC_DAM Manual, A Finite Element Analysis Computer Program to predict the Fracture and Damage Response of Concrete Structures". ***Report No. EPM/GCS-1993-04***, Dept. of Civil Engg, Ecole Polytechnique, Montreal, 1994.
3. S.S. Bhattacharjee, P. Léger, and R. Tinawi, "Flood safety evaluation of plain and post-tensioned concrete gravity dams considering a poro-fracture constitutive model". ***Report No. EPM/GCS-1994-02***, Dept. of Civil Engg., Ecole Poly., Montreal, 1994.
4. S.S. Bhattacharjee, and P. Léger, "Fracture response of gravity dams to an incremental rise of reservoir elevation", ***ASCE J. of Struct. Engg.***, 1994 (submitted).
5. S.S. Bhattacharjee, and P. Léger, "Application of NLFM models to predict cracking in concrete gravity dams", ***ASCE J. of Structural Engg.***, 120(4), 1255-1271, 1994.
6. S.S. Bhattacharjee, "Smeared Fracture Analysis of Concrete Gravity Dams for Static and Seismic Loads", ***Ph.D. Thesis***, Department of Civil Engineering & Applied Mechanics, McGill University, Montreal, February, 1993.
7. S.S. Bhattacharjee and P. Léger, "Seismic cracking and energy dissipation in concrete gravity dams", ***Earthquake Engineering & Structural Dynamics***, 22, 991-1007, 1993.
8. S.S. Bhattacharjee and P. Léger, "Finite-element modelling of the tensile strain softening behaviour of plain concrete structures", ***Engg Compu.***, 10(3), 205-221, 1993.
9. S.S. Bhattacharjee, P. Léger, and J. Venturelli, "Thermo-seismic analysis of concrete gravity dams", in ***Fracture Mechanics of Concrete Structures***, Ed. Z.P. Bažant, Elsevier Applied Science, Proc. Int. Conf. Frac. Mech. Con. Struc., Breckenridge, Colorado, 361-366, 1992.
10. S.S. Bhattacharjee, and P. Léger, "Concrete constitutive models for nonlinear seismic analysis of gravity dams - state-of-the-art", ***Canadian J. Civil Engg.***, 492-509, 1992.
11. P. Léger and S.S. Bhattacharjee, "Energy concepts in seismic fracture analysis of concrete gravity dams", ***International Workshop on Dam Fracture and Damage***, pp. 231-240, Chambéry, France, March, 1994.
12. P. Léger and S.S. Bhattacharjee, "Seismic fracture analysis of concrete gravity dams", ***Canadian Journal of Civil Engineering***, February, 1995 (to be published).
13. P. Léger, S.S. Bhattacharjee, and J. Venturelli, "Seismic analysis of gravity dams considering severe seasonal temperature variations", ***Int. Workshop on Dam Safety Evaluation***, Vol. 2, pp. 217-228, Grindelwald, Switzerland, April, 1993.
14. R. Tinawi, P. Léger, S.S. Bhattacharjee, and F. Ghrib, "Safety evaluation of gravity dams for floods and earthquakes using crack propagation analyses", Symp. on ***Fracture Mechanics for Hydroelectric Power Systems***, Vancouver, Canada, Sept., 1994.
15. F. Ghrib, "Sur l'analyse de la fissuration des barrages en béton par la mécanique de l'endommagement continu-comportement statique et dynamique", ***Ph.D. Thesis***, Department de Genie Civil, Ecole Polytechnique de Montreal, Canada, May, 1994.
16. D.R.J. Owen, and A.J. Fawkes, ***Engineering Fracture Mechanics: Numerical Methods and Applications***, Pineridge Press Ltd., Swansea, U.K., 1983.

Table 1 : Critical temperature response of the dam with a rigid foundation.

L m	DT ^{0}C	d_{max} m	yd_{max} m
0.5	-10.76	0.07409e-3	0.25
2.0	-5.64	0.15025e-3	1.00
10.0	-3.02	0.32248e-3	5.00
20.0	-2.66	0.56199e-3	10.0
40.0	-3.17	1.08907e-3	20.0

Table 2 : Critical temperature response of the dam with a flexible foundation.

L m	DT ^{0}C	d_{max} m	yd_{max} m
0.5	-17.14	0.08426e-3	0.250
2.0	-9.05	0.17067e-3	1.000
10.0	-5.00	0.38776e-3	4.375
20.0	-4.61	0.66585e-3	10.00
40.0	-5.82	1.40052e-3	10.00

Table 3 : Horizontal displacements of the nodes on the crack-lip (rigid foundation).

L=0.5 m		L=2.0 m		L=10.0 m		L=20.0 m		L=40.0 m	
y m	ux(y) m	y m	ux(y) m	y m	ux(y) m	y m	ux(y) m	y m	ux(y) m
-	-	-	-	-	-	-	-	40.0000	0.00000e-3
-	-	-	-	-	-	-	-	39.9030	0.03365e-3
-	-	-	-	-	-	20.0000	0.00000e-3	39.7790	0.05378e-3
-	-	-	-	10.0000	0.00000e-3	19.9030	0.03357e-3	39.6010	0.07317e-3
-	-	-	-	9.9032	0.03349e-3	19.7790	0.05346e-3	39.3450	0.09402e-3
-	-	-	-	9.7787	0.05319e-3	19.6010	0.07233e-3	38.9860	0.11662e-3
-	-	-	-	9.6010	0.07145e-3	19.3450	0.09214e-3	38.5000	0.14037e-3
-	-	-	-	9.3448	0.09012e-3	18.9860	0.11285e-3	37.5000	0.18152e-3
0.5000	0.0000000	2.0000	0.0000000	8.9859	0.10867e-3	18.5000	0.13337e-3	35.6250	0.24785e-3
0.4839	0.01353e-3	1.9355	0.02705e-3	8.5000	0.12508e-3	17.5000	0.16687e-3	30.0000	0.40274e-3
0.4631	0.02110e-3	1.8525	0.04225e-3	7.5000	0.14757e-3	15.6250	0.21775e-3	20.0000	0.54453e-3
0.4335	0.02754e-3	1.7340	0.05521e-3	6.1010	0.16069e-3	10.0000	0.28100e-3	10.0000	0.48677e-3
0.3908	0.03316e-3	1.5632	0.06664e-3	5.0000	0.16124e-3	4.3750	0.20195e-3	4.3750	0.29711e-3
0.3310	0.03698e-3	1.3239	0.07460e-3	2.5000	0.13009e-3	2.5000	0.14366e-3	2.5000	0.20392e-3
0.2500	0.03705e-3	1.0000	0.07513e-3	1.5000	0.09964e-3	1.5000	0.10421e-3	1.5000	0.14400e-3
0.1690	0.03287e-3	0.6761	0.06705e-3	1.0141	0.07963e-3	1.0141	0.08099e-3	1.0141	0.11012e-3
0.1092	0.02623e-3	0.4368	0.05378e-3	0.6551	0.05911e-3	0.6551	0.05902e-3	0.6551	0.07923e-3
0.0665	0.01912e-3	0.2660	0.03937e-3	0.3990	0.04096e-3	0.3990	0.04035e-3	0.3990	0.05366e-3
0.0369	0.01248e-3	0.1475	0.02578e-3	0.2213	0.02574e-3	0.2213	0.02513e-3	0.2213	0.03317e-3
0.0161	0.00648e-3	0.0646	0.01342e-3	0.0968	0.01297e-3	0.0968	0.01258e-3	0.0968	0.01652e-3
0.0000	0.0000000	0.0000	0.0000000	0.0000	0.00000e-3	0.0000	0.00000e-3	0.0000	0.00000e-3

Table 4 : Horizontal displacements of the nodes on the crack-lip (flexible foundation).

L=0.5 m		L=2.0 m		L=10.0 m		L=20.0 m		L=40.0 m	
y m	ux(y) m	y m	ux(y) m	y m	ux(y) m	y m	ux(y) m	y m	ux(y) m
-	-	-	-	-	-	-	-	40.0000	0.00000e-3
-	-	-	-	-	-	-	-	39.9030	0.03367e-3
-	-	-	-	-	-	20.0000	0.00000e-3	39.7790	0.05389e-3
-	-	-	-	10.0000	0.00000e-3	19.9030	0.03361e-3	39.6010	0.07345e-3
-	-	-	-	9.9032	0.03352e-3	19.7790	0.05363e-3	39.3450	0.09464e-3
-	-	-	-	9.7787	0.05339e-3	19.6010	0.07277e-3	38.9860	0.11786e-3
-	-	-	-	9.6010	0.07202e-3	19.3450	0.09312e-3	38.5000	0.14266e-3
-	-	-	-	9.3448	0.09144e-3	18.9860	0.11481e-3	37.5000	0.18632e-3
0.5000	0.00000e-3	2.0000	0.00000e-3	8.9859	0.11137e-3	18.5000	0.13704e-3	35.6250	0.25794e-3
0.4839	0.01358e-3	1.9355	0.02715e-3	8.5000	0.13018e-3	17.5000	0.17464e-3	30.0000	0.43610e-3
0.4631	0.02131e-3	1.8525	0.04268e-3	7.5000	0.15862e-3	15.6250	0.23445e-3	20.0000	0.65621e-3
0.4335	0.02812e-3	1.7340	0.05638e-3	5.6250	0.18727e-3	10.0000	0.33293e-3	10.0000	0.70026e-3
0.3908	0.03448e-3	1.5632	0.06928e-3	4.3750	0.19388e-3	4.3750	0.30285e-3	4.3750	0.54756e-3
0.3310	0.03968e-3	1.3239	0.08000e-3	2.5000	0.18449e-3	2.5000	0.25774e-3	2.5000	0.45113e-3
0.2500	0.04213e-3	1.0000	0.08534e-3	1.5000	0.16317e-3	1.5000	0.21920e-3	1.5000	0.37628e-3
0.1690	0.04076e-3	0.6761	0.08297e-3	1.0141	0.14547e-3	1.0141	0.19199e-3	1.0141	0.32632e-3
0.1092	0.03628e-3	0.4368	0.07411e-3	0.6551	0.12367e-3	0.6551	0.16140e-3	0.6551	0.27246e-3
0.0665	0.03028e-3	0.2660	0.06202e-3	0.3990	0.10032e-3	0.3990	0.12993e-3	0.3990	0.21831e-3
0.0369	0.02350e-3	0.1475	0.04822e-3	0.2213	0.07639e-3	0.2213	0.09843e-3	0.2213	0.16486e-3
0.0161	0.01534e-3	0.0645	0.03151e-3	0.0968	0.04925e-3	0.0968	0.06322e-3	0.0968	0.10565e-3
0.0000	0.00000e-3	0.0000	0.00000e-3	0.0000	0.00000e-3	0.0000	0.00000e-3	0.0000	0.00000e-3

Table 5 : Horizontal nodal displacements along the line y=L/2 (rigid foundation).

L=0.5 m		L=2.0 m		L=10.0 m		L=20.0 m		L=40.0 m	
x (y=L/2) m	ux(x) m	x (y=L/2) m	ux(x) m	x(y=L/2) m	ux(x) m	x(y=L/2) m	ux(x) m	x(y=L/2) m	ux(x) m
0.0000	0.0000371	0.0000	0.0000751	0.0000	0.16124e-3	0.0000	0.28100e-3	0.0000	0.54453e-3
0.0646	0.0000312	0.2586	0.0000629	5.0000	0.05244e-3	5.0000	0.18553e-3	5.0000	0.39433e-3
0.1522	0.0000231	0.6089	0.0000457			10.0000	0.07463e-3	10.0000	0.24859e-3
0.2398	0.0000174	0.9592	0.0000337			15.0000	-0.000002	15.0000	0.10702e-3
0.5260	0.0000067	2.1041	0.0000105			20.0000	-0.000061	20.0000	-0.0000237
						25.0000	-0.000109	25.0000	-0.0001458
						30.0000	-0.000152	30.0000	-0.0002643
						35.0000	-0.000189	35.0000	-0.0003896
						40.0000	-0.000234		

Table 6 : Horizontal nodal displacements along the line y=L/2 (flexible foundation).

L=0.5 m		L=2.0 m		L=10.0 m		L=20.0 m		L=40.0 m	
x (y=L/2) m	ux(x) m	x (y=L/2) m	ux(x) m	x(y=L/2) m	ux(x) m	x(y=L/2) m	ux(x) m	x(y=L/2) m	ux(x) m
0.0000	0.04213e-3	0.0000	0.08534e-3	0.0000	0.18918e-3	0.0000	0.33293e-3	0.0000	0.65621e-3
0.0646	0.03198e-3	0.2586	0.06380e-3	5.0000	-0.02797e-3	5.0000	0.13274e-3	5.0000	0.36982e-3
0.1522	0.01755e-3	0.6089	0.03327e-3			10.0000	-0.08869e-3	10.0000	0.08515e-3
0.2398	0.00507e-3	0.9592	0.00669e-3			15.0000	-0.27976e-3	15.0000	-0.20106e-3
0.5260	-0.02935e-3	2.1041	-0.06682e-3			20.0000	-0.45407e-3	20.0000	-0.47992e-3
						25.0000	-0.61919e-3	25.0000	-0.75246e-3
						30.0000	-0.77958e-3	30.0000	-1.02306e-3
						35.0000	-0.93582e-3	35.0000	-1.30068e-3
						40.0000	-1.10437e-3		

MERLIN Analysis

Theme A2

Evaluation of Critical Uniform Temperature Decrease of a Cracked Buttress Dam

Third ICOLD Benchmark Workshop
On Numerical Analysis of Dams
Paris (France), Sept. 29-30 1994

Submitted by:
Akira Shinmura
Jan Červenka
Howard Boggs
Giovanni Plizzari
Victor Saouma

Dept. of Civil Engineering
University of Colorado,
Boulder, CO 80309-0428, USA Program Funded by the

Electric Power Research Institute
3412 Hillview Avenue
Palo Alto, California 94304

EPRI Project Manager
D.I. Morris
Hydroelectric and Storage Systems Division

EPRI Project Monitor
H. Boggs

1 Introduction

Analysis of this dam, was undertaken using the MERLIN[1] program developed by the University of Colorado under contract from the Electric Power Research Institute (Palo-Alto).

Because MERLIN does not support symmetrical cracks, we have used pre-MERLIN (a 2D/3D mesh generator) to generate the full mesh of the dam under consideration. The generated mesh has approximately the same number of nodes as the one supplied by the organizing committee.

2 Finite Element Meshes

As indicated above, preMERLIN was used to generate the finite element meshes shown in Fig. 1. The crack lengths are assumed to be 0.5m, 2.0m, 10.0m, 20.0m, and 40.0m. Plane-stress 3-node elements were used for dam and plane-strain 3-node elements were used for foundation.

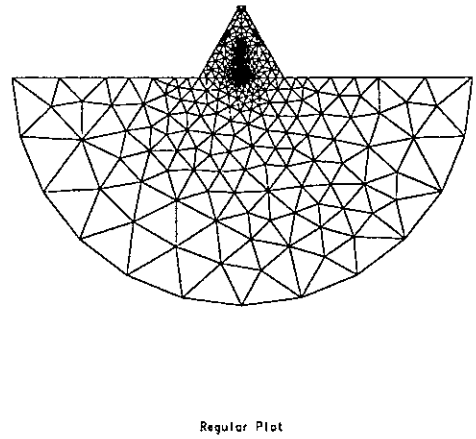

Figure 1: Finite Element Mesh Generated with preMERLIN (Crack length=40m)

[1]MERLIN is separately described in the appendix.

3 Mechanical Parameteras

The mechanical parameters are shown in Table 1.

Material -	Young's modulus $10^{10}\mathrm{Nm}^{-2}$	Poisson's ratio -	Thermal dilatation coefficient $10^{-5}{}^{o}\mathrm{C}^{-1}$	Fracture toughness $10^{6}\mathrm{Nm}^{-3/2}$
Concrete	3.0	0.16	1.0	2.3
Rock	1.0	0.2	-	-

Table 1: Mechanical Parameteras

4 Critical Temperatures

Results of the parametric study for critical temperature are summarized in Table 2, and plotted in Fig. 2

L m	Δ T ^{o}C	COD_{max} mm	y COD_{max} m
Rigid Foundation			
0.5	11.23	0.073	0.292
2.0	5.79	0.158	1.00
10.	3.00	0.378	5.00
20.	2.64	0.585	10.00
40.	3.22	1.085	25.00
Deformable Foundation			
0.5	11.90	0.082	0.25
2.0	6.42	0.182	1.00
10.	3.59	0.442	3.75
20.	3.26	0.698	7.50
40.	6.62	2.248	22.50

Table 2: Critical Temperature

5 Horizontal Displacements Along the Crack

Horizontal displacements along the cracks are tabulated in Table 3,Table 4, and plotted in Fig. 3 Fig. 4 Fig. 5 Fig. 6 Fig. 7.

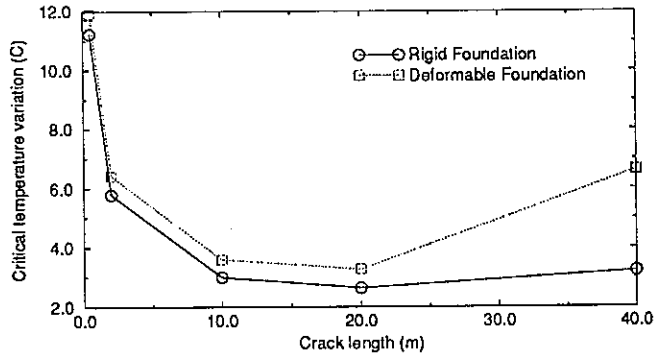

Figure 2: Critical Temperatures

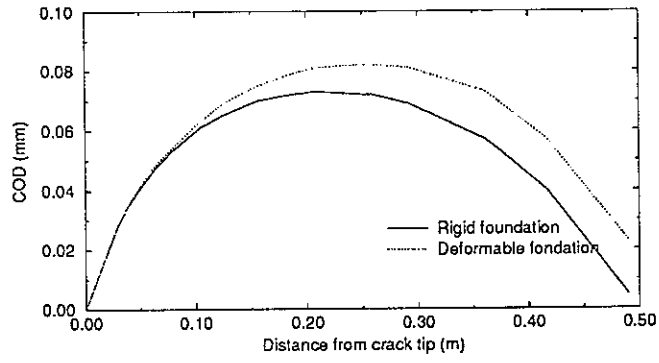

Figure 3: Crack Opening Displacements: Crack Length 0.5m

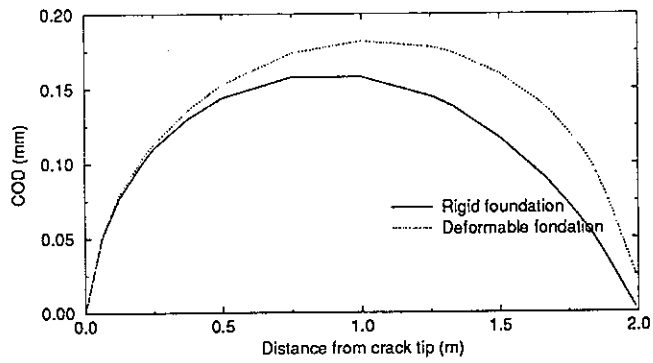

Figure 4: Crack Opening Displacements: Crack Length 2m

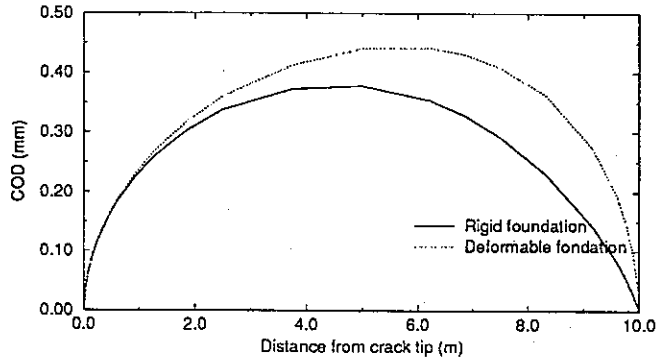

Figure 5: Crack Opening Displacements: Crack Length 10m

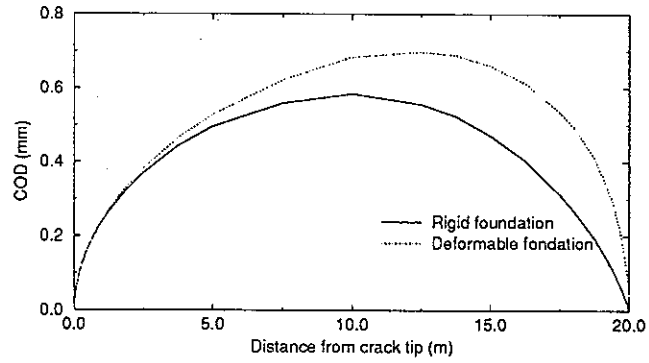

Figure 6: Crack Opening Displacements: Crack Length 20m

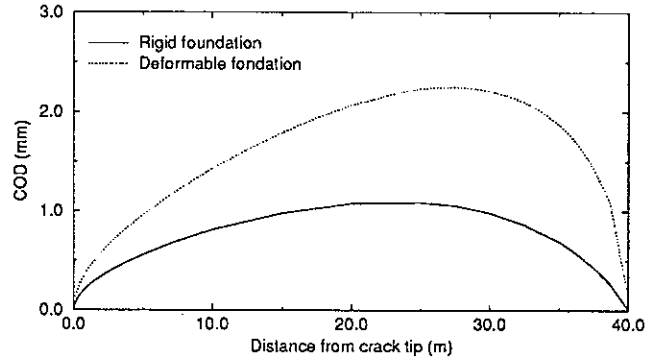

Figure 7: Crack Opening Displacements: Crack Length 40m

L=0.5 m		L=2.0 m		L=10.0 m		L=20.0 m		L=40.0 m	
y m	COD 10^{-3} m	y m	COD 10^{-3}m	y m	COD 10^{-3}m	y m	COD 10^{-3}m	y m	COD 10^{-3}m
0.00	0.000	0.00	0.000	0.00	0.000	0.00	0.000	0.00	0.000
0.02	0.027	0.06	0.051	0.03	0.040	0.03	0.038	0.03	0.029
0.03	0.035	0.12	0.077	0.07	0.062	0.07	0.058	0.07	0.051
0.05	0.042	0.21	0.101	0.15	0.091	0.15	0.089	0.15	0.082
0.06	0.047	0.25	0.110	0.23	0.113	0.23	0.111	0.31	0.125
0.07	0.053	0.37	0.130	0.31	0.131	0.31	0.130	0.46	0.157
0.10	0.061	0.50	0.144	0.46	0.162	0.46	0.162	0.62	0.184
0.12	0.065	0.75	0.158	0.62	0.187	0.62	0.188	0.93	0.228
0.15	0.070	1.00	0.158	0.93	0.226	0.93	0.231	1.25	0.267
0.18	0.072	1.25	0.145	1.25	0.258	1.25	0.266	1.87	0.328
0.20	0.073	1.33	0.138	1.87	0.304	1.87	0.323	2.50	0.385
0.25	0.072	1.50	0.117	2.50	0.338	2.50	0.370	3.75	0.476
0.25	0.072	1.66	0.090	3.75	0.373	3.75	0.443	5.00	0.557
0.29	0.069	1.74	0.073	5.00	0.378	5.00	0.495	7.50	0.693
0.36	0.057	1.80	0.061	6.23	0.354	7.50	0.559	10.00	0.809
0.37	0.053	1.83	0.053	6.25	0.354	10.00	0.585	15.00	0.979
0.41	0.040	1.88	0.036	6.25	0.353	12.49	0.556	20.00	1.077
0.49	0.005	1.99	0.003	6.87	0.328	13.75	0.523	24.99	1.085
				7.50	0.292	15.00	0.471	27.49	1.056
				8.33	0.229	16.23	0.405	29.99	0.983
				9.16	0.142	16.25	0.403	32.50	0.863
				9.58	0.083	17.50	0.312	35.00	0.692
				9.76	0.053	18.12	0.257	36.24	0.575
				9.88	0.027	18.75	0.193	37.49	0.433
				9.99	0.002	19.38	0.112	38.66	0.265
						19.69	0.063	39.98	0.011
						19.85	0.033	39.99	0.004
						19.92	0.019		
						19.99	0.002		

Table 3: Crack Opening Displacements, Rigid Foundation

L=0.5 m		L=2.0 m		L=10.0 m		L=20.0 m		L=40.0 m	
y m	COD 10^{-3} m	y m	COD 10^{-3}m	y m	COD 10^{-3}m	y m	COD 10^{-3}m	y m	COD 10^{-3}m
0.00	0.00	0.00	0.00	0.00	0.00	0.00	0.00	0.00	0.00
0.03	0.03	0.06	0.05	0.04	0.04	0.04	0.04	0.04	0.06
0.04	0.04	0.13	0.08	0.08	0.06	0.08	0.06	0.08	0.09
0.05	0.04	0.21	0.10	0.16	0.09	0.16	0.09	0.16	0.14
0.06	0.05	0.25	0.11	0.23	0.11	0.23	0.11	0.23	0.18
0.08	0.05	0.38	0.14	0.31	0.13	0.31	0.13	0.31	0.21
0.10	0.06	0.50	0.15	0.47	0.16	0.47	0.16	0.39	0.24
0.13	0.07	0.75	0.17	0.63	0.19	0.63	0.19	0.47	0.26
0.16	0.08	1.00	0.18	0.94	0.23	0.94	0.23	0.63	0.31
0.19	0.08	1.25	0.18	1.25	0.27	1.25	0.27	0.78	0.35
0.21	0.08	1.33	0.17	1.88	0.32	1.88	0.33	0.94	0.39
0.25	0.08	1.50	0.16	2.50	0.36	2.50	0.38	1.25	0.45
0.26	0.08	1.67	0.14	3.75	0.41	3.75	0.46	1.56	0.51
0.29	0.08	1.75	0.12	5.00	0.44	5.00	0.53	1.88	0.56
0.36	0.07	1.80	0.11	6.24	0.44	7.50	0.62	2.19	0.61
0.38	0.07	1.83	0.10	6.25	0.44	10.00	0.68	2.50	0.65
0.42	0.06	1.89	0.08	6.25	0.44	12.50	0.70	3.13	0.74
0.49	0.02	1.99	0.03	6.87	0.43	13.75	0.69	3.75	0.82
				7.50	0.41	15.00	0.66	4.38	0.89
				8.33	0.36	16.24	0.62	5.00	0.96
				9.17	0.27	16.26	0.61	6.25	1.09
				9.59	0.20	17.50	0.54	7.50	1.21
				9.76	0.15	18.12	0.48	8.71	1.32
				9.89	0.10	18.75	0.41	10.00	1.43
				9.99	0.03	19.38	0.30	12.50	1.62
						19.69	0.21	15.00	1.79
						19.85	0.14	17.50	1.94
						19.92	0.10	20.00	2.07
						19.99	0.04	22.50	2.16
								23.13	2.18
								23.75	2.20
								24.37	2.22
								25.00	2.23
								25.01	2.23
								26.25	2.25
								27.50	2.25
								28.75	2.24
								29.99	2.21
								31.26	2.17
								32.51	2.10
								33.74	2.01
								35.01	1.88
								35.62	1.80
								36.25	1.70
								36.25	1.70
								36.86	1.58
								37.49	1.44
								38.67	1.09
								39.99	0.14
								39.99	0.14

Table 4: Crack Opening Displacements, Deformabale Foundation

6 Horizontal Displacements measured at mid crack height.

Horizontal displacements measured at mid crack height y=L/2 are tabulated in Table 5 and Table 6, and plotted in Fig. 8 and Fig. 9.

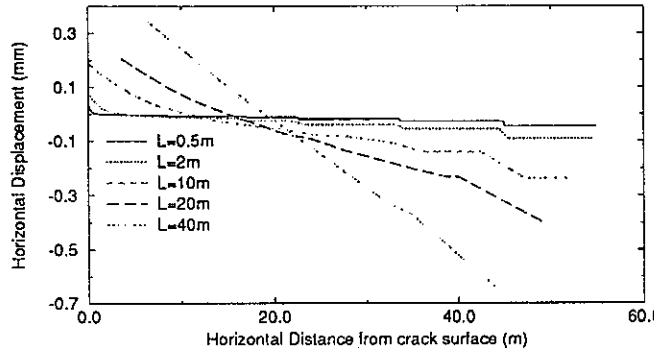

Figure 8: Horizontal Displacements at y=L/2, Rigid Foundation

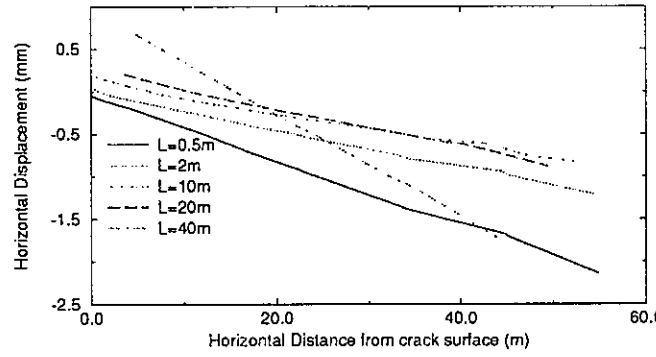

Figure 9: Horizontal Displacements at y=L/2, Deformable Foundation

L=0.5 m		L=2.0 m		L=10.0 m		L=20.0 m		L=40.0 m	
x m	Disp. 10^{-3} m	x m	Disp. 10^{-3}m	x m	Disp. 10^{-3}m	x m	Disp. 10^{-3}m	x m	Disp. 10^{-3}m
0.00	0.036	0.00	0.079	0.00	0.188	3.63	0.205	5.94	0.356
0.00	0.036	0.29	0.063	1.21	0.155	3.67	0.204	7.63	0.308
0.02	0.033	0.37	0.060	1.22	0.155	6.20	0.147	11.20	0.210
0.03	0.033	0.64	0.048	2.10	0.131	6.42	0.143	12.87	0.159
0.03	0.032	0.69	0.046	3.10	0.109	8.52	0.099	18.07	0.024
0.10	0.025	1.09	0.032	3.34	0.103	10.14	0.071	18.33	0.017
0.18	0.020	1.14	0.030	3.65	0.097	11.49	0.048	24.46	-0.135
0.24	0.016	1.20	0.029	4.86	0.070	15.15	-0.001	26.52	-0.187
0.35	0.010	1.62	0.019	5.79	0.057	15.39	-0.004	32.27	-0.327
0.49	0.007	1.82	0.016	6.42	0.046	15.60	-0.006	35.00	-0.372
0.58	0.005	2.21	0.010	7.69	0.029	20.95	-0.072	35.00	-0.372
0.91	0.002	3.07	0.004	9.29	0.013	24.14	-0.094	43.81	-0.635
0.95	0.002	3.15	0.003	10.10	0.005	27.60	-0.134	43.88	-0.637
0.96	0.002	3.27	0.003	10.69	0.002	35.46	-0.206		
0.97	0.002	4.42	-0.003	13.71	-0.025	38.75	-0.232		
1.40	-0.000	4.89	-0.003	15.56	-0.033	40.00	-0.232		
1.67	-0.001	6.11	-0.006	20.16	-0.055	40.00	-0.232		
1.95	-0.001	6.97	-0.006	20.39	-0.055	44.44	-0.313		
2.25	-0.001	8.10	-0.009	25.13	-0.080	49.28	-0.401		
2.72	-0.001	9.04	-0.012	26.97	-0.080	49.44	-0.404		
3.10	-0.002	10.74	-0.012	32.23	-0.103				
3.98	-0.002	11.88	-0.015	36.25	-0.141				
4.35	-0.003	15.19	-0.015	42.50	-0.141				
5.47	-0.003	16.38	-0.018	42.50	-0.141				
5.87	-0.004	17.19	-0.024	44.72	-0.186				
7.83	-0.004	21.64	-0.024	47.22	-0.237				
8.24	-0.004	22.48	-0.030	52.22	-0.237				
8.52	-0.006	23.46	-0.040						
11.10	-0.006	33.08	-0.040						
11.38	-0.008	34.25	-0.056						
16.53	-0.008	44.50	-0.056						
16.80	-0.009	44.50	-0.056						
17.01	-0.012	44.94	-0.073						
22.32	-0.012	45.44	-0.092						
22.52	-0.015	54.44	-0.092						
22.75	-0.019								
33.56	-0.019								
33.88	-0.027								
44.87	-0.027								
44.87	-0.027								
44.98	-0.035								
45.11	-0.045								
54.86	-0.045								

Table 5: Horizontal Displacements at y=L/2, Rigid Foundation

L=0.5 m		L=2.0 m		L=10.0 m		L=20.0 m		L=40.0 m	
x m	Disp. 10^{-3} m	x m	Disp. 10^{-3}m	x m	Disp. 10^{-3}m	x m	Disp. 10^{-3}m	x m	Disp. 10^{-3}m
0.03	-0.03	0.30	0.04	1.22	0.16	3.64	0.21	4.40	0.71
0.03	-0.03	0.37	0.03	2.10	0.13	3.67	0.21	5.36	0.65
0.04	-0.03	0.65	0.02	3.10	0.10	6.20	0.13	10.10	0.35
0.11	-0.04	0.70	0.01	3.35	0.09	6.42	0.13	10.47	0.32
0.18	-0.05	1.09	-0.01	3.66	0.08	8.53	0.06	10.76	0.30
0.25	-0.05	1.15	-0.01	4.86	0.04	10.15	0.02	16.29	-0.05
0.36	-0.06	1.21	-0.01	5.80	0.02	11.50	-0.02	16.44	-0.05
0.50	-0.07	1.62	-0.03	6.43	0.00	15.16	-0.11	21.59	-0.37
0.59	-0.07	1.83	-0.03	7.70	-0.03	15.39	-0.11	24.92	-0.56
0.92	-0.08	2.21	-0.05	9.30	-0.06	15.61	-0.12	31.89	-0.98
0.95	-0.08	3.07	-0.07	10.11	-0.08	20.95	-0.24	35.00	-1.13
0.96	-0.09	3.15	-0.07	10.69	-0.09	24.15	-0.30	35.00	-1.13
0.97	-0.09	3.28	-0.07	13.71	-0.16	27.60	-0.37	43.82	-1.71
1.40	-0.10	4.43	-0.10	15.56	-0.19	35.46	-0.54	43.89	-1.71
1.68	-0.11	4.90	-0.11	20.16	-0.27	38.75	-0.60		
1.96	-0.12	6.11	-0.14	20.39	-0.27	40.00	-0.61		
2.25	-0.13	6.97	-0.16	25.13	-0.36	40.00	-0.61		
2.72	-0.15	8.11	-0.19	26.97	-0.38	44.45	-0.74		
3.10	-0.16	9.05	-0.21	32.23	-0.47	49.29	-0.87		
3.98	-0.19	10.75	-0.24	36.25	-0.56	49.44	-0.88		
4.35	-0.20	11.88	-0.27	42.50	-0.61				
5.48	-0.24	15.19	-0.35	42.50	-0.61				
5.88	-0.26	16.39	-0.38	44.72	-0.68				
7.84	-0.33	17.20	-0.40	47.23	-0.75				
8.25	-0.35	21.65	-0.49	52.22	-0.82				
8.52	-0.36	22.49	-0.52						
11.10	-0.46	23.46	-0.55						
11.38	-0.47	33.09	-0.75						
16.53	-0.69	34.26	-0.79						
16.80	-0.70	44.50	-0.94						
17.01	-0.71	44.50	-0.94						
22.33	-0.91	44.94	-0.96						
22.53	-0.92	45.45	-0.99						
22.76	-0.94	54.44	-1.21						
33.57	-1.36								
33.88	-1.38								
44.88	-1.68								
44.88	-1.68								
44.99	-1.69								
45.11	-1.70								
54.86	-2.14								

Table 6: Horizontal Displacements at y=L/2, Deformabale Foundation

7 Contour Maps

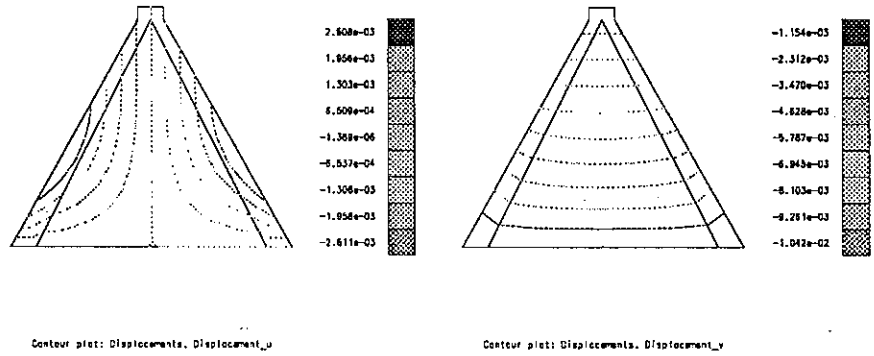

Figure 10: Contour maps of horizontal and vertical displacement: Rigid Foundation L=0.5m

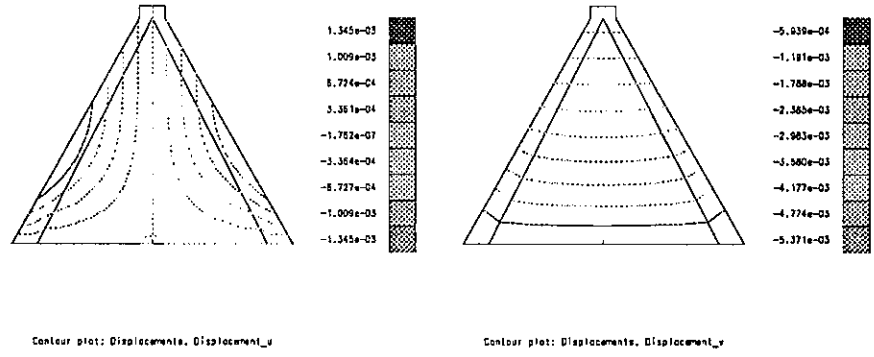

Figure 11: Contour maps of horizontal and vertical displacement: Rigid Foundation L=2m

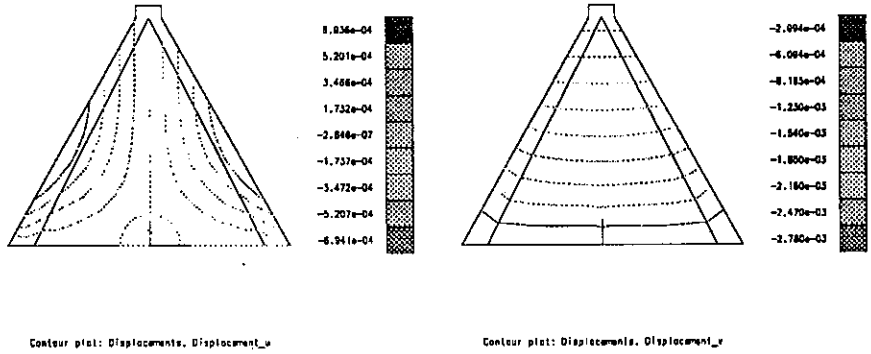

Figure 12: Contour maps of horizontal and vertical displacement: Rigid Foundation L=10m

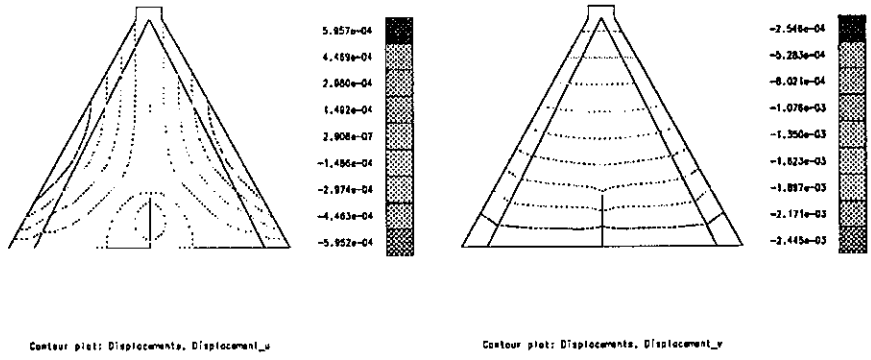

Figure 13: Contour maps of horizontal and vertical displacement: Rigid Foundation L=20m

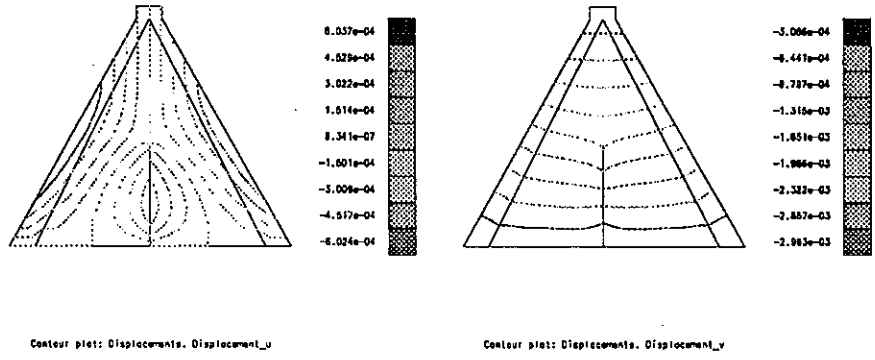

Figure 14: Contour maps of horizontal and vertical displacement: Rigid Foundation L=40m

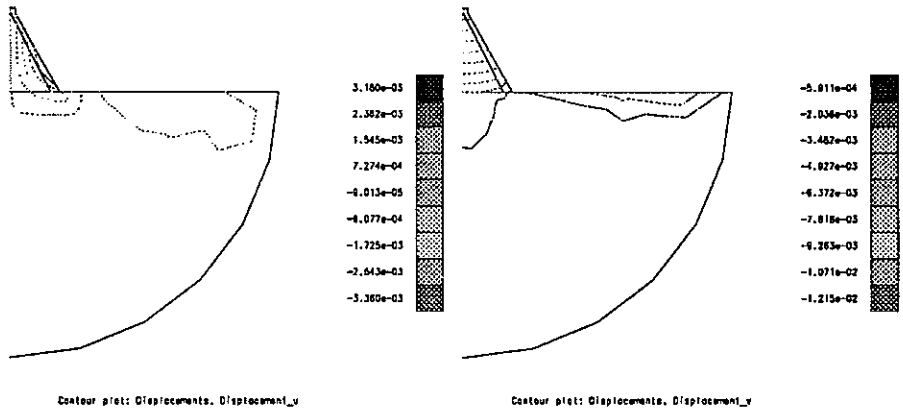

Figure 15: Contour maps of horizontal and vertical displacement: Deformable Foundation L=0.5m

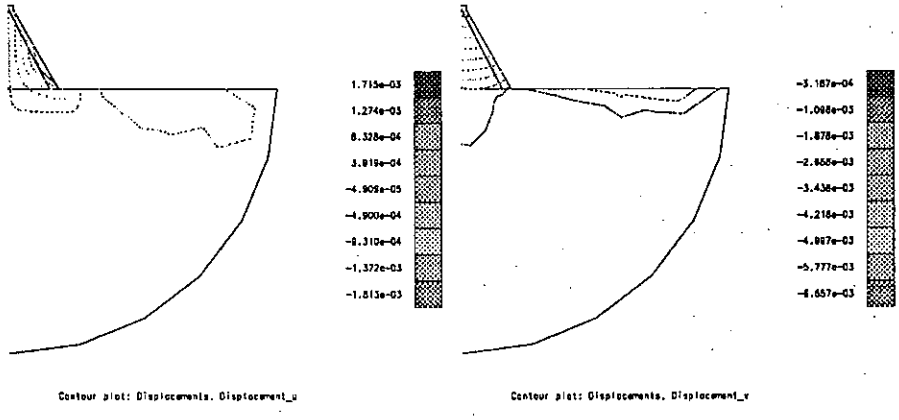

Figure 16: Contour maps of horizontal and vertical displacement: Deformable Foundation L=2m

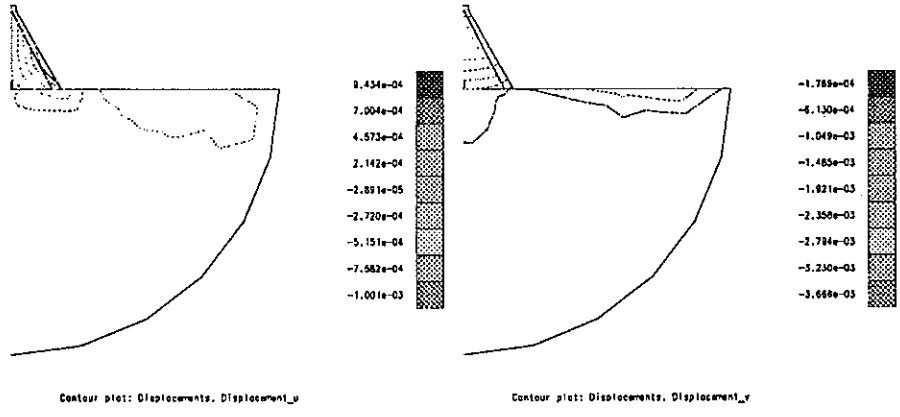

Figure 17: Contour maps of horizontal and vertical displacement: Deformable Foundation L=10m

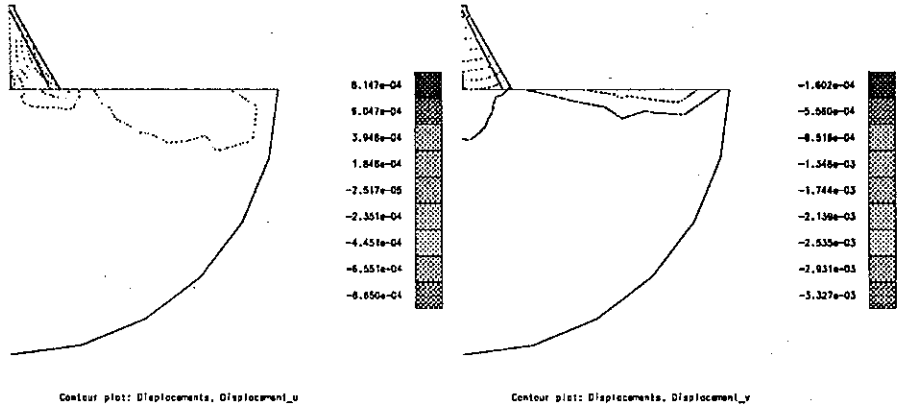

Figure 18: Contour maps of horizontal and vertical displacement: Deformable Foundation L=20m

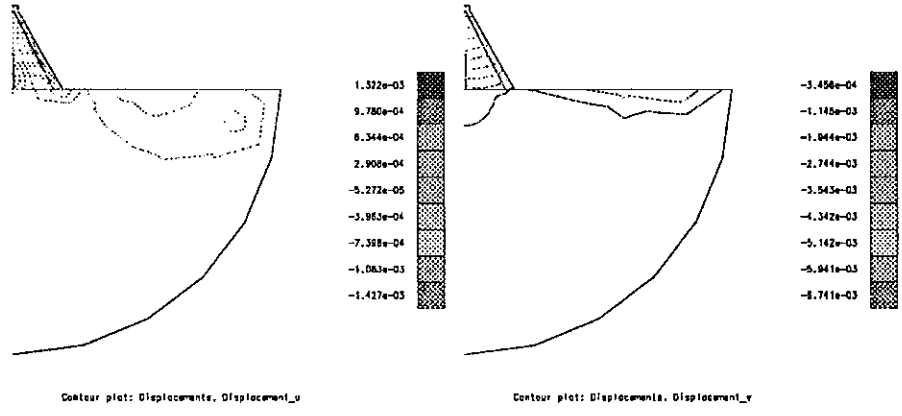

Figure 19: Contour maps of horizontal and vertical displacement: Deformable Foundation L=40m

A MERLIN Description

MERLIN, is a library of three programs

	Pre-Processor/Remeshing	Analysis	Post-Processor
	PreMERLIN	MERLIN	PostMERLIN
Language	C/C++	Fortran & C	C
Environment	UNIX	UNIX, Cray	UNIX
Standards	X & PHIGS	-	X & PHIGS
GUI	MOTIF	-	OPEN LOOK, MOTIF
Size (lines)	38,000	52,000	41,000
% Completed	80	95	100

A.1 PreMERLIN

Fully automatic 2D/3D mesh generator, used for both generation of initial meshes as for adaptive mesh regeneration to capture the crack propagation. Define boundaries of the structure (including crack). Use mesh generator, analyse, determine if a crack propagation occurs, alter the original boundary representation. An arbitrary curvilinear crack propagation can be modeled using this approach. Also, includes capabilities for automatic adaptive remeshing.

A.2 MERLIN

- Includes capabilities for 2- and 3-dimensional:
  1. linear and nonlinear elasto-statics,
  2. steady state and transient linear heat transfer,
  3. uncoupled thermo-elasticity,
  4. steady state and transient linear seepage flow,
  5. uncoupled poro-elasticity,
- Fracture mechanics in 2D/3D.
- Modern element technology and solution strategies are incorporated:
  1. high performance elements with selective reduced integration,
  2. compatible families of heat transfer/seepage flow and stress analysis elements,
  3. modified Newton-Raphson method with:
     - line search,
     - secant-Newton update,
     - indirect displacement control algorithms:
       (a) spherical arc-length.

(b) relative displacement between two nodes, i.e. COD.

(c) tractions due to interface constraints.

4. mixed-iterative method for stress analyses.
5. implicit time integration using α-method for transient heat transfer/seepage flow analyses.

- User subroutines.

A.2.1 Loads Supported by MERLIN

- For stress analysis, the following applied loads are supported:

  1. point loads,
  2. surface tractions,
  3. body forces,
  4. centrifugal forces,
  5. hydrostatic forces,
  6. nonlinear uplift pressures in cracks,
  7. pressures (from seepage flow analysis),
  8. temperatures (from heat transfer analysis).

- For heat transfer/seepage flow analyses, the following applied "loads" are supported:

  1. point fluxes,
  2. surface fluxes,
  3. body fluxes (for heat transfer only),
  4. films (for heat transfer only).

A.2.2 Material models Supported in MERLIN

- Includes the following stress-strain idealizations:

  1. truss/spring,
  2. plane stress,
  3. plane strain,
  4. 3D continuum,
  5. 2D and 3D interface.

- Includes linearly isotropic and anisotropic materials for both stress and heat transfer/seepage flow analyses.

- Includes the following nonlinear constitutive models for stress analysis:
  1. J-2 plasticity.
  2. Drucker-Prager plasticity.
  3. Coulomb friction model (for interface elements).
  4. Fictitious Crack Model,
  5. Interface Crack model.

A.2.3 User Defined Subroutines in MERLIN

- UTRACT for user defined surface tractions,
- UBODY for user defined body forces,
- UFLUX for user defined surface fluxes,
- UHEAT for user defined body fluxes,
- UFILM for user defined films,
- UFCMLW for user defined FCM softening laws.
- UCRFLD provides an interface with CRFLOOD to evaluate the influence of drains in a crack.

A.2.4 Fracture Mechanics Capabilities in MERLIN

- Linear elastic fracture mechanics (LEFM) both in 2D and 3D using:
  1. displacement correlation method,
  2. path-independent contour integrals,
  3. volume integrals.
  4. Mixed mode crack propagation in LEFM and NLFM.
- Supports the Fictitious Crack Model (FCM) using:
  1. an incremental formulation,
  2. linear, bilinear, or user defined softening models,
  3. maximum principal stress criterion for crack propagation,
  4. continuous interface elements to simulate stress transfer in the fracture process zone (FPZ).
- Supports the Interface Crack Model (ICM) using:
  1. an incremental formulation,

2. shear and tensile softening, modeled by decreasing the cohesion c, and the tensile strength σ_t respectively, as a function of the norm of effective inelastic opening displacement $u_{i\epsilon ff}$,
3. stiffness degradation, modeled using a damage parameter D,
4. dilatancy ϕ_d and dilatancy degradation,
5. linear, bilinear, or user defined softening models,
6. continuous interface elements to simulate stress transfer in the fracture process zone (FPZ).

A.3 PostMERLIN

Visualization of results for 2D & 3D analyses:

1. Deformed mesh
2. Vector Plots
   (a) Principal stresses
   (b) Displacements
   (c) Forces
   (d) Fluxes
3. Contour lines/surfaces and shaded contours for:
   (a) Cartesian stresses
   (b) Principal stresses
   (c) Temperatures
   (d) Heads
4. Carpet plots
5. Arbitrary line/plane cuts in 2D/3D for display along x-y plot/shaded surfaces
6. Could be used with other FE analysis programs
7. Supports CGM file format for transfer of information
8. Supports color postscript file format for hardcopy output
9. "State-of-the-art" environment combining PHIGS for real time 3D graphics and X Windows for the user-interface
10. C program based on X Windows and PHIGS

NOTES

Third ICOLD Benchmark Workshop on **Numerical Analysis of Dams**, Paris, Sept. 29-30, 1994

Contribution to Theme A2: Evaluation of critical uniform temperature decrease for a cracked buttress dam

Thermal Effects on Cracking in Concrete Dams - Fracture Mechanics Approach

H.N. Linsbauer, University of Technology Vienna

R. Promper, Österreichische Tauernkraftwerke AG, Salzburg

1. INTRODUCTION

Thermal effects on cracking mechanisms in mass concrete as mainly used in dam construction generally may be related to two different forms of appearance. The most critical phase is given during the "juvenile stage" of the concrete where high temperatures generated during the process of hydration may lead to thermal stress related cracking as a consequence of internal or external restraint of volume change. Despite precautionary measures as lowering of the cement content, adding of special admixtures (blast-furnace slag, fly ash), precooling, postcooling, insulating, optimizing of block dimensions, etc., the development of crack like defects often is not to avoid. Except for the fact that those cracks a priori may influence the reliability of the structure, very often they serve as starting points for further cracking due to temperature variations resulting from climatic conditions near the dam site.

According to the task of theme A2 the stability of a vertical macro-crack in a buttress dam spreading from the foundation area subjected to uniform temperature decrease is investigated in view of a potential crack propagation. The LEFM -investigation results in mode-1 Stress-Intensity-Factor developments for different initial crack lengths. Based on an "assumed" *valid* -size independent- fracture toughness material parameter the critical temperature decrease is shown up.

The analyses are performed by Finite Element Method (FEM) both for rigid and elastic foundation conditions. The crack tip area is represented by a rosette of triangular quarter-point-elements.

2. GENERAL CONSIDERATIONS

The problem in question, before direct analytical attack, requires some general considerations. First of all as necessary for such problems the field of validity of "Linear Elastic Fracture Mechanics (LEFM)" has to be defined. A purely geometrical point of view concerning the ratio of crack length (and estimated size of fracture process zone) to the dimension of the structure may be seen as first assessment.

In this connection it is to state that the LEFM-requirements for the shortest crack in the buttress dam with 0.5 m of length are questionable.

A further quite essential part concerning failure assessment considerations (critical temperatures) via a LEFM-fracture criterion is the material assigned term. Valid LEFM material values for dam concrete with aggregate sizes up to 120 mm call for characteristic test-sample sizes of 2 and more meters which are unrealistic in fracture mechanics materials testing, especially for already existing dams. This item (size effect problem) up to now practically is unsolved and has been a matter of concern and discussion on the International "Workshop on Dam Fracture and Damage" in Chambery in March 1994.

Despite of this crucial situation the assumed value of 2.3 $MN/m^{3/2}$ may be seen as conservative and fit quite well to K_{IC}-transferred values of fracture energy tests of drilling cores from Koelnbrein dam in Austria /1/.

The aim of this contribution besides the intention of the "Benchmark Workshop" was to use very simple equipment and procedures which are common available. This means PC-computers and FE-programs with 8-node isoparametric (plane) elements implemented. As well known the so called quarter-point -elements /2,3/ represent the $1/\sqrt{r}$ singularity which is characteristic for LEFM - this is quite useful both in energy release rate and stress-intensity-factor studies.

The easy way for the determination of critical temperature in this case (symmetry both in geometry and loading $\Rightarrow$ pure mode 1-problem) obviously is given by an energy release rate analysis due to the simple $G \Leftrightarrow K_I$ conversion.

Unfortunately this routine is only available for elastic and not for thermoelastic material in the PC-FEM-program applied to the present investigation.

3 FEATURES

In accordance with the object of the Benchmark Workshop the following items are specified:

- **methodology of the analysis**

  determination of critical temperatures for different crack lengths via a LEFM-criterion ($K_I = K_{IC}$)

- **selected computation method**

  Finite Element Method (FEM)

- **main assumptions of the numerical model**

  validity of Linear Elastic Fracture Mechanics (LEFM) - determination of K_I via the displacements of the quarterpoint and the endpoint of the crack-tip-elements adjacent to the crack faces ($\varphi = \pm 180^o$)

- **software**

  SOLVIA System Version 90.2 (implemented on PC - 4 MB RAM)

- **hardware**

  PC- 486 DX2/66 EISA

- **computation time**

Rigid Foundation

Crack Length [m]	No. of Nodes	No. of Elements	Total Time [CPU sec.]
0,5	674	221	14,39
2,0	636	213	12,74
10,0	658	223	14,61
20,0	653	220	14,06
40,0	653	220	13,73

Deformable Foundation

Crack Length [m]	No. of Nodes	No. of Elements	Total Time [CPU sec.]
0,5	1212	395	41,90
2,0	1120	369	39,77
10,0	1142	379	49,98
20,0	1137	376	46,35
40,0	1137	376	43,17

4 FORMULATION OF THE PROBLEM

The formulation of the problem is given by the project theme: Evaluation of critical uniform temperature decrease for a cracked buttress dam considering cracks with different lengths spreading vertically from the dam foundation interface. The investigation was to carry out both for rigid and deformable foundation conditions.

For reason of comparison the proposed (Benchmark Workshop) finite element mesh was taken as a basis. Some adaptations were necessary especially by moving the midside nodal points of the crack tip elements to quarter point position and to prepare an adequate input file for SOLVIA.

The proposed geometry and the assumed material values are shown in Fig. 1

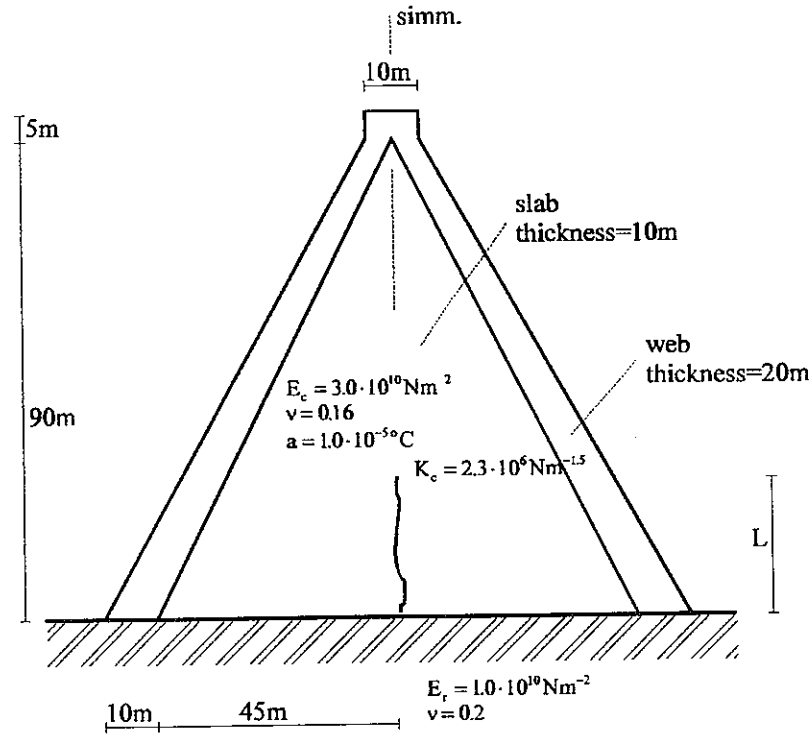

Fig. 1 Geometry and characteristic material values

5 RESULTS

The results of the investigation are presented in the following section .

5.1 Critical temperatures and associated maximum crack opening

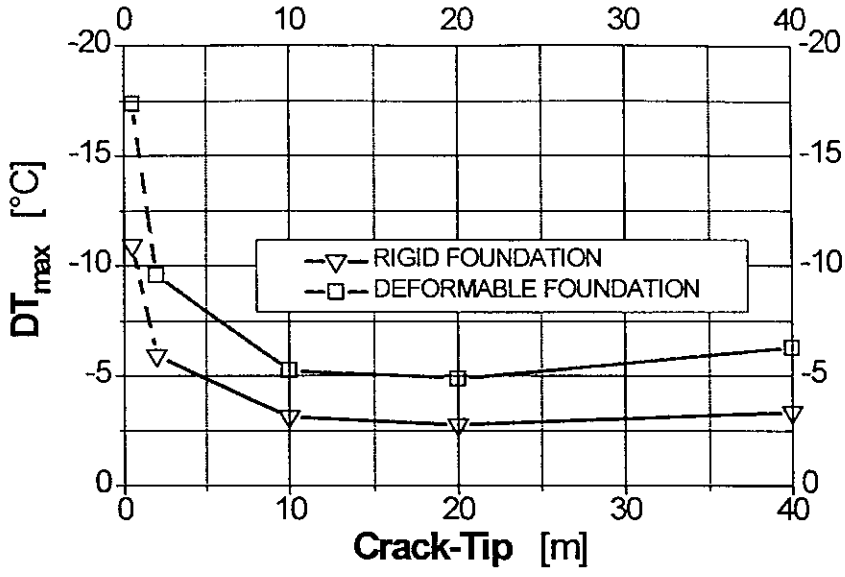

TABLE 1
RIGID FOUNDATION

L m	DT °C	Yd_{max} m	d_{max} m
0,5	-10,9381	0,29	4,07E-5
2,0	-5,9167	1,16	8,5E-5
10,0	-3,1253	5,62	2,024E-4
20,0	-2,7693	10,0	3,109E-4
40,0	-3,3392	20,0	5,831E-4

TABLE 2
DEFORMABLE FOUNDATION

L m	DT °C	Yd_{max} m	d_{max} m
0,5	-17,39	0,25	4,59E-5
2,0	-9,589	1,0	9,62E-5
10,0	-5,2461	4,38	2,36E-4
20,0	-4,8678	7,19	3,786E-4
40,0	-6,2753	15,0	7,666E-4

5.2 Crack opening due to "critical temperature" loading

a) Rigid foundation

(L = 0.5 m)

Y m	Ux(y) m
0,5	0
0,496	7,8374E-6
0,484	1,5874E-5
0,473	2,0341E-5
0,463	2,3474E-5
0,448	2,7184E-5
0,433	3,0139E-5
0,412	3,3405E-5
0,391	3,5895E-5
0,361	3,8427E-5
0,331	3,9964E-5
0,29	4,0711E-5
0,25	4,0121E-5
0,21	3,8268E-5
0,169	3,5056E-5
0,139	3,1776E-5
0,109	2,7608E-5
0,088	2,4122E-5
0,067	2,0055E-5
0,052	1,6741E-5
0,037	1,2992E-5
0,027	1,0195E-5
0,016	6,7001E-6
0,008	3,7481E-6
0	0

(L = 2.0 m)

Y m	Ux(y) m
2	0
1,98375	1,5919E-5
1,935	3,2486E-5
1,894	4,1145E-5
1,852	4,8025E-5
1,793	5,5686E-5
1,734	6,1823E-5
1,649	6,8832E-5
1,563	7,4267E-5
1,444	7,9669E-5
1,324	8,3065E-5
1,162	8,4895E-5
1	8,3915E-5
0,838	8,0215E-5
0,676	7,3747E-5
0,556	6,6991E-5
0,437	5,8423E-5
0,351	5,0956E-5
0,266	4,2305E-5
0,207	3,5423E-5
0,147	2,7487E-5
0,106	2,1385E-5
0,065	1,4466E-5
0,032	7,9964E-6
0	0

(L = 10.0 m)

Y m	Ux(y) m
10	0
9,97575	1,9677E-5
9,903	4,0605E-5
9,841	5,2073E-5
9,779	6,1302E-5
9,69	7,2282E-5
9,601	8,1619E-5
9,473	9,3185E-5
9,345	1,0319E-4
9,165	1,1528E-4
8,986	1,2561E-4
8,743	1,3787E-4
8,5	1,4847E-4
8	1,6519E-4
7,5	1,7944E-4
6,563	1,9539E-4
5,625	2,024E-4
5	2,0228E-4
4,375	1,9701E-4
3,438	1,8001E-4
2,5	1,5654E-4
2	1,3706E-4
1,5	1,1562E-4
1,257	1,0272E-4
1,014	8,8428E-5
0,835	7,6998E-5
0,655	6,4369E-5
0,527	5,4591E-5
0,399	4,4013E-5
0,31	3,6094E-5
0,221	2,7533E-5
0,159	2,1098E-5
0,097	1,4005E-5
0,048	7,6912E-6
0	0

(L= 20.0 m)

Y m	Ux(y) m
20	0
19,97575	1,973E-5
19,903	4,0817E-5
19,841	5,2455E-5
19,779	6,1884E-5
19,69	7,32E-5
19,601	8,2922E-5
19,473	9,5114E-5
19,345	1,0582E-4
19,165	1,1903E-4
18,986	1,3061E-4
18,743	1,4473E-4
18,5	1,5736E-4
18	1,7899E-4
17,5	1,9853E-4
16,563	2,2775E-4
15,625	2,5208E-4
12,813	2,9877E-4
10	3,1091E-4
7,188	2,9369E-4
4,375	2,3747E-4
3,438	2,0686E-4
2,5	1,7143E-4
2	1,47E-4
1,5	1,2101E-4
1,257	1,0634E-4
1,014	9,0561E-5
0,835	7,82E-5
0,655	6,4818E-5
0,527	5,4635E-5
0,399	4,3774E-5
0,31	3,5737E-5
0,221	2,7134E-5
0,159	2,0724E-5
0,097	1,371E-5
0,	0

(L=40.0m)

Y m	Ux(y) m
40	0
39,841	5,2681E-5
39,779	6,2231E-5
39,69	7,3749E-5
39,601	8,3703E-5
39,473	9,6272E-5
39,345	1,074E-4
39,165	1,2129E-4
38,986	1,3364E-4
38,743	1,4888E-4
38,5	1,6275E-4
38	1,8744E-4
37,5	2,1032E-4
36,563	2,4729E-4
35,625	2,8104E-4
32,813	3,6581E-4
30	4,3455E-4
25	5,2511E-4
20	5,7678E-4
15	5,831E-4
10	5,2191E-4
7,188	4,5033E-4
4,375	3,3901E-4
3,438	2,8983E-4
2,5	2,3535E-4
2	2,0004E-4
1,5	1,6292E-4
1,257	1,4246E-4
1,014	1,2074E-4
0,835	1,0387E-4
0,655	8,5764E-5
0,527	7,2093E-5
0,399	5,76E-5
0,31	4,6931E-5
0,221	3,5563E-5
0,159	2,7123E-5
0	0

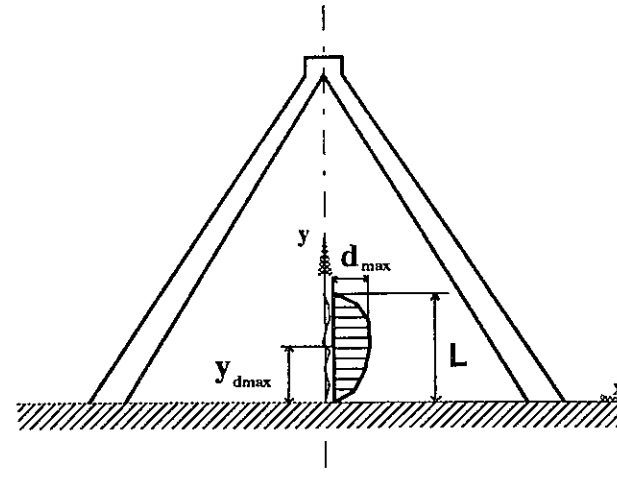

b) Deformable foundation

(L = 0.5 m)

Y m	Ux(y) m
0,5	0
0,496	7,8686E-6
0,484	1,5999E-5
0,473	2,0577E-5
0,463	2,383E-5
0,448	2,775E-5
0,433	3,0945E-5
0,412	3,4596E-5
0,391	3,7522E-5
0,361	4,0765E-5
0,331	4,3105E-5
0,29	4,5108E-5
0,25	4,5908E-5
0,21	4,5564E-5
0,169	4,4014E-5
0,139	4,1986E-5
0,109	3,9026E-5
0,088	3,6264E-5
0,067	3,2729E-5
0,052	2,9553E-5
0,037	2,5555E-5
0,027	2,2145E-5
0,016	1,7285E-5
0,008	1,1671E-5
0	0

(L = 2.0 m)

Y m	Ux(y) m
2	0
1,98375	1,5985E-5
1,935	3,2747E-5
1,894	4,162E-5
1,852	4,8763E-5
1,793	5,6852E-5
1,734	6,3484E-5
1,649	7,1312E-5
1,563	7,7692E-5
1,444	8,4587E-5
1,324	8,9687E-5
1,162	9,4154E-5
1	9,6171E-5
0,838	9,5733E-5
0,676	9,278E-5
0,556	8,8709E-5
0,437	8,2705E-5
0,351	7,6838E-5
0,266	6,9351E-5
0,207	6,2764E-5
0,147	5,4328E-5
0,106	4,691E-5
0,065	3,7427E-5
0,032	2,5424E-5
0	0

(L= 10.0 m)

Y m	Ux(y) m
10	0
9,97575	1,9706E-5
9,903	4,0722E-5
9,841	5,2285E-5
9,779	6,1628E-5
9,69	7,2798E-5
9,601	8,2352E-5
9,473	9,4271E-5
9,345	1,0467E-4
9,165	1,174E-4
8,986	1,2843E-4
8,743	1,4175E-4
8,5	1,5353E-4
8	1,7306E-4
7,5	1,9033E-4
6,563	2,1337E-4
5,625	2,2853E-4
5	2,3444E-4
4,375	2,3602E-4
3,438	2,2944E-4
2,5	2,1649E-4
2	2,022E-4
1,5	1,8546E-4
1,257	1,7425E-4
1,014	1,6069E-4
0,835	1,4897E-4
0,655	1,3495E-4
0,527	1,231E-4
0,399	1,0907E-4
0,31	9,7452E-5
0,221	8,3514E-5
0,159	7,1467E-5
0,097	5,6377E-5
0,048	3,8178E-5
0	0

(L = 20.0 m)

Y m	Ux(y) m
20	0
19,97575	1,9749E-5
19,903	4,0892E-5
19,841	5,2591E-5
19,779	6,2092E-5
19,69	7,3529E-5
19,601	8,3388E-5
19,473	9,5804E-5
19,345	1,0676E-4
19,165	1,2037E-4
18,986	1,324E-4
18,743	1,4717E-4
18,5	1,6052E-4
18	1,8387E-4
17,5	2,0527E-4
16,563	2,387E-4
15,625	2,6793E-4
12,813	3,3332E-4
10	3,693E-4
7,188	3,7868E-4
4,375	3,5078E-4
3,438	3,2688E-4
2,5	2,9706E-4
2	2,7314E-4
1,5	2,4643E-4
1,257	2,2992E-4
1,014	2,1057E-4
0,835	1,9421E-4
0,655	1,7505E-4
0,527	1,5911E-4
0,399	1,4047E-4
0,31	1,252E-4
0,221	1,0702E-4
0,159	9,1424E-5
0,097	7,1988E-5
0	0

(L = 40.0 m)

Y m	U(x)y m
40,0	0.0
39,841	5,277E-5
39,779	6,2367E-5
39,69	7,3962E-5
39,601	8,4005E-5
39,473	9,6718E-5
39,345	1,0801E-4
39,165	1,2216E-4
38,986	1,3479E-4
38,743	1,5045E-4
38,5	1,6478E-4
38	1,9059E-4
37,5	2,1469E-4
36,563	2,5442E-4
35,625	2,9143E-4
32,813	3,8884E-4
30	4,7399E-4
25	6,0251E-4
20	7,0274E-4
15	7,6658E-4
10	7,6559E-4
7,188	7,2349E-4
4,375	6,3134E-4
3,438	5,7938E-4
2,5	5,184E-4
2	4,7332E-4
1,5	4,2378E-4
1,257	3,94E-4
1,014	3,5961E-4
0,835	3,308E-4
0,655	2,9739E-4
0,527	2,6982E-4
0,399	2,3777E-4
0,31	2,1164E-4
0,221	1,8068E-4
0,159	1,542E-4
0	0

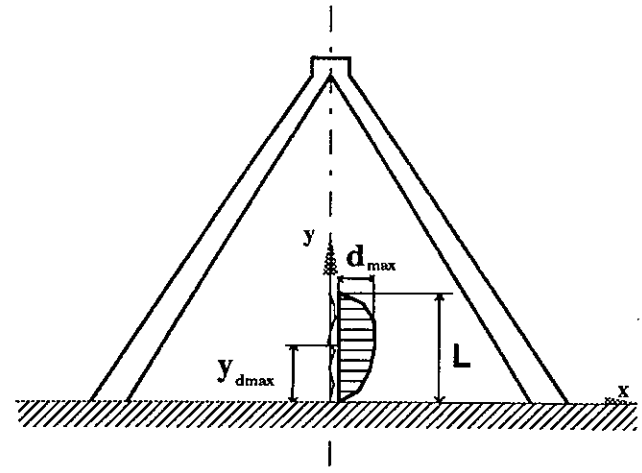

c) Crack opening for <u>equal</u> values of K ($K=2.3MN/m^{3/2}$) due to different critical temperatures (Table 1 and Table 2)

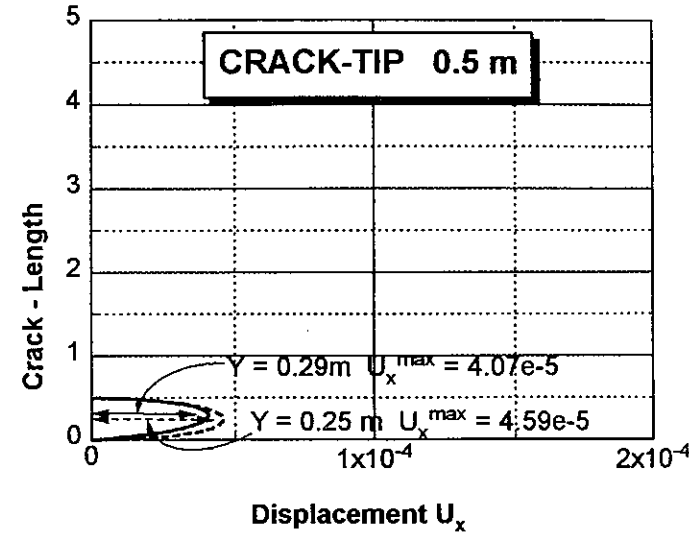

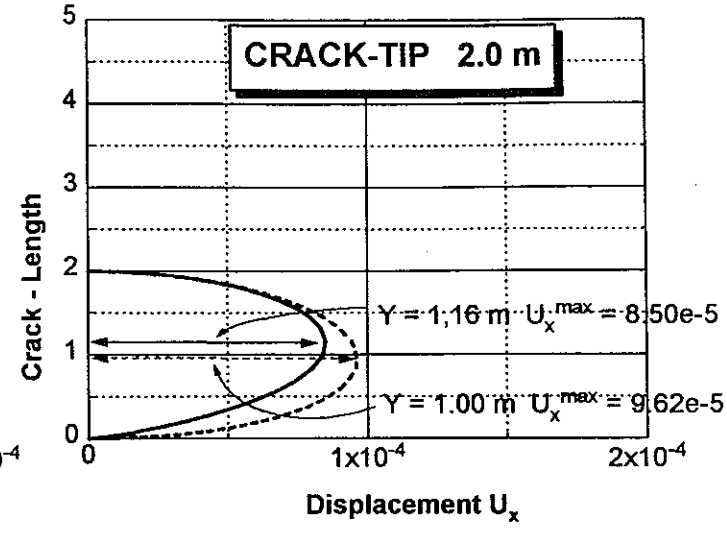

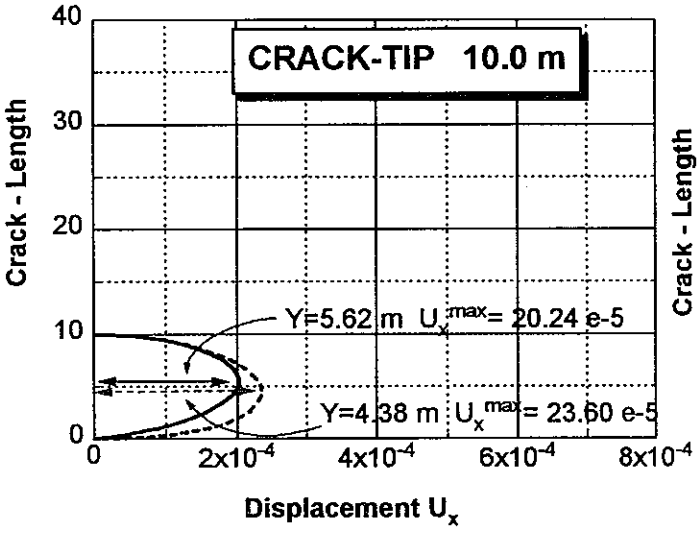

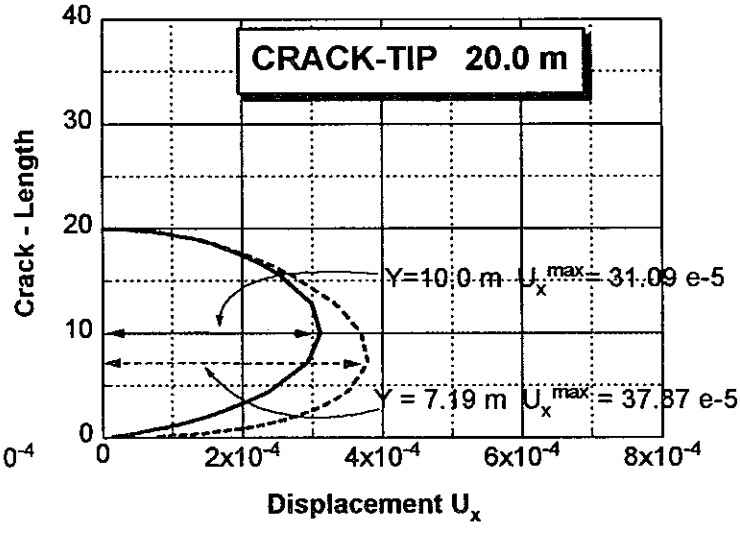

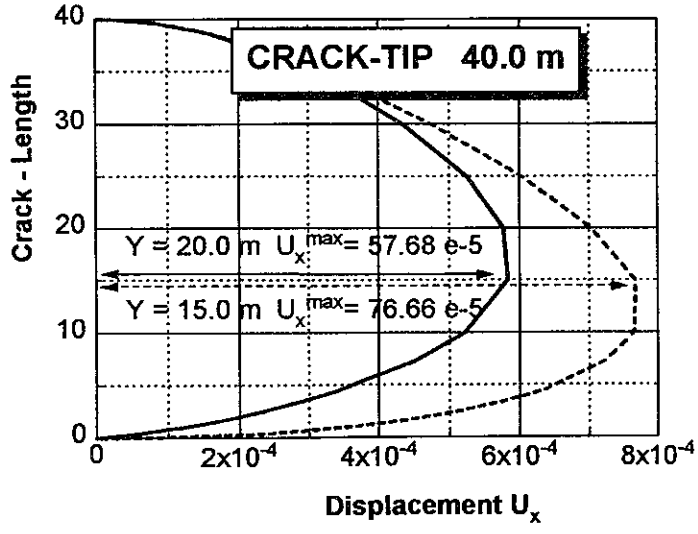

5.3 Displacements $u_x(x)$ at level L/2 due to "critical temperature" loading

a) rigid foundation

(L = 0.5 m)

x(x=L/2) m	Ux(x) m
0	4,0121E-5
0,033	3,7027E-5
0,065	3,4031E-5
0,152	2,6038E-5
0,196	2,2509E-5
0,24	1,9457E-5
0,361	1,3259E-5
0,526	8,0004E-6
0,833	3,7051E-6
1,667	9,3597E-7
2,833	-6,0935E-7

(L = 2.0 m)

x(x=L/2) m	Ux(x) m
0	8,3915E-5
0,13	7,7365E-5
0,259	7,0833E-5
0,609	5,3528E-5
0,784	4,5925E-5
0,959	3,933E-
1,444	2,5622E-5
2,10	1,3586E-

(L = 10.0 m)

x(x=L/2) m	Ux(x) m
0	2,0228E-4
2,247	1,4065E-4
5	7,8696E-5
10	6,4584E-6
15	-3,1347E-5
20	-5,8661E-5
25	-8,1652E-5
30	-1,028E-4
35	-1,2255E-4
40	-1,3938E-4
42,5	-1,4233E-4

(L = 20.0 m)

x(x=L/2) m	Ux(x) m
0	3,1091E-4
2,5	2,5118E-4
5	1,9241E-4
7,5	1,3404E-4
10	8,6388E-5
12,5	4,2111E-5
15	4,8099E-6
17,5	-2,8806E-5
20	-5,8458E-5
22,5	-8,6199E-5
25	-1,1173E-4
27,5	-1,3632E-4
30	-1,5982E-4
32,5	-1,8325E-4
35	-2,0599E-4
37,5	-2,2938E-4
40	-2,5243E-4

(L = 40.0 m)

x(x=L/2) m	Ux(x) m
0	5,7678E-4
2,5	5,0022E-4
5	4,221E-4
7,5	3,4535E-4
10	2,6774E-4
12,5	1,9353E-4
15	1,2116E-4
17,5	5,1488E-5
20	-1,585E-5
22,5	-8,1292E-5
25	-1,4531E-4
27,5	-2,0831E-4
30	-2,7098E-4
32,5	-3,3461E-4
35	-3,9923E-4

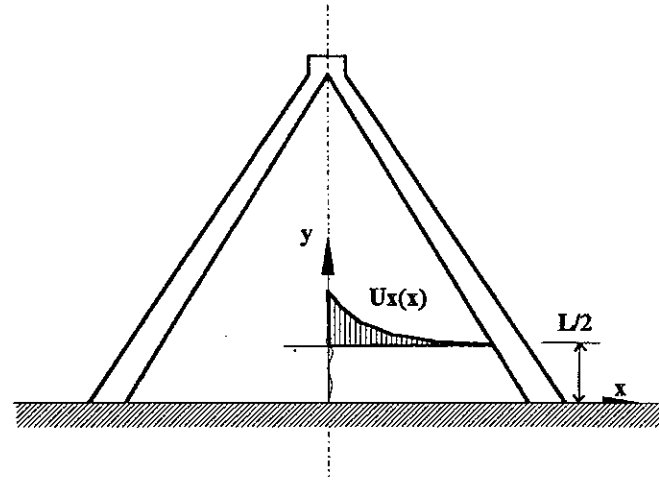

b) deformable foundation

(L = 0.5 m)

x(x=L/2) m	Ux(x) m
0	4,5908E-5
0,033	4,0607E-5
0,065	3,5433E-5
0,152	2,1162E-5
0,196	1,4246E-5
0,24	7,7115E-6
0,361	-8,4463E-6
0,526	-2,7723E-5
0,833	-5,8991E-5
1,667	-1,3564E-4
2,833	-2,3976E-4

(L = 2.0 m)

x(x=L/2) m	Ux(x) m
0	9,6171E-5
0,13	8,4648E-5
0,259	7,3102E-5
0,609	4,1432E-5
0,784	2,6205E-5
0,959	1,1786E-5
1,444	-2,4419E-5
2,104	-6,8212E-5

(L = 10.0 m)

x(x=L/2) m	Ux(x) m
0	2,3444E-4
2,247	1,2256E-4
5	-7,5276E-6
10	-2,0959E-4
15	-3,816E-4
20	-5,4327E-4
25	-6,9933E-4
30	-8,5181E-4
35	-1,0015E-3
40	-1,1488E-3
42,5	-1,221E-3

(L = 20.0 m)

x(x=L/2) m	Ux(x) m
0	3,693E-4
2,5	2,5499E-4
5	1,4002E-4
7,5	2,3574E-5
10	-8,3895E-5
12,5	-1,8956E-4
15	-2,8896E-4
17,5	-3,8494E-4
20	-4,7755E-4
22,5	-5,6835E-4
25	-6,5748E-4
27,5	-7,4581E-4
30	-8,3376E-4
32,5	-9,2226E-4
35	-1,0109E-3
37,5	-1,0994E-3
40	-1,1918E-3

(L = 40.0 m)

x(x=L/2) m	Ux(x) m
0	7,0274E-4
2,5	5,5148E-4
5	3,9834E-4
7,5	2,4537E-4
10	8,9953E-5
12,5	-6,3249E-5
15	-2,161E-4
17,5	-3,6704E-4
20	-5,1653E-4
22,5	-6,6476E-4
25	-8,1216E-4
27,5	-9,5924E-4
30	-1,1061E-3
32,5	-1,2535E-3
35	-1,4031E-3

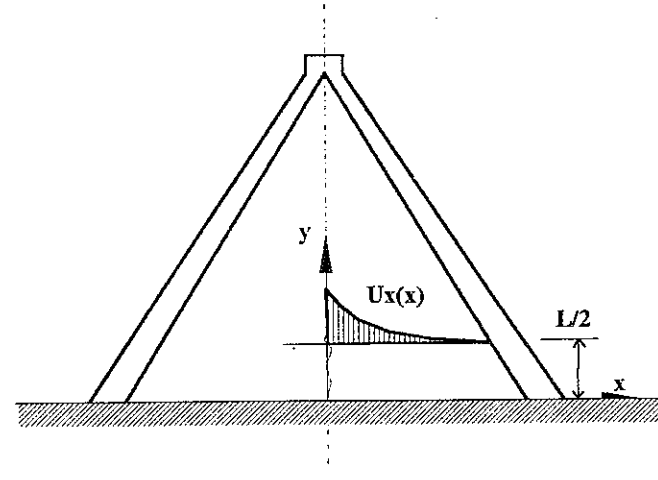

c) Displacements $u_x(x)$ at level L/2 for <u>equal</u> values of K ($K=2.3MN/m^{3/2}$) due to different critical temperatures (Table 1 and Table 2)

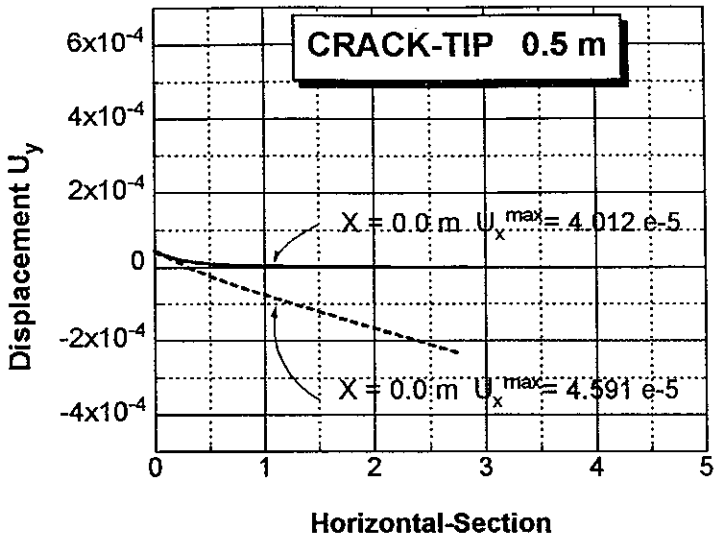

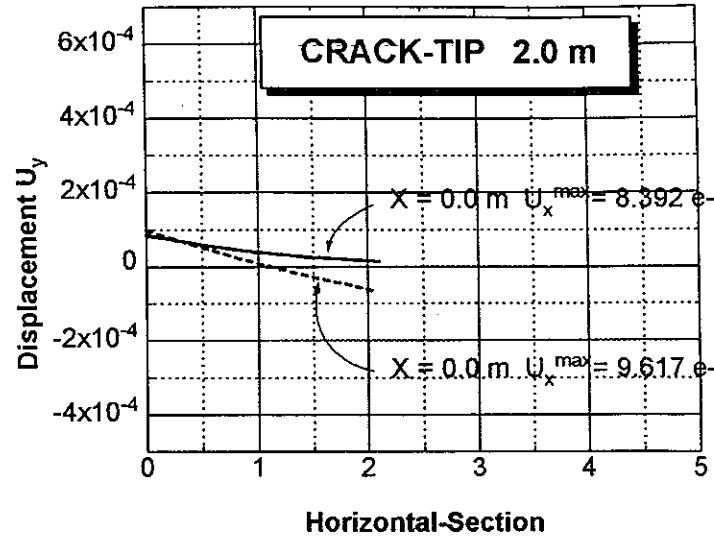

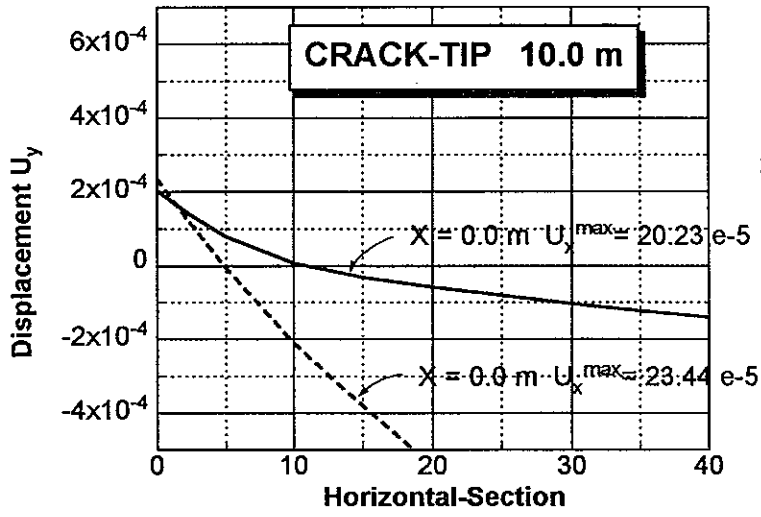

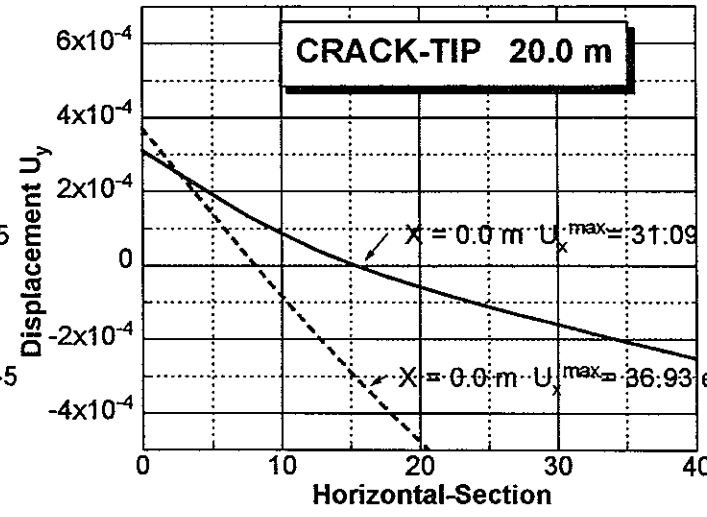

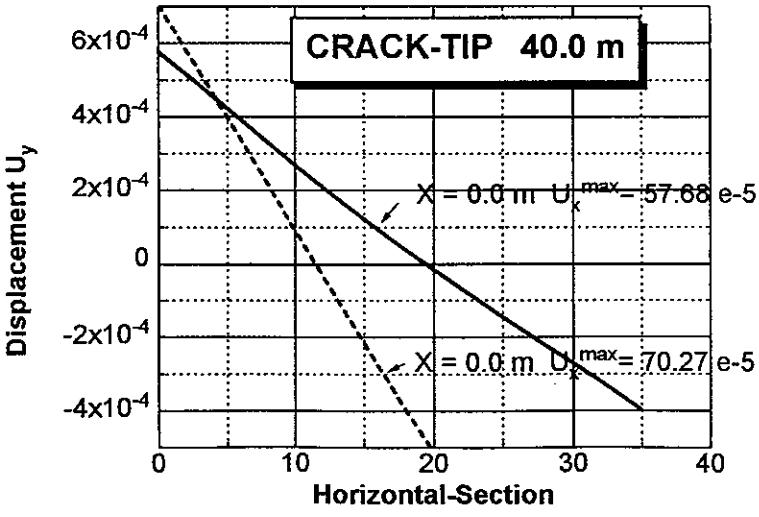

——— RIGID FOUNDATION

------- DEFORMABLE FOUNDATION

5.4 Contour plots for horizontal and vertical displacements CL=0.5m

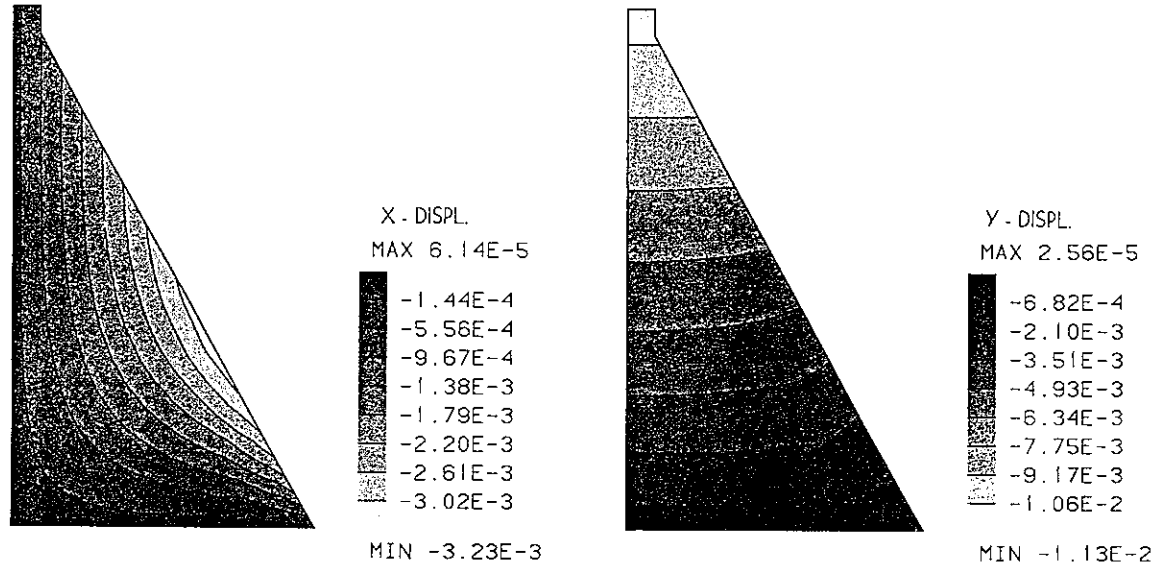

a) rigid foundation

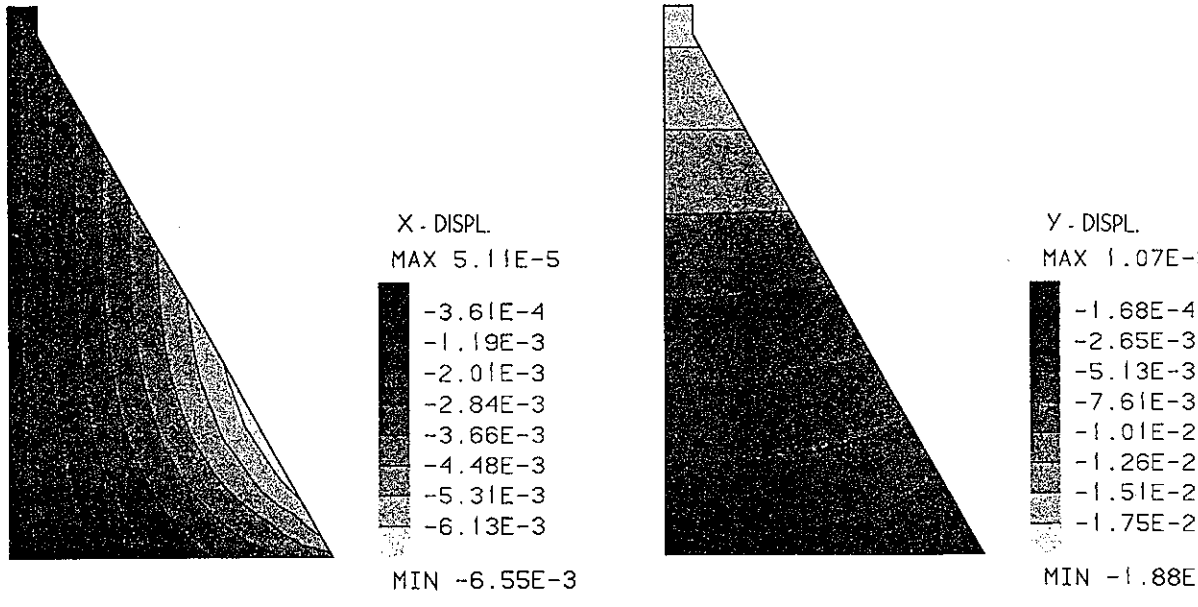

b) deformable foundation

5.5 Contour plots for horizontal and vertical displacements CL=2.0 m

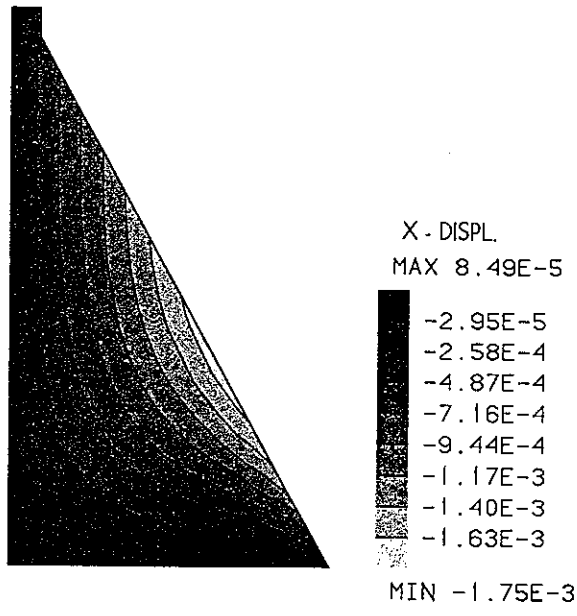

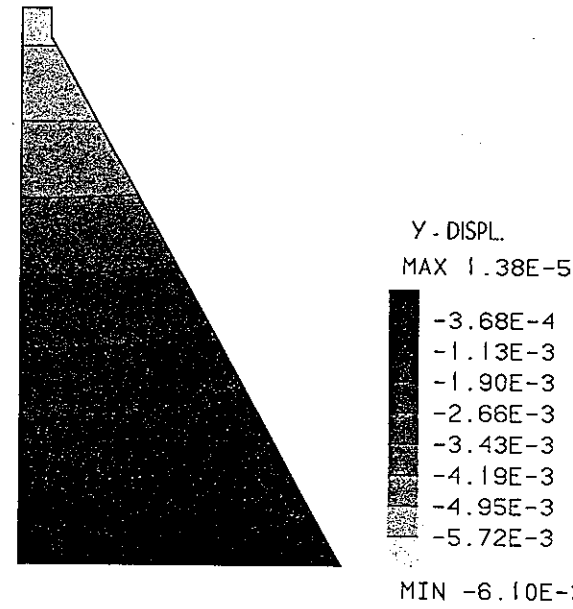

a) rigid foundation

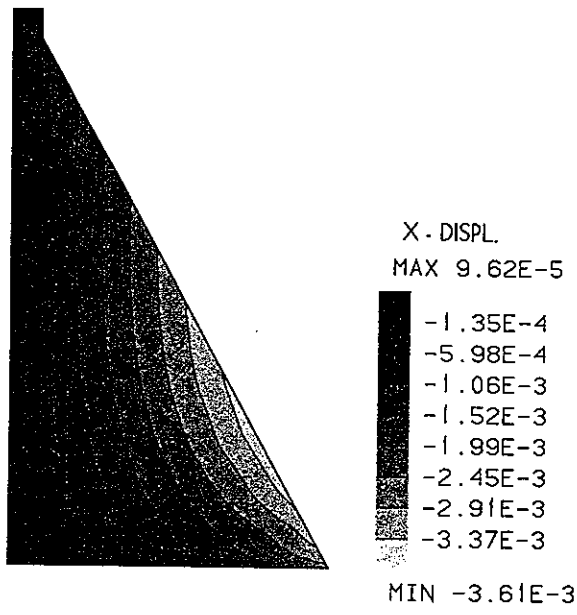

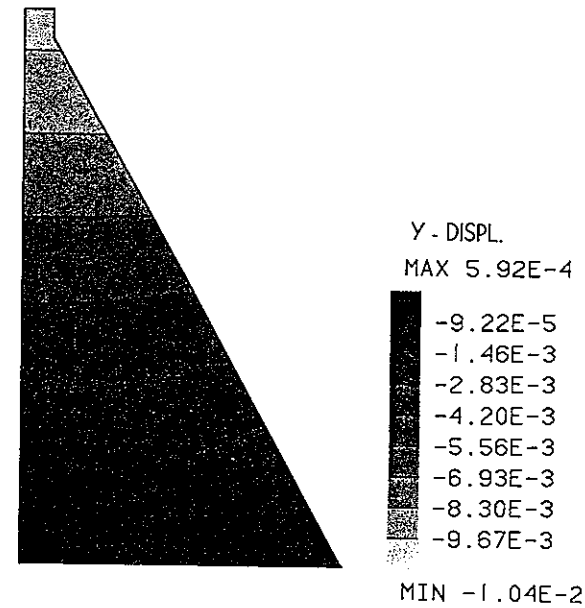

b) deformable foundation

5.6 Contour plots for horizontal and vertical displacements CL=10.0 m

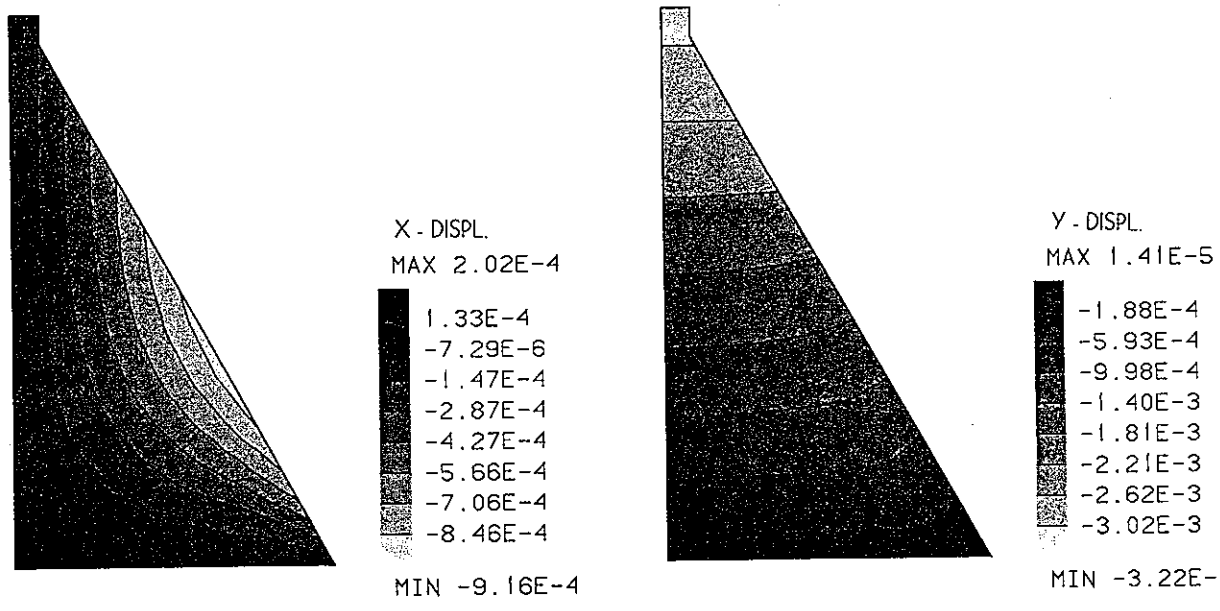

a) rigid foundation

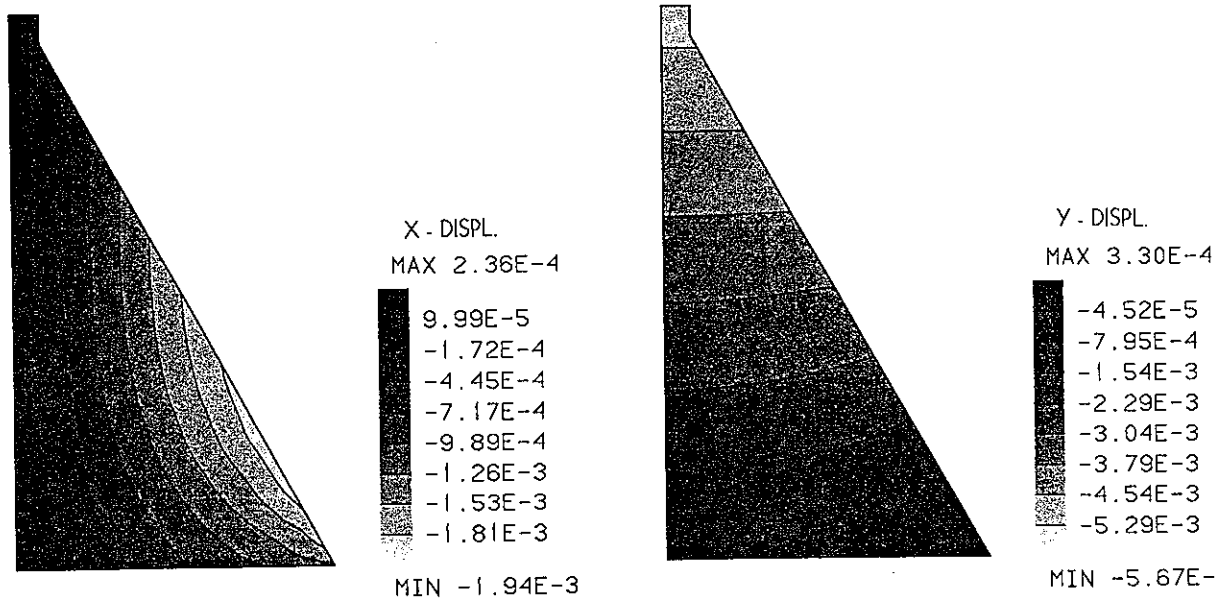

b) deformable foundation

5.7 Contour plots for horizontal and vertical displacements CL=20.0 m

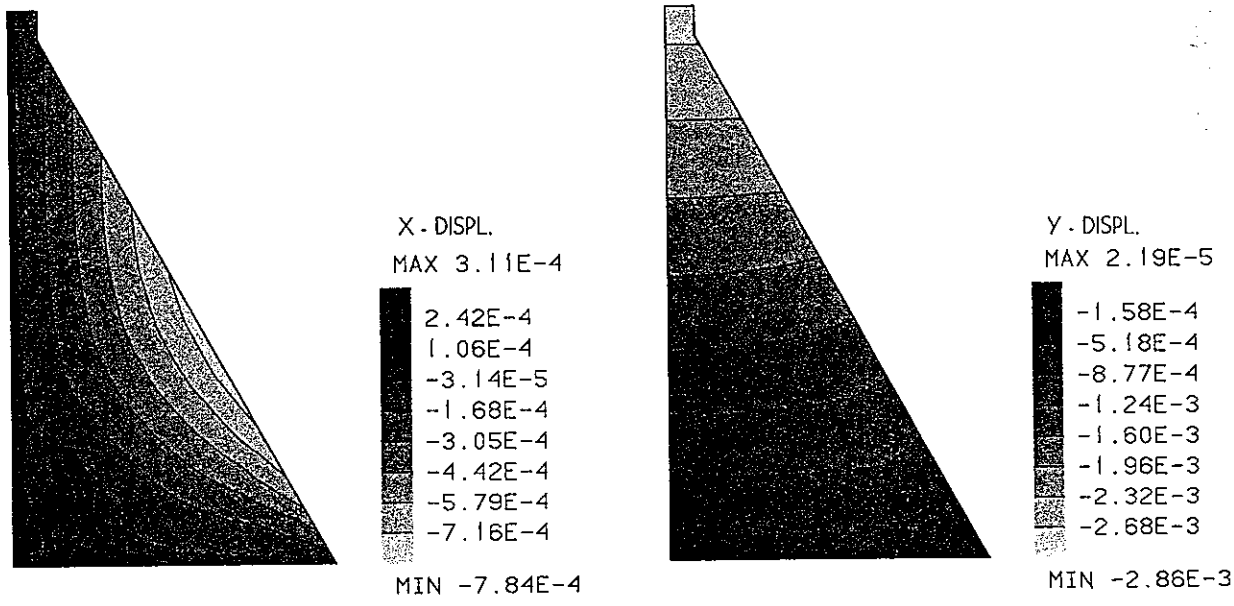

a) rigid foundation

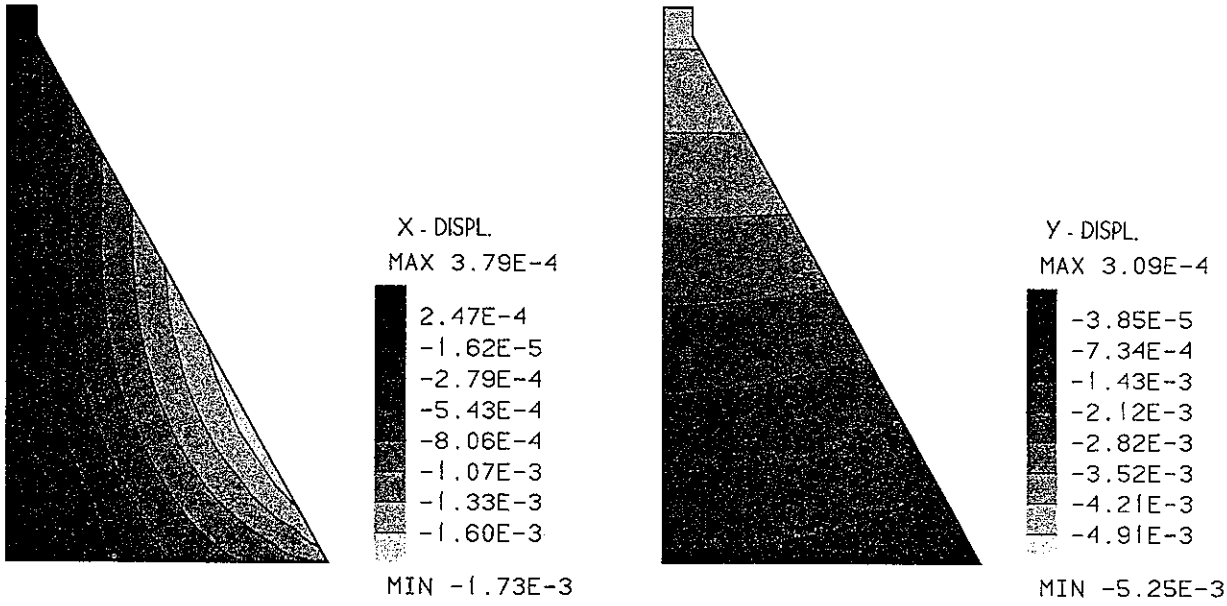

b) deformable foundation

5.8 Contour plots for horizontal and vertical displacements CL=40.0 m

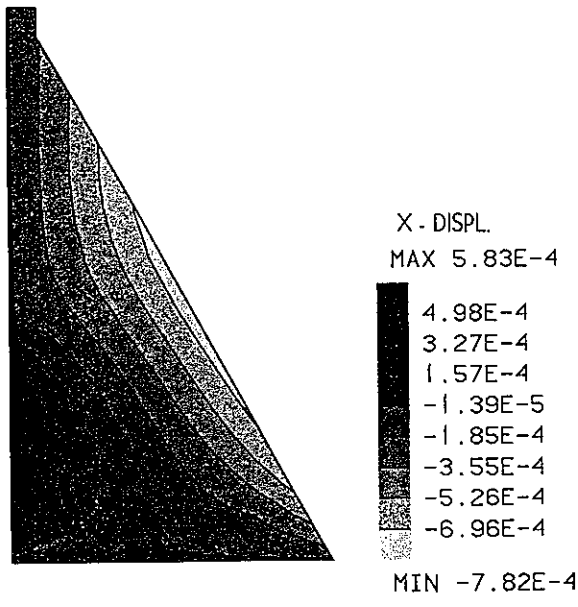

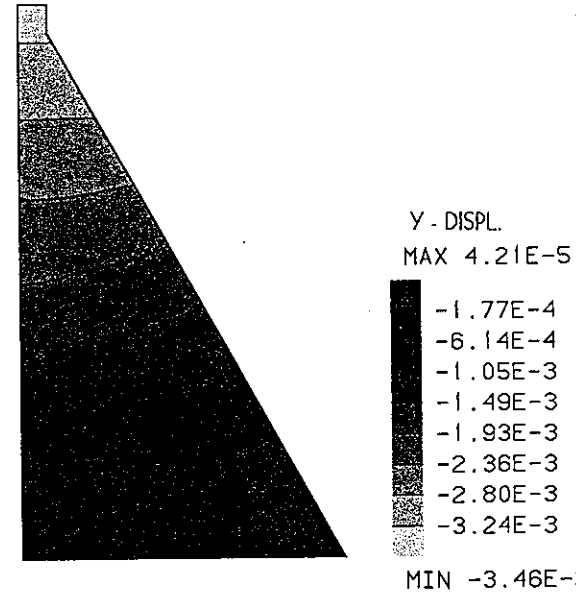

a) rigid foundation

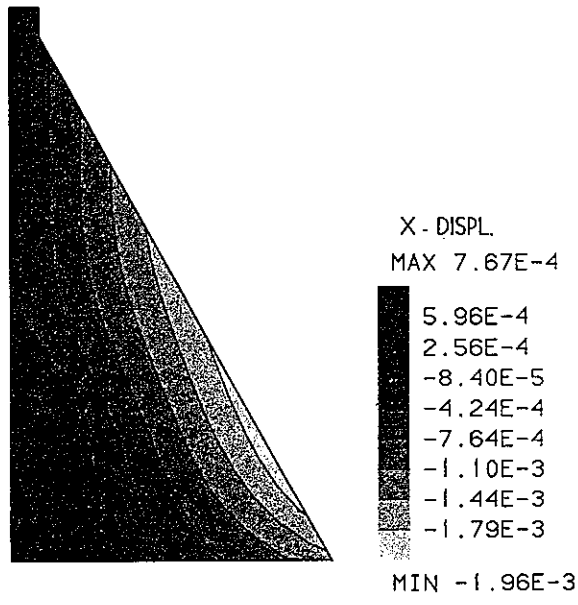

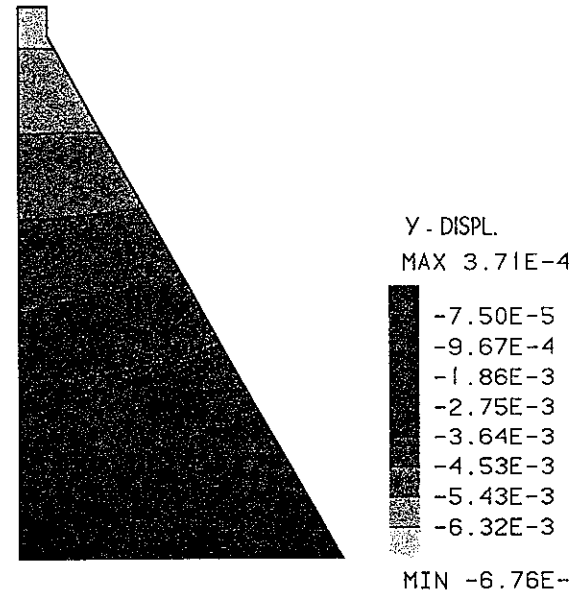

b) deformable foundation

6 CONCLUSION

Besides the intention of the ICOLD Benchmark Workshop to compare existing software for investigation of cracking in concrete dams, generally the physical-mathematical modeling of the problem should be discussed. In particular the call for more sophisticated methods in describing the fracture process in mass concrete structures. Shortly spoken - linear elastic fracture mechanics versus nonlinear (fracture energy related) methods.

Comparing the simplicity of LEFM with the complexity which is significant for all of the present discussed nonlinear models and considering the crucial size effect problem in material testing (of dam concrete) subjected to both methods it is to state that at present nonlinear models are not suitable for investigation of cracking in concrete dams.

The application of LEFM to actual cases of cracking in dams on the other side often has been successful (e.g. /4/).

7 LITERATURE

/1/ Linsbauer, H.N.: Fracture Mechanics Material Parameters of Mass Concrete Based on Drilling Core Tests - Review and Discussion. In: van Mier,J.G.M.; Rots,J.G.; Bakker,A.(eds.): Fracture Processes in Concrete, Rock and Ceramics, RILEM, E.&F.N.Spon, (1991) 779-787

/2/ Henshell, R.D. and Shaw, K.G.:Crack tip finite elements are unnessesary, Int.J.num.Meth.Engng,9 (1975) 495-507

/3/ Barsoum, R.S.: On the use of isoparametric finite elements in linear fracture mechanics, Int.J.num.Meth.Engng 10 (1976) 25-37

/4/ Linsbauer, H.N.:Fracture mechanics application in dam engineering in Austria: Review and discussion,. In : E. Boudarot, J. Mazars, V. Saouma, eds.: Dam Fracture and Damage, A.A.Balkema, Rotterdam, 1994 (241-246)

Acknowledgment: The authors would like to express their thanks to Dipl.Ing. A. Šajna for computer support and layout.